03

E74 10705
CR-139434

A RECONNAISSANCE SPACE SENSING INVESTIGATION OF CRUSTAL STRUCTURE FOR A STRIP FROM THE EASTERN SIERRA NEVADA TO THE COLORADO PLATEAU

ARGUS EXPLORATION COMPANY
555 South Flower Street – Suite 3670
Los Angeles, California 90071

August 1974

Final Report of Investigation

ORIGINAL CONTAINS
COLOR ILLUSTRATIONS

Prepared for

GODDARD SPACE FLIGHT CENTER
Greenbelt, Maryland 20771

1103A

CYPRUS

BIBLIOGRAPHIC DATA SHEET

1. Report No.

2.

3. Recipient's Accession No.

4. Title and Subtitle

A RECONNAISSANCE SP[illegible]E SENSING INVESTIGATION OF CRUSTAL STRUCTURE FO[illegible]TRIP FROM THE EASTERN SIERRA NEVADA TO TH[illegible]OLORADO PLATEAU

5. Report Date

August 1974

6.

7. Author(s)

Mark A. Liggett and Research Staff

8. Performing Organization Rept. No.

9. Performing Organization Name and Address

Argus Exploration Company *
555 South Flower Street - Suite 3670
Los Angeles, California 90071

10. Project/Task/Work Unit No.

11. Contract/Grant No.

NAS5-21809

12. Sponsoring Organization Name and Address

National Aeronautics and Space Administration
Goddard Space Flight Center
Greenbelt, Maryland 20771

13. Type of Report & Period Covered

Type III Final Report of Investigation

14.

15. Supplementary Notes

* A research subsidiary of Cyprus Mines Corporation

16. Abstracts

This report summarizes an investigation of geologic applications of ERTS-1 MSS imagery over parts of southern Nevada, eastern California, northwestern Arizona and southwestern Utah in a test site located between lat 35° and 38° N. and long 113° and 119° W. Studies were conducted in key field areas in the Sierra Nevada, the Basin Range Province and the Colorado Plateau to evaluate the origins and significance of geologic and structural anomalies expressed in the ERTS-1 data. The investigation included development of image enhancement and analysis techniques and comparison of remote sensing data available over the test site. The ERTS-1 MSS imagery has proven to be an effective tool for studying the interrelationships between Cenozoic tectonic patterns and the distributions of Cenozoic plutonism and volcanism, seismic activity, geologic hazards, and known mineral, geothermal and ground water resources. Recommendations are made for applications of ERTS-1 data to natural resource exploration and management.

17. Key Words and Document Analysis. 17a. Descriptors

Tectonics
Geology
ERTS-1

ORIGINAL CONTAINS
COLOR ILLUSTRATIONS

17b. Identifiers/Open-Ended Terms

Basin Range Province
Image enhancement techniques
mineral exploration
geothermal exploration
hydrologic exploration
geologic hazards

Original photography may be purchased from
EROS Data Center
10th and Dakota Avenue
Sioux Falls, SD 57198

18. Availability Statement

Release unlimited

19. Security Class (This Report) UNCLASSIFIED

20. Security Class (This Page) UNCLASSIFIED

21. No. of Pages

22. Price

PREFACE

The following report summarizes the results of an 18-month research program on geologic applications of data from the NASA Earth Resources Technology Satellite (ERTS-1). The Argus Exploration Company test site traverses the southern Basin Range Province from the Sierra Nevada to the western Colorado Plateau in parts of eastern California, southern Nevada, southwestern Utah and northwestern Arizona.

The following objectives define the scope of this investigation:

1. Analysis, interpretation and evaluation of ERTS-1 MSS data for use in the study of regional crustal structure and related geologic phenomena.

2. Field investigation and literature research to support imagery interpretation and to evaluate the origins and significance of anomalies recognized in ERTS-1 MSS data. Evaluation of potential applications of ERTS-1 data to natural resource exploration and management.

3. Comparison and evaluation of selected spacecraft and aerial remote sensing imagery over the test site. Experimentation with image enhancement and analysis techniques.

The results of this investigation support the following conclusions:

1. The synoptic scale of the ERTS-1 MSS imagery has permitted the recognition of large geologic features, trends and patterns often obscured by detail at the scale of low altitude aerial photography or conventional geologic mapping. These anomalies are expressed in ERTS-1 imagery by such characteristics as surface coloring and texture, topography and vegetation patterns. Ground based reconnaissance of anomalies recognized in ERTS-1 imagery has resulted in identification of previously unreported strike-slip and normal fault systems, structural ground water traps, dike swarms, domal plutonic structures, volcanic centers, and areas of hydrothermal alteration.

2. Using ERTS-1 MSS imagery, the Cenozoic tectonic framework of the test site has been studied at a scale and level of detail not possible using available tectonic map compilations. This study has documented an interrelationship between the Cenozoic tectonics of the southern Basin Range Province and the regional distribution of seismic activity, volcanism, plutonism and related mineralization and geothermal activity. This research has resulted in new concepts of Basin Range tectonics and related structural control of igneous activity and mineralization.

3. Several image enhancement techniques have been developed for effective

A RECONNAISSANCE SPACE SENSING INVESTIGATION OF CRUSTAL STRUCTURE FOR A STRIP FROM THE EASTERN SIERRA NEVADA TO THE COLORADO PLATEAU

ARGUS EXPLORATION COMPANY
555 South Flower Street – Suite 3670
Los Angeles, California 90071

August 1974

Final Report of Investigation

Prepared for

GODDARD SPACE FLIGHT CENTER
Greenbelt, Maryland 20771

analysis of the ERTS-1 data. High resolution false-color compositing of multispectral imagery, with precise control of image color balance and contrast range, has been a primary tool. Edge enhancement printing has proven useful for studying structural trends expressed by patterns of topography and drainage. False-color spectral ratio imaging has been effective for enhancing subtle reflectance differences between rock and soil types, and in studying the distribution and density of vegetation.

4. A primary limitation of the ERTS-1 imagery has been in studying at a local scale, geologic and structural features such as folds, foliation and irregular lithologic contacts. Although large exposures of surface material can often be distinguished by color, texture or erosional morphology, specific rock or soil types cannot generally be identified by composition. Surface coloring and small structural features are easily masked by vegetation.

5. The repetitive ERTS-1 imagery coverage has provided unique information related to seasonal changes of vegetation patterns and varied illumination of topography. Similar repetitive aircraft imagery has not generally been available. However, the scale and resolution of available U-2 photography and SLAR have proven useful for guiding detailed laboratory and field studies of geologic and structural anomalies interpreted in the ERTS-1 data.

6. ERTS-1 MSS imagery can be a valuable tool for reconnaissance exploration of mineral, geothermal and ground water resources, and for regional study of geologic hazards. Used as part of an integrated exploration or research program, anomalies selected from ERTS-1 data can be economically narrowed and evaluated using a variety of geophysical, geochemical and geologic techniques. Within the geologic and climatic terrane of the test site, the use of ERTS-1 MSS imagery in natural resource exploration and management is estimated to permit cost savings of approximately 10 to 1 over conventional reconnaissance techniques.

CONTENTS

LIST OF TABLES

LIST OF FIGURES

LIST OF PLATES

LIST OF APPENDICES

1.0 INTRODUCTION

Objectives:

The following report summarizes the results of an eighteen-month investigation of geologic applications of data from the Earth Resources Technology Satellite (ERTS-1). This investigation was undertaken with the following objectives:

1. Analysis, interpretation and evaluation of ERTS-1 MSS data for use in the study of regional crustal structure and related geologic phenomena.

2. Field investigation and literature research to support imagery interpretation and to evaluate the origins and significance of anomalies recognized in ERTS-1 data. Evaluation of potential applications of ERTS-1 data to natural resource exploration and management.

3. Comparison of selected spacecraft and aerial remote sensing imagery over the test site. Experimentation with image enhancement and analysis techniques.

The Argus Exploration Company test site occupies an area of more than 180,000 square km (70,000 square miles) in parts of eastern California, southern Nevada, southwestern Utah, and northwestern Arizona, as shown in the index map of Figure 1. This test site was chosen for its span of diverse structural and geologic terranes from the Sierra Nevada granitic massif, across the complexly faulted Basin Range Province, to the relatively stable terrane of the Colorado Plateau. The variation in geology and structure across the test site is similar to that of major mountain belts on other continents, and it is within these mobile belts that most of the world's metallic mineral and geothermal energy resources are found. This research program was undertaken with the premise that a better understanding of regional tectonics and more effective tools for reconnaissance geologic mapping will have important roles in the future exploration and management of natural resources.

Because of its broad scope, this investigation has combined many different tasks which are summarized in separate sections of this report.

Field Investigations:

An extensive program of ground based field reconnaissance, geologic mapping and literature research was undertaken in order to evaluate the origins and significance of key geologic and structural anomalies interpreted in the ERTS-1 MSS imagery. These investigations were conducted in the diverse geologic, topographic and climatic terranes of the test site, and have formed the basis for evaluating data analysis and interpretation techniques and potential applications of the ERTS-1 data. Summaries of these investigations are included in the Appendices of this report.

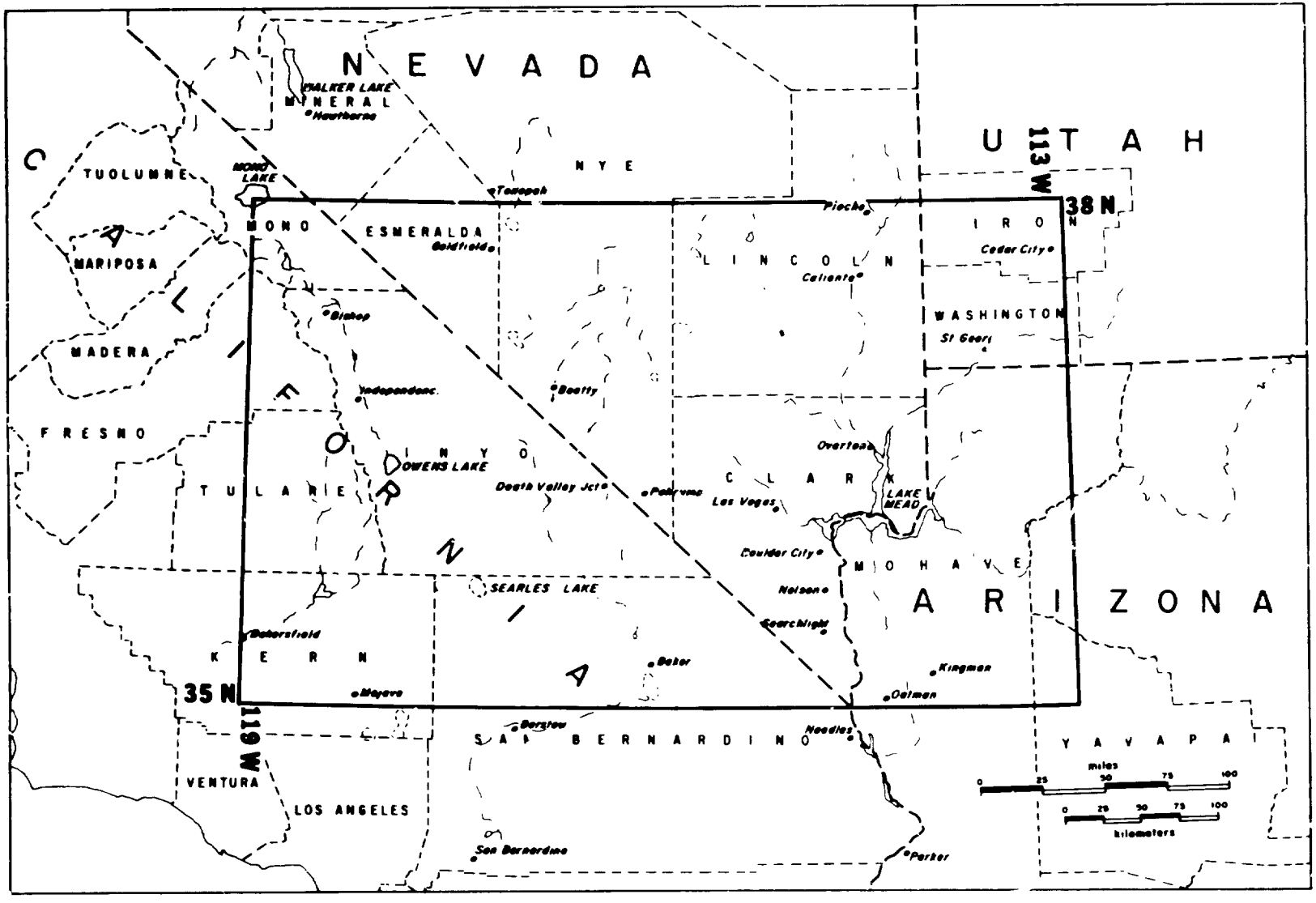

Figure 1: Index map of the Argus Exploration Company test site.

Program Support:

Analysis and interpretation of ERTS-1 MSS imagery were coordinated with the study of other remote sensing data available over the test site. These include DAPP and NIMBUS weather satellite data, Apollo-9 photography, NASA-USAF X-15 photography, NASA and USAF U-2 photography, and NASA Side Looking Aerial Radar (SLAR). The comparison of data over key areas established a basis for evaluating the applications of different imaging techniques.

The geologic and structural information contained in the ERTS-1 MSS imagery and subsidiary remote sensing data was studied with the aid of a variety of experimental photographic, photomechanical, optical and digital image enhancement and analysis techniques, which are summarized in this report.

Regional Investigations:

The ERTS-1 MSS imagery over the test site was used as a basis for studying the regional interrelationship of Cenozoic structural features and tectonic patterns with other geologic phenomena, including the distributions of Cenozoic plutonic and volcanic centers, the locations and characteristic expressions of known mineral deposits and potential geothermal sources, and the distributions of recorded earthquake epicenters. These investigations have coordinated the use of imagery analysis, field reconnaissance and literature research.

Potential Applications of ERTS-1 MSS Data:

On the basis of field investigations and regional studies of geologic phenomena in the test site, we have evaluated concepts and techniques for operational applications of ERTS-1 MSS data to natural resource exploration and management. The disciplines considered include reconnaissance exploration for mineral, ground water and geothermal resources, and reconnaissance study of geologic hazards. Recommended procedures and analytical techniques, and the cost and time advantages gained by use of ERTS-1 data are outlined in this report.

The synoptic view of the earth recorded by the ERTS-1 satellite provides a perspective of regional geology and crustal structure not achieved from aircraft based sensors or conventional ground based geologic mapping. This perspective permits the recognition and mapping of structural features and other geologic phenomena obscured by detail in smaller fields of view. Although the effectiveness of ERTS-1 data may vary with geologic and climatic settings, we are confident that the analysis and interpretation procedures developed in this investigation will help extend the use of ERTS-1 data to other parts of the world, where regional structural reconnaissance and related applications to resource exploration have not been economically feasible in the past.

This report is organized in sections which summarize the procedures and results of the separate research tasks conducted in this investigation. Detailed reports on key geologic field studies and ERTS-1 data processing techniques are included in the Appendices to this report.

2.0 PROGRAM SUPPORT

2.1 ACKNOWLEDGEMENTS

The research program summarized in this report has benefited from the support of many individuals, to whom the research staff wishes to express its appreciation.

We wish to thank our principal NASA monitors, Paul D. Lowman, Jr. and Edward W. Crump for their patience and support during the course of this program. We are especially grateful to Dr. Lowman for his scientific advice, and for his generosity in sharing time, enthusiasm and unparalleled experience in geologic applications of spacecraft remote sensing techniques.

Wally MacGalliard has provided masterful skill in the technical processing and reproduction of the color imagery used in this investigation. Dr. Alexander K. Baird, Pomona College, Claremont, California, has contributed valuable advice and an experienced perspective of geologic problems, research techniques and applications.

Many other individuals have furnished data, ideas and encouragement in support of this investigation. Among these, we would particularly like to thank R. Ernest Anderson, U.S. Geological Survey, Denver, Colorado; Lucy Birdsall, U.S. Geological Survey, Los Angeles, California; and Alexis Volborth, University of California, Irvine, California. Charlotte P. Teshar has patiently typed and edited many drafts of this report.

Ira C. Bechtold made many contributions to the planning of the early phases of this investigation, and this support is gratefully acknowledged.

This research program was supported by Cyprus Mines Corporation and the National Aeronautics and Space Administration under contract NAS 5-21809.

2.2 PERSONNEL

The following personnel have served as members of the Argus Exploration Company research staff:

Scientific Staff

Mark A. Liggett, Field Geologist and acting Principal Investigator: *
tectonics and imagery analysis techniques

John F. Childs, Field Geologist:
geologic reconnaissance, mapping, and applications research

Helmut E. Ehrenspeck, Assistant Geologist:
volcanology

Technical Staff

Jack W. Barth, Research Assistant:
remote sensing, data procurement

Alexander Costa, Research Assistant:
seismology

Richard L. Hutchens, Technician and Field Assistant:
literature research

Paul L. McClay, Technician and Field Assistant:
photography

Clerical Staff

Charlotte P. Teshar, Technical Secretary

Claudine G. Gove, Technical Secretary

* Mr. Ira C. Bechtold was Principal Investigator for this project from June 1972 to June 1973.

2.3 ERTS-1 MSS IMAGERY

The positions of key ERTS-1 MSS frames over the Argus Exploration Company test site are shown in Figure 2. False color composites of this imagery are included in Figures 4 - 14 accompanied by index maps that show the topography and the principal geographic features in the image areas.

The false color composites were produced using the following ERTS-1 MSS band and printing filter combinations:

MSS Band	Spectral Range	Printing Filter
#4	Green and yellow (0.5-0.6 micron)	Blue
#5	Red (0.6-0.7 micron)	Green
#7	Near-infrared (0.8-1.1 micron)	Red
	or	
#6	Near-infrared (0.7-0.8 micron)	Red

As a result of this color convention, green vegetation appears in the composites as intense red, due to the high reflectance of vegetation in the near-infrared portion of the spectrum. Most buff to brown rock or soil units in the composites reproduce in approximately their natural colors. Neutral colored granites, sandstones or concrete generally appear with gray to slightly blue coloring; and dark, mafic igneous and metamorphic rocks reproduce with dark brown to steel gray coloring. Red, iron-rich sedimentary rocks and iron oxide staining associated with hydrothermal alteration appear as yellow coloring, sometimes varying between greenish yellow and orange, depending on the mineralogy and moisture content of the surface material. Water bodies appear dark blue or black due to the high absorption by water in the spectral bands recorded by the ERTS-1 MSS sensors. The techniques used in production of this imagery are outlined in Appendix J of this report.

Prior to the availability of ERTS-1 MSS imagery, several preliminary studies were conducted in the test site using oblique Apollo-9 Ektachrome photography recorded in March 1969. A key example of this photography is included as Figure 3 for comparison with the ERTS-1 MSS data.

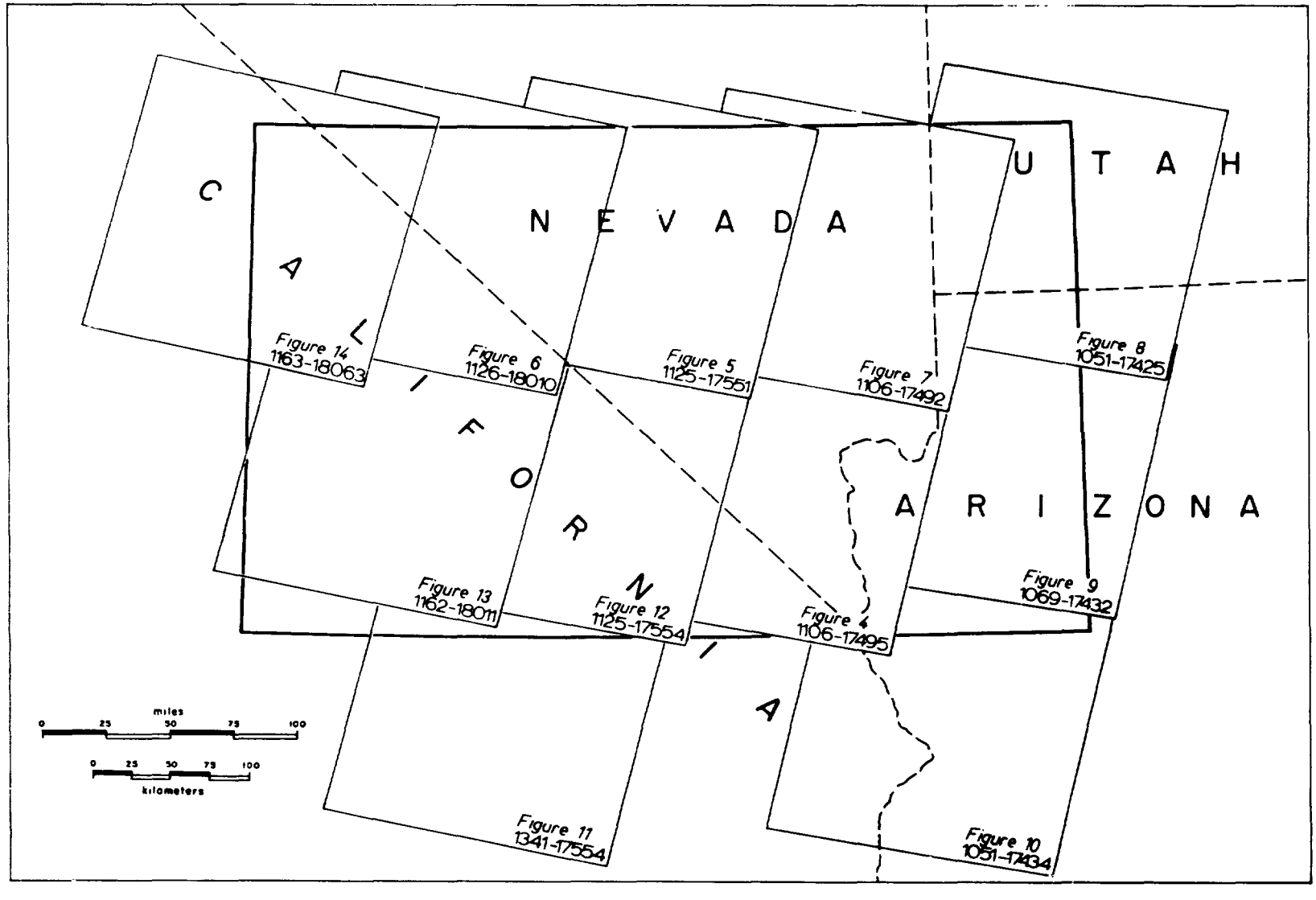

Figure 2: Locations, figure numbers and frame numbers of ERTS-1 MSS imagery included in this report. Heavy lines indicate the boundary of the Argus Exploration Company test site. See Figure 1 for geographic details.

Figure 3: Lake Mead area, Nevada, California & Arizona.
Apollo 9 Photograph AS 9-20-3135, March 1969

FOLDOUT FRAME

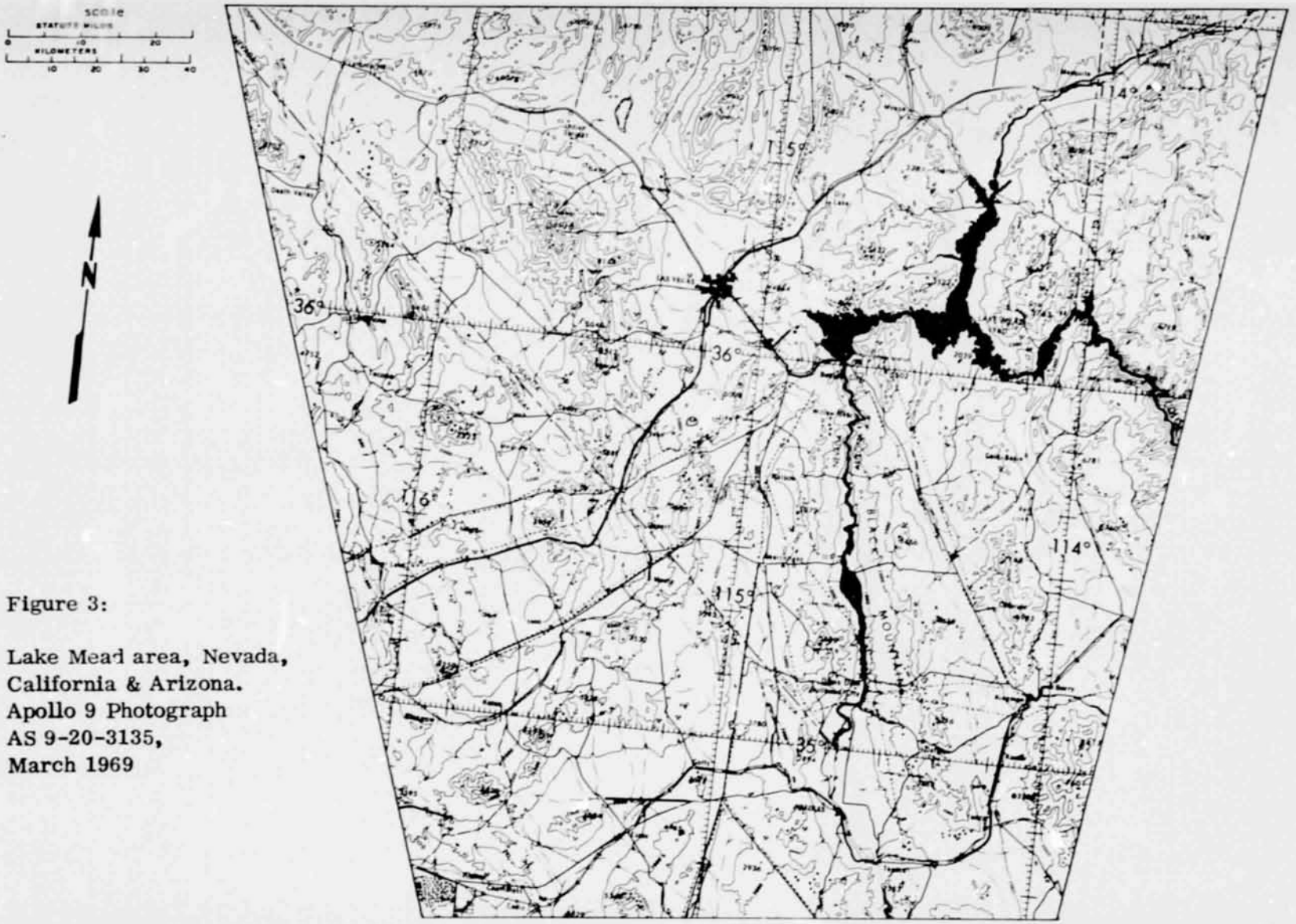

FOLDOUT FRAME 2

Figure 3:

Lake Mead area, Nevada,
California & Arizona.
Apollo 9 Photograph
AS 9-20-3135,
March 1969

Figure 4: Lake Mead area, Nevada, California & Arizona.
ERTS-1 MSS Frame #1106-17495

FOLDOUT FRAME

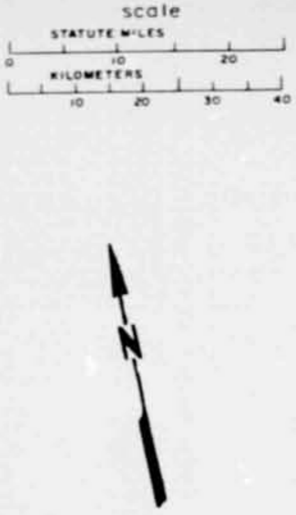

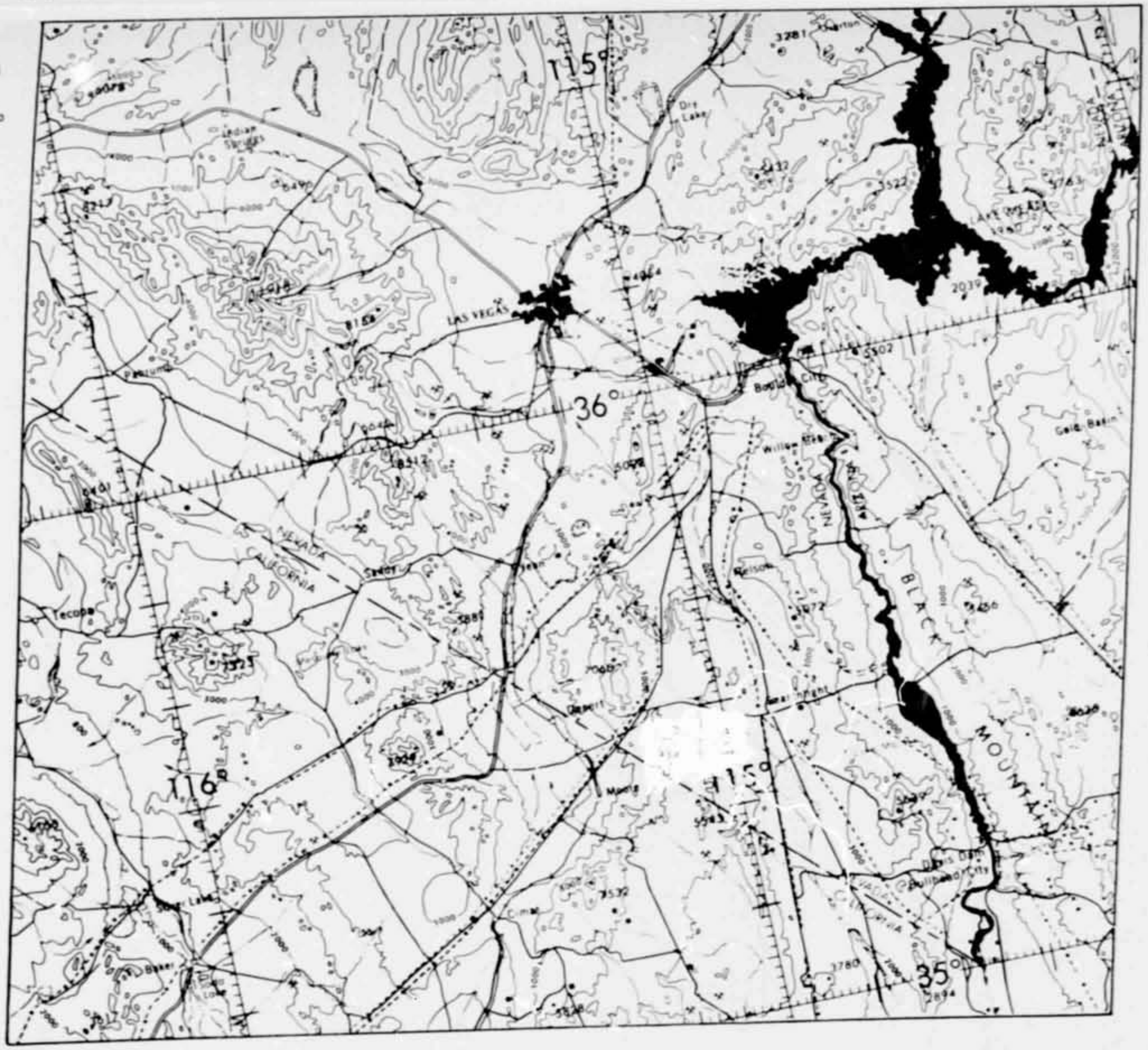

Figure 4:

Lake Mead area,
Nevada, California
& Arizona.
ERTS-1 MSS Frame
#1106-17495

FOLDOUT FRAME 2

Figure 5: Beatty area, Nevada.
ERTS-1 MSS Frame #1125-17551

FOLDOUT FRAME

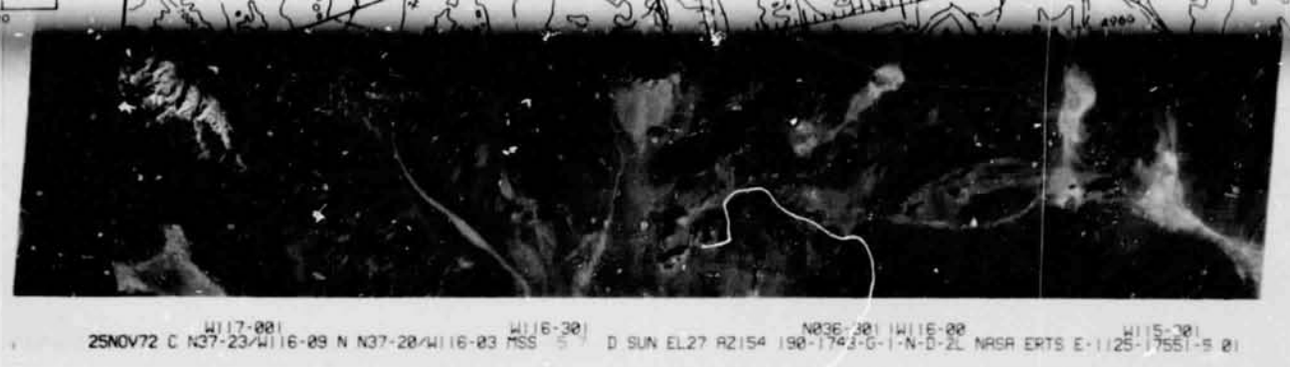

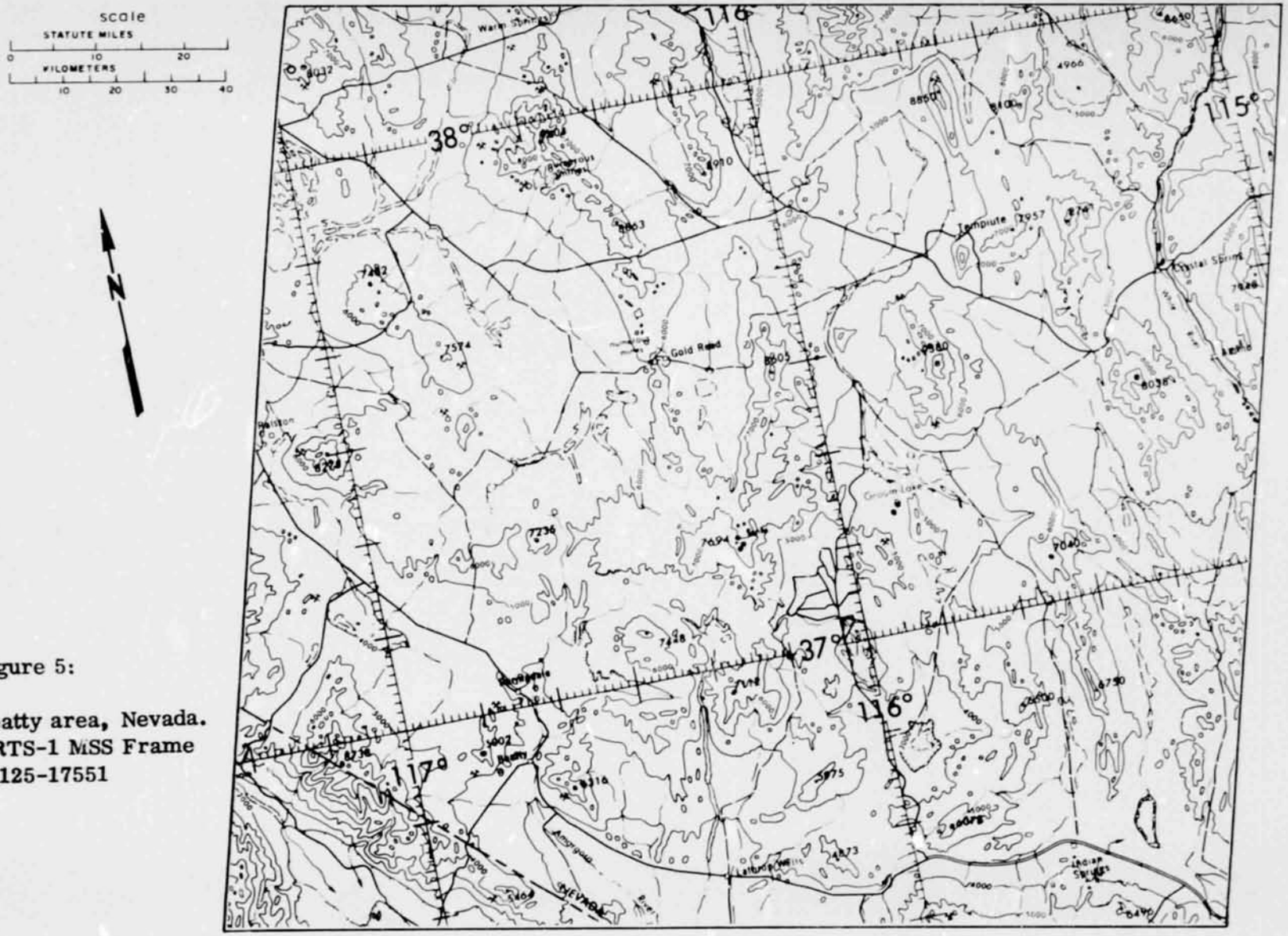

FOLDOUT FRAME 2

Figure 5:

Beatty area, Nevada. ERTS-1 MSS Frame #1125-17551

Figure 6: Goldfield area, Nevada & California.
ERTS-1 MSS Frame #1126-18010

FOLDOUT FRAME

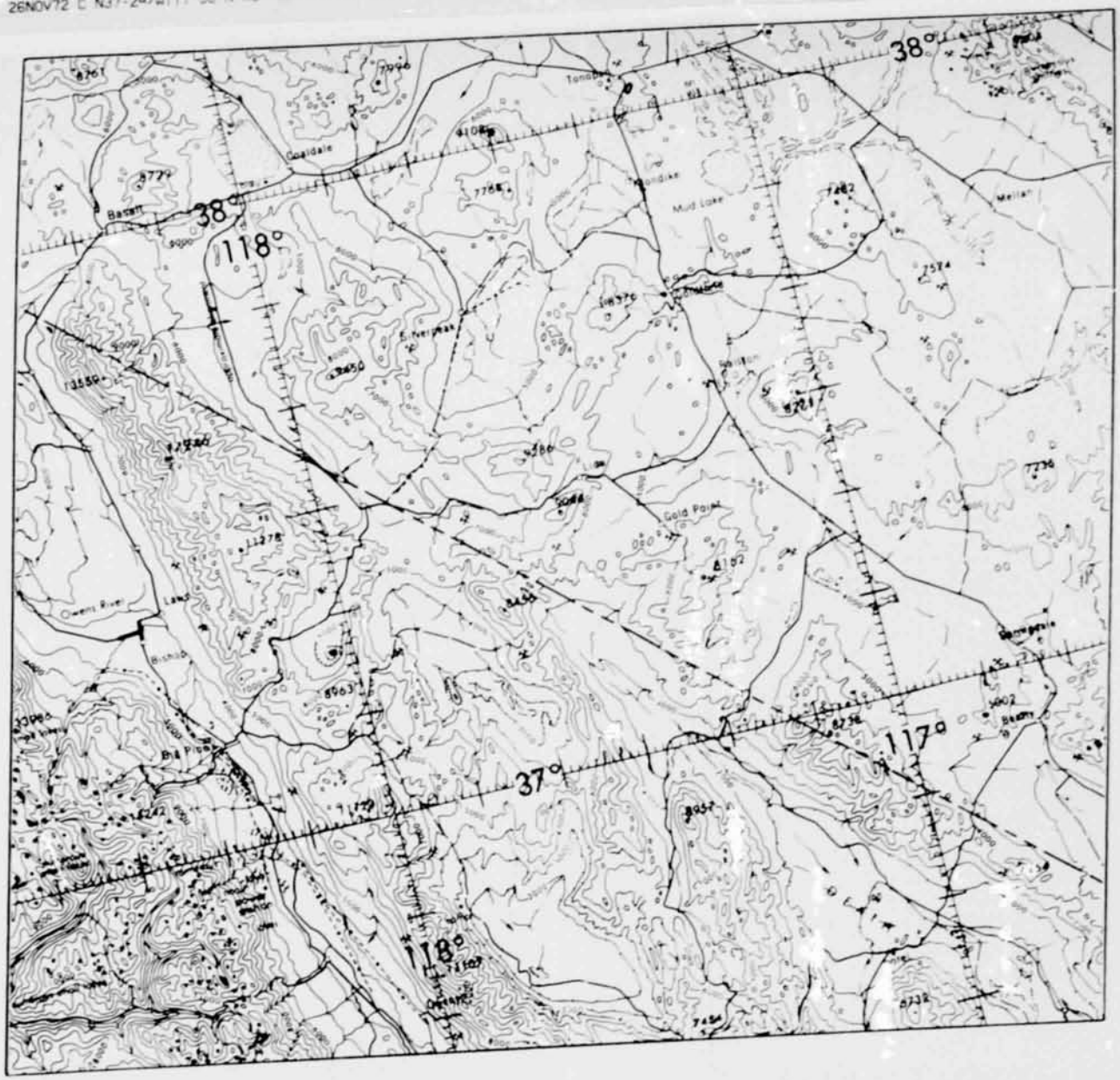

FOLDOUT FRAME

Figure 6:

Goldfield area,
Nevada & California.
ERTS-1 MSS Frame
#1126-18010

Figure 7: Caliente area, Nevada.
ERTS-1 MSS Frame #1106-17492

FOLDOUT FRAME

W115-30|
RENOV72 C N37-18/W114-45 N N37-14/W114-30 MSS

N036-30|

W115-00

W114-30|
D SUN EL32 AZ153 190-1478-G-1-N-D-2L NASA ERTS E-1106-17492-7 |

scale
STATUTE MILES
0 10 20
KILOMETERS

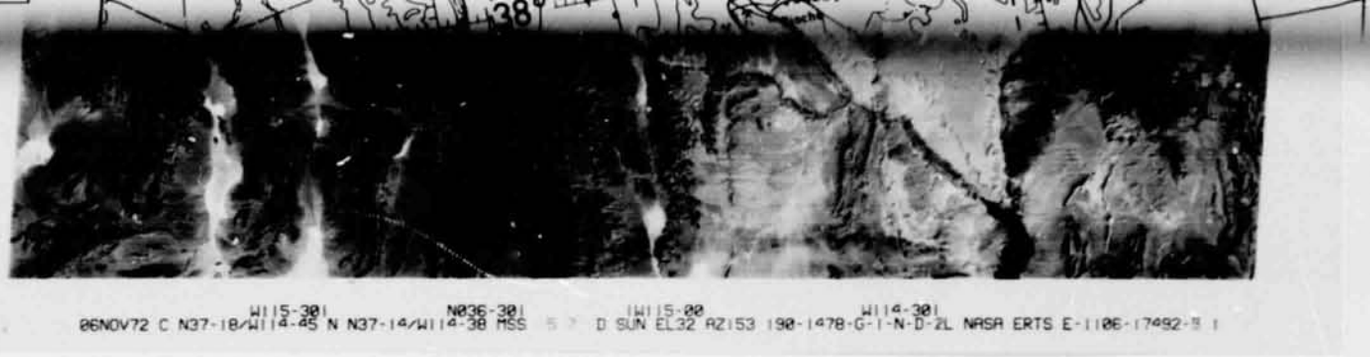

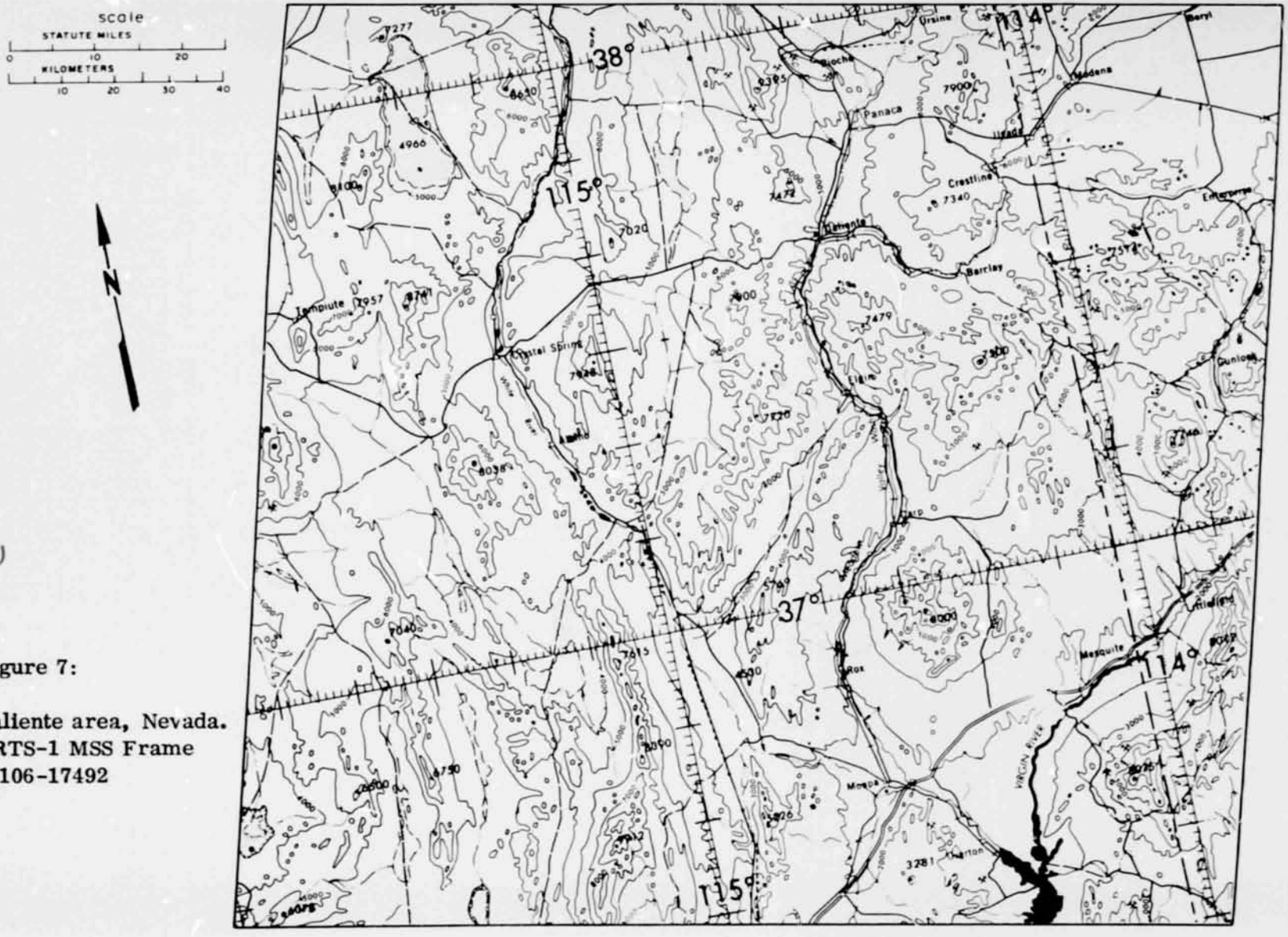

FOLDOUT FRAME 2

Figure 7:

Caliente area, Nevada. ERTS-1 MSS Frame #1106-17492

Figure 8: Cedar City area, Utah & Arizona.
ERTS-1 MSS Frame #1051-17425

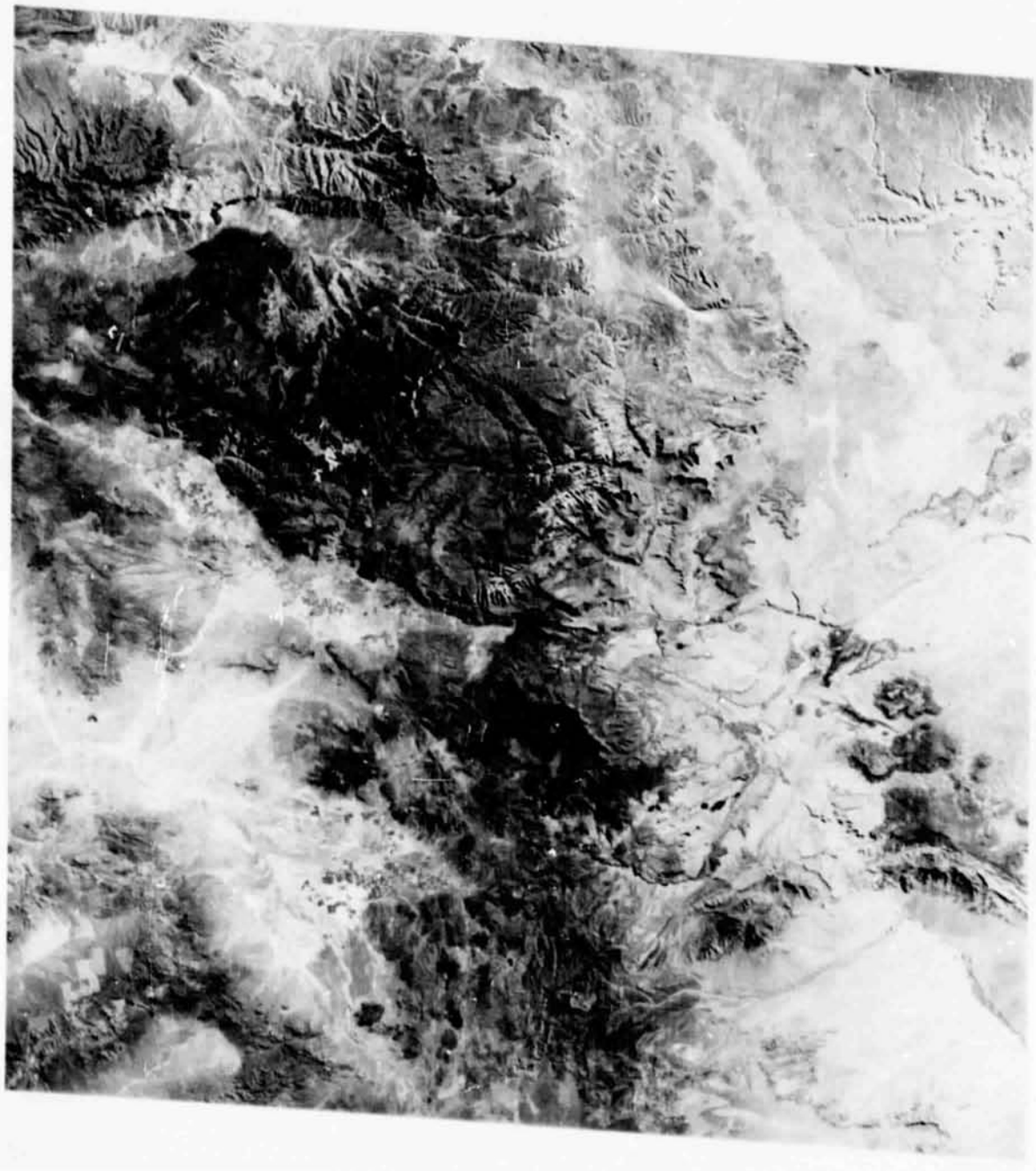

FOLDOUT FRAME

W114-00| W113-30| W113-00| N036-30|
12SEP72 C N37-26/W113-09 N N37-26/W113-03 MSS 5 D SUN EL48 AZ137 190-0711-G-1-N-D-2L NASA ERTS E-1051-17425-5 01

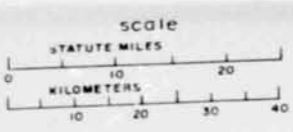

FOLDOUT FRAME

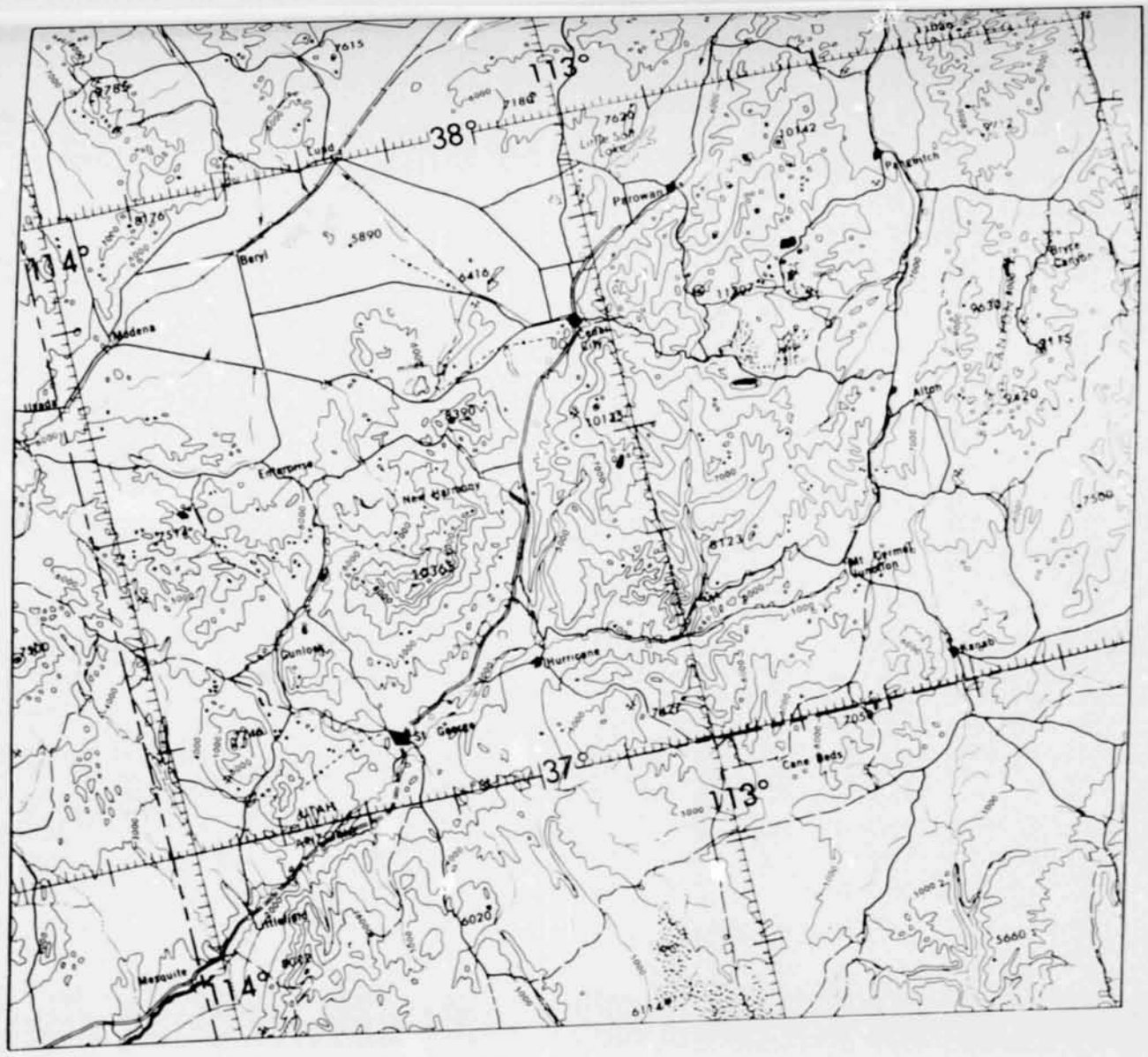

Figure 8:

Cedar City area,
Utah & Arizona.
ERTS-1 MSS Frame
#1051-17425

Figure 9: Grand Canyon area, Arizona.
ERTS-1 MSS Frame #1069-17432

FOLDOUT FRAME

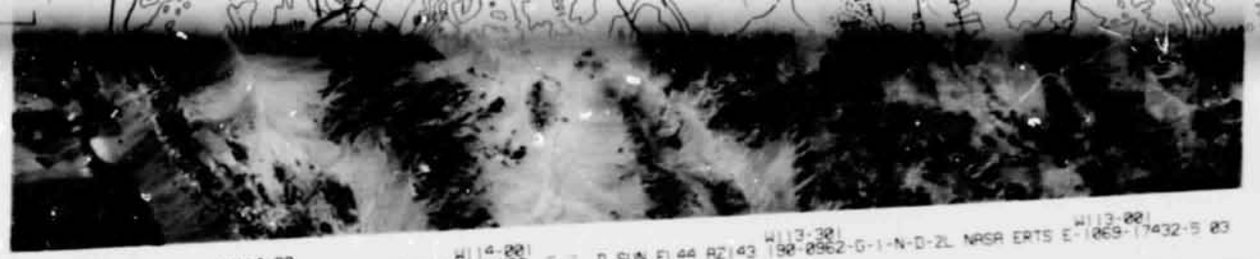

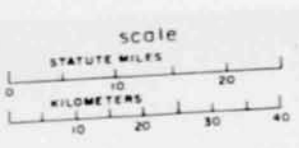

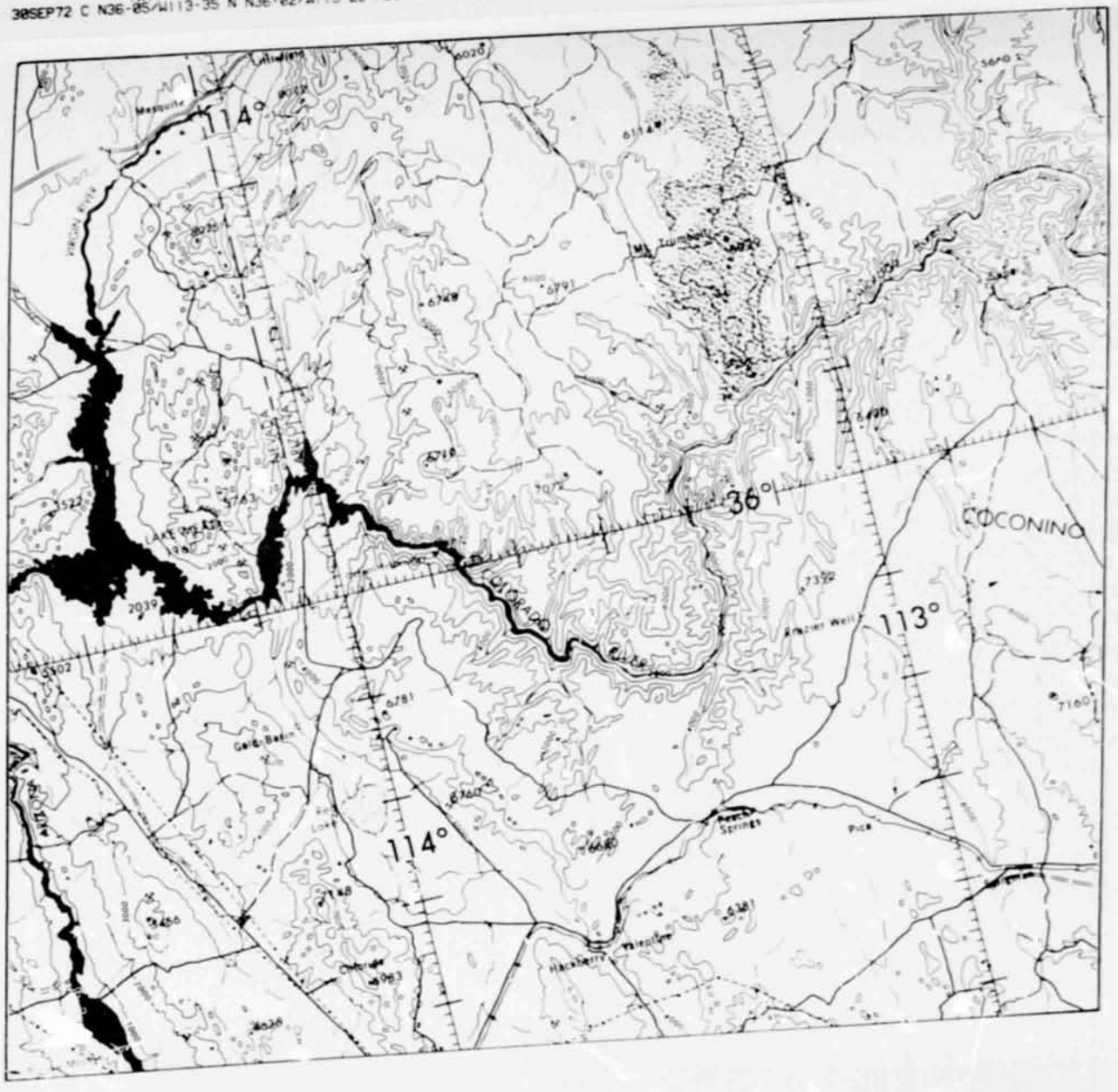

Figure 9:

Grand Canyon area, Arizona.
ERTS-1 MSS Frame #1069-17432

FOLDOUT FRAME 2

Figure 10: Kingman-Needles area, Arizona & California.
ERTS-1 MSS Frame #1051-17434

FOLDOUT FRAME

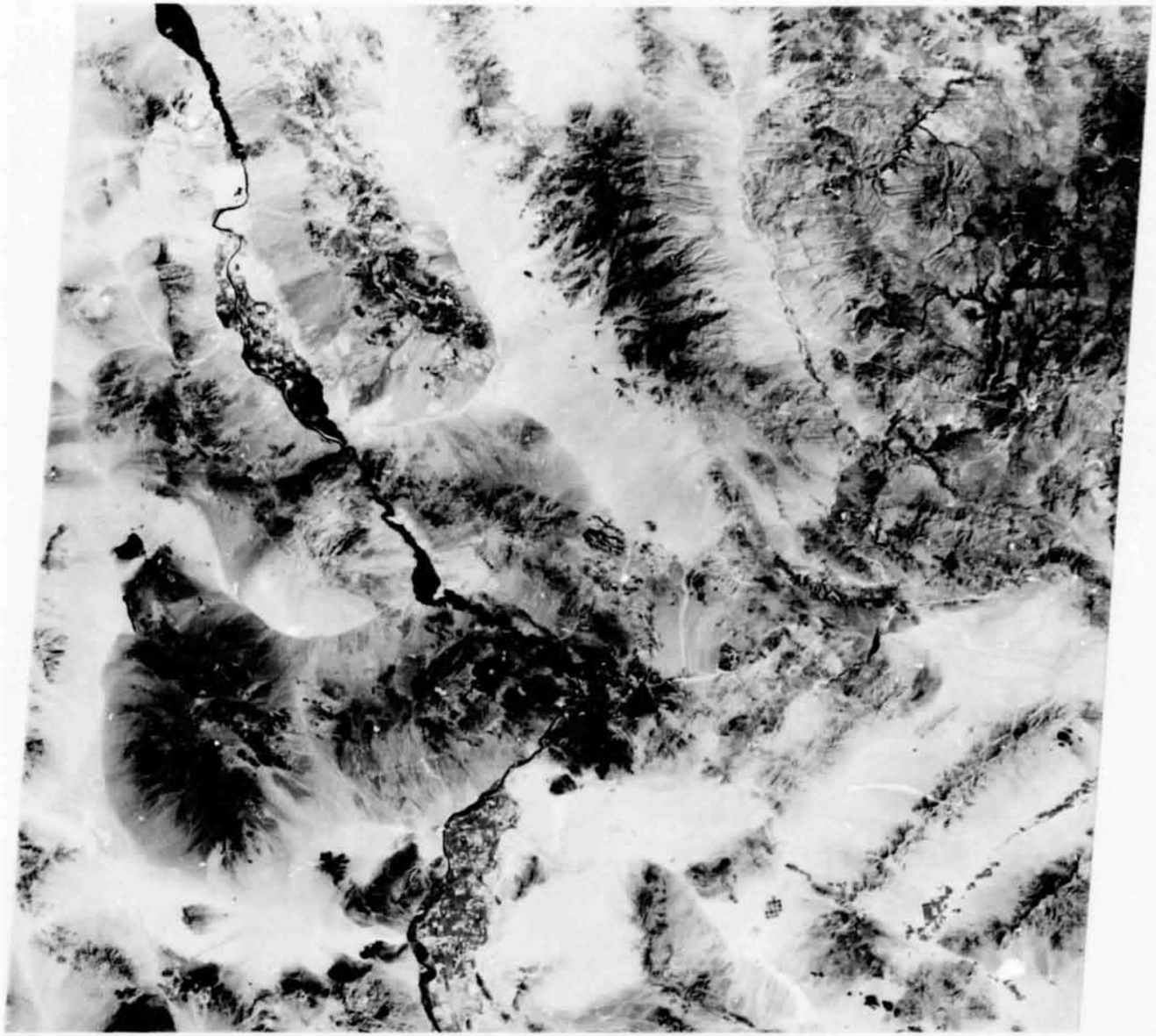

1W115-00 W114-30 W114-00 W113-30
12SEP72 C N34-35/W114-04 N N34-34/W113-58 MSS 5G D SUN EL50 AZ134 190-0711-G-1-N-D-2L NASA ERTS E-1051-17434-R 01

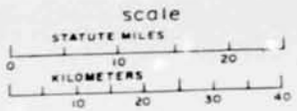

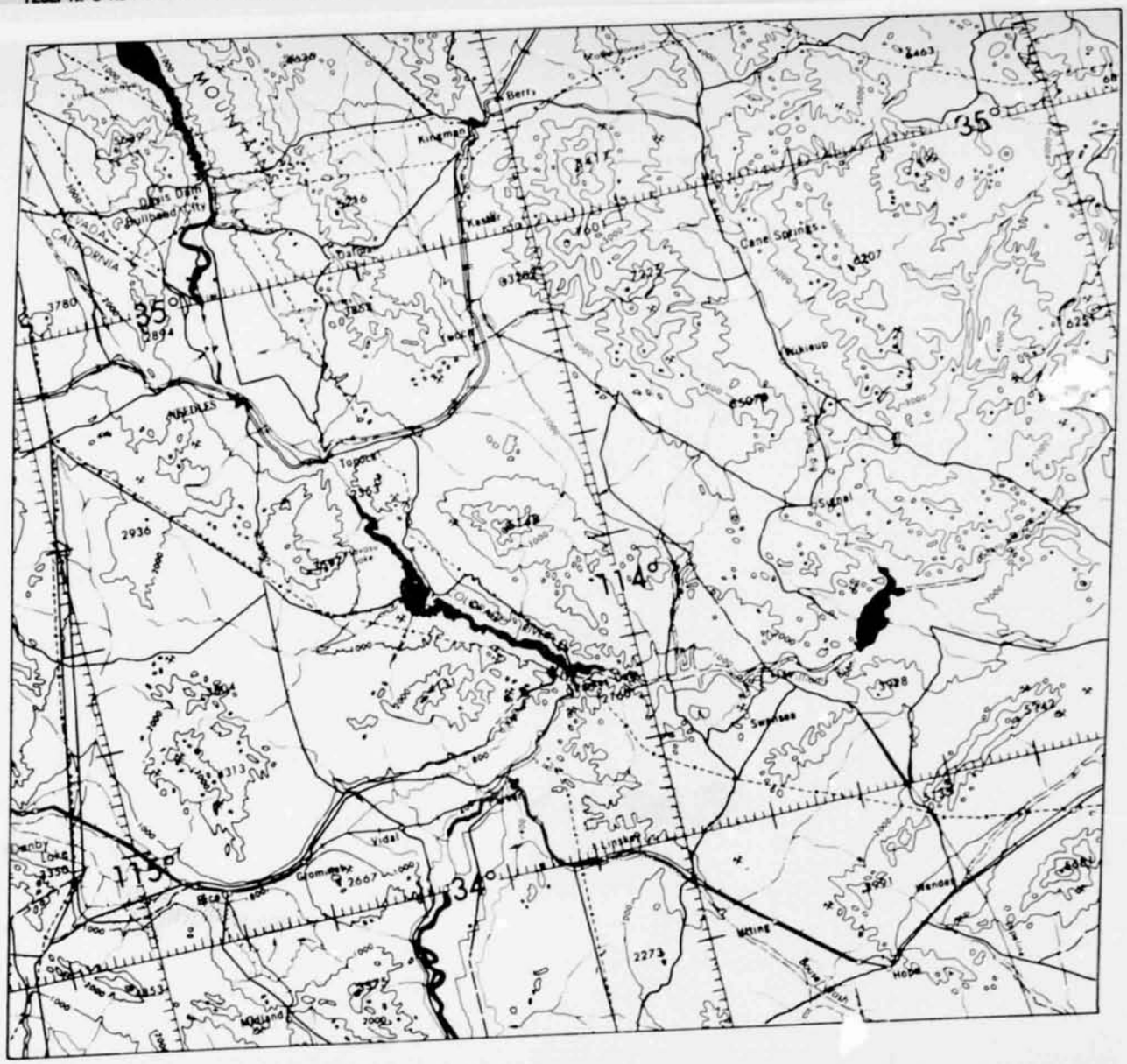

FOLDOUT FRAME 2

Figure 10:

Kingman - Needles area, Arizona & California. ERTS-1 MSS Frame #1051-17434

Figure 11: Barstow area, Mojave Desert, California.
ERTS-1 MSS Frame #1341-17554

FOLDOUT FRAME

29JUN73 C N34-36/W117-12 N N34-36/W117-03 MSS D SUN EL62 AZ108 190-4755-0-1-N-D-2L NASA ERTS E-1341-17554-5

scale
STATUTE MILES
0 10 20

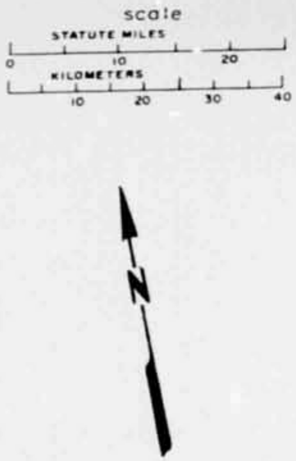

Figure 11:

Barstow area, Mojave Desert, California. ERTS-1 MSS Frame #1341-17554

Figure 12: Death Valley area, California & Nevada.
ERTS-1 MSS Frame #1125-17554

FOLDOUT FRAME

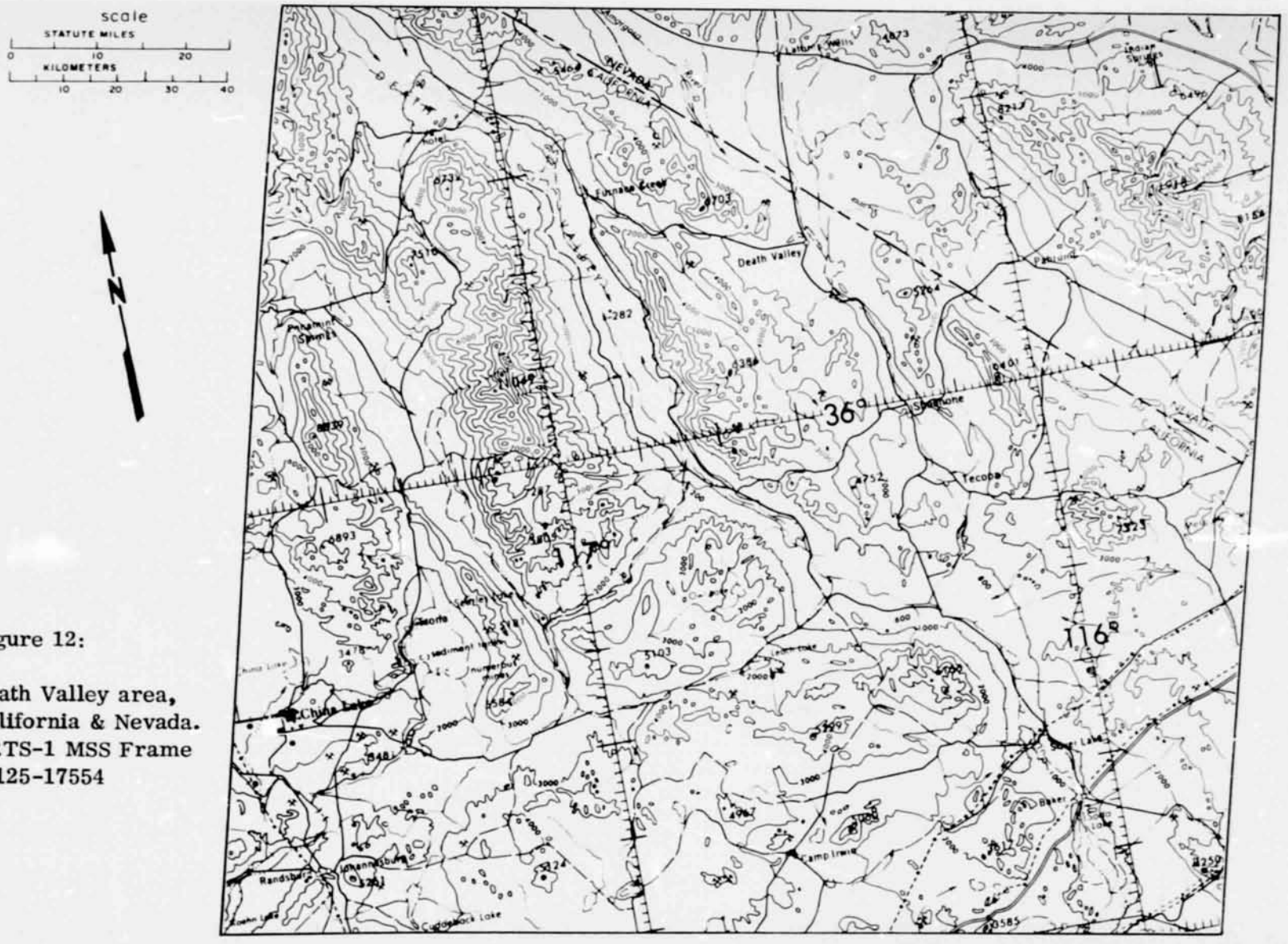

FOLDOUT FRAME 2

Figure 12:

Death Valley area, California & Nevada. ERTS-1 MSS Frame #1125-17554

Figure 13: Owens Lake-Sierra Nevada, California.
ERTS-1 MSS Frame #1162-18011

FOLDOUT FRAME

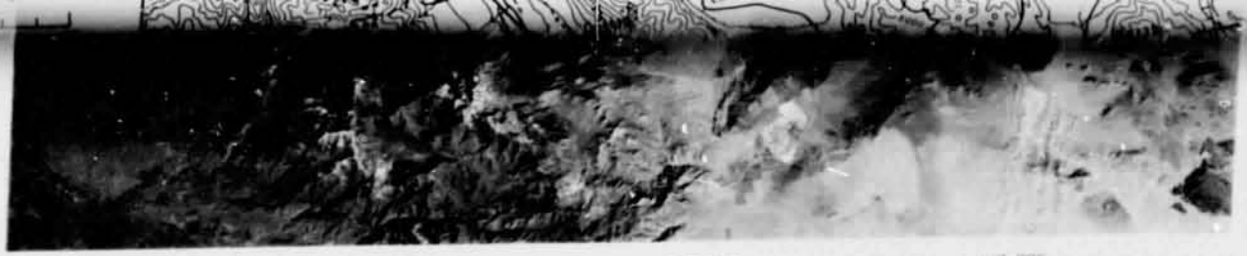

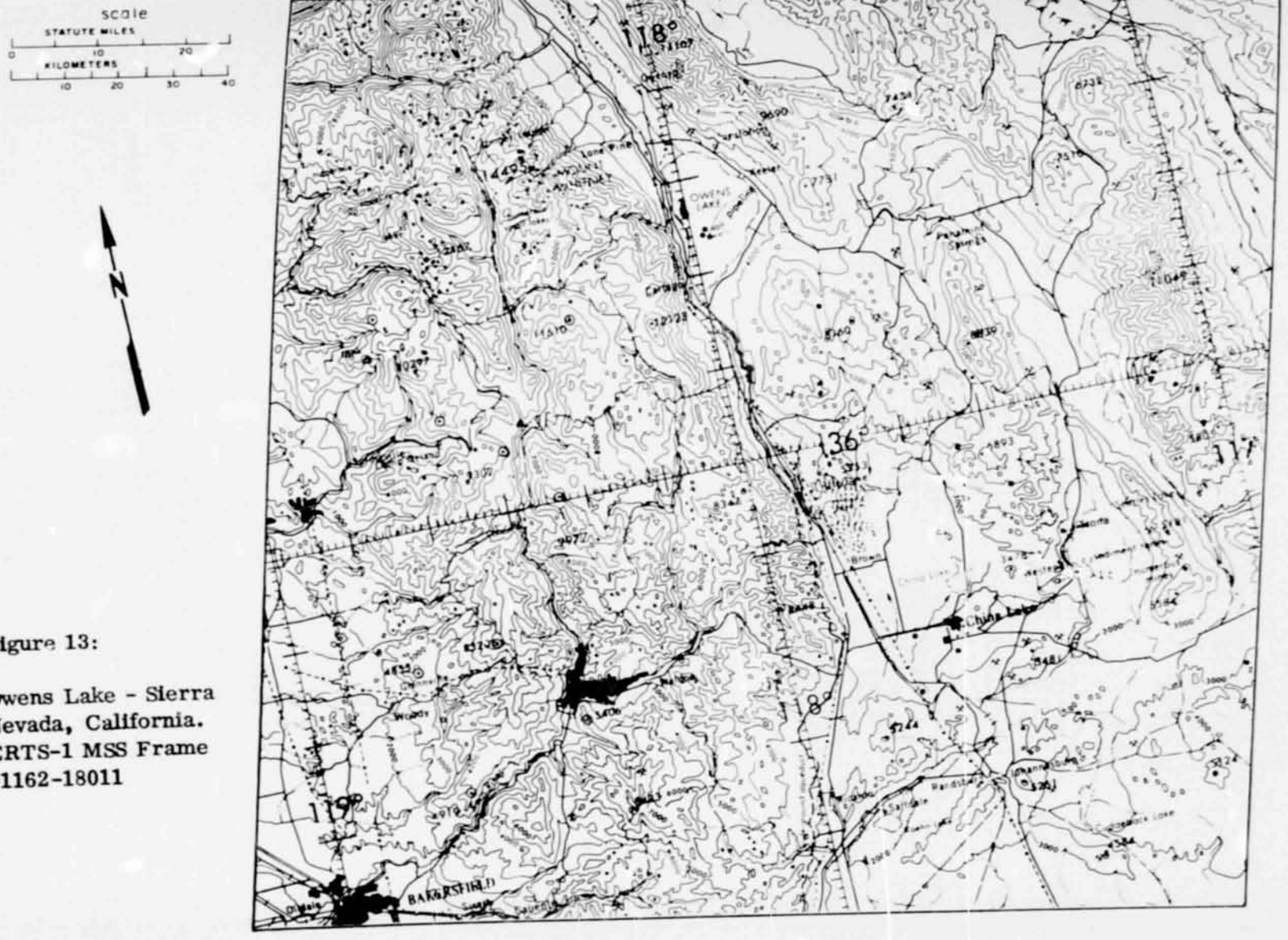

FOLDOUT FRAME 2

Figure 13:

Owens Lake - Sierra Nevada, California. ERTS-1 MSS Frame #1162-18011

Figure 14: Mono Lake-Sierra Nevada, California.
ERTS-1 MSS Frame #1163-18063

FOLDOUT FRAME

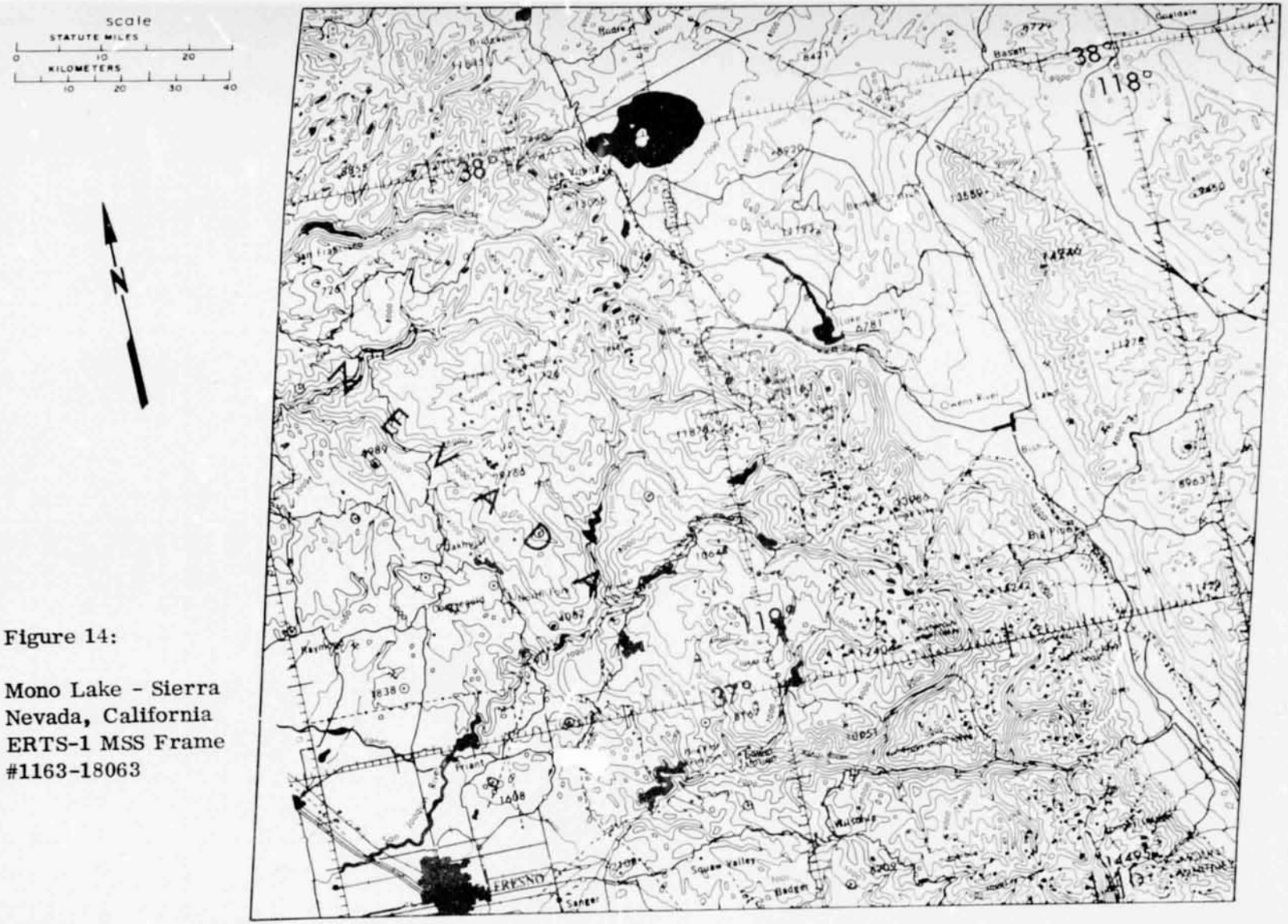

FOLDOUT FRAME 2

Figure 14:

Mono Lake - Sierra Nevada, California ERTS-1 MSS Frame #1163-18063

2.4 IMAGE ENHANCEMENT AND ANALYSIS TECHNIQUES

2.4.1 Introduction:

A variety of image processing, analysis and enhancement techniques has been applied in studying the ERTS-1 MSS imagery and other remote sensing data available over the Argus Exploration Company test site. These techniques include the photographic, photomechanical, optical and digital processing techniques summarized in the following sections.

The significant applications of these techniques are cited below and in the separate studies included in the Appendices to this report. Several of these techniques are standard photographic laboratory procedures which are discussed in detail in most standard photographic manuals. These techniques are reviewed here in order to stress the importance of conventional processing for effective use of ERTS-1 MSS and other imagery. Other enhancement and analysis techniques discussed below are experimental and are described here in the interest of encouraging further research or experimentation in their application.

Much of the black and white photography, photographic reproduction and special processing was performed by Argus Exploration Company personnel. Technical color processing and much of the experimentation on technique development was done in cooperation with:

Mr. Wally MacGalliard
MacGalliard Colorprints
4129 Cahuenga Boulevard
North Hollywood, California 91602

2.4.2 Black and White Photographic Reproduction:

Black and white reproduction of maps, aerial photographs, SLAR and other data has been done for adjustment of image scale and multiple reproduction. Standard copy work has been done in 4 x 5-and 8 x 10-inch formats using Kodak Professional Copy Film and standard enlarging papers. Positive transparencies for SLAR, NIMBUS, and ERTS-1 imagery have been reproduced by enlarging or contact printing on Kodak Professional Copy Film or on orthographic/lithographic films.

Variable contrast films and papers, print toning, and other special printing procedures have been used on a variety of photographic data. Two standard laboratory masking techniques used in printing black and white photographs are "dodging" and "burning". Dodging is used in printing negatives which have areas of low density that would result in an excessively dark positive image. The negative image is projected with an enlarger onto a sheet of photographic paper, and a photographic mask is used to shield the light portions of the image during part of the exposure time. Burning is a similar procedure in which photographic masks are used to extend the exposure time for dark portions of a projected image. These

laboratory procedures have been used in the printing of key ERTS-1 MSS, X-15, and U-2 imagery in which valuable detail would have otherwise been obscured by extreme image contrast.

Sepia color toning of black and white photographic prints has been used in several applications, such as with annotated image overlays. Standard or variable contrast photographic papers are toned by using an additional chemical bath during development. The toning chemicals are available as standard photographic reagents.

2.4.3 Edge Enhancement Processing:

A simple photographic technique known as "edge enhancement" or "line breakdown" has proven useful in pattern analysis of ERTS-1 MSS imagery. The effect of this technique is to reduce density variation in an image, enhancing the "edges" or peripheries of separate image areas having density contrast. In this manner a gradual change from light to dark gray is reduced to a single neutral-gray level; an abrupt contact of light and dark areas is enhanced to a line, separating areas of equal density.

Edge enhancement processing has been used with ERTS-1 MSS imagery to accentuate structural patterns expressed by such features as drainage, topography, or surface texture. An example of edge enhancement processing is shown in Figure 15 for ERTS-1 MSS Frame #1106-17495. Because much of the topographic expression in an image is due to shadowing, the low sun elevations recorded in winter ERTS-1 imagery are particularly useful. Because of its enhancement of spatial information, edge enhancement processing is a valuable tool for use in conjunction with Moiré patterns or Fourier transform analysis, as discussed in following sections.

Edge enhancement processing is performed by using a set of balanced contrast positive and negative transparencies. The transparencies are registered and "sandwiched" together in a prirting frame, using registration techniques such as those discussed by MacGalliard and Liggett (1973*). The "sandwich" is used to expose a high contrast photographic film or paper by contact printing with either perpendicular or oblique illumination. Various parameters can be modified in using this procedure to obtain the desired results. Perfect registration of the "sandwich" is effective for most applications; however, controlled misregistration may be used to enhance or subdue specific directional trends in an image.

A similar analysis technique can be performed digitally, using equipment such as that manufactured by Spatial Data Systems, Inc., Goleta, California, and Interpretation Systems, Inc., Lawrence, Kansas. Digital enhancement techniques have the advantage of real-time variation of image orientation, contrast range, degree of tonal elimination, etc., but they generally have lower resolution than a photographic process.

---

* Appendix J, this report

Figure 15: Black & white edge enhancement print of ERTS-1 MSS Frame #1106-17495. Compare with the false color composite shown in Figure 4.

FOLDOUT FRAME

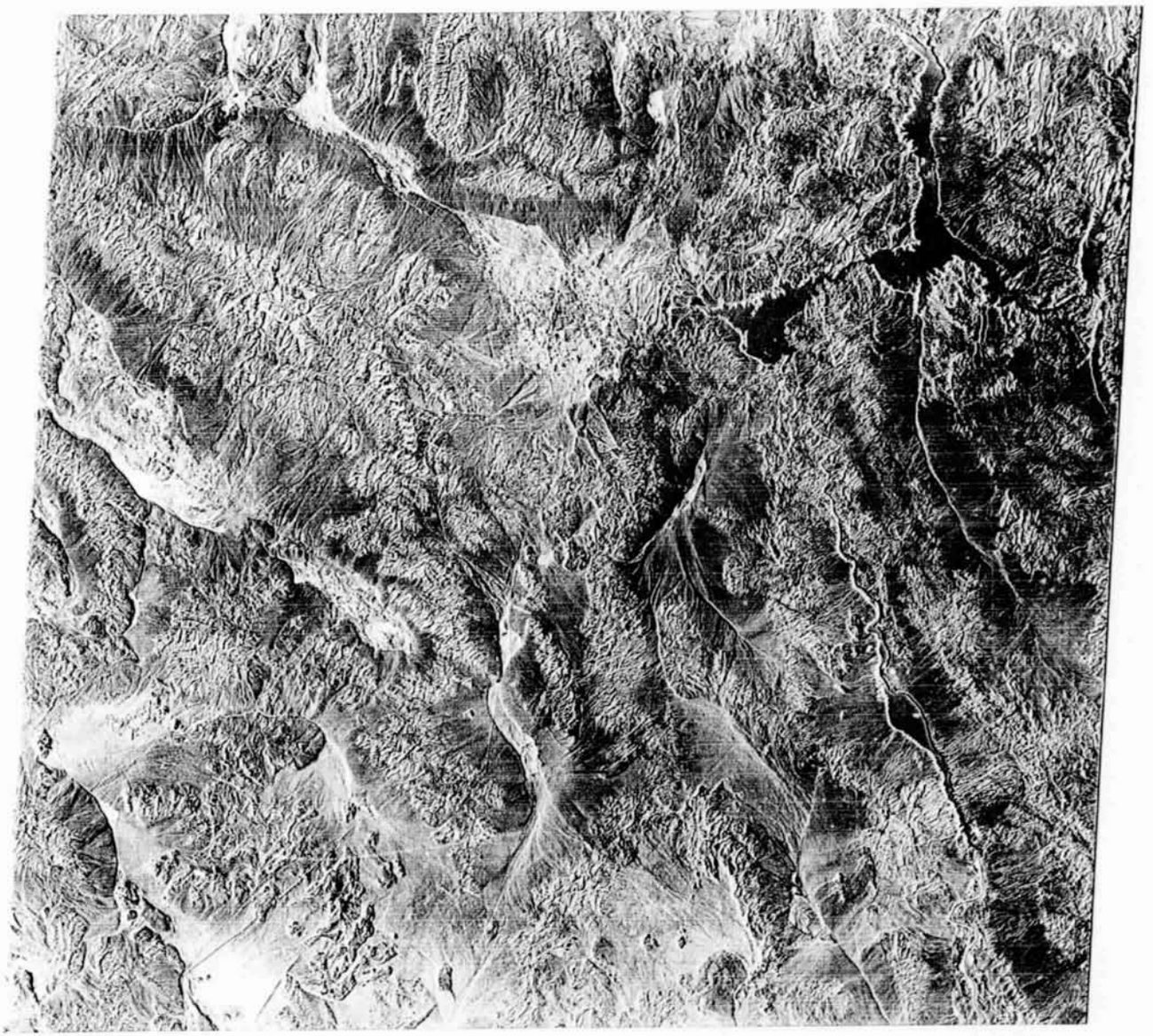

W116-001 W115-301 N035-001 W115-00 W114-301
06NOV72 C N35-52/W115-1? N N35-49/W115-05 MSS 7 D SUN EL33 AZI52 190-1478-G-1-N-D-IL NASA ERTS E-1106-17495-7 1

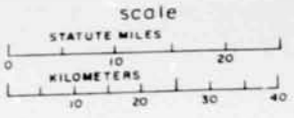

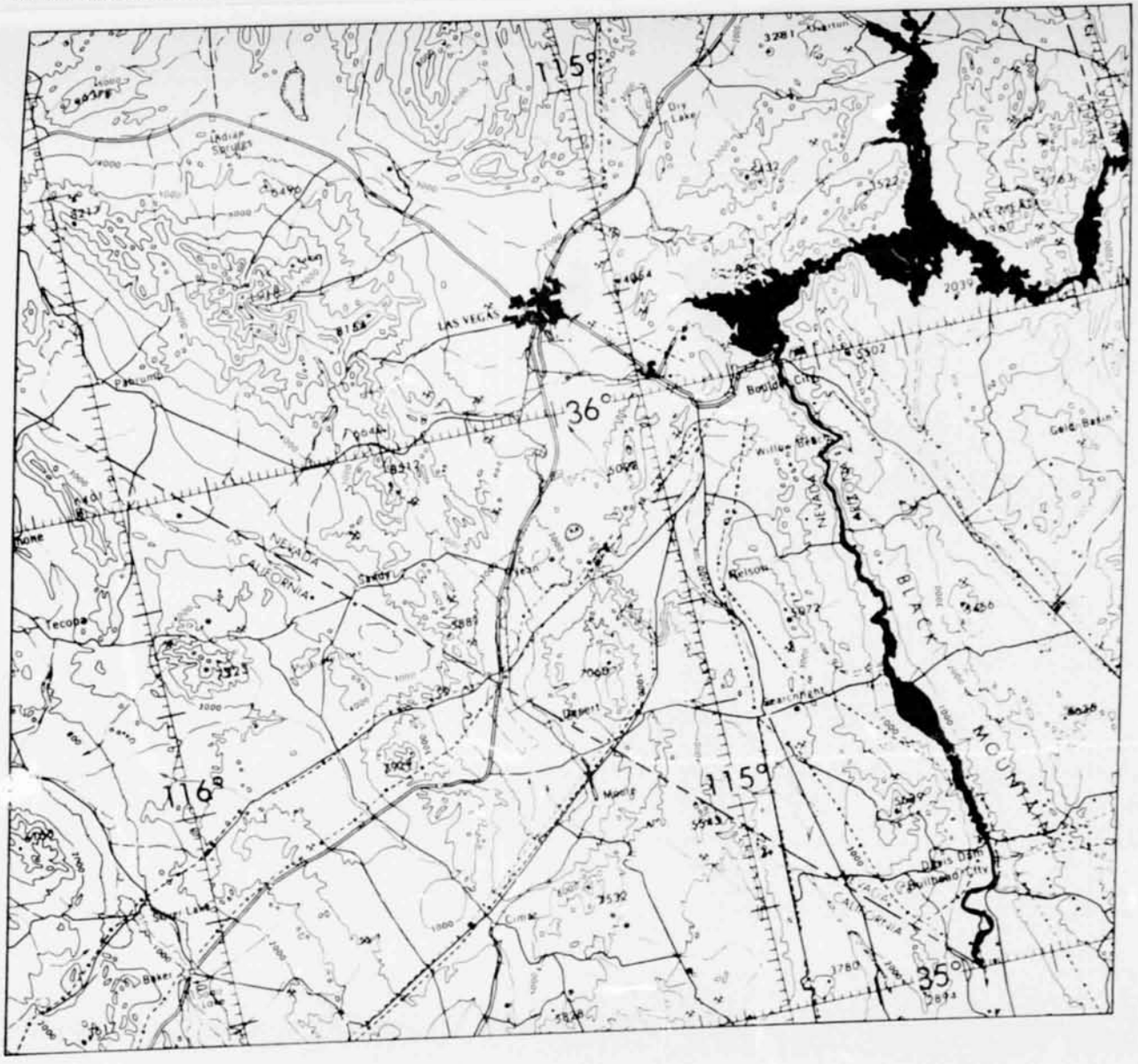

FOLDOUT FRAME 2

Figure 15:

Black & white edge enhancement print. ERTS-1 MSS Frame #1106-17495

2.4.4 Additive Color Viewing:

Additive color viewing of ERTS-1 MSS and other multispectral imagery available over the Argus Exploration Company test site has proven to be a primary tool for image analysis and interpretation. Our work has been performed using a Model-61 multispectral viewer manufactured by Spectral Data Corporation, Long Island, New York. This viewer has four channels, each with independent registration, independent illumination intensity controls, and a filter wheel containing three additive primary color filters and a clear filter. NASA-NDPF positive film chips are used as the data input.

Because of the small size of the viewer screen and the relatively poor image resolution, the most effective use of the viewer has been in determining the optimum MSS band-filter combination and color balance for discrimination of specific geologic features. This choice of color balance can then be used to guide production of high resolution color composite photographs, using the techniques discussed in Sections 2.4.5 and 2.4.6 below. The coordinated use of additive color viewing and laboratory processing has proven valuable for effective use of multispectral imagery.

Experiments have been conducted with additive color viewing of multiseasonal ERTS-1 MSS imagery recorded over the test site. This work has been facilitated by independent scale adjustment on the four viewer channels. However, the use of an additive color viewer for interpretation of multiseasonal imagery is complicated by variables such as cloud cover, instrument noise, and variation in illumination angle. False-color compositing of multipolarization SLAR imagery (NASA Mission 103) has resulted in recognition of surface anomalies caused by differences in polarization of the reflected radar signals.

2.4.5 High Resolution False-Color Compositing:

High resolution false-color photographic composites of the ERTS-1 MSS imagery have been used as the primary tool for detailed laboratory analysis and field study in this investigation. The choice of optimum MSS band-filter combinations and color balance has been guided by additive color viewing of the primary multispectral data.

Composite imagery was initially produced by photographing the screen of an additive color multispectral viewer. This technique is outlined in the Argus Exploration Company Type II report of 19 January 1973. Excellent duplication of color balance has been achieved by this method, although the resolution is less than that of black and white prints of single MSS bands.

An operational technique for producing high resolution, false-color composites of ERTS-1 MSS imagery has been developed for use in a standard photographic laboratory equipped for color processing and printing. The procedures are out-

lined in detail by MacGalliard and Liggett (1973*). The positive transparencies of ERTS-1 MSS bands are manually registered and punched for accurate locking in a printing frame. An internegative film is sequentially exposed by each of the MSS bands with an appropriate color filter. Both illumination intensity and exposure time may be varied for each band to control final color balance. Once a suitable internegative is produced, contact prints or enlargements can be made using standard Kodak Ektacolor papers and chemicals. For detailed analysis, enlargements up to 30 x 30 inches have been made with excellent resolution and color reproduction. This compositing technique uses standard NASA-NDPF or EROS 70-mm or 9 x 9-inch positive transparencies and is adaptable to data from a variety of multispectral imaging systems, including multiseasonal and multipolarization data.

Examples of ERTS-1 MSS composites produced using this technique appear in Section 2.3 of this report.

2.4.6 Dye Transfer Color Compositing:

Limited experimentation has been done on production of color composites using the dye transfer printing technique. This technique is a three-color process in which yellow, magenta and cyan dye images are superimposed on a paper or film printing medium. A separate preregistered dye transfer mat is used for each of the three dye images. These transfer mats are made photographically from the MSS bands by contact printing of the NASA 9 x 9-inch positive transparencies. Dye transfer prints have high resolution and excellent color range, often superior to that attained with photographic papers or films. In addition, dye transfer printing is well suited for a variety of enhancement techniques, such as photographic density slicing or variable contrast color printing. For most normal uses, however, dye transfer printing is relatively expensive and has therefore not proven economical for operational reproduction requirements.

2.4.7 Spectral Ratioing:

A photomechanical technique has been developed for ratioing pairs of ERTS-1 MSS bands and compiling the band ratios into false-color composite images. The technique results in enhancement of subtle spectral differences in the ERTS-1 MSS imagery and has proven effective in geologic analysis and interpretation.

The spectral ratio images are produced using standard NASA-NDPF 9 x 9-inch positive transparencies. Because emulsion density is proportional to the logarithm of scene brightness, the subtraction of one emulsion density from another approximates a mathematical ratio of the two brightness values. This is done by producing a set of positive and negative ERTS-1 MSS transparencies which have

---

* Appendix J, this report

matching density ranges (D log E curves). A registered "sandwich" is then assembled which consists of a positive transparency of one MSS band and a negative transparency of a second. This sandwich is used to expose a high-gamma film transparency to produce a black and white ratio image.

For example, a sandwich consisting of a negative MSS band #7 transparency and a positive MSS band #5 transparency is used to produce a positive image designated as R7/5. Three sets of these individual black and white ratio images can be combined to make a false-color composite using the technique outlined by MacGalliard and Liggett (1973*). The false-color spectral ratio image shown in Figure 16 was produced using the following ratio combinations and printing filters:

Ratio	Printing Filter
R7/5	Red
R5/4	Green
R4/7	Blue

Where the ratio R7/5 is greater than 1.0, the composite image is bright red; where it is less than 1.0, the image is cyan or various shades of blue or green, depending on the other two image ratios. The color coding of the spectral ratio print shown in Figure 16 is similar, although greatly enhanced over that of the conventional false-color composite shown in Figure 4. Preliminary results using this technique show promise in facilitating the use of ERTS-1 MSS imagery for discrimination of rock and soil types and for analysis of vegetation distribution and variation. Examples of applications are summarized in Section 4.0 of this report.

The principles and applications of digital computer spectral ratioing of ERTS-1 MSS data are outlined by Billingsley and Goetz (1973), Billingsley and others (1970), and Vincent (1973).

2.4.8 Moiré Pattern Analysis:

A Moiré pattern is the figure produced by superposition of two or more repetitive geometric patterns, such as ruled-line gratings or dot patterns. This phenomenon can be used as a tool for measuring the orientation of pervasive linear patterns expressed in ERTS-1 MSS imagery by topography and shadowing. Linear topographic patterns can be expressions of such structural features as fault systems, joint patterns, metamorphic and igneous foliation, dike swarms, and sedimentary or other compositional layering.

In this investigation Moiré patterns have been generated using a black-lined grating on an 8-1/2 x 11-inch clear acetate base, which can be overlain on the 9 x 9-inch

---

* Appendix J, this report

Figure 16: False color spectral ratio image. ERTS-1 MSS Frame #1106-17495.

FOLDOUT FRAME

W116-00| W115-30| N035-00| W115-00 W114-30|
06NOV72 C N35-52/W115-12 N N35-49/W115-05 MSS 5 7 D SUN EL33 AZ152 190-1478-G-1-N-D-2L NASA ERTS E-1186-17495-5

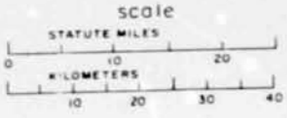

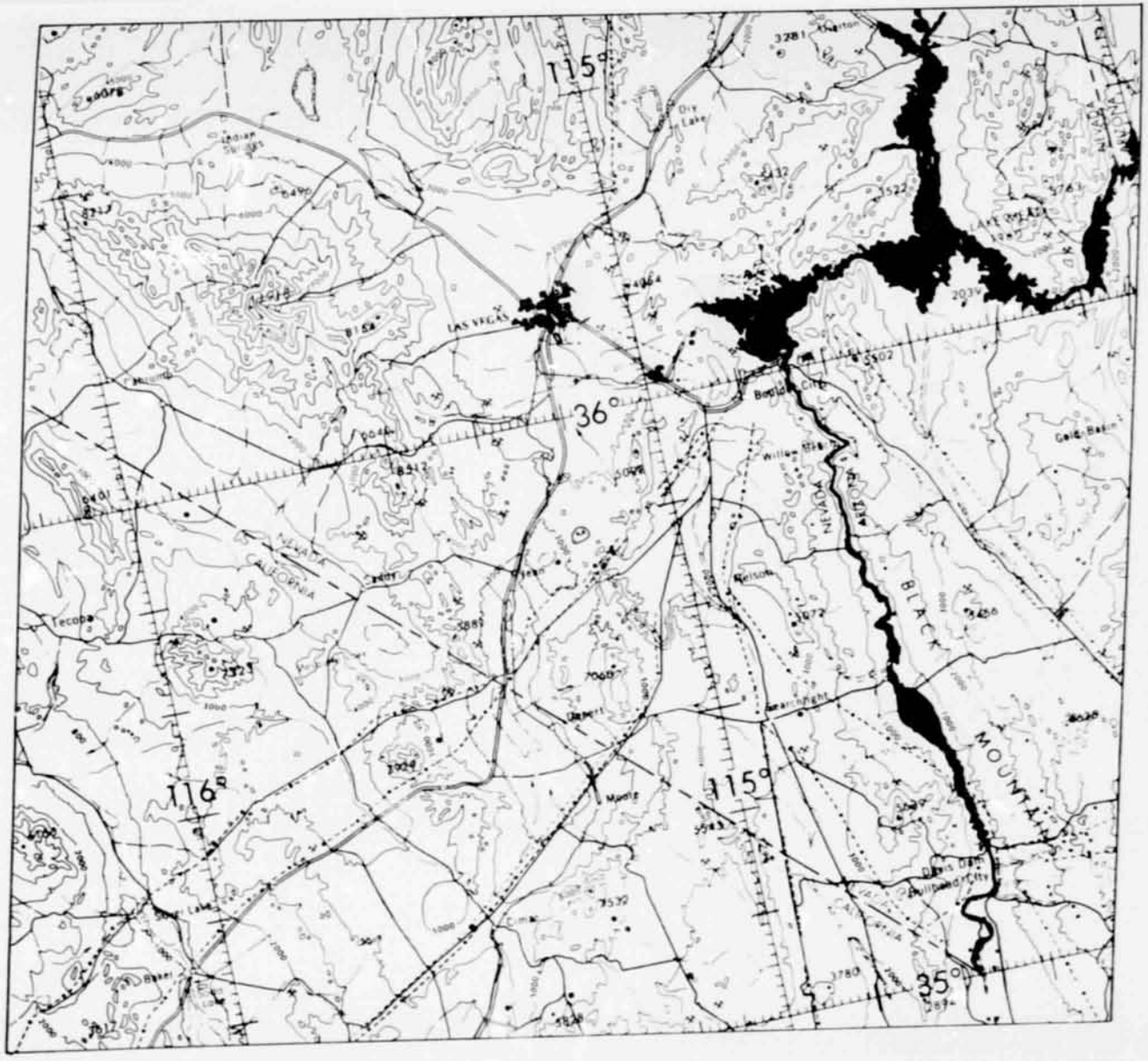

FOLDOUT FRAME 2

Figure 16:

False color spectral ratio image. ERTS-1 MSS Frame #1106-17495

ERTS-1 MSS prints. Gratings of various line spacing have been tried, but the best results have been obtained using a grating with a line spacing of approximately 10 lines/cm (27 lines/in.). The line widths and the spacings between lines are approximately 0.6 mm and 0.4 mm, respectively. This particular grating is available through Edmund Scientific Company, Barrington, New Jersey (stock no. 60534, Pattern 2).

The grating is used by holding it above the image within the near-field focus of the eyes. The optimum distance above the image varies with the spacing and size of linear elements in the image and should thus be determined experimentally. The grating is rotated slowly until an enhanced directional trend is recognized. Gratings can be mounted on a simple goniometer for precise measurements of directional trends.

Moiré patterns may also be generated using black and white or false-color images projected on the screen of a multispectral viewer. The technique has been found to be particularly effective when used with edge enhancement prints, as outlined in Section 2.4.3. Other applications of Moiré patterns for measurement of linear directional trends on lunar and terrestrial photography are discussed by Cummings and Pohn (1966).

2.4.9 Optical Fourier Transform Analysis:

A preliminary study was made of the use of optical Fourier transforms for structural analysis of ERTS-1 MSS imagery. A Fourier transform is produced as a diffraction pattern by illumination of an image transparency with a collimated laser beam. Fourier transforms may be used for precise measurement of the directional orientations and spatial frequencies of linear image elements. Geologic applications of the techniques have been discussed by Dobrin (1968), Pincus and Dobrin (1966) and Nyberg and others (1971).

Fourier transform analysis of satellite imagery shows promise in the quantitative study of linear patterns controlled by a variety of geologic features. Examples include faults, folds, dike swarms and joint patterns, which are often expressed as linear topographic alignments, such as ridges, valleys, or local drainage patterns. Fourier transforms can be used for pattern analysis of an entire image or of separate domains within an image, thereby providing a measure of pattern variation by subarea.

A problem apparent in the application of this technique to ERTS-1 MSS imagery is the dominant expression of scan lines and resolution elements in the Fourier transform, which mask more subtle image elements. Preliminary discussions and experimentation were conducted with the support of:

Recognition Systems, Inc.
15531 Cabrito Road
Van Nuys, California 91406

and

Thomas Doe
Department of Geology and Geophysics
University of Wisconsin
Madison, Wisconsin 53706

2.4.10 Pseudo-Relief Enhancement:

A planoconvex Fresnel lens has been used experimentally for pseudo-relief enhancement of false-color ERTS-1 MSS imagery. The three-dimensional perception is due in part to chromatic aberration of the lens, which causes separation of focal planes for different colors in the imagery. Because focal length is inversely proportional to wavelength, red areas appear raised above yellow; yellow above green; and green above blue areas. Magnification by the lens may have an additional psychological effect on perception.

The best results have been obtained by viewing false-color composites on the projection screen of an additive color viewer. The projection screen is viewed from a distance of approximately 25-50 cm with the Fresnel lens held 5-15 cm from the screen. A similar pseudo-relief effect has been described by McIlroy and Vaughan (1970) using a more complex optical system for viewing small color transparencies. A similar effect can be achieved by viewing a pair of identical ERTS-1 images with a standard stereoscopic viewer.

A variety of inexpensive plastic Fresnel lenses is available through Edmund Scientific Company, Barrington, New Jersey. The lens used in our experimentation is a 28 cm square Fresnel lens with a focal length of approximately 40 cm (16 inches), Stock No. 70533. The experimental application of a Fresnel lens for pseudo-relief enhancement is described in an abstract by Bechtold and others (1973*).

---

* Appendix C, this report

2.4.11 References Cited in Text:

Bechtold, I.C., Liggett, M.A., and Childs, J.F., January 1973, Pseudo-relief enhancement of color imagery (abs.): NASA Rept. Inv., NASA-CR-129969, E73-10028, 1 p.

Billingsley, F.C., Goetz, A.F.H., and Lindsley, J.N., 1970, Color differentiation by computer image processing: Photographic Sci. and Engineering, v. 14, no. 1, p. 28-35.

Billingsley, F.C., and Goetz, A.F.H., 1973. Computer techniques used for some enhancements of ERTS images, in Freden, S.C., Mercanti, E.P., and Becker, M.A., eds., Symposium on significant results obtained from the Earth Resources Technology Satellite-1: New Carrollton, Maryland, v. 1, sect. B., paper I 9, NASA-SP-327, E73-10824, p. 1159-1168.

Cummings, David, and Pohn, H.A., 1966, Application of Moiré patterns to lunar mapping, in Astrogeologic studies, Annual Progress Report 1965-66, part A (lunar and planetary investigation): U.S. Geol. Survey, p. 183-187.

Dobrin, M.B., 1968, Optical processing in the earth sciences: Inst. Electrical and Electronic Engineers Spectrum, v. 5, no. 9, p. 59-66.

MacGalliard, Wally, and Liggett, M.A., November 1973, False-color compositing of ERTS-1 MSS imagery: NASA Rept. Inv., NASA-CR-135859, E74-10018, 5 p.

McLeroy, D.F., and Vaughan, O.H., Jr., 1970, Enhancement and application of space photographs for earth resources studies with special emphasis on regional geologic investigations: NASA-ASEE Summer Faculty Fellowship, Marshall Space Flight Center, Grant No. NGT-01-003-45.

Nyberg, Sten, Orhaug, Torleiv, and Svensson, Harald, 1971, Optical processing for pattern properties: Photogrammetric Engineering, v. 37, p. 547-554.

Pincus, H.J., and Dobrin, M.B., 1966, Optical processing of geological data: Jour. Geophys. Res., v. 71, no. 20, p. 4861-4870.

Vincent, R.K., March 1973, Ratio maps of iron ore deposits, Atlantic City District, Wyoming, in Freden S.C., Mercanti, E.P., and Becker, M.A., eds., Symposium on significant results obtained from the Earth Resources Technology Satellite-1: New Carrollton, Maryland, v. 1, sect. A, paper G16, NASA-SP-327, E73-10824, p. 379-386.

2.5 EVALUATION OF REMOTE SENSING DATA

2.5.1 Introduction:

This report section constitutes a brief review of the formats, spectral ranges, scales, resolutions and applications of subsidiary remote sensing data used in this investigation. The evaluation of these techniques is based on field investigations of geologic and structural problems in varied topographic and climatic terranes within the Argus Exploration Company test site.

The broad spectral range of the imaging systems discussed here has been advantageous in studying the distributions of vegetation, soil and rock types, and water bodies. However, in applications to the study of regional geology and tectonics, the most important variation between sensors has been the scale of the imagery produced. The imagery can be broadly grouped into two categories: small-scale imagery, which provides a synoptic view of terrane; and large-scale imagery, which provides resolution of detail in small areas. Data from both categories have proven valuable in reconnaissance studies in which regional interpretations have been based on geologic or structural detail in key local areas. The ERTS-1 MSS imagery has provided an effective combination of both scale and resolution.

The sources of subsidiary remote sensing data used in this investigation are listed in Appendix P of this report.

2.5.2 DAPP Satellite Imagery:

The DAPP (Data Acquisition and Processing Program) satellite is an operational weather satellite operated by the United States Air Force. Imagery from this satellite system is archived by the Space Science and Engineering Center at the University of Wisconsin. The two scanner systems on the DAPP satellite record imagery in spectral bands of 0.4 to 1.1 microns and 8.0 to 13.0 microns with resolutions of approximately 0.5 km and 3 km respectively. The images are recorded as continuous strips having fields of view approximately 2,400 km across.

A visible near-infrared DAPP image (0.4 to 1.1 microns) recorded on 18 June 1973, has proven extremely useful in studying the subcontinental tectonic setting of the test site. The lower resolution of the thermal infrared DAPP imagery (8.0 to 13.0 microns) have proven less useful, and no significant geologic or structural features have been recognized in the thermal infrared data.

2.5.3 NIMBUS-1 ATS Imagery:

A limited amount of synoptic imagery over the Argus Exploration Company test site was recorded by the NIMBUS-1 weather satellite in September 1964. This imagery was recorded by the Advanced Vidicon Camera System (AVCS) which has a spectral range of 0.45 to 0.65 micron. The images have a field of view approximately 700 km across. The NIMBUS-1 data used in this investigation was obtained from the

NIMBUS ATS Data Utilization Center (NADUC), Goddard Space Flight Center, Greenbelt, Maryland.

The NIMBUS-1 data provided the first vertical looking spacecraft imagery available over portions of the test site prior to the launch of the ERTS-1 satellite. Although used extensively for studying regional structural patterns in the test site, the initial value of the NIMBUS-1 data was largely superseded by the availability of DAPP and ERTS-1 MSS imagery.

2.5.4 Apollo-9 Photography:

Oblique color Ektachrome photographs from the Apollo-9 spacecraft (Frames AS9-20-3134, 3135, and 3136) were recorded over parts of the Argus Exploration Company test site in March 1969 using a hand-held Hasselblad 70-mm camera. These photographs have been used in the form of color enlargements which were produced from transparencies provided by the NASA Johnson Space Center, Houston, Texas. The color enlargements were printed using controlled exposure and color balance for enhancement of geologic detail.

Because of the oblique-look angle of the Apollo-9 photographs, scale and resolution vary from the far to near portions of the scenes. At middle range, however, the scale and effective resolution of the photographs are comparable to those of the ERTS-1 MSS imagery. Apollo-9 photography was the first synoptic imagery available over much of the test site and formed the basis for the first four months of this investigation. The natural color of the Apollo-9 photographs has complemented analysis and interpretation of the ERTS-1 MSS false-color imagery. An example of the Apollo-9 photography is shown in Figure 3, Section 2.3 of this report.

The geometric distortion of the Apollo-9 photographs can be largely compensated by transferring image anomalies to base maps. In several instances, however, this distortion has led to false interpretation of terrane alignments. In a study of the New York and Eldorado Mountains of eastern California and southern Nevada, Barth (1974*) has shown that a lineament expressed in an Apollo-9 photograph was largely caused by fortuitous alignment of terrane features, low elevation solar illumination, and the extreme oblique-look angle of the photograph.

2.5.5 SLAR Imagery:

Side Looking Aerial Radar (SLAR) imagery over a portion of the Argus Exploration Company test site was flown by NASA in October and November of 1965, using the Westinghouse APQ-97, K-Band (0.86 cm) radar system. The imagery was flown as part of the NASA Earth Observation Aircraft Program operated by the Johnson Space Center, Houston, Texas. The SLAR imagery used in this investigation in-

---

* Appendix N, this report

cludes all or part of NASA Missions 97, 99 to 101, 103 and 104. A detailed list of these missions is presented in Appendix P of this report.

The primary value of SLAR is the ability to image topographic and textural patterns using radar illumination of various look directions. Such radar images are completely independent of solar illumination. Like U-2 photography (Section 2.5.7) SLAR has proven of value in structural interpretation at a scale intermediate between ERTS-1 and ground based reconnaissance. Enhancement of subtle structure is frequently superior to that achieved in U-2 imagery, and SLAR is not degraded by the presence of haze, fog or clouds. The SLAR imagery has provided detailed structural information in areas that are otherwise obscurred by shadowing of solar illumination. Although the orientation of structural trends may be biased by SLAR look directions, structural anomalies are easily cross checked in other imagery or by field reconnaissance. Analysis of the APQ-97 SLAR data has included false-color compositing of the cross-polarized images.

The ability to recognize structural features in SLAR (NASA Mission 100) that are not apparent in U-2 or low altitude aerial photographs has been demonstrated in the Long Valley-Mono Craters area of California (Bailey, written communication, 1972). SLAR (NASA Mission 103) has also been used effectively in supplementing interpretation of ERTS-1 imagery in a structurally complex area north of Lake Mead, Nevada, which includes the probable eastward termination of the Las Vegas shear zone (Liggett and Childs, March 1974*).

2.5.6 X-15 Photography:

Portions of the test site are covered by photographs recorded from the experimental USAF-NASA X-15 spacecraft. Most of the X-15 data used in this investigation are 5-inch panchromatic black and white photographs recorded on 9 October 1962 (NASA Flight No. 2-30-51). A limited quantity of near-infrared color imagery has also been available. These photographs were recorded using a Hycon HR-236 camera at altitudes up to approximately 40 km. Because of highly oblique look directions, the scales of the photographs are variable from the near to far portions of the scenes. Most of the X-15 photographs used in this investigation have a near field of view approximately 80 km across.

The X-15 photographs provide a synoptic scale intermediate between ERTS-1 MSS imagery and U-2 aircraft photography, and they have been used in several areas of interest where U-2 photographs were unavailable. X-15 photography along the California-Nevada border has complemented U-2 and ERTS-1 imagery analysis and supported field reconnaissance of fault patterns in Pahrump Valley (Liggett and Childs, July 1973**). Oblique, southeast looking, X-15 photographs have also

---

* Appendix O, this report

** Appendix H, this report

been used in studying the northwesterly trending fault patterns in alluvium and bedrock in the western part of the Mojave Desert, California. Some of the X-15 photographs used in these studies were poorly exposed, and special photographic printing techniques have been required to support effective analysis.

2.5.7 U-2 Photography:

The USGS-USAF and NASA U-2 aircraft photography used in this investigation was recorded with a variety of camera and film types. These include 70-mm multispectral photography and 9.5-inch and 70-mm color, near-infrared color and panchromatic films. Most of the U-2 photography was recorded at altitudes of approximately 20 km. The scale of this imagery is somewhat variable although the photographs typically have fields of view approximately 30 km across. The USGS-USAF U-2 photographic coverage of the Argus Exploration Company test site is shown in Plate 8; the NASA Pre-ERTS Investigator Support (PEIS) flight lines are shown in Plate 7; and the NASA Earth Observation Aircraft Program data are indexed in Appendix P.

The U-2 photography has been the most generally available and most widely used subsidiary data in this investigation. The primary use of the U-2 imagery has been in providing detail for geologic studies of anomalies recognized in the ERTS-1 imagery. The stereoscopic U-2 coverage has been extremely useful in detailed structural analysis and has guided selection of key areas to be studied on the ground. The color infrared U-2 photography has provided excellent detail of vegetation, soil, and rock-type variation and has been used in the detailed mapping of faults in alluvium in the Lake Mead area (Bechtold and others, January 1973*) and in interpretation of fault patterns in volcanic rocks in Fish Lake Valley, Nevada (Childs, 1974**).

The U-2 multispectral photography recorded over the test site has proven to be of generally poor quality. Exposure, clarity, and scale variations between the multispectral bands have caused severe registration problems, preventing effective additive color analysis or compositing of the data.

2.5.8 Low Altutude Aerial Photography and Fixed-Wing Reconnaissance:

Low altitude aerial black and white photography over most of the Argus Exploration Company test site is available through the United States Army, Department of Interior, Department of Agriculture or private aerial survey companies. This imagery has been used in support of ERTS-1 imagery analysis and field reconnaissance in many separate parts of the test site. In areas for which large-scale topographic base maps have not been available, low altitude aerial photography has

---

* Appendix B, this report

** Appendix K, this report

been used for plotting detailed field data.

To complement field reconnaissance in critical areas, low altitude fixed-wing reconnaissance has been flown by Argus Exploration Company personnel. During these flights, color and color infrared 35-mm photographs have been taken at various times of day to provide detailed views of inaccessible areas. Fixed-wing reconnaissance has played an important part in studying the style, continuity and patterns of deformation in a large area south of Lake Mead, Nevada (Liggett and Childs, March 1974*) and the late Tertiary and Quaternary fault pattern in Esmeralda County, Nevada (Childs, 1974**).

Fixed-wing aerial reconnaissance has proven to be an economical method for preliminary evaluation of geologic and structural anomalies interpreted in ERTS-1 MSS imagery. The information obtained from airborne reconnaissance can be an effective tool for planning and guiding detailed field investigations.

2.5.9 ERTS-1 MSS Imagery:

The ERTS-1 MSS imagery has proven to have an effective balance of scale, resolution and spectral range for applications to reconnaissance geologic investigations. The primary advantage of the ERTS-1 MSS imagery is the synoptic perspective of terrane, which permits the study of regional distributions or patterns of spectral and spatial features related to geologic and structural phenomena. The ERTS-1 MSS images are recorded as continuous strips which have fields of view approximately 185 km across.

The spectral range and the multispectral format of the ERTS-1 MSS data have proven suitable for a variety of image enhancement and analysis techniques, as outlined in Section 2.4 of this report. The control of color balance and contrast range possible in false-color compositing of the ERTS-1 MSS imagery is greater than that feasible in the processing of conventional color photography.

The resolution of the ERTS-1 MSS false-color imagery has been limited as much by imperfect registration of the MSS bands as by the size of the image picture elements. Nevertheless, the MSS resolution has been highly effective in the reconnaissance geologic applications conducted in this investigation.

The repetitive ERTS-1 MSS coverage has facilitated the acquisition of imagery having minimum cloud and snow cover, and maximum exposure of surface soil and rock coloring which can be seasonally masked by vegetation. In addition, the repetitive coverage has permitted observation of terrane under varied conditions of illumination and shadowing controlled by seasonal variations in solar azimuth and

---

* Appendix O, this report

** Appendix K, this report

elevation.

Recommendations of operational modifications for consideration in future ERTS and other spacecraft remote sensing programs are summarized in Section 5.0 of this report.

2.5.10 References Cited in Text:

Barth, J.W., March 1974, Investigation of a lineament expressed in an oblique Apollo 9 photograph: NASA Rept. Inv., NASA-CR-137255, E74-10410, 7 p.

Bechtold, I.C., Liggett, M.A., and Childs, J.F., January 1973, Remote sensing reconnaissance of faulting in alluvium, Lake Mead to Lake Havasu, California, Nevada and Arizona: An application of ERTS-1 satellite imagery: NASA Rept. Inv., NASA-CR-130011, E73-10070, 9 p.

Childs, J.F., January 1974, Fault pattern at the northern end of the Death Valley-Furnace Creek Fault Zone, California and Nevada: NASA Rept. Inv., NASA-CR-136387, E74-10205, 8 p.

Liggett, M.A., and Childs, J.F., July 1973, Evidence of a major fault zone along the California-Nevada state line, 35°30' to 36°30' N latitude: NASA Rept. Inv., NASA-CR-133140, E73-10773, 10 p.

Liggett, M.A., and Childs, J.F., March 1974, Crustal extension and transform faulting in the southern Basin Range Province: NASA Rept. Inv., NASA-CR-137256, E74-10411, 28 p.

2.6 ARGUS EXPLORATION COMPANY REPORTS

2.6.1 Type I Progress Reports:

A Reconnaissance Space Sensing Investigation of Crustal Structure for a Strip from the Eastern Sierra Nevada to the Colorado Plateau. NASA Contract NAS 5-21809.

8 September, 1972

9 November, 1972

15 March, 1973

11 May, 1973

10 September, 1973

9 November, 1973

2.6.2 Type II Progress Reports:

A Reconnaissance Space Sensing Investigation of Crustal Structure for a Strip from the Eastern Sierra Nevada to the Colorado Plateau. NASA Contract NAS 5-21809.

19 January, 1973: NASA-CR-129969, E73-10028, 31 p.

20 July, 1973: NASA-CR-133141, E73-10774, 45 p.

19 January, 1974: NASA-CR-136389, E74-10207, 26 p.

2.6.3 Reports of Investigation:

Bechtold, I.C., Liggett, M.A., and Childs, J.F., January 1973, Remote sensing reconnaissance of faulting in alluvium, Lake Mead to Lake Havasu, California, Nevada and Arizona: An application of ERTS-1 satellite imagery: NASA Rept. Inv., NASA-CR-130011, E73-10070, 9 p.

Liggett, M.A., and Childs, J.F., July 1973, Evidence of a major fault zone along the California-Nevada state line, 35°30' to 36°30' N. latitude: NASA Rept. Inv., NASA-CR-133140, E73-10773, 10 p.

MacGalliard, Wally, and Liggett, M.A., November 1973, False-color compositing of ERTS-1 MSS imagery: NASA Rept. Inv., NASA-CR-135859, E74-10018, 5 p.

Liggett, M.A., and Ehrenspeck, H.E., January 1974, Pahranagat Shear System, Lincoln County, Nevada: NASA Rept. Inv., NASA-CR-136388, E74-10206, 10 p.

Childs, J.F., January 1974, Fault pattern at the northern end of the Death Valley-Furnace Creek Fault Zone, California and Nevada: NASA Rept. Inv., NASA-CR-136387, E74-10205, 8 p.

Liggett, M.A., and Childs, J.F., February 1974, Structural lineaments in the southern Sierra Nevada, California: NASA Rept. Inv., NASA-CR-136665, E74-10279, 9 p.

Barth, J.W., March 1974, Investigation of a lineament expressed in an oblique Apollo 9 photograph: NASA Rept. Inv., NASA-CR-137255, E74-10410, 7 p.

Liggett, M.A., and Childs, J.F., March 1974, Crustal extension and transform faulting in the southern Basin Range Province: NASA Rept. Inv., NASA-CR-137256, E74-10411, 28 p.

2.6.4 Abstracts:

Bechtold, I.C., Liggett, M.A., and Childs, J.F., November 1972, Structurally controlled dike swarms along the Colorado River, northwestern Arizona and southern Nevada (abs.) in Type I Progress Report: NASA-CR-128390, E72-10192, 2 p.

Bechtold, I.C., Liggett, M.A., and Childs, J.F., January 1973, Pseudo-relief enhancement of color imagery (abs.) in Type II Progress Report: NASA-CR-129969, E73-10028, 1 p.

Childs, J.F., January 1973, Preliminary investigation of rock type discrimination near Wrightwood, California (abs.) in Type II Progress Report: NASA-CR-129969, E73-10028, 1 p.

Childs, J.F., July 1973, The Salt Creek Fault, Death Valley, California (abs.) in Type II Progress Report, NASA-CR-133141, E73-10774, 6 p.

Childs, J.F., and Liggett, M.A., July 1973, Structure and volcanism, Ubehebe Craters, Death Valley, California (abs.) in Type II Progress Report: NASA-CR-133141, E73-10774, 6 p.

Childs, J.F., November 1973, A major normal fault in Esmeralda County, Nevada (abs.) in Type I Progress Report: NASA-CR-135859, E74-10018, 6 p.

2.6.5 Other Publications:

Bechtold, I. C., Liggett, M. A., and Childs, J. F., March 1973, Regional tectonic control of Tertiary mineralization and Recent faulting in the southern Basin-Range Province: An application of ERTS-1 data, in Freden, S. C., Mercanti, E. P., and Becker, M. A., eds., Symposium on significant results obtained from the Earth Resources Technology Satellite-1: New Carrollton, Maryland, v. 1, sect. A, paper G 21, NASA-SP-327, E73-10824, p. 425-432.

Bechtold, I. C., Liggett, M. A., and Childs, J. F., October 1973, Remote sensing of faulting in alluvium, Lake Mead to Lake Havasu, California, Nevada and Arizona, in Moran, D. E., Slosson, J. E., Stone, R. O., and Yelverton, C. A., eds., Geology, seismicity, and environmental impact: Association of Engineering Geologists Spec. Pub., p. 157-161.

2.6.6 Presentations:

Liggett, M. A., July 1972, Applications of ERTS-A imagery to structural geology: ERTS Users News Briefing, NASA Headquarters, Washington. D. C.

Bechtold, I. C., July 1972, Geologic Applications of Satellite Imagery - A Preview of ERTS-A: ERTS-A Launch Panel Discussion, Santa Maria, California.

Bechtold, I. C., and Liggett, M. A., January 1973, Orbital remote sensing for mineral resources exploration: Ninth Annual Meeting of the AIAA, Washington, D. C.

Bechtold, I. C., Liggett, M. A., and Childs, J. F., March 1973, Regional tectonic control of Tertiary mineralization and Recent faulting in the southern Basin-Range Province: An application of ERTS-1 data: ERTS-1 Symposium, New Carrollton, Maryland.

2.6.7 Newspaper Articles:

Batt, Leo, 7 December 1973, Subterranean conditions mapped by eye in the sky: Los Angeles, Herald-Examiner, p. A-10.
(This article discusses the NASA ERTS-1 program and practical applications of ERTS-1 data made by Argus Exploration Company in the study of geologic hazards and potential ground water sources related to the Pahrump Fault Zone of eastern California and southwestern Nevada).

3.0 REGIONAL INVESTIGATIONS IN THE ARGUS EXPLORATION COMPANY TEST SITE

The diverse geology and structure of the Argus Exploration Company test site is shown in U.S. Geological Survey Map I-532-C (Carlson and Willden, 1968) in the map pocket of this report. The test site includes a variety of physiographic and climatic settings which are expressed in ERTS-1 MSS imagery by varied patterns of vegetation, weathering and erosional topography.

A primary emphasis in this investigation has been on detailed ground based reconnaissance and mapping of anomalous geologic and structural features or patterns observed in the ERTS-1 imagery in different parts of the test site. Reports which summarize the results of these studies are included as Appendices.

In order to evaluate the origin and significance of regional geologic and structural patterns expressed in the ERTS-1 data over the test site, a second emphasis in this investigation has been the study of interrelationships between Cenozoic structural patterns and other regional geologic phenomena. These include patterns of recorded seismic activity, the distributions and compositions of Cenozoic igneous rocks and the locations and characteristics of known areas of alteration and mineralization. These regional syntheses are summarized in the following sections of this report.

3.1 CENOZOIC TECTONIC PATTERNS

3.1.1 Introduction:

The tectonic map compilation of Plate 1 shows the major Cenozoic fault patterns expressed in the ERTS-1 MSS imagery over the Argus Exploration Company test site. These faults are expressed in the imagery by linear topographic alignments of such features as valleys, ridges and escarpments, linear patterns of vegetation, and linear contacts of contrasting rock or soil types. Several previously unmapped structures have been recognized in the ERTS-1 imagery and confirmed by our field reconnaissance. These structures are discussed in separate reports included in the Appendix to this report. The other structural information included in Plate 1 has been documented by published geologic data of other workers as cited in Section 3.1.7.

The purpose of Plate 1 is to illustrate the expression in ERTS-1 imagery of the Cenozoic tectonics of the test site. The Cenozoic deformation of this region is dominated by systems of strike-slip and extensional normal faults which are superposed on complex geologic and structural terranes formed in earlier episodes of deposition, igneous activity and compressional deformation. Although the pre-Cenozoic structure is locally expressed, the younger deformation has produced the dominant regional structural patterns apparent in the ERTS-1 imagery. In order to emphasize the continuity of these regional patterns and the variations in tectonic styles across the test site, minor faults have been omitted from the compilation.

This section includes a brief summary of the geologic history and the primary characteristics of Cenozoic tectonics in the structural provinces of the test site. The generalized boundaries of these structural provinces are shown in Figure 17.

3.1.2 Basin Range Province:

The distinctive physiographic and structural terrane of the Basin Range Province can be traced from Idaho and Oregon southward into northern Mexico and is characterized by systems of northerly trending mountain blocks separated by range-front faults from deep, intermontane valleys (see for example, ERTS-1 Frame #1106-17492, Figure 7, west half). The portion of the Basin Range Province included in the Argus Exploration Company test site is outlined in Figure 17, and the tectonic pattern characteristic of the region is shown in Plate 1.

Much of the Basin Range Province is underlain by a crystalline basement of Precambrian age. Throughout most of the province, this basement is mantled by later Precambrian, Paleozoic and Mesozoic sediments of the Cordilleran geosyncline, deformed during several orogenies of late Paleozoic and Mesozoic age (Armstrong, 1968).

The Mesozoic deformation culminated in late Cretaceous time in a belt of eastward overthrusting and related folding, which extends along the eastern margin of the

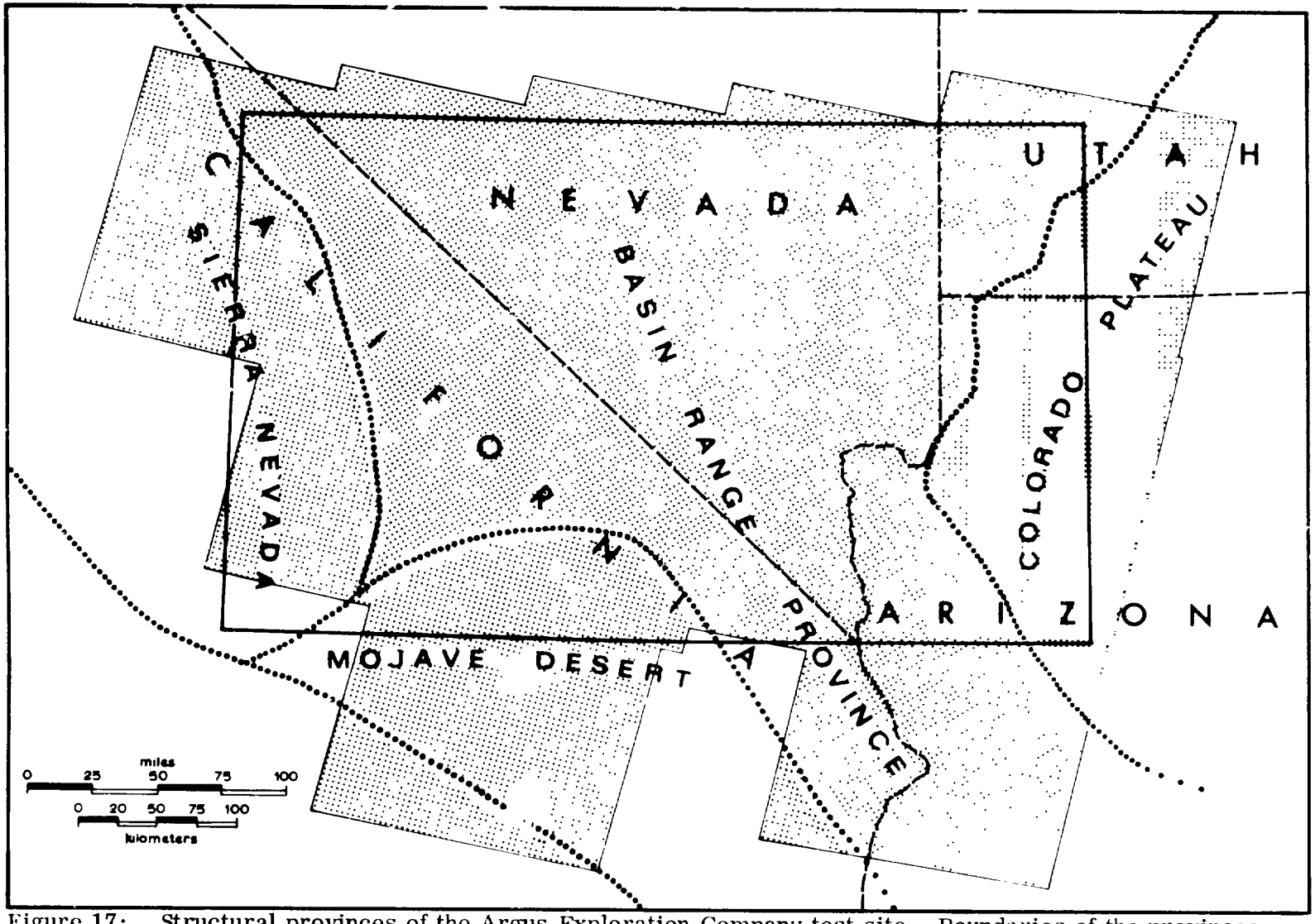

Figure 17: Structural provinces of the Argus Exploration Company test site. Boundaries of the provinces are indicated by dotted lines. Shading indicates areas of each province covered by ERTS-1 MSS imagery included in this report. See Figure 1 for geographic details.

Great Basin from southeastern California to Idaho. West of the frontal zone of thrusting, these orogenies are expressed by abundant plutonic and associated metamorphic rocks of Mesozoic age (Burchfiel and Davis, 1972).

A long period of post-Cretaceous stability was followed in mid-Tertiary time by the onset of regional normal faulting, widespread volcanic activity and the formation of the characteristic Basin Range physiography. The Cenozoic structure of the province is characterized by northerly trending systems of complex grabens, horsts and tilted blocks bounded by normal faults (Stewart, 1971; Liggett and Childs, March 1974*). The major range-front faults generally dip at approximately 60 degrees and are believed to shallow at depth (Hamilton and Myers, 1966). However, in several areas normal faults having large displacements and dips of less than 25 degrees have been mapped (Longwell, 1945; Anderson, 1973; Liggett and Ehrenspeck, 1974**).

Cenozoic volcanism throughout the Basin Range Province is dominated by voluminous ignimbrites and flows of intermediate to silicic composition. These volcanic rocks are closely associated with volcanotectonic features, such as the caldera structures of southern Nye County, Nevada (Ekren, 1968; Cornwall, 1972; Liggett and Childs, March 1974*). Some of these caldera structures are expressed in ERTS-1 imagery by localized patterns of concentric and radial faults, which are superimposed on, and have locally influenced the development of Basin Range faults (see Plate 1; and ERTS-1 Frame #1125-17551, Figure 5, southwest quarter).

In several areas erosion has exposed Cenozoic intrusive bodies genetically related to the widespread silicic and intermediate volcanic rocks. Examples are the Eldorado and Newberry Mountains south of Lake Mead in Clark County, Nevada (Volborth, 1973; ERTS-1 Frame #1106-17495, Figure 4, southeast quarter). Plutons and dike swarms in this area are aligned along northerly trends, and their emplacement was both temporally and spatially related to Basin Range normal faulting (Liggett and Childs, March 1974*).

Systems of right-and left-lateral strike-slip faults have been recognized within the Basin Range Province, generally striking at high angles to the northerly trends typical of the province. Movement on several of these strike-slip fault systems is inferred to have been synchronous with Basin Range normal faulting, and the estimated lateral displacement on these fault systems ranges up to tens of kilometers. Examples are the right-lateral Las Vegas Valley shear zone (Liggett and Childs, March 1974*), Pahrump fault zone (Liggett and Childs, 1973***), Death Valley-Furnace Creek fault zone (Childs, 1974****); and the left-lateral Garlock

---

* Appendix O, this report
** Appendix L, this report
*** Appendix H, this report
**** Appendix K, this report

fault (Davis and Burchfiel, 1973), Pahranagat shear system (Liggett and Ehrenspeck, 1974*), and Hamolin Bay fault (Anderson, 1973). These structures are well expressed in ERTS-1 imagery (see for example, ERTS-1 Frame #1106-17495, Figure 4, northeast quarter) and have been the subject of detailed study as part of this investigation.

Various theories proposed for the origin of Basin Range structure are discussed in excellent summaries by Nolan (1943), Gilluly (1963), Roberts (1968) and Stewart (1971). Most concepts can be separated into the following three categories:

1. Basin Range structure has resulted from the collapse of the upper crust caused by such mechanisms as lateral transfer of lower crustal material (Gilluly, 1963) or eruption of huge volumes of volcanic rocks (Mackin, 1960; Le Conte, 1889).

2. Basin Range structure has formed en echelon to deep-seated, conjugate sets of right-and left-lateral strike-slip movement (Shawe, 1965; Sales, 1966).

3. Basin Range structure is the result of regional crustal extension in an east-west direction (Hamilton and Myers, 1966; Cook, 1966; Roberts, 1968; Stewart, 1971). This process is believed to have occurred by plastic extension of the lower crust, perhaps accompanied by intrusion of plutons beneath Basin Range grabens (Thompson, 1966). The net amount of crustal extension has been estimated to be as great as 300 km, or 100 percent (Hamilton and Myers, 1966).

Supported by recent geologic mapping and geophysical surveys, most current theories of Basin Range structure presume the existence of net crustal extension within the province during late Cenozoic time. Analysis of ERTS-1 imagery, supported by field reconnaissance and literature research, has led to the conception of a tectonic model which relates strike-slip faulting and Cenozoic igneous activity to crustal extension in part of the southern Basin Range Province (Liggett and Childs, March 1974**).

3.1.3 Sierra Nevada and Western Basin Range Province:

The terrane north of the Garlock fault in eastern California and western Nevada is dominated by a system of rugged northwest trending ranges, separated by deep, alluvium-filled troughs. The Cenozoic structure of this area is dominated by a northwest trending pattern of right-lateral oblique-slip faults which form a belt extending from the California-Nevada border to the Sierra Nevada (see Plate 1, and

---

* Appendix L, this report

** Appendix O, this report

Figure 17). Although conventionally considered a part of the western Basin Range Province, the Cenozoic structure of this belt contrasts markedly with the less complex horst and graben structure of southern Nevada. These contrasting styles of deformation are clearly expressed in ERTS-1 imagery and Plate 1.

In pre-Cenozoic time, the region of the Sierra Nevada and western Basin Range Province formed part of the southern Cordilleran geosyncline. Nearly 13 km of geosynclinal sedimentary rocks of late Precambrian through late Paleozoic age were deposited on crystalline basement of the North American continental platform (Bateman and Wahrhaftig, 1966; Burchfiel and Davis, 1972). During the Mesozoic, these rocks were intensely folded, faulted, and regionally metamorphosed in one or more orogenies that accompanied the formation of a broad plutonic and volcanic arc which extended northwest from Baja California into Idaho (Burchfiel and Davis, 1972). This Mesozoic deformation and igneous activity was followed by a prolonged period of relative stability lasting until middle Tertiary time. During this period, regional erosion removed as much as 8 km of rock from the ancestral Sierra Nevada region (Bateman and Wahrhaftig, 1966). Gradual uplift of the Sierra Nevada and adjoining ranges to the east began in Miocene time with the onset of Basin Range normal faulting and has continued to the present, accompanied by intermittent and scattered volcanic activity. Specific examples of the spatial and temporal relationships between the late Cenozoic structural development and volcanism of the Sierra Nevada and adjacent areas are discussed in Section 3.3.4 of this report.

The Sierra Nevada is a westward-tilted block of granitic rock, detached by major normal faulting on its east and south sides from other parts of a large Mesozoic batholithic complex. The Sierra Nevada block now forms the western border of the Basin Range Province and constitutes a structural boundary between extensional tectonics to the east and the dominantly compressional and strike-slip tectonics of the California Coast Ranges (Hamilton and Myers, 1966).

Only minor Cenozoic deformation has been recognized within the Sierra Nevada batholith. The Kern Canyon fault is a nearly continuous, north striking fault of probable Cenozoic age, although its precise age and sense of displacement are unknown (see Plate 1; and ERTS-1 Frame #1162-18011, Figure 13, west half). Numerous intersecting lineament systems in the southern Sierra Nevada can be traced in ERTS-1 MSS imagery for as far as 30 km. These structures are believed to have resulted in part from Cenozoic faulting (Liggett and Childs, February 1974*).

From northwest of Mono Lake to Big Pine, California, the eastern escarpment of the Sierra Nevada consists of a discontinuous pattern of branching and en echelon, east dipping normal faults (ERTS-1 Frame #1163-18063, Figure 14). Together, these features have a net dip-slip displacement of approximately 2-3 km between the crest of the Sierra Nevada and the floor of Owens Valley (Bateman and

---

* Appendix M, this report

Wahrhaftig, 1966). From Big Pine southward to Owens Lake, as much as 6 km of total dip-slip displacement has occurred on two or more subparallel range front fault zones. South of Owens Lake, the Sierran escarpment is formed by a single fault zone that terminates at the Garlock fault (ERTS-1 Frame #1162-18011, Figure 13).

East of the Sierra Nevada the most continuous and prominent Cenozoic structures are the Owens Valley fault zone, the Death Valley-Furnace Creek fault zone, the Death Valley fault zone, and the Pahrump fault zone, as shown in Plate 1. These fault zones strike northwest within deep structural troughs in which they have locally cut alluvium of Recent age.

Significant components of right-lateral strike-slip have been postulated for each of these Cenozoic fault zones. Net displacement on the Owens Valley fault zone may be as great as several kilometers, based on the apparent offset of a Mesozoic pluton (Ross, 1962) and dike swarms (Moore and Hopson, 1961) across the fault zone. Estimates of net displacement on the Death Valley-Furnace Creek fault zone, summarized by Stewart (1967), and Stewart and others (1968), range as high as 80 to 125 km. However, for the southern Death Valley fault zone, Wright and Troxel (1967; 1970) have presented evidence which would limit lateral displacement to less than 8 km. Net displacement on the Pahrump fault zone has been estimated at approximately 13 km (Liggett and Childs, 1973*).

An elongate, northwest trending structural belt about 100 km long and 30 to 40 km wide and situated between the Owens Valley and Death Valley-Furnace Creek fault zones is dominated by a pattern of closely spaced, north to northeast striking normal faults (Ross, 1967, 1970). The individual faults have dip-slip displacements of up to 2 km (Hamilton and Myers, 1966) and border horsts, grabens and tilted blocks, most of which are clearly expressed in ERTS-1 imagery (see Plate 1; and ERTS-1 Frame #1126-18010, Figure 6, south half). The development of this structural pattern has been at least in part synchronous with oblique-slip, or strike-slip movement on the Owens Valley and Death Valley-Furnace Creek fault systems. During late Pliocene time, the normal faulting was accompanied by an episode of widespread basaltic volcanism which formed the Saline Range volcanic field (Ross, 1970). The close relationship between this episode of volcanism and the normal faulting are discussed in Section 3.3.4 of this report. This structural belt is believed to represent regional, extensional fragmentation related to the major Cenozoic right-lateral deformation that characterizes the western margin of the Basin Range Province (Hamilton and Myers, 1966; Stewart, 1971).

3.1.4 Colorado Plateau:

The Colorado Plateau is a physiographically and structurally distinct portion of the

---

* Appendix H, this report

continental platform of North America. This enormous structural province is characterized by a Precambrian crystalline basement overlain by several kilometers of nearly flat lying, late Precambrian to Mesozoic sedimentary strata which are locally intruded by Cenozoic igneous rocks and overlain by Cenozoic sedimentary and volcanic rocks. Except for monoclinal upwarps and minor normal faults, the interior region of this block is essentially undeformed. The western margin of the Colorado Plateau which lies within the Argus Exploration Company Test Site is shown in Figure 17 and Plate 1. During the Sevier orogeny of late Cretaceous age, the western portion of the ancestral Colorado Plateau was delineated by a northeast trending belt of folding and eastward thrust faulting. Several large open folds which formed during this deformation occur along the present western margin of the plateau in southwestern Utah.

Following a long period of early Tertiary erosion, uplift of the Colorado Plateau began by about 18 million years ago along the major normal faults that form the present western border of the province (Lucchitta, 1972). Uplift of the Colorado Plateau continued through the late Tertiary and was synchronous with major normal faulting and silicic to intermediate volcanism and plutonism in the Basin Range Province to the west. From late Miocene through Recent time, intermittent normal faulting in the Colorado Plateau has been temporally and spatially associated with basaltic volcanism of modest volume, as outlined in Section 3.3.2 of this report.

The western boundary of the Colorado Plateau is marked in the ERTS-1 imagery by two prominent west-facing escarpments formed by the Hurricane and Grand Wash fault zones (see ERTS-1 Frame #1051-17425, Figure 8; and ERTS-1 Frame #1069-17432, Figure 9). These faults border two elongate plateaus of gently eastward dipping strata. Estimated displacement on the Grand Wash fault zone decreases northward from nearly 5 km at the mouth of the Grand Canyon to less than 300 meters west of St. George, Utah (Hamblin, 1970). North of St. George, the fault zone ends in a region of many small faults of divergent trends (see Plate 1).

The Hurricane fault zone and subsidiary fault systems of the Shivwitz Plateau and St. George basin form a complex pattern of branching northwest and northeast striking faults (see Plate 1). Dip-slip displacement on the Hurricane fault zone increases northward from a few hundred meters in the Grand Canyon region to nearly 3 km near Cedar City, Utah. Along most of its trace, the Hurricane fault zone is marked by a prominent west-facing escarpment (see ERTS-1 Frame #1051-17425, Figure 8), but north of Cedar City the fault fans out into a series of horsts and grabens, as shown in Plate 1.

East of the Hurricane fault zone, the Toroweap-Sevier fault can be traced in ERTS-1 imagery for nearly 500 km from south of Peach Springs, Arizona to central Utah (see Plate 1; and ERTS-1 Frame #1069-17432, Figure 9, east half). Although the dip-slip displacement on this fault is variable along strike, it does not exceed about 600 meters (Hamblin, 1970).

3.1.5 Mojave Desert Block:

The Mojave Desert of south-central to southeastern California is a westward-tapering wedge of generally subdued topography, characterized by eroded remnants of mountain blocks largely buried by Cenozoic basin deposits (see ERTS-1 Frame #1341-17554, Figure 11). This structural block is bounded on the northwest by the Garlock fault and on the southwest by the San Andreas fault zone. However, to the east and southeast, the block passes gradually into typical Basin Range terrane in the region south and east of the Death Valley fault zone (see Plate 1; and Figure 17).

Scattered remnants of Precambrian crystalline basement within and peripheral to the Mojave Desert indicate that this region has been part of the North American continental platform since the Precambrian. From late Precambrian through late Paleozoic time, several kilometers of geosynclinal sedimentary rocks were deposited on this basement. In Mesozoic time, however, deposition was scattered and discontinuous.

During the Mesozoic, the thick sedimentary cover of the western Mojave Desert region was intensely deformed and regionally metamorphosed by orogenies that accompanied plutonism and volcanism in the ancestral Sierra Nevada region. In the eastern Mojave Desert region the Mesozoic orogenies are represented by northerly trending fold belts and westward dipping thrust faults of the Sevier orogenic belt (Burchfiel and Davis, 1972).

From late Cretaceous to mid-Tertiary time the Mojave Desert Block is believed to have undergone at least 5 km of gradual uplift accompanied by extensive erosion. The present pattern of localized deposition in elongate, northwest trending basins probably began in middle Miocene time (Bassett and Kupfer, 1964; Dibblee, 1967).

The Cenozoic structure of the Mojave Desert region is dominated by a system of northwest striking high-angle faults, several of which can be traced for 40 to 70 km in the ERTS-1 imagery (see Plate 1; and ERTS-1 Frame #1341-17554, Figure 11, east-central part). Elongate ranges and depositional basins and silicic to basaltic volcanic centers occur between and along these faults (see Rogers, 1967). The faults of this system are generally parallel to the San Andreas fault zone, and most are known or suspected to have undergone significant right-lateral strike-slip movement. However, unlike the San Andreas, displacement on the individual faults is at most a few kilometers (Bassett and Kupfer, 1964; Dibblee, 1967). The displacement of Quaternary sediments, and occurrence of recent seismic activity near some of these faults indicate that this system is presently active.

A subordinate structural trend in the Mojave Desert is represented by numerous east to northeast striking faults. These faults are generally discontinuous and are offset by, or terminate against the northwest trending faults (see Plate 1). At least one of these structures, the Pinto Mountain fault of the southern Mojave Desert, appears to have been important in the Cenozoic tectonic development of the province. This fault can be traced in ERTS-1 imagery for more than 50 km eastward from the San Andreas fault zone (see Plate 1), and is estimated to have undergone several kilometers of left-lateral strike-slip movement (Dibblee, 1967; Davis and Burchfiel, 1973).

The Garlock fault borders the Mojave Desert Block on the north and northwest (see Plate 1) and is expressed in ERTS-1 imagery as a nearly continuous topographic lineament which can be traced westward for 260 km from near the Avawatz Mountains to its termination against the San Andreas fault zone. The easternmost portion of the Garlock fault is poorly understood and has been variously interpreted to terminate against a southward extension of the Death Valley fault zone, or to continue eastward an unknown distance beneath alluvium (see Davis and Burchfiel, 1973; Plate 1; and ERTS-1 Frame #1125-17554, Figure 12, south half).

Movement on the Garlock fault is thought to have begun in Miocene time and is known to be continuing at present. Left-lateral strike-slip displacement on the Garlock fault is estimated to be approximately 50-70 km at its western end, possibly decreasing to zero east of the Avawatz Mountains (Davis and Burchfiel, 1973). The Garlock fault separates the strike-slip deformation and subdued topography of the Mojave Desert Block from the oblique-slip, extensional tectonics and rugged physiography of the Sierra Nevada, Argus, Panamint and Black Mountains in the Basin Range Province to the north (ERTS-1 Frame #1125-17554, Figure 12, south half). Davis and Burchfiel (1973) have interpreted this major physiographic and tectonic boundary to represent an intracontinental transform fault.

3.1.6 References Cited in Text:

Anderson, R.E., 1973, Large-magnitude late Tertiary strike-slip faulting north of Lake Mead, Nevada: U.S. Geol. Survey Prof Paper 794, 18 p.

Armstrong, R.L., 1968, Sevier orogenic belt in Nevada and Utah: Geol. Soc. America Bull., v. 79, p. 429-458.

Bassett, A.M., and Kupfer, D.H., 1964, A geologic reconnaissance in the southeastern Mojave Desert, California: California Div. Mines and Geology Spec. Rept. 83, 43 p.

Bateman, P.C., and Wahrhaftig, Clyde, 1966, Geology of the Sierra Nevada, in Bailey, E.H., ed., Geology of northern California: California Div. Mines and Geology Bull. 190, p. 107-172.

Burchfiel, B.C., and Davis, G.A., 1972, Structural framework and evolution of the southern part of the Cordilleran orogen, western United States: Am Jour. Sci., v. 272, p. 97-118.

Carlson, J.E., and Willden, Ronald, 1968, Transcontinental Geophysical Survey (35°-39° N) geologic map from 112° W longitude to the coast of California: U.S. Geol. Survey Misc. Geologic Inv. Map I-532-C, scale 1:1,000,000.

Childs, J.F., January 1974, Fault pattern at the northern end of the Death Valley-Furnace Creek Fault Zone, California and Nevada: NASA Rept. Inv., NASA-CR-136387, E74-10205, 8 p.

Cook, K.L., 1966, Rift system in the Basin and Range province, in The world rift system: Canada Geol. Survey Paper 66-14, p. 246-279.

Cornwall, H.R., 1972, Geology and mineral deposits of southern Nye County, Nevada: Nevada Bur. Mines and Geology Bull. 77, 49 p.

Davis, G.A., and Burchfiel, B.C., 1973, Garlock Fault: An intracontinental transform structure, southern California: Geol. Soc. America Bull., v. 84, p. 1407-1422.

Dibblee, T.W., Jr., 1967, Areal geology of the western Mojave Desert, California: U.S. Geol. Survey Prof. Paper 522, 153 p.

Ekren, E.B., 1968, Geologic setting of Nevada Test Site and Nellis Air Force Range: in Eckel, E.B., ed., Nevada Test Site: Geol. Soc. America Memoir 110, p. 11-19.

Gilluly, James, 1963, The tectonic evolution of the western United States: Geol. Soc. London Quart. Jour., v. 119, p. 133-174.

Hamblin, W.K., 1970, Structure of the western Grand Canyon region, in Hamblin, W.K., and Best, M.G., eds., Guidebook to the geology of Utah: Utah Geol. Soc., no. 23, p. 3-20.

Hamilton, Warren, and Myers, W.B., 1966, Cenozoic tectonics of the western United States: Rev. Geophysics, v. 4, no. 4, p. 509-549.

Le Conte, Joseph, 1889, On the origin of normal faults and of the structure of the Basin region: Am. Jour. Sci., Third series, v. 38, no. 226, p. 257-263.

Liggett, M.A., and Childs, J.F., July 1973, Evidence of a major fault zone along the California-Nevada state line, 35°30' to 36°30' N. latitude: NASA Rept. Inv., NASA-CR-133140, E73-10773, 10 p.

Liggett, M.A., and Childs, J.F., February 1974, Structural lineaments in the southern Sierra Nevada, California: NASA Rept. Inv., NASA-CR-136665, E74-10279, 9 p.

Liggett, M.A., and Childs, J.F., March 1974, Crustal extension and transform faulting in the southern Basin Range Province: NASA Rept. Inv., NASA-CR-137256, E74-10411, 28 p.

Liggett, M.A., and Ehrenspeck, H.E., January 1974, Pahranagat Shear System, Lincoln County, Nevada: NASA Rept. Inv., NASA-CR-136388, E74-10206, 10 p.

Longwell, C.R., 1945, Low-angle normal faults in the Basin-and-Range Province: Trans. Amer. Geophys. Union, v. 26, part 1, p. 107-118.

Lucchitta, Ivo, 1972, Early history of the Colorado River in the Basin and Range province: Geol. Soc. America Bull., v. 83, p. 1933-1948.

Mackin, J.H., 1960, Structural significance of Tertiary volcanic rocks in southwestern Utah: Am. Jour. Sci., v. 258, p. 81-131.

Moore, J.G., and Hopson, C.A., 1961, The Independence dike swarm in eastern California: Am. Jour. Sci., v. 259, p. 241-259.

Nolan, T.B., 1943, The Basin and Range province in Utah, Nevada, and California: U.S. Geol. Survey Prof. Paper 197-D, p. 141-196.

Roberts, R.J., 1968, Tectonic framework of the Great Basin: Rolla, Univ. Missouri Res. Jour., no. 1, p. 101-119.

Rogers, T.H., 1967, Geologic map of California, San Bernardino sheet, Olaf P. Jenkins edition: California Div. Mines and Geology, scale 1:250,000.

Ross, D.C., 1962, Correlation of granitic plutons across faulted Owens Valley, California: U.S. Geol. Survey Prof. Paper 450-D, p. D86-D88.

Ross, D.C., 1967, Generalized geologic map of the Inyo Mountains region, California: U.S. Geol. Survey Misc. Geologic Inv. Map I-506, scale 1:125,000.

Ross, D.C., 1970, Pegmatitic trachyandesite plugs and associated volcanic rocks in the Saline Range-Inyo Mountains region, California: U.S. Geol. Survey Prof. Paper 614-D, 29 p.

Sales, J.K., 1968, Structural analysis of the Basin Range province in terms of wrench faulting (Ph.D. dissert.): Reno, Univ. Nevada, 289 p.

Shawe, D.R., 1965, Strike-slip control of Basin-Range structure indicated by historical faults in western Nevada: Geol. Soc. America Bull., v. 76, p. 1361-1378.

Stewart, J.H., 1967, Possible large right-lateral displacement along fault and shear zones in the Death Valley-Las Vegas area, California and Nevada: Geol. Soc. America Bull., v. 78, p. 131-142.

Stewart, J.H., 1971, Basin and Range structure: A system of horsts and grabens produced by deep-seated extension: Geol. Soc. America Bull., v. 82, p. 1019-1044.

Stewart, J.H., Albers, J.P., and Poole, F.G., 1968, Summary of regional evidence for right-lateral displacement in the western Great Basin: Geol. Soc. America Bull., v. 79, p. 1407-1414.

Thompson, G.A., 1966, The rift system of the western United States, in The world rift system: Canada Geol. Survey Paper 66-14, p. 280-290.

Volborth, Alexis, 1973, Geology of the granite complex of the Eldorado, Newberry and northern Dead Mountains, Clark County, Nevada: Nevada Bur. Mines and Geology Bull. 80, 40 p.

Wright, L.A., and Troxel, B.W., 1967, Limitations on right-lateral, strike-slip displacement, Death Valley and Furnace Creek fault zones, California: Geol. Soc. America Bull., v. 78, p. 933-950.

Wright, L.A., and Troxel, B.W., 1970, Summary of regional evidence for right-lateral displacement in the western Great Basin: Discussion: Geol. Soc. America Bull., v. 81, p. 2167-2174.

3.1.7 References Used in Compiling Plate 1:

Albers, J. P., and Stewart, J. H., 1972, Geology and mineral deposits of Esmeralda County, Nevada: Nevada Bur. Mines and Geology Bull. 78, 80 p.

Anderson, R. E., 1971, Thin skin distension in Tertiary rocks of southeastern Nevada: Geol. Soc. America Bull., v. 82, p. 43-58.

Anderson, R. E., 1973, Large-magnitude late Tertiary strike-slip faulting north of Lake Mead, Nevada: U. S. Geol. Survey Prof. Paper 794, 18 p.

Bassett, A. M., and Kupfer, D. H., 1964, A geologic reconnaissance in the southeastern Mojave Desert, California: California Div. Mines and Geology Spec. Rept. 83, 43 p.

Bateman, P. C., 1965, Geologic map of the Blackcap Mountain quadrangle, Fresno County, California: U. S. Geol. Survey Geol. Quad. Map GQ-428, scale 1:62,500.

Bateman, P. C., and Moore, J. G., 1965, Geologic map of the Mount Goddard quadrangle, Fresno and Inyo Counties, California: U. S. Geol. Survey Geol. Quad. Map GQ-429, scale 1:62,500.

Bechtold, I. C., Liggett, M. A., and Childs, J. F., March 1973, Regional tectonic control of Tertiary mineralization and Recent faulting in the southern Basin-Range Province: An application of ERTS-1 data, in Freden, S. C., Mercanti, E. P., and Becker, M. A., eds., Symposium on significant results obtained from the Earth Resources Technology Satellite-1: New Carrollton, Maryland, v. 1, sect. A. paper G 21, NASA-SP-327, E73-10824, p. 425-432.

Bishop, C. C., 1963, Geologic map of California, Needles sheet, Olaf P. Jenkins edition: California Div. Mines and Geology, scale 1:250,000.

Bowen, O. E., Jr., 1954, Geology and mineral deposits of Barstow quadrangle, San Bernardino County, California: California Div. Mines Bull. 165, 208 p.

Callaghan, Eugene, 1939, Geology of the Searchlight district, Clark County, Nevada: U. S. Geol. Survey Bull. 906-D, p. 135-185.

Childs, J. F., November 1973, A major normal fault in Esmeralda County, Nevada (abs.): in Type I Progress Rept.: NASA-CR-135859, E74-10018, 6 p.

Childs, J. F., January 1974, Fault pattern at the northern end of the Death Valley-Furnace Creek Fault Zone, California and Nevada: NASA Rept. Inv.,

NASA-CR-136387, E74-10205, 8 p.

Clary, M. R., 1967, Geology of the eastern part of the Clark Mountain Range, San Bernardino County, California: California Div. Mines and Geology Map Sheet 6.

Cook, E. F., 1957, Geology of the Pine Valley Mountains, Utah: Utah Geol. and Mineralog. Survey Bull. 58, 111 p.

Cook, E. F., 1960, Geologic atlas of Utah, Washington County: Utah Geol. and Mineralog. Survey Bull. 70, 119 p.

Cornwall, H. R., 1972, Geology and mineral deposits of southern Nye County, Nevada: Nevada Bur. Mines and Geology Bull. 77, 49 p.

Crowder, D. F., Robinson, P. F., and Harris, D. L., 1972, Geologic map of the Benton quadrangle, Mono County, California and Esmeralda and Mineral Counties, Nevada: U. S. Geol. Survey Geol. Quad. Map GQ-1013, scale 1:62,500.

Ekren, E. B., Anderson, R. E., Rogers, C. L., and Noble, D. C., 1971, Geology of northern Nellis Air Force Base Bombing and Gunnery Range, Nye County, Nevada: U. S. Geol. Survey Prof. Paper 651, 91 p.

Gilbert, C. M., Christensen, M. N., Al-Rawi, Yehya, and Lajoie, K. R., 1968, Structural and volcanic history of Mono Basin, California-Nevada, in Coats, R. R., Hay, R. L., and Anderson, C. A., eds., Studies in volcanology: Geol. Soc. America Memoir 116, p. 275-329.

Gillespie, J. B., and Bentley, C. B., 1971, Geohydrology of Hualapai and Sacramento Valleys, Mohave County, Arizona: U. S. Geol. Survey Water-Supply Paper 1899-H, 37 p.

Goodwin, J. G., 1958, Mines and mineral resources of Tulare County, California: California Jour. Mines and Geology, v. 54, no. 3, p. 317-492.

Gregory, H. E., 1950, Geology of eastern Iron County, Utah: Utah Geol. and Mineralog. Survey Bull. 37, 153 p.

Hall, W. E., and MacKevett, E. M., 1958, Economic geology of the Darwin quadrangle, Inyo County, California: California Div. Mines Spec. Rept. 51, 73 p.

Hall, W. E., and Stephens, H. G., 1963, Economic geology of the Panamint Butte quadrangle and Modoc district, Inyo County, California: California Div. Mines and Geology Spec. Rept. 73, 39 p.

Hamblin, W.K., 1970, Structure of the western Grand Canyon region, in Hamblin, W.K., and Best, M.G., eds., Guidebook to the geology of Utah: Utah Geol. Soc., no. 23, p. 3-20.

Hansen, S.M., 1962, The geology of the Eldorado mining district, Clark County, Nevada (Ph.D. dissert.): Rolla, Univ. Missouri, 262 p.

Hewett, D.F., 1931, Geology and ore deposits of the Goodsprings quadrangle, Nevada: U.S. Geol. Survey Prof. Paper 162, 172 p.

Heylmun, E.B., ed., 1963, Guidebook to the geology of southwestern Utah: Intermountain Assoc. Petroleum Geologists Guidebook 12, Salt Lake City, Utah, 232 p.

Hintze, L.F., 1963, Geologic map of southwestern Utah: Utah Geol. and Mineralog. Survey, scale 1:250,000

Huber, N.K., and Rinehart, C.D., 1965, Geologic map of the Devils Postpile quadrangle, Sierra Nevada, California: U.S. Geol. Survey Geol. Quad. Map GQ-437, scale 1:62,500.

Jahns, R.H., ed., 1954, Geology of southern California: California Div. Mines Bull. 170.

Jennings, C.W., 1958, Geologic map of California, Death Valley sheet, Olaf P. Jenkins edition: California Div. Mines, scale 1:250,000.

Jennings, C.W., 1961, Geologic map of California, Kingman sheet, Olaf P. Jenkins edition: California Div. Mines, scale 1:250,000.

Jennings, C.W., 1973, State of California, preliminary fault and geologic map: California Div. Mines and Geology Preliminary Report 13, scale 1:750,000.

Jennings, C.W., Burnett, J.L., and Troxel, B.W., 1962, Geologic map of California, Trona sheet, Olaf P. Jenkins edition: California Div. Mines and Geology, scale 1:250,000.

Jennings, C.W., and Strand, R.G., 1969, Geologic map of California, Los Angeles sheet, Olaf P. Jenkins edition: California Div. Mines and Geology, scale 1:250,000.

Koenig, J.B., 1963, Geologic map of California, Walker Lake sheet, Olaf P. Jenkins edition: California Div. Mines and Geology, scale 1:250,000.

Krauskopf, K.B , 1971, Geologic map of the Mt. Barcroft quadrangle, California-Nevada: U.S. Geol. Survey Geol. Quad. Map GQ-960, scale 1:62,500.

Kupfer, D.H., 1960, Thrust faulting and chaos structure, Silurian Hills, San Bernardino County, California: Geol. Soc. America Bull., v. 71, p. 181-214.

Liggett, M.A., and Childs, J.F., July 1973, Evidence of a major fault zone along the California-Nevada state line 35°30'-36°30' N. latitude: NASA Rept. Inv., NASA-CR-133140, E73-10773, 10 p.

Liggett, M.A., and Childs, J.F., February 1974, Structural lineaments in the southern Sierra Nevada, California: NASA Rept. Inv., NASA-CR-136665, E74-10279, 9 p.

Liggett, M.A., and Ehrenspeck, H.E., January 1974, Pahranagat Shear System, Lincoln County, Nevada: NASA Rept. Inv., NASA-CR-136388, E74-10206, 10 p.

Longwell, C.R., Pampeyan, E.H., Bowyer, Ben, and Roberts, R.J., 1965, Geology and mineral deposits of Clark County, Nevada: Nevada Bur. Mines Bull. 62, 218 p.

Malmberg, G.T., 1967, Hydrology of the valley-fill and carbonate-rock reservoirs, Pahrump Valley, Nevada-California: U.S. Geol. Survey Water-Supply Paper 1832, 47 p.

Matthews, R.A., and Burnett, J.L., 1965, Geologic map of California, Fresno sheet, Olaf P. Jenkins edition: California Div. Mines and Geology, scale 1:250,000.

Maxey, G.B., and Jameson, C.H., 1948, Geology and water resources of Las Vegas, Pahrump, and Indian Spring Valleys, Clark and Nye Counties, Nevada: Nevada Water Resources Bull. 5, 121 p.

McAllister, J.F., 1952, Rocks and structure of the Quartz Spring area, northern Panamint Range, California: California Div. Mines Spec. Rept. 25, 38 p.

McAllister, J.F., 1956, Geology of the Ubehebe Peak quadrangle, California: U.S. Geol. Survey Geol. Quad. Map GQ-95, scale 1:62,500.

McAllister, J.F., 1970, Geology of the Furnace Creek borate area, Death Valley, Inyo County, California: California Div. Mines and Geology Map Sheet 14, scale 1:24,000.

McKee, E.H., and Nelson, C.A., 1967, Geologic map of the Soldier Pass quadrangle, California and Nevada: U.S. Geol. Survey Geol. Quad. Map GQ-654, scale 1:62,500.

McKee, E.H., 1968, Geology of the Magruder Mountain area, Nevada-California:

C-2

U.S. Geol. Survey Bull. 1[illegible]H, 40 p.

McKee, E.H., 1968, Age and rate of movement of the northern part of the Death Valley-Furnace Creek fault zone, California: Geol. Soc. America Bull., v. 79, p. 509-512.

Nelson, C.A., 1966, Geologic map of the Blanco Mountain quadrangle, Inyo and Mono Counties, California: U.S. Geol. Survey Geol. Quad. Map GQ-529, scale 1:62,500.

Nelson, C.A., 1966, Geologic map of the Waucoba Mountain quadrangle, Inyo County, California: U.S. Geol. Survey Geol. Quad. Map GQ-528, scale 1:62,500.

Nelson, C.A., 1971, Geologic map of the Waucoba Spring quadrangle, Inyo County, California: U.S. Geol. Survey Geol. Quad. Map GQ-921, scale 1:62,500.

Noble, D.C., 1968, Kane Springs Wash volcanic center, Lincoln County, Nevada, in Eckel, E.B., ed., Nevada Test Site: Geol. Soc. America Memoir 110, p. 109-116.

Norman, L.A., Jr., and Stewart, R.M., 1951, Mines and mineral resources of Inyo County: California Jour. Mines and Geology, v. 47, no. 1, p. 17-223.

Ransome, F.L., 1909, The geology and ore deposits of Goldfield, Nevada: U.S. Geol. Survey Prof. Paper 66, 258 p.

Ransome, F.L., 1923, Geology of the Oatman gold district, Arizona: A preliminary report: U.S. Geol. Survey Bull. 743, 58 p.

Rinehart, C.D., and Ross, D.C., 1956, Economic geology of the Casa Diablo Mountain quadrangle, California: California Div. Mines Spec. Rept. 48, 17 p.

Rinehart, C.D., Ross, D.C., and Pakiser, L.C., 1964, Geology and mineral deposits of the Mount Morrison quadrangle, Sierra Nevada, California; With a section on a gravity study of Long Valley: U.S. Geol. Survey Prof. Paper 385, 106 p.

Robinson, P.T., McKee, E.H., and Moiola, R.J., 1968, Cenozoic volcanism and sedimentation, Silver Peak region, western Nevada and adjacent California, in Coats, R.R., Hay, R.L., and Anderson, C.A., eds., Studies in volcanology: Geol. Soc. America Memoir 116, p. 577-611.

Rogers. T.H., 1967, Geologic map of California, San Bernardino sheet, Olaf P.

Jenkins edition: California Div. Mines and Geology, scale 1:250,000.

Ross, D.C., 1961, Geology and mineral deposits of Mineral County, Nevada: Nevada Bur. Mines Bull. 58, 98 p.

Ross, D.C., 1965, Geology of the Independence quadrangle, Inyo County, California: U.S. Geol. Survey Bull. 1181-O, 64 p.

Ross, D.C., 1967, Geologic map of the Waucoba Wash quadrangle, Inyo County, California: U.S. Geol. Survey Geol. Quad. Map GQ-612, scale 1:62,500.

Ross, D.C., 1967, Generalized geologic map of the Inyo Mountains region, California: U.S. Geol. Survey Misc. Geologic Inv. Map I-506, scale 1:125,000.

Ross, D.C., 1970, Pegmatitic trachyandesite plugs and associated volcanic rocks in the Saline Range-Inyo Mountains region, California: U.S. Geol. Survey Prof. Paper 614-D, 29 p.

Schrader, F.C., 1909, Mineral deposits of the Cerbat Range, Black Mountains, and Grand Wash Cliffs, Mohave County, Arizona: U.S. Geol. Survey Bull. 397, 226 p.

Smith, A.R., 1964, Geologic map of California, Bakersfield sheet, Olaf P. Jenkins edition: California Div. Mines and Geology, scale 1:250,000.

Smith, G.I., Troxel, B.W., Gray, C.H., Jr., and von Huene, Roland, 1968, Geologic reconnaissance of the Slate Range, San Bernardino and Inyo Counties, California: California Div. Mines and Geology Spec. Rept. 96, 33 p.

Stokes, W.L., and Heylmun, E.B., 1963, Tectonic history of southwestern Utah, in Heylmun, E.B., ed., Guidebook to the geology of southwestern Utah: Intermountain Assoc. Petroleum Geologists Guidebook 12, p. 19-25.

Strand, R.G., 1967, Geologic map of California, Mariposa sheet, Olaf P. Jenkins edition: California Div. Mines and Geology, scale 1:250,000.

Threet, R.L., 1963, Structure of the Colorado Plateau margin near Cedar City, Utah, in Heylmun E.B., ed., Guidebook to the geology of southwestern Utah: Intermountain Assoc. Petroleum Geologists Guidebook 12, p. 104-117.

Troxel, B.W., and Morton, P.K., 1962, Mines and mineral resources of Kern County, California: California Div. Mines and Geology, County Rept. no. 1, 370 p.

Tschanz, C.M., and Pampeyan, E.H., 1970, Geology and mineral deposits of Lincoln County, Nevada: Nevada Bur. Mines Bull. 73, 187 p.

Volborth, Alexis, 1973, Geology of the granite complex of the Eldorado, Newberry, and northern Dead Mountains, Clark County, Nevada: Nevada Bur. Mines and Geology Bull. 80, 40 p.

Wilson, E. D., Moore, R. T., and Cooper, J. R., 1969, Geologic map of Arizona: U. S. Geol. Survey, and Arizona Bur. Mines, scale 1:500,000.

Young, R. A., and Brennan, W. J., 1974, Peach Springs Tuff: Its bearing on structural evolution of the Colorado Plateau and development of Cenozoic drainage in Mohave County, Arizona: Geol. Soc. America Bull., v. 85, p. 83-90.

3.2 DISTRIBUTION OF SEISMIC ACTIVITY

3.2.1 Introduction:

The distributions of recorded earthquake epicenters and focal depths in the Argus Exploration Company test site have been compiled in order to investigate the interrelationships between seismicity and regional Cenozoic structural patterns visible in the ERTS-1 MSS imagery.

The seismicity of the Basin Range Province has been studied in many investigations of regional seismology and tectonics. Among these are the works of Gianella and Callaghan (1934), Slemmons and others (1965), Ryall and others (1966), Gumper and Scholz (1971), Scholz and others (1971), and Sbar and others (1972). Several of these reports are somewhat limited in scope and data, and for this reason tend to be conflicting in interpretation. Using ERTS-1 imagery and available seismic data, we have attempted to resolve some of the controversy over the relationship of tectonics and seismicity in the area of the test site. To gain a perspective of this relationship we have studied correlations between the distributions of recorded earthquake epicenters, known systems of active faulting and the Cenozoic structural patterns visible in the ERTS-1 MSS imagery.

3.2.2 Data:

The map compilation of Plate 3 shows epicenter locations and focal depths for recorded earthquakes of magnitude 3.0 Richter units or greater in the test site. Most of the earthquakes shown in this compilation were recorded in the period from 1961 to 1972, although major pre-1961 earthquakes are also included. The primary source of this seismic data is the Earthquake Data File (National Geophysical Data Center, 1972) published by the National Oceanic and Atmospheric Administration (NOAA) for the period January 1961 through December 1971. Sources of data for major pre-1961 earthquakes include Gianella and Callaghan (1934), Callaghan and Gianella (1935), Richter (1947), Chakrabarty and Richter (1949), Richter (1960), and Bateman (1961), as summarized in Section 3.2.9.

3.2.3 Accuracy and Limitations of Seismic Data:

The reliability of seismic data such as epicenter locations, focal depths and magnitudes is highly variable within the area of the test site. This reliability is primarily determined by the proximity of an earthquake to a seismographic station or group of stations.

The epicenter locations of post-1961 earthquakes are generally known to within a few tenths of a degree, or approximately 15 km (National Geophysical Data Center, 1972). Locations of major pre-1961 earthquake epicenters are less precisely known but are considered to be generally accurate at the scale of Plate 3.

Within the test site, earthquake focal depths are generally considered to be accurate

in areas where the distance from an epicenter to the recording instruments does not exceed the focal depth of the earthquake (Nordquist, 1974, personal communication). The areas with the most accurate focal depth measurements include the Nevada Test Site in Nye County, Nevada; the region surrounding Lake Mead in Clark County, Nevada; and southern Owens Valley, California. Focal depths recorded in these areas are characteristically less than 40 km. Other focal depths cited in the seismic literature of the southern Basin Range Province have been estimated on the basis of currently accepted crustal parameters and are of uncertain accuracy. This limitation must be considered in interpreting the focal depths shown in Plate 3.

The majority of earthquakes reported in the test site range in magnitude from 3.0 to 4.5 Richter units. Most post-1961 earthquake magnitudes have been determined by averaging the magnitudes recorded at several seismic stations for each earthquake; however, some magnitudes are based on single station recordings. In their study of microseismic events in the Basin Range Province, Gumper and Scholz (1971) have estimated a reliability of $\pm$ 0.3 Richter units. This figure probably represents a reasonable minimum value for much of the data cited here, although reliability may be as poor as $\pm$ 1.0 Richter units for some data (Nordquist, 1974, personal communication). Because of the small range of recorded magnitudes in the test site, and the short time span of accurate measurement (about 12 years), the patterns of earthquake magnitudes are not considered geologically significant and have not been shown in Plate 3.

In areas of good seismographic control, numerous small-magnitude earthquakes have been recorded which do not necessarily reflect the true regional distribution of seismic activity. In order to gain a more accurate perspective of this distribution, it has been necessary to establish a "threshold" magnitude which represents the lowest magnitude event in the test site that can be recorded regardless of the distance from its epicenter to a seismographic station. Although there is no generally accepted "threshold" magnitude for this region, a magnitude of 3.0 Richter units is believed to be a reasonable lower limit, based on seismographic station coverage from 1961 to the present (Nordquist, 1974, personal communication; and U.S.G.S. Branch of Seismic Engineering, Las Vegas, 1974, personal communication). Although this lower "threshold" value may not totally eliminate the areal bias of earthquake data shown in Plate 3, it is believed to provide a reasonably accurate view of the natural distribution of epicenters in the test site.

In addition to bias introduced during measurement, the regional pattern of seismic activity may be further complicated by man-made seismic events, such as the release of tectonic stress and collapse phenomena following nuclear testing in the Nevada Test Site. The abundance of earthquakes centered around Lake Mead is thought to be related to changes in isostatic loading controlled by varying water levels in the reservoir (Jones 1944; Carder 1970).

3.2.4 Correlations of Active Faulting and Seismic Activity:

Fault movement has been documented for all major historical earthquakes in the

Basin Range Province (see Plate 3). Right-lateral displacement was measured on fault scarps formed during the Cedar Mountain earthquake of 1932 (Gianella and Callaghan, 1934), the Fairview Peak earthquake of 1954 (Slemmons, 1957), the Wonder earthquake of 1903 (Slemmons and others, 1959), and the Owens Valley earthquake of 1872 (Bateman, 1961). Left-lateral movement was inferred from en echelon fissures formed during the Excelsior Mountains earthquake of 1934 (Callaghan and Gianella, 1935).

Faults with dip-slip displacement were associated with the Pleasant Valley earthquake of 1915 (Page, 1935), the Rainbow Mountain earthquake of 1954 (Byerly and others, 1956), and the Dixie Valley earthquake of 1954 (Slemmons, 1957). In addition to "natural" earthquakes, strike-slip, dip-slip and oblique-slip surface faulting has been observed associated with the release of tectonic stress following nuclear explosions in the Nevada Test Site (Dickey, 1968, 1969; Bucknam, 1969; and McKeown and Dickey, 1969).

The sense of motion on faults in the southern Basin Range Province has been interpreted from first motion and composite fault plane solution (CFPS) studies at locations shown in Plate 3. First motion studies of the Fairview Peak earthquake of 1954 (Romney, 1957) indicated that right-lateral oblique-slip motion occurred on generally north striking faults. Subsequent CFPS studies on microearthquakes in this area by Stauder and Ryall (1967) found dip-slip motion to be predominant. CFPS studies by Gumper and Scholz (1971) have indicated right-lateral oblique-slip motion on northerly trending faults in the Cedar Mountains and Cedar Valley areas of Mineral and Esmeralda Counties, Nevada, and left-lateral strike-slip motion on east-northeast striking faults in the Excelsior Mountains area of Mineral County.

A microseismic CFPS study conducted by the U.S. Geological Survey during October 1972 in Long Valley, California has been interpreted as indicating right-lateral strike-slip motion on north striking faults (U.S. Dept. of Interior, 1973). In southern Owens Valley, Lindh (1974, personal communication) has interpreted right-lateral strike-slip motion on generally northerly striking faults. In the Nevada Test Site of southern Nye County, Nevada, CFPS measurements have been interpreted by Lindh (1974, personal communication) as indicating right-lateral strike-slip motion on northerly striking faults. However, the CFPS measurements in the Nevada Test Site can be alternately interpreted as indicating left-lateral motion on generally west striking faults.

In Lincoln County, Nevada, CFPS studies (Lindh, 1974, personal communication) indicate dip-slip motion on north to northeast striking faults in the Pahroc Valley north of Crystal Springs. In the Clover Mountains south of Barclay, similar data support alternate interpretations of left-lateral motion on west-northwest striking faults, or right-lateral motion on northeast striking faults. Likewise, CFPS data south of Lake Mead (Lindh, 1974, personal communication) support alternate interpretations of right-lateral strike-slip motion on northerly striking faults, or left-lateral motion on easterly striking faults. Dip-slip motion is interpreted by Sbar and others (1972) for northerly striking faults northeast of Cedar City, Utah.

Normal and oblique-slip displacements of Quaternary alluvium have been observed in many areas in the southern Basin Range Province. Notable examples have been reported by Slemmons (1956) in the Fairview Peak-Dixie Valley area; Liggett and Childs (1973*) in the Pahrump Valley of Clark County, Nevada; Bechtold and others (1973**) in a broad area south of Lake Mead; and Tschanz and Pampeyan (1970) and Liggett and Ehrenspeck (1974***) in the Pahranagat area of Lincoln County, Nevada. Many of these fault systems are considered to be presently active, although they may not correspond to seismic events recorded in the short time span of observation.

As discussed in Section 3.1.2, the dominant Cenozoic tectonic features in the southern Basin Range Province are northerly striking normal faults that have formed the characteristic horst and graben structural pattern. The major range-front faults generally dip at moderate angles away from the uplifted ranges toward the structural troughs. As a result of this structural geometry, earthquake foci located along Basin Range normal faults would be expected to be clustered beneath topographic basins. This pattern holds true for the majority of epicenters shown in Plate 3.

Other than the clustering of earthquake epicenters within structural basins, the distributions of recorded epicenters shown in Plate 3 are not recognized to be grouped along the major structural features shown in the tectonic map of Plate 1. No clear patterns of epicenter distributions or focal depths are recognized which permit a distinction between known strike-slip and dip-slip fault systems.

3.2.5 Regional Seismic Patterns:

The regional distribution of earthquake epicenters in the map compilation of Plate 3 indicates a generally northward trending zone of relatively high seismic activity along the western margin of the Basin Range Province. This seismic zone is bounded on the west by the eastern front of the Sierra Nevada and varies in width from approximately 175 km north of lat 38° N., to less than 25 km near lat 37° N.

A similar northerly trending seismic pattern is evident in the distribution of earthquake epicenters of magnitude 4.0 or greater, compiled by Slemmons and others (1965) for the period 1352-1960. They have described this pattern as two subparallel northerly trending zones, one along the eastern Sierra Nevada front including Carson City and Reno, Nevada, the other to the east along the 118° meridian, which includes most major historic earthquakes in Nevada. However, much of this data is dependent on non-instrumental reports and on pre-1932 instrumental recordings made with poor seismographic station coverage. As noted by Slemmons and others (1965), this limitation in the data has biased the density of recorded epicenters toward population centers, such as Carson City and Reno, Nevada.

---

* Appendix H, this report
** Appendix B, this report
*** Appendix L, this report

A recent interpretation of microseismic data in the western Basin Range by Gumper and Scholz (1971) has indicated a seismic pattern similar to that shown in Plate 3, which they have named the Nevada Seismic Zone. Based on the distribution of recorded microseismic epicenters, Gumper and Scholz (1971) suggest that the Nevada Seismic Zone is displaced westward by approximately 75 km along a northeast trending feature in the vicinity of the Excelsior Mountains, east of Mono Lake. Such a displacement is not apparent either from the seismic data presented in Plate 3 or from the pre-1961 instrumental data of Slemmons and others (1965).

The Sierra Nevada which forms the western boundary of the Nevada Seismic Zone, is characterized by a conspicuously low level of seismic activity with exceptions along the Kern Canyon fault and in the Tehachapi Mountains. The southern terminus of the Nevada Seismic Zone appears to be the Garlock fault, which also forms the physiographic and structural boundary between the Sierra Nevada and Basin Range Province to the north and the Mojave Desert Block to the south (see Plate 1). This seismic pattern was noted by Allen and others (1965, p. 577) in their statement that "the entire Garlock fault zone .... seems to have served more as a boundary between seismic provinces than as a locus of seismic activity." Like the Sierra Nevada, the Mojave Desert Block is a province of low earthquake activity.

An east-west zone of seismic activity 70-120 km wide crosses southern Nevada approximately between lat 37° N. and lat 38° N. and extends into western Utah at approximately lat 38° N. This east-west zone is well defined in Plate 3, although an artificial density of epicenter locations in the Nevada Test Site and Caliente, Nevada areas appears to contribute significantly to this trend. Using pre-1961 data, Slemmons and others (1965) described a similar belt of seismic activity that includes the Lake Mead region. They named this belt the Southern Nevada Transverse Zone.

The data of Plate 3 suggests that the Southern Nevada Transverse Zone does not extend far enough to the south to include the Lake Mead activity, and is perhaps only half as wide as the zone postulated by Slemmons and others (1965). In addition, the seismic data of Plate 3 suggests that the Southern Nevada Transverse Zone is not restricted to the southern Basin Range Province, but extends eastward a short distance into the western Colorado Plateau. With the exception of this eastward extension of the seismic zone, the western portion of the Colorado Plateau appears to have a low level of seismic activity.

3.2.6 Regional Tectonic Implications:

Nevada Seismic Zone:

The high earthquake activity in the Nevada Seismic Zone coincides with a broad belt of right-lateral oblique-slip faulting which forms the western margin of the Basin Range Province (see Section 3.1.3 and Plate 1). Within this belt are the generally northwest trending Owens Valley, Death Valley-Furnace Creek, and

Pahrump fault zones. This belt of right-lateral oblique-slip deformation appears to be structurally transitional between the northerly trending dip-slip faulting typical of the Basin Range Province and the northwest trending right-lateral strike-slip faulting of the San Andreas fault system. The change in orientation and style of deformation within this area is apparent in the tectonic compilation of Plate 1.

Seismic refraction, seismic velocity, and gravity data were compiled by Thompson and Talwani (1964) in a study of the crust and upper mantle structure along a traverse across the Sierra Nevada batholith and into central Nevada. This seismic refraction data suggests that the crust thins rapidly from over 40 km in the Sierra Nevada to 22 km near Fallon, Nevada in the western Basin Range Province. The regional gravity pattern along this traverse is postulated by Thompson and Talwani (1964) to indicate the presence of unusually dense crust beneath the Sierra Nevada, and anomalously thick and/or low density mantle beneath the Basin Range Province. The anomalous crust and mantle within the Basin Range Province may be related to the Cenozoic crustal extension in the province. The marked change in style of deformation within this area, coincident with major changes in the thickness and/or density of the crust and mantle, suggests that the earthquake activity of the Nevada Seismic Zone reflects a major crustal discontinuity.

Southern Nevada Transverse Zone:

The east trending Southern Nevada Transverse Zone of seismic activity shown in Plate 3 does not coincide with major known transverse structural features or patterns apparent in ERTS-1 imagery (see Plate 1). Instead, northerly trending normal faults of Tertiary age typical of the Basin Range Province dominate the Cenozoic structure of the Southern Nevada Transverse Zone. However, some transverse structural features are apparent in the ERTS-1 imagery. These include northeast trending structures such as the left-lateral strike-slip Pahranagat shear system (Liggett and Ehrenspeck, 1974*) and possible strike-slip faulting in Kane Springs Wash in Lincoln County, Nevada. In addition, a pervasive pattern of generally east striking faults and joints is exposed in the volcanic cover between Caliente, Nevada, and Cedar City, Utah (see Plate 1). Although the abundance of scarps in Quaternary alluvium indicate that faulting is currently active in the Southern Nevada Transverse Zone, the origin of the seismic activity and its relationship to the structure of the area are not known.

This zone is coincident with a broad belt of middle to late Tertiary felsic volcanism and related plutonism, as shown in the compilation of Plate 2. Genetic relationships between this igneous activity and the present earthquake activity are not apparent.

3.2.7 Conclusions:

This study has documented an interrelationship between Cenozoic tectonic patterns

---

* Appendix L, this report

visible in ERTS-1 MSS imagery, and the distribution of recorded seismic activity in the Argus Exploration Company test site. The following conclusions are indicated:

1. The regional seismic activity of the southern Basin Range Province is higher than that of the adjoining Sierra Nevada and Mojave Desert Blocks.

2. First motion studies and composite fault plane solutions of microearthquakes are consistent with field evidence that both strike-slip and dip-slip faulting are presently active in the southern Basin Range Province.

3. Within the southern Basin Range Province, recorded epicenters are generally clustered within topographic depressions. This clustering is believed to be the result of movement on normal faults which have formed the structural troughs. However, recorded epicenters do not appear to be aligned along specific fault zones.

4. The high seismic activity of the Nevada Seismic Zone of Gumper and Scholz (1971) generally coincides with a belt of right-lateral oblique-slip deformation along the western margin of the Basin Range Province. This belt is postulated to be a major crustal discontinuity, transitional between the extensional tectonics of the Basin Range Province and the right-lateral strike-slip deformation of the San Andreas fault system.

5. The Southern Nevada Transverse Zone of Slemmons and others (1965) is coincident with a belt of Tertiary volcanic and plutonic centers of felsic to intermediate composition. No regional transverse structural patterns coincident with this seismic zone have been recognized in the ERTS-1 imagery.

3.2.8 References Cited in Text:

Allen, C.R., St. Amand, P., Richter, C.F., and Nordquist, J.M., 1965, Relationship between seismicity and geologic structure in the southern California region: Seis. Soc. America Bull., v. 55, p. 753-797.

Bateman, P.C., 1961, Willard D. Johnson and the strike-slip component of fault movement in the Owens Valley, California, earthquake of 1872: Seis. Soc. America Bull., v. 51, p. 483-493

Bechtold, I.C., Liggett, M.A., and Childs, J.F., January 1973, Remote sensing reconnaissance of faulting in alluvium, Lake Mead to Lake Havasu, California, Nevada and Arizona: An application of ERTS-1 satellite imagery: NASA Rept. Inv., NASA-CR-130011, E73-10070, 9 p.

Bucknam, R.C., 1969, Geologic effects of the Benham underground nuclear explosion, Nevada Test Site: Seis. Soc. America Bull., v. 59, p. 2209-2220.

Byerly, Perry, Slemmons, D.B., Tocher, Don, Steinbrugge, K.V., Moran, D. F., and Cloud, W.K., 1956, The Fallon-Stillwater earthquakes of July 6, 1954 and August 23, 1954: Seis. Soc. America Bull., v. 46, p. 1-40.

Callaghan, Eugene, and Gianella, V.P., 1935, The earthquake of January 30, 1934 at Excelsior Mountains, Nevada: Seis. Soc. America Bull., v. 25, p. 161-168.

Carder, D.S., 1970, Reservoir loading and local earthquakes, in Adams, ., ed., Engineering Seismology: The works of man: Geol. Soc. ..rica Engineering Geology Case Histories, no. 8, p. 51-61.

Chakrabarty, S.K., and Richter, C.F., 1949, The Walker Pass earthquakes and structure of the southern Sierra Nevada: Seis. Soc. America Bull., v. 39, p. 93-107.

Dickey, D.D., 1968, Fault displacement as a result of underground nuclear explosions, in Eckel, E.B., ed., Nevada Test Site: Geol. Soc. America Memoir 110, p. 219-232.

Dickey, D.D., 1969, Strain associated with the Benham underground nuclear explosion: Seis. Soc. America Bull., v. 59, p. 2221-2230.

Gianella, V.P., and Callaghan, Eugene, 1934, The Cedar Mountain, Nevada earthquake of December 20, 1932: Seis. Soc. America Bull., v. 24, p. 345-377.

Gumper, F.J., and Scholz, Christopher, 1971, Microseismicity and tectonics of the Nevada Seismic Zone: Seis. Soc. America Bull., v. 61, p. 1413-1432.

Jones, A.E., 1944, Earthquake magnitudes, efficiency of stations, and perceptibility of local earthquakes in the Lake Mead area: Seis. Soc. America Bull., v. 34, p. 161-173.

Liggett, M.A., and Childs, J.F., July 1973, Evidence of a major fault zone along the California-Nevada state line, 35°30' to 36°30' N. latitude: NASA Rept. Inv., NASA-CR-133140, E73-10773, 10 p.

Liggett, M.A., and Ehrenspeck, H.E., January 1974, Pahranagat Shear System, Lincoln County, Nevada: NASA Rept. Inv., NASA-CR-136388, E74-10206, 10 p.

McKeown, F.A., and Dickey, D.D., 1969, Fault displacements and motion related to nuclear explosions: Seis. Soc. America Bull., v. 59, p. 2253-2269.

National Geophysical Data Center, 1972, Earthquake data file, January 1961 through December 1971 (geographically sorted): National Oceanic and Atmospheric Administration, Environmental Data Service, National Geophys. Data Center, p. 256-285.

Page, B.M., 1935, Basin-Range faulting of 1915 in Pleasant Valley, Nevada: Jour. Geology, v. 43, p. 690-707.

Richter, C.F., 1947, The Manix (California) earthquake of April 10, 1947: Seis. Soc. America Bull., v. 37, p. 171-179.

Richter, C.F., 1960, Earthquakes in Owens Valley, California, January-February, 1959: Seis. Soc. America Bull., v. 50, p. 187-196.

Romney, Carl, 1957, Seismic waves from the Dixie Valley-Fairview Peak earthquakes: Seis. Soc. America Bull., v. 47, p. 301-319.

Ryall, Alan, Slemmons, D.B., and Gedney, L.D., 1966, Seismicity, tectonism, and surface faulting in the western United States during historic time: Seis. Soc. America Bull., v. 56, p. 1105-1135.

Sbar, M.L., Barazangi, Muawia, Dorman, James, Scholz, C.H., and Smith, R.B., 1972, Tectonics of the Intermountain Seismic Belt, western United States: Microearthquake seismicity and composite fault plane solutions: Geol. Soc. America Bull., v. 83, p. 13-28.

Scholz, C.H., Barazangi, Muawia, and Sbar, M.L., 1971, Late Cenozoic evolution of the Great Basin, western United States, as an ensialic interarc

basin: Geol. Soc. America Bull., v. 82, p. 2979-2990.

Slemmons, D.B., 1956, Geologic setting for the Fallon-Stillwater earthquakes of 1954: Seis. Soc. America Bull., v. 46, p. 4-9.

Slemmons, D.B., 1957, Geological effects of the Dixie Valley-Fairview Peak, Nevada, earthquakes of December 16, 1954: Seis. Soc. America Bull., v. 47, p. 353-375.

Slemmons, D.B., Steinbrugge, K.V., Tocher, Don, Oakeshott, G.B., and Gianella, V.P., 1959, Wonder, Nevada, earthquakes of 1903: Seis. Soc. America Bull., v. 49, p. 251-265.

Slemmons, D.B., Jones, A.E., and Gimlett, J.I., 1965, Catalog of Nevada earthquakes, 1852-1960: Seis. Soc. America Bull., v. 55, p. 537-583.

Stauder, William, and Ryall, Alan, 1967, Spatial distribution and source mechanism of microearthquakes in central Nevada: Seis. Soc. America Bull., v. 57, p. 1317-1345.

Thompson, G.A., and Talwani, Manik, 1964, Crustal structure from the Pacific Basin to central Nevada: Jour. Geophys. Res., v. 69, no. 22, p. 4813-4837.

Tschanz, C.M., and Pampeyan, E.H., 1970, Geology and mineral deposits of Lincoln County, Nevada: Nevada Bur. Mines Bull. 73, 187 p.

U.S. Department of Interior, 1973, Final environmental statement for the Geothermal Leasing Program: v. 2, chap. 5.

3.2.9 References Used in Compiling Plate 3:

Bateman, P.C., 1961, Willard D. Johnson and the strike-slip component of fault movement in the Owens Valley, California, earthquake of 1872: Seis. Soc. America Bull., v. 51, p. 483-493.

Bayer, K.C., 1972a, Seismicity of the southern Nevada region; December 22, 1971 to July 1, 1972: National Oceanic and Atmospheric Administration, NVO-746-3, 12 p.

Bayer, K.C., 1972b, A preliminary seismicity study of the southern Nevada region for the month of July, 1972: National Oceanic and Atmospheric Administration, NVO-746-4, 9 p.

Callaghan, Eugene, and Gianella, V.P., 1935, The earthquake of January 30, 1934, at Excelsior Mountains, Nevada: Seis. Soc. America Bull., v. 25, p. 161-168.

Chakrabarty, S.K., and Richter, C.F., 1949, The Walker Pass earthquakes and structure of the southern Sierra Nevada: Seis. Soc. America Bull., v. 39, p. 93-107.

Gianella, V.P., and Callaghan, Eugene, 1934, The Cedar Mountain, Nevada, earthquake of December 20, 1932: Seis. Soc. America Bull., v. 24, p. 345-377.

Gumper, F.J., and Scholz, Christopher, 1971, Microseismicity and tectonics of the Nevada Seismic Zone: Seis. Soc. America Bull., v. 61, p. 1413-1432.

Gutenberg, Beno, 1943, Earthquakes and structure in southern California: Geol. Soc. America Bull., v. 54, p. 499-526.

Gutenberg, Beno, 1955, Epicenter and origin time of the main shock on July 21 and travel times of major phases, in Oakeshott, G.B., ed., Earthquakes in Kern County, California during 1952: California Div. Mines Bull. 171, p. 157-163.

Gutenberg, Beno, 1955, The first motion in longitudinal and transverse waves of the main shock and the direction of slip, in Oakeshott, G.B., ed., Earthquakes in Kern County, California during 1952: California Div. Mines Bull. 171, p. 165-170.

Jones, A.E., 1944, Earthquake magnitudes, efficiency of stations, and perceptibility of local earthquakes in the Lake Mead area: Seis. Soc. America Bull., v. 34, p. 161-173.

King, K.W., Bayer, K.C., and Brockman, S.R., 1971, Earthquakes on and around the Nevada Test Site, 1950-1971: National Oceanic and Atmospheric Administration, Earth Sciences Laboratories, CGS-746-12, 29 p.

National Geophysical Data Center, 1972, Earthquake data file, January 1961 through December 1971 (geographically sorted): National Oceanic and Atmospheric Administration, Environmental Data Service, National Geophys. Data Center, p. 256-285.

Richter, C.F., 1947, The Manix (California) earthquake of April 10, 1947: Seis. Soc. America Bull., v. 37, p. 171-179.

Sbar, M.L., Barazangi, Muawia, Dorman, James, Scholz, C.H., and Smith R. B., 1972, Tectonics of the Intermountain Seismic Belt, western United States: Microearthquake seismicity and composite fault plane solutions: Geol. Soc. America Bull., v. 83, p. 13-28.

Slemmons, D.B., Gimlett, J.I., Jones, A.E., Greensfelder, Roger, and Koenig, James, 1965, Earthquake epicenter map of Nevada: Nevada Bur. Mines Map 29, scale 1:1,000,000.

Stauder, William, and Ryall, Alan, 1967, Spatial distribution and source mechanism of microearthquakes in central Nevada: Seis. Soc. America Bull., v. 57, p. 1317-1345.

U.S. Department of Interior, 1973, Final environmental statement for the Geothermal Leasing Program: v. 2, chap. 5, p. 180-182.

3.2.10 Supplemental References:

Albers, J. P., 1967, Belt of sigmoidal bending and right-lateral faulting in the western Great Basin: Geol. Soc. America Bull., v. 78, p. 143-156.

Brogan, G. E., and Slemmons, D. B., 1970, Late Quaternary fault patterns along the Death Valley-Furnace Creek fault zones, Death Valley and Fish Lake Valley, California and Nevada: Geol. Soc. America, Abs. with Programs (Cordilleran section), v. 2, no. 2, p. 74-75.

Dibblee, T. W., Jr., 1967, Areal geology of the western Mojave Desert, California: U.S. Geol. Survey Prof. Paper 522, 153 p.

Gardner, L. S., 1941, The Hurricane fault in southwestern Utah and northwestern Arizona: Am. Jour. Sci., v. 239, no. 4, p. 241-260.

Hill, M. L., 1954, Tectonics of faulting in southern California, in Jahns, R. H., ed., Geology of southern California: California Div. Mines Bull. 170, chap. 4, part 1, p. 5-13.

Larson, E. R., 1957, Minor features of the Fairview fault, Nevada: Seis. Soc. America Bull., v. 47, p. 377-386.

Longwell, C. R., 1930, Faulted fans west of the Sheep Range, southern Nevada: Am. Jour. Sci., v. 20, p. 1-13.

Longwell, C. R., 1950, Tectonic theory viewed from the Basin Ranges: Geol. Soc. America Bull., v. 61, p. 413-434.

McKee, E. H., 1968, Age and rate of movement of the northern part of the Death Valley-Furnace Creek fault zone, California: Geol. Soc. America Bull., v. 79, p. 509-512.

Nielsen, R. L., 1965, Right-lateral strike-slip faulting in the Walker Lane, west-central Nevada: Geol. Soc. America Bull., v. 76, p. 1301-1307.

Pakiser, L. C., 1963, Structure of the crust and upper mantle in the western United States: Jour. Geophys. Res., v. 68, no. 20, p. 5747-5756.

Ross, D. C., 1962, Correlation of granitic plutons across faulted Owens Valley, California: U.S. Geol. Survey Prof. Paper 450-D, p. D86-D88.

Savage, J. C., and Hastie, L. M., 1969, A dislocation model for the Fairview Peak, Nevada, earthquake: Seis. Soc. America Bull., v. 59, p. 1937-1948.

Stewart, J. H., 1967, Possible large right-lateral displacement along fault and shear zones in the Death Valley-Las Vegas area, California and Nevada:

Geol. Soc. America Bull., v. 78, p. 131-142.

Stewart, J.H., 1971, Basin and Range structure: A system of horsts and grabens produced by deep-seated extension: Geol. Soc. America Bull., v. 82, p. 1019-1044

Stewart, J.H., Albers, J.P., and Poole, F.G., 1968, Summary of regional evidence for right-lateral displacement in the western Great Basin: Geol. Soc. America Bull., v. 79, p. 1407-1414.

Wright, L.A., and Troxel, B.W., 1967, Limitations on right-lateral, strike-slip displacement, Death Valley and Furnace Creek fault zones, California: Geol. Soc. America Bull., v. 78, p. 933-950.

Wright, L.A., and Troxel, B.W., 1970, Summary of regional evidence for right-lateral displacement in the western Great Basin: Discussion: Geol. Soc. America Bull., v. 81, p. 2167-2174.

3.3 CENOZOIC VOLCANISM AND PLUTONISM

3.3.1 Introduction:

The map compilation presented in Plate 2 shows the distributions and compositions of late Cenozoic volcanic and intrusive rocks in the Argus Exploration Company test site. This compilation is based on published and unpublished data cited in Section 3.3.7 of this report. The information shown on Plate 2, combined with literature research and field studies, suggests the presence of four generalized volcanic provinces which may be differentiated on the basis of compositional trends, age ranges and eruptive styles. These volcanic provinces are temporally and spatially related to the dominant structural patterns in the test site visible in the ERTS-1 MSS imagery (see Plate 1).

The characteristics of Cenozoic igneous activity and the tectonic patterns delineate the following provinces:

1. The western margin of the Colorado Plateau of southern Utah and northern Arizona is characterized by late Cenozoic normal faults on which movement was temporally and spatially associated with the eruption of relatively small volumes of basaltic rocks.

2. The formation of the pervasive north trending horst and graben structure, typical of the Basin Range Province of southern Nevada, northwestern Arizona and southwestern Utah, was temporally and spatially associated with the eruption of huge volumes of silicic to intermediate ignimbrites and flows and the intrusion of compositionally similar plutonic rocks during late Miocene to Pliocene time.

3. The area of complex late Cenozoic right-lateral oblique-slip faulting along the western margin of the Basin Range Province, east of the Sierra Nevada, is characterized by compositionally diverse and geographically scattered volcanic centers.

4. The Mojave Desert Block of southern California is dominated by northwest trending, right-lateral strike-slip faulting of Miocene to Recent age, which is spatially and temporally associated with volumetrically modest volcanism of predominantly basaltic and intermediate composition.

The above generalizations have notable exceptions, and the provinces are both structurally and volcanogenically gradational. However, the similarities between the respective tectonic and volcanic provinces suggest genetic ties between regional structure and the distribution, chemistry and petrography of igneous centers. Such a relationship has important implications for the origin and evolution of the Basin Range Province and provides a guide in the search for mineral and geothermal resources.

3.3.2 Colorado Plateau Margin:

Along the western margin of the Colorado Plateau in southwestern Utah and north-central Arizona, a large basaltic volcanic province developed synchronously with episodic, late Cenozoic normal faulting. Within this province, numerous separate and coalesced basalt fields occur within a broad belt that extends southward from the high plateaus of south-central Utah, through the western Grand Canyon region and into the San Francisco Mountains, Verde River and Mount Hope regions of Arizona. Most of the lava in these separate volcanic fields consists of nearly uniform alkali-olivine basalt (Best and Brimhall, 1970; Lowder, 1973) with subordinate occurrences of tholeiitic or andesitic basalt (McKee and Anderson, 1971; Lowder, 1973).

Within this belt of volcanism, many of the local basalt fields and their vent areas are associated with specific structures. For example, in northern Arizona numerous small cinder cones and basalt flows are located near or along subsidiary strands of the Hurricane and Toroweap-Sevier fault zones (see Plate 1; ERTS-1 Frame #1069-17432, Figure 9; and Hamblin, 1970a). In the Markagunt Plateau region of southwestern Utah, several cinder cones occur at or near the intersections of prominent joint systems or minor faults (Cook, 1960; Threet, 1963, p. 105).

Geochronologic data (Mackin, 1960, p. 97; Armstrong, 1970; Noble and McKee, 1972) and field studies (Cook, 1957; 1960) indicate that initial movement on the Hurricane fault, approximately 20 million years ago, was temporally associated with silicic volcanism and plutonism in the adjacent Basin Range Province. Subsequent, late Miocene to Recent movement on the Hurricane and other faults on the Colorado Plateau has been accompanied or followed by distinct episodes of basalt extrusion. This relationship of volcanism and structure has been documented in the St. George basin of southwestern Utah (Gardner, 1941; Cook, 1960; Hamblin, 1963, 1970b), and in the western Grand Canyon and southern Colorado Plateau regions of Arizona (Wilson and others, 1969; Hamblin, 1970b; McKee and Anderson, 1971).

3.3.3 Southern Basin Range Province:

The volcanism and plutonism of the southern Basin Range Province are characterized by huge volumes of silicic to intermediate ignimbrites, flows and chemically similar intrusive bodies. Most of this igneous activity occurred during late Tertiary time and was both spatially and temporally associated with Basin Range normal faulting. The distribution of intermediate to silicic igneous rocks of Cenozoic age shown in Plate 2, suggests the existence of three or four distinctive volcanic terranes within the southern Basin Range Province. The locations and characteristics of these volcanic terranes are summarized below, proceeding from west to east across the test site.

Nye County Volcanism:

A large volcanic terrane of intermediate to silicic composition occurs in southern

Nye County, Nevada. The geology of this region is discussed by Ekren (1968), Ekren and others (1968, 1971), Cornwall (1972) and in several studies of mining areas associated with the Tertiary volcanism (see for example, Albers and Kleinhampl, 1970). Based on age and general compositional ranges, the extrusive and intrusive rocks of this terrane fall into two distinct groupings: a late Oligocene to middle Miocene succession (Marvin and others, 1970) of predominantly intermediate composition, and a late Miocene to Pliocene sequence of largely silicic composition.

Complex assemblages of intrusive and extrusive rocks, ranging in age from about 26.5 to 18 million years (Anderson and Ekren, 1968; Cornwall, 1972) are exposed in large horsts that form the Cactus, Kawich and Belted Ranges, and the Goldfield Hills of southern Nye County. The volcanic rocks consist largely of voluminous calcalkaline andesitic flows, breccias, and ignimbrites and represent the southern end of a broad belt of volcanic activity which extends northward and westward into central Nevada and eastern California (see Plate 2). Emplacement of these widespread volcanic rocks predated much of the Basin Range faulting (Christiansen and Lipman, 1972; Noble, 1972).

The distinct late Miocene to Pliocene episode of silicic volcanism in southern Nye County is related to at least 10 major eruptive centers, half of which are believed to be collapsed calderas. The eruptive centers are loosely grouped along a northerly trend and their voluminous ignimbrites and flows overlap the older volcanic succession to the north. The silicic volcanism appears to have begun in the Mt. Helen region about 15-16 million years ago and to have ended with eruptions from the Black Mountain caldera about 6.2 million years ago. The bulk of the volcanism occurred between about 13.5 and 10 million years ago in the Jackass Flats centers, the Bullfrog Hills caldera and the Timber Mountain caldera. Since middle Pliocene time, only scattered basaltic volcanism has occurred in this area.

Variations in the thickness and distribution of the volcanic units, and direct structural evidence (see for example, Ekren and others, 1968) indicate that Basin Range normal faulting in the Nye County area was synchronous with the bulk of the silicic igneous activity. The Nye County volcanic terrane lies entirely north of the western termination of the Las Vegas shear zone, on which major right-lateral strike-slip displacement was at least in part synchronous with normal faulting and igneous activity. Guided by analysis of ERTS-1 imagery, a structural model has been proposed by Liggett and Childs (March 1974*) which relates right-lateral strike-slip displacement on the Las Vegas shear zone to volcanism, plutonism, and inferred crustal extension in southern Nye County and in the Black Mountains area south of Lake Mead, Nevada.

Black Mountains Volcanism:

---

* Appendix O, this report

A silicic to intermediate volcanic terrane, similar to that of Nye County, forms a north-south trending belt along the Colorado River from south of Lake Mead, Nevada, to near Parker, Arizona (see ERTS-1 Frame #1106-17495, Figure 4, east half). This volcanic terrane lies south of the eastern termination of the Las Vegas shear zone. Plutons, dike swarms and normal faults within this belt are oriented with northerly trends (Bechtold and others, 1972*) and are well expressed in ERTS-1 imagery. In the southern Black Mountains, a probable caldera structure has been mapped in the Oatman district (Thorson, 1971). A composite batholith of Miocene age is exposed west of the Colorado River in the Newberry and Eldorado Mountains, and similar plutons have been recognized in other parts of this terrane. These plutons range in composition from leucocratic granite to gabbro, although granite, quartz monzonite and quartz diorite predominate (Volborth, 1973). The regional geology of this area has been discussed by Longwell (1963) and by Anderson and others (1972). The structural setting and the synchroneity of volcanism and faulting are discussed by Liggett and Childs (March 1974**).

Lincoln County Volcanism:

Several important silicic volcanic and plutonic centers of middle to late Miocene age occur in Lincoln County, Nevada. Igneous rocks from these centers form the western part of a northeast trending belt of volcanic rocks that extends from southeastern Nevada into southwestern Utah (see Plate 2, and ERTS-1 Frame #1106-17492, Figure 7, northeast quarter).

At the eastern end of this group of centers, the Caliente depression has been identified as the probable source of voluminous and widespread ignimbrites found in southeastern Nevada and adjacent Utah (Noble and McKee, 1972). These ignimbrites range in age from approximately 21-17 million years (Mackin, 1960; Cook, 1965).

In the Clover Mountains about 15 km south of Caliente, a large rhyolitic igneous complex, possibly a caldera, has been mapped at a reconnaissance scale by Tschanz and Pampeyan (1970). In the southern Delamar Range, the Kane Springs Wash volcanic center is thought to be the source of regionally extensive ignimbrites and lavas approximately 14-12 million years in age (Noble, 1968; Armstrong, 1970; Noble and McKee, 1972). Several small intrusive bodies of intermediate to silicic composition occur in the Delamar Range, Clover Mountains, and Caliente depression. Supported by analysis of ERTS-1 imagery, field reconnaissance along the west side of the Delamar Range has indicated that at least some of these small stocks and dikes are intrusive into the volcanic cover.

The structural setting of the Lincoln County volcanic terrane is not well known; however, deformation is regionally dominated by northerly trending normal faults

---

* Appendix A, this report

** Appendix O, this report

typical of the Basin Range Province (see Plate 1). This faulting is known to be at least in part synchronous with the silicic volcanism (Mackin, 1960; Cook, 1965; Noble, 1972). The youngest known volcanic rocks of this region are local Pliocene basalt flows erupted approximately 8 million years ago (Armstrong, 1970, p. 212).

Southwestern Utah Intermediate and Silicic Volcanism:

Several large, shallow intrusions and associated volcanic rocks of predominantly intermediate composition form a northeast trending belt extending from near St. George nearly to Black Rock in southwestern Utah (see Plate 3). These igneous rocks have intruded and blanketed a widespread succession of volcanic and sedimentary rocks of late Oligocene to middle Miocene age. The intrusive bodies are believed to be laccolithic protrusions of a large igneous mass (Cook, 1960) which invaded along the axis of a northeast trending anticlinal structure of Laramide age (Cook, 1960; Mackin, 1960). At least two of the laccolithic bodies reached the surface and vented voluminous dacitic to latitic tuffs and flows. The largest of the intrusions, the Pine Valley Mountains laccolith (see ERTS-1 Frame #1051-17425, Figure 8, left center) intruded its own extrusive cover of thick latite flows (Cook, 1957, 1960) to form a body which is nearly 1 km thick and exceeds 100 square km in area.

Geochronologic data (Armstrong, 1970; Noble and McKee, 1972) indicate that this episode of igneous activity occurred approximately 21-19 million years ago. Field studies in southwestern Utah by Cook (1957, 1960) and others suggest that the initiation of Basin Range faulting, as illustrated by the Hurricane fault zone, also occurred during this time.

A later period of predominantly silicic volcanism is represented by ignimbrites and flows ranging in age from about 19 to less than 14 million years (Mackin, 1960, p. 98; Armstrong, 1970; Noble and McKee, 1972). These silicic volcanic rocks are associated with small intrusive bodies and eruptive centers that tend to be aligned along Basin Range faults (Christiansen and Lipman, 1972). The late Miocene silicic volcanic rocks in southwestern Utah are overlain by a succession of basaltic rocks, which are spatially and temporally associated with episodic normal faulting along the Colorado Plateau margin.

3.3.4 Sierra Nevada and Western Basin Range Province:

An area believed to be transitional between the extensional deformation of the Basin Range Province and the strike-slip tectonics of the San Andreas fault system (Hamilton and Myers, 1966) lies along the western margin of the Basin Range Province in eastern California (see Section 3.1.3). This area is characterized by Cenozoic volcanic and plutonic centers of varied compositions, ages and structural associations. Although it is beyond the scope of this summary to review each of these igneous centers, the following examples illustrate the diversity of structural and volcanic associations that characterize this province.

Central to Southern Sierra Nevada, California:

Cenozoic volcanism within the Sierra Nevada includes a wide range of compositions and eruptive styles. Because of differences in the regional tectonic evolution and Cenozoic volcanism of the central and the southern part of the Sierra Nevada, these two regions are considered separately.

In the central Sierra Nevada north of the Tuolomne River, Tertiary volcanism began with widespread eruption of rhyolitic tuffs during a period which lasted from about 33-20 million years ago (Dalrymple, 1964; Slemmons, 1966). These volcanic units extend far beyond the present eastern margin of the Sierra Nevada and are believed to have been erupted from sources located along and east of the present mountain range (Slemmons, 1966; Gilbert and others, 1968).

Latite flows and tuffs unconformably overlie all older volcanic sequences in the Sonora Pass region and were erupted during a geochronologically well-defined episode of volcanism about 9.5 million years ago (Noble and others, 1974). The latite ignimbrites extend eastward from the Sierra Nevada into western Nevada, and their emplacement predates most of the uplift of the range (Slemmons, 1966; Gilbert and others, 1968; Christiansen and Lipman, 1972).

Major uplift and tilting of the central Sierra Nevada occurred during middle to late Pliocene time and was generally synchronous with the emplacement of voluminous andesitic and basaltic breccias and flows which range from about 9 million to less than 6 million years in age (Dalrymple, 1964; Slemmons, 1966). These flows and breccias are locally capped by late Pliocene basalt flows which grade northward to regionally continuous flood basalts. Scattered eruptions of rhyolitic to basaltic volcanic rocks within and along the eastern Sierra Nevada range front have accompanied late Pliocene to Recent tectonism (Slemmons, 1966; Bateman and Wahrhaftig, 1966; Christensen and others, 1969).

The Sierra Nevada block south of the Tuolomne River has undergone nearly continuous erosion during most of the Cenozoic (see Section 3.1.3) and pre-Pliocene volcanic rocks are almost entirely absent from this region. Volcanism in the southern Sierra Nevada appears to fall into three main episodes, occurring about 9-10 million, 2-4 million, and less than 1 million years ago (Bateman and Wahrhaftig, 1966). This volcanic activity is characterized by scattered basalt and andesite flows, and rhyolitic to latitic tuffs, flows and domes.

Although the bulk of volcanism is spatially associated with faulting along the Sierra Nevada range front, several small eruptive centers with apparent structural associations are located in the central and eastern part of the range. Near the mouth of the Little Kern River in Kern Canyon, small basalt fields of late Pliocene age (Dalrymple, 1963) are located over and along the trace of the north striking Kern Canyon fault (Matthews and Burnett, 1965; Bateman and Wahrhaftig, 1966). Field reconnaissance of lineaments visible in ERTS-1 imagery over the southern Sierra Nevada (see ERTS-1 Frame #1162-18011, Figure 13, northwest quarter;

and Liggett and Childs, February 1974*) has suggested structural control of the locations of Quaternary cinder cones in the Toowa volcanic field (Webb, 1950; see also Mayo, 1947, p. 501), and of two nearby latite domes, Monache and Templeton Mountains, of probable Quaternary age (Bateman and Wahrhaftig, 1966). These volcanic centers are situated at the intersections of generally north and west trending lineaments, which appear to be zones of crustal weakness (Mayo, 1947, p. 499; Liggett and Childs, February 1974*).

Mono Basin and Long Valley, California:

Mono Basin is an elongate, northeast trending structural and topographic depression, which terminates on the west against the range-front faults of the Sierra Nevada. Geochronologic and geologic studies of this region, synthesized by Gilbert and others (1968) and by Christensen and others (1969), have established that the structural development of the basin and related volcanism postdates Miocene to early Pliocene volcanism of the Sierra Nevada and Basin Range Province.

The bulk of volcanic activity in the Mono Basin occurred approximately 3.5-1.5 million years ago, and began with the eruption of widespread, thin olivine basalt flows. These flows form a nearly continuous terrane of approximately 500 square km that extends from the Excelsior Mountains region on the eastern margin of the Mono Basin southwestward to the Sierra Nevada. This basaltic terrane is cut by a pervasive system of northeast trending faults of probable left-lateral strike-slip movement (Gilbert and others, 1968; Gilbert and Reynolds, 1973). In the southeast part of the Mono Basin, individual faults of this system typically bend southward and intersect or merge with a northerly trending system of normal faults. Many segments of this complex fault pattern are apparent in ERTS-1 imagery (see Plate 1; and ERTS-1 Frame #1163-18063, Figure 14, top center). The zone of intersection between the two synchronous fault systems is believed to have formed an elongate belt of crustal extension, from which additional, extensive basalt flows were vented (Gilbert and others, 1968). Although such widespread basaltic volcanism ceased by latest Pliocene time, continued movement on this fault system appears to have localized small Quaternary protrusions and flows of latite, rhyolite, andesite and minor basalt (Gilbert and others, 1968; Christensen and others, 1969).

Long Valley is expressed in ERTS-1 imagery as a roughly elliptical topographic depression about 30 km by 20 km in size, located about 35 km south of the Mono Basin (see ERTS-1 Frame #1163-18063, Figure 14, upper center). On the south and west it abuts against the Mammoth embayment of the eastern Sierra Nevada escarpment. Long Valley is bounded on all sides by known or geophysically inferred faults (Pakiser, 1960; Pakiser and others, 1964; Strand, 1967; Christensen and others, 1969) which formed as a result of subsidence and resurgence of a large caldera.

---

* Appendix M, this report

The general structural and volcanic history of the area is summarized in studies by Pakiser and others (1964); Gilbert and others (1968); and Christensen and others (1969). Important volcanism in this area began about 1 million years ago with rhyolitic volcanism in the Glass Mountain region. This volcanism was followed about 0.7 million years ago by the eruption of the voluminous Bishop Tuff, and the simultaneous subsidence of the Long Valley caldera. Subsequent resurgent doming within the caldera has been accompanied by eruption of rhyolitic to basaltic rocks (Bailey, 1973) from several prominent centers aligned along a northerly trend between Mammoth Mountain and Mono Lake (see Plate 2; and ERTS-1 Frame #1163-18063, Figure 14, upper center). The area is considered to be volcanically active.

Owens Valley Volcanic Field, California:

A volcanic field consisting of numerous Quaternary cinder cones and related alkali basalt flows occurs in Owens Valley between the Sierra Nevada and the White-Inyo Mountains escarpments, and extends from south of Big Pine to north of Independence, California (see Plate 2; and ERTS-1 Frame #1163-18063, Figure 14, southeast quarter). The most prominent volcanic centers of the region are Crater Mountain and Red Mountain, and several small cinder cones and basalt flows are situated over, and locally offset by strands of the active Owens Valley fault zone (see Plate 1; Bateman, 1965; and Strand, 1967). As noted in Section 3.1.3, the Owens Valley fault zone is postulated to have undergone post-Cretaceous right-lateral displacement of up to a few kilometers (see, for example, Ross, 1962).

The twenty or more basaltic cinder cones and fissure vents in the southern part of the Owens Valley volcanic field are aligned along the northerly trending normal faults of the Sierran escarpment (Moore, 1963; Matthews and Burnett, 1966). Many of these faults cut alluvium as well as flows and cinder cones of various ages (Moore, 1963), indicating a close relationship between episodic volcanism and recurrent fault movements.

Saline Range Volcanic Field, California:

The Saline Range volcanic field is a regionally extensive and voluminous succession of trachyandesitic basalt flows of late Pliocene age. The main field locally attains a thickness of 300 meters and forms a rhombohedrally shaped area of more than 300 square km bordered on the north and south by Eureka and Saline Valleys, respectively (see Jennings, 1958; Ross, 1967; Strand, 1967). Geochronologic and field studies by Ross (1967, 1970) indicate that widespread fissure eruptions of trachyandesite began shortly after the emplacement of small, compositionally similar intrusive bodies about 3.5 million years ago. The bulk of the volcanism ended by about 2.5 million years ago.

Field investigations and geochronologic evidence indicate that the volcanic activity in the Saline Range was synchronous with, and controlled by the development of a pervasive system of north to northeast striking normal faults. As outlined in Section 3.1.3, this belt of northwest-southeast extension is located between the

Owens Valley and Death Valley-Furnace Creek fault zones, both of which are known to have undergone strike-slip displacement during the Cenozoic (see Plate 1). This regional structural setting, and the characteristic local structure of the Saline Range are clearly expressed in ERTS-1 MSS Frame #1126-18010 (Figure 6, south half).

Kingston Peak Pluton, California:

The Kingston Peak pluton in northeastern San Bernardino County is a laccolithic body of porphyritic quartz monzonite intruded into Precambrian metamorphic and Paleozoic sedimentary rocks. This pluton has been radiometrically dated at between 18.6 and 12.5 million years (Sutter, 1968; Armstrong, 1970) and is the probable source of widespread rhyolitic and dacitic volcaniclastic sedimentary rocks in the area.

The Kingston Peak pluton is located north of, and adjacent to the eastern termination of the Garlock fault (see Plates 1 and 2; and ERTS-1 Frame #1125-17554, Figure 12, east central portion). Regional evidence for the onset of Basin Range normal faulting (Ekren and others, 1968) suggests that movement on the Garlock fault began approximately 26 million years before present and was at least in part synchronous with emplacement of the Kingston Peak pluton.

Silver Peak Volcanic Center, Nevada:

The Silver Peak volcanic center of Esmeralda County, Nevada, is located adjacent to the Death Valley-Furnace Creek fault zone, which terminates in northern Fish Lake Valley 40 km northwest of Silver Peak (see Plates 1 and 2). Right-lateral displacement of approximately 1 km since Pliocene time and nearly 50 km since Jurassic time has been postulated for the northern part of the Death Valley-Furnace Creek fault zone (McKee, 1968). The bulk of volcanism associated with the Silver Peak center occurred between about 6.1 and 4.8 million years ago (Robinson and others, 1968) and was synchronous with movement on the Death Valley-Furnace Creek fault zone.

Coso Range Volcanic Field, California:

A compositionally bimodal volcanic field of late Pliocene to Quaternary age is centered in the Coso Mountains region east and south of Owens Lake. The bulk of the volcanic rocks occurs as a succession of thin olivine basalt flows and numerous associated cinder cones (see Jennings, 1958; Jennings and others, 1962). This widespread basaltic volcanism was contemporaneous with less abundant silicic volcanism (Babcock and Wise, 1973) in the form of rhyolitic domes and tuff cones in the southern part of the field (see ERTS-1 Frame #1162-18011, Figure 13, center). These bimodal volcanic rocks unconformably overlie a succession of andesitic to basaltic flows and pyroclastic rocks of probable Pliocene age (Jennings, 1958; Hall and MacKevett, 1958).

The Coso Mountains region is dominated structurally by swarms of northerly striking normal faults that intersect a second system of northwest striking faults (see

ERTS-1 Frame #1162-18011, Figure 13). One of these northwest trending faults, the Darwin tear fault, has a known left-lateral displacement of 0.7 km (Hall and MacKevett, 1958).

Synchronous interaction of the two fault systems is indicated by the local merging of the two fault trends, the crosscutting of one fault system by the other, and the displacement of Quaternary alluvial and volcanic units by both systems (see Jennings and others, 1962). The close association of the basaltic and rhyolitic volcanism with both fault systems (Babcock and Wise, 1973) is exemplified by numerous vents in the region east of Little Lake that are aligned along both fault trends (see Jennings and others, 1962).

3.3.5 Mojave Desert, California:

Many separate intrusive centers and volcanic fields of Miocene to Recent age form a broad southeast trending belt of igneous activity in the Mojave Desert. This igneous activity occurs largely within the area of the Mojave Desert structural block which is dominated by a pervasive system of northwest trending faults of probable strike-slip displacement (see Plate 1 and Section 3.1.5).

Radiometric data suggest that volcanism in the Mojave Desert began about 22 million years ago (Armstrong and Higgins, 1973). Since early Miocene time, scattered volcanism accompanied the development of elongate depositional basins bounded by the northwest striking faults (Hewett, 1954; Dibblee, 1967). The Miocene and Pliocene volcanism is characterized by numerous local sequences of intermediate to silicic extrusive rocks and related hypabyssal intrusive rocks, intercalated with or capped by basaltic to andesitic volcaniclastic rocks and flows (Dibblee, 1967; Christiansen and Lipman, 1972). Quaternary volcanism in this region consists mostly of basaltic flows of local extent and modest volume, erupted from many separate vents (Dibblee, 1967; Wise, 1969).

A close interrelationship between the northwest striking faults and Tertiary volcanism is apparent in several areas of the Mojave Desert. In the Bullion Mountains, for example, movement on the Bullion fault followed shortly after eruption of a succession of basaltic and intermediate volcanic rocks. At least one sequence of basalt flows was vented from conduits along the Bullion fault and related breaks, and was later offset by further movement on the fault (Bassett and Kupfer, 1964, p. 37-39).

Synchroneity of Pleistocene and Recent volcanism and faulting is also evident. At the Pisgah and Sunshine Peak eruptive centers, for example, cinder cones are aligned over strands of the Pisgah fault, and basalt flows both predate and postdate movement on this fault (Bassett and Kupfer, 1964; Rogers, 1967; Wise, 1969).

3.3.6 Conclusions:

The purpose of this study has been to investigate the interrelationships between the distributions and characteristics of Cenozoic igneous activity and regional structural

patterns expressed in ERTS-1 MSS imagery over the Argus Exploration Company test site.

The data summarized here and in the accompanying tectonic and igneous map compilations (Plates 1 and 2) indicate close temporal and spatial relationships between Cenozoic plutonism, volcanism and deformation. These relationships are consistent within the terranes defined by patterns and styles of tectonic deformation. These include the structurally stable Colorado Plateau, the major extensional tectonics of the Basin Range Province, the right-lateral strike-slip deformation of the Mojave Desert Block, and a zone of right-lateral oblique-slip displacement in the western Basin Range Province adjacent to the Sierra Nevada.

The following general associations between volcanism and tectonism are postulated for the area of this investigation:

1. Large silicic volcanic and plutonic centers are located in terrane which has undergone regional crustal distension on major dip-slip fault systems. Although silicic igneous activity in many areas was synchronous with adjacent systems of strike-slip faulting, the igneous centers are not aligned along or displaced by strike-slip faults.

2. Predominantly basaltic to andesitic volcanism of modest volume is spatially associated and synchronous with systems of major strike-slip faulting and is also associated with areas of normal faulting of small to moderate displacement.

3. Within a local area, volumetrically minor basaltic volcanism has generally post-dated voluminous silicic to intermediate igneous activity.

The inferred temporal and spatial associations between igneous activity and structural deformation are supported by the homogeneity of igneous activity within the structural provinces of the test site and by the alignment and localization of igneous centers along key structural features or systems. However, this association does not prove a necessary cause-and-effect relationship between tectonism and volcanogenesis. It is possible that tectonic features may tap compositionally distinct magma sources at different depths or may influence magma genesis through control of heat flow or other physical or chemical parameters. Moreover, both structural and igneous activity may be the results of primary subcrustal processes.

Although considerations of the driving mechanisms for regional structural deformation and the possible physico-chemical controls of magma generation are beyond the scope of this study, it is hoped that the framework proposed here will help to define specific questions as a guide to investigation of these fundamental problems. An understanding of the relationship between tectonics and igneous activity will have important practical applications in the search for geothermal energy sources and the exploration of mineral deposits associated with these processes.

The ERTS-1 MSS imagery has proven to be an effective tool for interpreting regional

patterns of Cenozoic structural deformation, and for studying the local structural settings of volcanic and plutonic centers. This task was previously possible only with regional map compilations of limited accuracy and scope.

3.3.7 References Cited in Text:

Albers, J.P., and Kleinhampl, F.J., 1970, Spatial relation of mineral deposits to Tertiary volcanic centers in Nevada: U.S. Geol. Survey Prof. Paper 700-C, p. C1-C10.

Anderson, R.E., and Ekren, E.B., 1968, Widespread Miocene igneous rocks of intermediate composition, southern Nye County, Nevada, in Eckel, E.B., ed., Nevada Test Site: Geol. Soc. America Memoir 110, p. 57-63.

Anderson, R.E., Longwell, C.R., Armstrong, R.L., and Marvin, R.F., 1972, Significance of K-Ar ages of Tertiary rocks from the Lake Mead region, Nevada-Arizona: Geol. Soc. America Bull., v. 83, p. 273-288.

Armstrong, R.L., 1970, Geochronology of Tertiary igneous rocks, eastern Basin and Range Province, western Utah, eastern Nevada and vicinity, U.S.A.: Geochimica et Cosmochimica Acta, v. 34, p. 203-232.

Armstrong, R.L., and Higgins, R.E., 1973, K-Ar dating of the beginning of Tertiary volcanism in the Mojave Desert, California: Geol. Soc. America Bull., v. 84, p. 1095-1100.

Babcock, J.W., and Wise, W.S., 1973, Petrology of contemporaneous Quaternary basalt and rhyolite in the Coso Mountains, California: Geol. Soc. America, Abs. with Programs (Cordilleran section), v. 5, no. 1, p. 6.

Bailey, R.A., 1973, Post-subsidence volcanism and structure of Long Valley caldera, California: Geol. Soc. America, Abs. with Programs (Cordilleran section), v. 5, no. 1, p. 7.

Bassett, A.M., and Kupfer, D.H., 1964, A geologic reconnaissance in the southeastern Mojave Desert, California: California Div. Mines and Geology Spec. Rept. 83, 43 p.

Bateman, P.C., 1965, Geology and tungsten mineralization of the Bishop district, California: U.S. Geol. Survey Prof. Paper 470, 208 p.

Bateman, P.C., and Wahrhaftig, Clyde, 1966, Geology of the Sierra Nevada, in Bailey, E.H., ed., Geology of northern California: California Div. Mines and Geology Bull. 190, p. 107-172.

Bechtold, I.C., Liggett, M.A., and Childs, J.F., November 1972, Structurally controlled dike swarms along the Colorado River, northwestern Arizona and southern Nevada (abs.): NASA Rept. Inv., NASA-CR-128390, E72-10192, 2 p.

Best, M.G., and Brimhall, W.H., 1970, Late Cenozoic basalt types in the western Grand Canyon region, in Hamblin, W.K., and Best, M.G., eds., Guidebook to the geology of Utah: Utah Geol. Soc., no. 23, p. 57-74.

Christensen, M.N., Gilbert, C.M., Lajoie, K.R., and Al-Rawi, Yehya, 1969, Geological-geophysical interpretation of Mono basin, California-Nevada: Jour. Geophys. Res., v. 74, no. 22, p. 5221-5239.

Christiansen, R.L., and Lipman, P.W., 1972, Cenozoic volcanism and plate-tectonic evolution of the western United States, Part II, late Cenozoic: Royal Soc. London Philos. Trans., series A, v. 271, p. 249-284.

Cook, E.F., 1957, Geology of the Pine Valley Mountains, Utah: Utah Geol. and Mineralog. Survey Bull. 58, 111 p.

Cook, E.F., 1960, Geologic atlas of Utah, Washington County: Utah Geol. and Mineralog. Survey Bull. 70, 119 p.

Cook, E.F., 1965, Stratigraphy of Tertiary volcanic rocks in eastern Nevada: Nevada Bur. Mines Rept. 11, 61 p.

Cornwall, H.R., 1972, Geology and mineral deposits of southern Nye County, Nevada: Nevada Bur. Mines and Geology Bull. 77, 49 p.

Dalrymple, G.B., 1963, Potassium-argon dates of some Cenozoic volcanic rocks of the Sierra Nevada, California: Geol. Soc. America Bull., v. 74, p. 379-390.

Dalrymple, G.B., 1964, Cenozoic chronology of the Sierra Nevada, California: California Univ. Pubs. Geol. Sci., v. 47, 41 p.

Dibblee, T.W., Jr., 1967, Areal geology of the western Mojave Desert, California: U.S. Geol. Survey Prof. Paper 522, 153 p.

Ekren, E.B., 1968, Geologic setting of Nevada Test Site and Nellis Air Force Range, in Eckel, E.B., ed., Nevada Test Site: Geol. Soc. America Memoir 110, p. 11-19.

Ekren, E.B., Rogers, C.L., Anderson, R.E., and Orkild, P.P., 1968, Age of Basin and Range normal faults in Nevada Test Site and Nellis Air Force Range, Nevada, in Eckel, E.B., ed., Nevada Test Site: Geol. Soc. America Memoir 110, p. 247-250.

Ekren, E.B., Anderson, R.E., Rogers, C.L., and Noble, D.C., 1971, Geology of northern Nellis Air Force Base Bombing and Gunnery Range, Nye County, Nevada: U.S. Geol. Survey Prof. Paper 651, 91 p.

Gardner, L.S., 1941, The Hurricane fault in southwestern Utah and northwestern Arizona: Am. Jour. Sci., v. 239, no. 4, p. 241-260.

Gilbert, C.M., Christensen, M.N., Al-Rawi, Yehya, and Lajoie, K.R., 1968, Structural and volcanic history of Mono Basin, California-Nevada, in Coats, R.R., Hay, R.L., and Anderson, C.A., eds., Studies in volcanology: Geol. Soc. America Memoir 116, p. 275-329.

Gilbert, C.M., and Reynolds, M.W., 1973, Character and chronology of basin development, western margin of the Basin and Range Province: Geol. Soc. America Bull., v. 84, p. 2489-2510.

Hall, W.E., and, MacKevett, E.M., 1958, Economic Geology of the Darwin quadrangle, Inyo County, California: California Div. Mines Spec. Rept. 51, 73 p.

Hamblin, W.K., 1963, Late Cenozoic basalts of the St. George basin, Utah, in Heylmun, E.B., ed., Guidebook to the geology of southwestern Utah: Intermountain Assoc. Petroleum Geologists Guidebook 12, p. 84-89.

Hamblin, W.K., 1970a, Structure of the western Grand Canyon region, in Hamblin, W.K., and Best, M.G., eds., Guidebook to the geology of Utah: Utah Geol. Soc., no. 23, p. 3-20.

Hamblin, W.K., 1970b, Late Cenozoic basalt flows of the western Grand Canyon, in Hamblin, W.K., and Best, M.G., eds., Guidebook to the geology of Utah: Utah Geol. Soc., no. 23, p. 21-38.

Hamilton, Warren, and Myers, W.B., 1966, Cenozoic tectonics of the western United States: Rev. Geophysics, v. 4, no. 4, p. 509-549.

Hewett, D.F., 1954, General geology of the Mojave Desert region, California, in Jahns, R.H., ed., Geology of southern California: California Div. Mines Bull. 170, chap. 2, p. 5-20.

Jennings, C.W., 1958, Geologic map of California, Death Valley sheet, Olaf P. Jenkins edition: California Div. Mines, scale 1:250,000.

Jennings, C.W., Burnett, J.L., and Troxel, B.W., 1962, Geologic map of California, Trona sheet, Olaf P. Jenkins edition: California Div. Mines and Geology, scale 1:250,000.

Liggett, M.A., and Childs, J.F., February 1974, Structural lineaments in the southern Sierra Nevada, California: NASA Rept. Inv., NASA-CR-136665, E74-10279, 9 p.

Liggett, M.A., and Childs, J.F., March 1974, Crustal extension and transform faulting in the southern Basin Range Province: NASA Rept. Inv., NASA-CR-137256, E74-10411, 28 p.

Longwell, C.R., 1963, Reconnaissance geology between Lake Mead and Davis Dam, Arizona-Nevada: U.S. Geol. Survey Prof. Paper 374-E, 51 p.

Lowder, G.G., 1973, Late Cenozoic transitional alkali olivine-tholeiitic basalt and andesite from the margin of the Great Basin, southwest Utah: Geol. Soc. America Bull., v. 84, p. 2993-3012.

Mackin, J.H., 1960, Structural significance of Tertiary volcanic rocks in southwestern Utah: Am. Jour. Sci., v. 258, p. 81-131.

Marvin, R.F., Byers, F.M., Jr., Mehnert, H.H., Orkild, P.P., and Stern, T.W., 1970, Radiometric ages and stratigraphic sequence of volcanic and plutonic rocks, southern Nye and western Lincoln Counties, Nevada: Geol. Soc. America Bull., v. 81, p. 2657-2676.

Matthews, R.A., and Burnett, J.L., 1965, Geologic map of California, Fresno sheet, Olaf P. Jenkins edition: California Div. Mines and Geology, scale 1:250,000.

Mayo, E.B., 1947, Structure plan of the southern Sierra Nevada, California: Geol. Soc. America Bull., v. 58, p. 495-504.

McKee, E.H., 1968, Age and rate of movement of the northern part of the Death Valley-Furnace Creek fault zone, California: Geol. Soc. America Bull., v. 79, p. 509-512.

McKee, E.H., and Anderson, C.A., 1971, Age and chemistry of Tertiary volcanic rocks in north-central Arizona and relation of the rocks to the Colorado Plateaus: Geol. Soc. America Bull., v. 82, p. 2767-2782.

Moore, J.G., 1963, Geology of the Mount Pinchot quadrangle, southern Sierra Nevada, California: U.S. Geol. Survey Bull. 1130, 152 p.

Noble, D.C., 1968, Kane Springs Wash volcanic center, Lincoln County, Nevada, in Eckel, E.B., ed., Nevada Test Site: Geol. Soc. America Memoir 110, p. 109-116.

Noble, D.C., 1972, Some observations on the Cenozoic volcano-tectonic evolution of the Great Basin, western United States: Earth and Planetary Sci. Letters, v. 17, p. 142-150.

Noble, D.C., and McKee, E.H., 1972, Description and K-Ar ages of volcanic units of the Caliente volcanic field, Lincoln County, Nevada, and

Washington County, Utah: Isochron/West, no. 5, p. 17-24.

Noble, D. C., Slemmons, D. B., Korringa, M. K., Dickinson, W. R., Al-Rawi, Yehya, and McKee, E. H., 1974, Eureka Valley Tuff, east-central California and adjacent Nevada: Geology, v. 2, p. 139-142.

Pakiser, L. C., 1960, Transcurrent faulting and volcanism in Owens Valley, California: Geol. Soc. America Bull., v. 71, p. 153-160.

Pakiser, L. C., Kane, M. F., and Jackson, W. H., 1964, Structural geology and volcanism of Owens Valley region - a geophysical study: U. S. Geol. Survey Prof. Paper 438, 68 p.

Robinson, P. T., McKee, E. H., and Moiola, R. J., 1968, Cenozoic volcanism and sedimentation, Silver Peak region, western Nevada and adjacent California, in Coats, R. R., Hay, R. L., and Anderson, C. A., eds., Studies in volcanology: Geol. Soc. America Memoir 116, p. 577-611.

Rogers, T. H., 1967, Geologic map of California, San Bernardino sheet, Olaf P. Jenkins edition: California Div. Mines and Geology, scale 1:250,000.

Ross, D. C., 1962, Correlation of granitic plutons across faulted Owens Valley, California: U. S. Geol. Survey Prof. Paper 450-D, p. D86-D88.

Ross, D. C., 1967, Generalized geologic map of the Inyo Mountains region, California: U. S. Geol. Survey Misc. Geologic Inv. Map I-506, scale 1:125,000.

Ross, D. C., 1970, Pegmatitic trachyandesite plugs and associated volcanic rocks in the Saline Range-Inyo Mountains region, California: U. S. Geol. Survey Prof. Paper 614-D, 29 p.

Slemmons, D. B., 1966, Cenozoic volcanism of the central Sierra Nevada, California, in Bailey, E. H., ed., Geology of northern California: California Div. Mines and Geology Bull. 190, p. 199-208.

Strand, R. G., 1967, Geologic map of California, Mariposa sheet, Olaf P. Jenkins edition: California Div. Mines and Geology, scale 1:250,000.

Sutter, J. F., 1968, Geochronology of major thrusts, southern Great Basin, California (M. S. thesis): Houston, Rice University, 32 p.

Thorson, J. P., 1971, Igneous petrology of the Oatman District, Mohave County, Arizona (Ph. D. dissert.): Santa Barbara, Univ. California, 173 p.

Threet, R. L., 1963, Structure of the Colorado Plateau margin near Cedar City, Utah, in Heylmun, E. B., ed., Guidebook to the geology of southwestern

Utah: Intermountain Assoc. Petroleum Geologists Guidebook 12, p. 104-117.

Tschanz, C.M., and Pampeyan, E.H., 1970, Geology and mineral deposits of Lincoln County, Nevada: Nevada Bur. Mines Bull. 73, 187 p.

Volborth, Alexis, 1973, Geology of the granite complex of the Eldorado, Newberry, and northern Dead Mountains, Clark County, Nevada: Nevada Bur. Mines and Geology Bull. 80, 40 p.

Webb, R.W., 1950, Volcanic geology of Toowa Valley, southern Sierra Nevada, California: Geol. Soc. America Bull., v. 61, p. 349-357.

Wilson, E.D., Moore, R.T., and Cooper, J.R., 1969, Geologic map of Arizona: U.S. Geol. Survey, and Arizona Bur. Mines, scale 1:500,000.

Wise, W.S., 1969, Origin of basaltic magmas in the Mojave Desert area, California: Contr. Mineralogy and Petrology, v. 23, p. 53-64.

3.3.8 References Used in Compiling Plate 2:

Albers, J.P., and Kleinhampl, F.J., 1970, Spatial relation of mineral deposits to Tertiary volcanic centers in Nevada: U.S. Geol. Survey Prof. Paper 700-C, p. C1-C10.

Albers, J.P., and Stewart, J.H., 1972, Geology and mineral deposits of Esmeralda County, Nevada: Nevada Bur. Mines and Geology Bull. 78, 80 p.

Anderson, R.E., 1969, Notes on the geology and paleohydrology of the Boulder City pluton, southern Nevada: U.S. Geol. Survey Prof. Paper 650-B, p. B35-B40.

Anderson, R.E., 1973, Large-magnitude late Tertiary strike-slip faulting north of Lake Mead, Nevada: U.S. Geol. Survey Prof. Paper 794, 18 p.

Bassett, A.M., and Kupfer, D.H., 1964, A geologic reconnaissance in the southeastern Mojave Desert, California: California Div. Mines and Geology Spec. Rept. 83, 43 p.

Bishop, C.C., 1963, Geologic map of California, Needles sheet, Olaf P. Jenkins edition: California Div. Mines and Geology, scale 1:250,000.

Carlson, J.E., and Willden, Ronald, 1968, Transcontinental Geophysical Survey (35°-39° N) geologic map from 112° W longitude to the coast of California: U.S. Geol. Survey Misc. Geologic Inv. Map I-532-C, scale 1:1,000,000.

Cook, E.F., 1960, Geologic atlas of Utah, Washington County: Utah Geol. and Mineralog. Survey Bull. 70, 119 p.

Cornwall, H.R., 1972, Geology and mineral deposits of southern Nye County, Nevada: Nevada Bur. Mines and Geology Bull. 77, 49 p.

Davis, G.A., February 1974, unpub. mapping.

Dibblee, T.W., Jr., 1967, Areal geology of the western Mojave Desert, California: U.S. Geol. Survey Prof. Paper 522, 153 p.

Ekren, E.B., Anderson, R.E., Rogers, C.L., and Noble, D.C., 1971, Geology of northern Nellis Air Force Base Bombing and Gunnery Range, Nye County, Nevada: U.S. Geol. Survey Prof. Paper 651, 91 p.

Gilbert, C.M., Christensen, M.N., Al-Rawi, Yehya, and Lajoie, K.R., 1968, Structural and volcanic history of Mono Basin, California-Nevada, in Coats, R.R., Hay, R.L., and Anderson, C.A., eds., Studies in

volcanology: Geol. Soc. America Memoir 116, p. 275-329.

Hintze, L.F., 1963, Geologic map of southwestern Utah: Utah Geol. and Mineralog. Survey, scale 1:250,000.

Jennings, C.W., 1958, Geologic map of California, Death Valley sheet, Olaf P. Jenkins edition: California Div. Mines, scale 1:250,000.

Jennings, C.W., 1961, Geologic map of California, Kingman sheet, Olaf P. Jenkins edition: California Div. Mines, scale 1:250,000.

Jennings, C.W., Burnett, J.L., and Troxel, B.W., 1962, Geologic map of California, Trona sheet, Olaf P. Jenkins edition: California Div. Mines and Geology, scale 1:250,000.

Jennings, C.W., and Strand, R.G., 1969, Geologic map of California, Los Angeles sheet, Olaf P. Jenkins edition: California Div. Mines and Geology, scale 1:250,000.

Koenig, J.B., 1963, Geologic map of California, Walker Lake sheet, Olaf P. Jenkins edition: California Div. Mines and Geology, scale 1:250,000.

Longwell, C.R., Pampeyan, E.H., Bowyer, Ben, and Roberts, R.J., 1965, Geology and mineral deposits of Clark County, Nevada: Nevada Bur. Mines Bull. 62, 218 p.

Matthews, R.A., and Burnett, J.L., 1965, Geologic map of California, Fresno sheet, Olaf P. Jenkins edition: California Div. Mines and Geology, scale 1:250,000.

Noble, D.C., 1968, Kane Springs Wash volcanic center, Lincoln County, Nevada, in Eckel, E.B., ed., Nevada Test Site: Geol. Soc. America Memoir 110, p. 109-116.

Robinson, P.T., McKee, E.H., and Moiola, R.J., 1968, Cenozoic volcanism and sedimentation, Silver Peak region, western Nevada and adjacent California, in Coats, R.R., Hay, R.L., and Anderson, C.A., eds., Studies in volcanology: Geol. Soc. America Memoir 116, p. 577-611.

Rogers, T.H., 1967, Geologic map of California, San Bernardino sheet, Olaf P. Jenkins edition: California Div. Mines and Geology, scale 1:250,000.

Ross, D.C., 1961, Geology and mineral deposits of Mineral County, Nevada: Nevada Bur. Mines Bull. 58, 98 p.

Smith, A.R., 1964, Geologic map of California, Bakersfield sheet, Olaf P. Jenkins edition: California Div. Mines and Geology, scale 1:250,000.

Strand, R.G., 1967, Geologic map of California, Mariposa sheet, Olaf P. Jenkins edition: California Div. Mines and Geology, scale 1:250,000.

Tschanz, C.M., and Pampeyan, E.H., 1970, Geology and mineral deposits of Lincoln County, Nevada: Nevada Bur. Mines Bull. 73, 187 p.

Volborth, Alexis, 1973, Geology of the granite complex of the Eldorado, Newberry, and northern Dead Mountains, Clark County, Nevada: Nevada Bur. Mines and Geology Bull. 80, 40 p.

Wilson, E.D., Moore, R.T., and Cooper, J.R., 1969, Geologic map of Arizona: U.S. Geol. Survey, and Arizona Bur. Mines, scale 1:500,000.

3.4 DISTRIBUTION AND EXPRESSION OF KNOWN MINERAL DEPOSITS

3.4.1 Introduction:

The map compilation of Plate 4 shows the distribution of major known ore deposits in the Argus Exploration Company test site. This compilation has been used in investigating the regional patterns of mineralization and the expression of altered and mineralized areas in ERTS-1 MSS imagery. The investigation has focused on nine major types of mineralization found in the test site:

1. Gold
2. Lead, zinc, silver
3. Mercury
4. Iron
5. Copper, molybdenum
6. Tungsten
7. Fluorite
8. Uranium, thorium
9. Rare earth elements

A program of literature research and field reconnaissance of key ore deposits has been conducted to determine the causes and significance of their expression in the ERTS-1 imagery. The following geologic features or associations have been recognized in studying these ore deposits:

1. Color anomalies (Section 3.4.3)
2. Structural anomalies (Section 3.4.4)
3. Topographic expression (Section 3.4.5)
4. Rock-type associations (Section 3.4.6)

The expressions of the ore deposits studied in this investigation have been found to vary with age, type of alteration and mineralization, lithologic host, and climatic setting. The regional and local geologic settings of the ore deposits have been studied to evaluate possible regional similarities in the mineralization, structure, and rock types that characterize the deposits.

In the following report sections emphasis is placed on mineralized areas for which ground based data is available, either through our own field work or through published maps and reports. The expression of known mineralized areas has been studied with the objective of recognizing criteria that can be applied to regions where less is known of the economic geology. The results of this study are incorporated in an evaluation of potential applications of ERTS-1 MSS data to mineral exploration summarized in Section 4.1 of this report.

3.4.2 Methods:

The data of Plate 4 were originally compiled on AMS 1:250,000-scale base maps

to obtain suitable topographic detail. The bibliographies in Sections 3.4.9, 3.4.10, and 3.4.11 list the important literature and map sources used in the map compilation, as well as those used in studying the detailed geology of the mineral deposits and districts.

The spectral and spatial expression of mineral deposits included in the compilation have been studied in high resolution ERTS-1 color composites at a scale of 1:500,000. Slight variations were made in the color balance between frames to enhance discrimination of rock and soil units.

The color composites used in this investigation were produced by Argus Exploration Company from 70-mm and 9-inch positive film transparencies (see Section 2.4). The standard ERTS-1 MSS band-filter conventions used in most of these color composites are as follows:

MSS Band	Spectral Range	Printing Filter
4	.5-.6 micron (green and yellow)	Blue
5	.6-.7 micron (red)	Green
7	.8-1.1 micron (near-infrared)	Red

With this color convention, vegetation appears bright red because of its characteristically high near-infrared reflectance; white or neutral playa deposits, rock units, or alteration areas appear white or neutral with a minor shift toward blue; and red, ferruginous sedimentary rocks and iron oxide staining associated with alteration appear as yellow, sometimes shifting toward orange or green.

Examples of the false-color ERTS-1 MSS composites used in this study are shown in Section 2.3 of this report. These images should be used along with the map of Plate 4 in reviewing the following sections which summarize the characteristics of anomalies recognized in the ERTS-1 MSS imagery. Each section is accompanied by a table in which key anomalies are listed in order of their occurrence from west to east across the Argus Exploration Company test site.

3.4.3 Color Anomalies Associated with Altered or Mineralized Areas:

Color anomalies discussed in this section are caused by alteration or mineralization of a variety of host rocks. Distinctive host rock types, including those primarily formed by metamorphic recrystallization rather than alteration, are discussed in Section 3.4.6.

Color anomalies associated with ore deposits included in this study are of two main

types, as outlined below. The reader is referred to Table 1 for examples of known areas of mineralization and their associated color anomalies.

1. Portions of playas characteristically appear white in both natural color and in the ERTS-1 composites. This is due to the high reflectance of the playa materials over the entire spectrum imaged by the ERTS-1 MSS scanner. The playa deposits carry economic deposits of gypsum, clays, diatomite, evaporites and barite.

Alteration associated with ore deposits frequently appears white in the ERTS-1 composites as a result of the presence of light colored minerals, such as clays, quartz, feldspar, and sericite. Alteration zones are commonly more extensive than the actual zone of mineralization and are, therefore, more likely to be identified in the ERTS-1 imagery. Of the generalized types of alteration considered in this section, the white anomalies produced by silicic and argillic alteration have proven to be the most useful in recognizing mineralized areas.

An example of a white alteration anomaly is found in the Eldorado Mountains in the eastern part of the Searchlight gold district, Nevada. In this area, granitic dikes and plutons of Tertiary age and Precambrian granitic rocks have undergone intense silicic and argillic alteration (see Table 1; and ERTS-1 MSS Frame #1106-17495, Figure 4, southeast quarter).

2. Many mineral deposits, especially those containing abundant pyrite and hematite exhibit strong red iron oxide staining or gossans. This red coloration appears in the ERTS-1 composites as yellow or orange anomalies. A prominent example of such iron-stained altered rocks is visible along the northern margin of Turquoise Mountain, approximately 7 km north-northwest of Halloran Springs and 21 km northeast of Baker, California (see Table 1; and ERTS-1 MSS Frame #1106-17495, Figure 4, southwest quarter). The anomaly trends approximately east-west for a distance of 6 km and results from weathering of sulfide-bearing granitic rocks. A less pronounced white anomaly caused by silicic and argillic alteration of the same granitic complex is also present.

The expression of color anomalies in ERTS-1 MSS imagery is easily masked by vegetation cover. Thus, the most easily recognized anomalies are found in arid to semiarid parts of the test site where vegetation is scarce. Indirect evidence of alteration coloring must often be sought in the alluvium shed from altered and potentially mineralized areas. For example, a light colored anomaly over alluvium derived from adjacent altered bedrock is found northeast of Searchlight, Nevada on the east side of the Eldorado Mountains (see ERTS-1 Frame #1106-17495, Figure 4, southeast quarter).

COLOR ANOMALIES ASSOCIATED WITH ALTERED OR MINERALIZED AREAS TABLE 1

Mining Area and ERTS-1 Frame Number	Argillic, Silicic and Other Light Colored Alteration Recognized in ERTS-1 Imagery	Iron Staining Recognized in ERTS-1 Imagery
Randsburg district, centered at Randsburg, Kern and San Bernardino Cos., Cal. (Au, Ag, W) ERTS-1 MSS Frame #1162-18011, Fig. 13, southeast quarter		A yellow-brown anomaly in the Red Mountain area is due to iron staining in the Rand schist and a quartz monzonite intrusive body.
Antelope Springs, Wilson Camp, Gold Crater, Trappman Hills, and parts of the Cactus Range, centered approximately 48 km east-southeast of Goldfield, Nye Co., Nev. (Au, Ag) ERTS-1 MSS Frame #1126-18010, Fig. 6, northeast quarter	An irregular, light colored anomaly in Tertiary volcanic rocks is due to widespread argillic, alunitic and silicic alteration. Alteration is most intense along faults and near intrusive bodies.	
Silver Bow (Tickabo) Mines, Kawich Range, 72 km east-northeast of Goldfield, Nye Co., Nev. (Au, Ag) ERTS-1 MSS Frame #1126-18010, Fig. 6, northeast quarter	A white to yellow anomaly on the south side of the Kawich Range is due to a combination of silicic alteration and iron staining. Host rocks are intermediate to felsic Tertiary volcanic rocks.	
Turquoise Mountain north of Highway 41, approximately 16 km northeast of Baker, San Bernardino Co., Cal. (Cu, Mo, Ag, Au, Fe) ERTS-1 MSS Frame #1106-17495, Fig. 4, southwest quarter		A strong yellow anomaly approximately 6 km long and 1 km wide is present where Mesozoic and Tertiary granitic bodies have intruded dark colored Precambrian metamorphic rocks. The anomaly is due to intense iron staining in mineralized areas.
Silurian Hills,24 km north of Baker, San Bernardino Co., Cal. (Ag) ERTS-1 MSS Frame #1106-17495, Fig. 4, southwest quarter		An orange anomaly is present where Paleozoic carbonate rocks are altered and mineralized along north-northeast striking faults.
Copper World and Dewey mines, north of Highway 91, west slope of Clark Mountains, approximately 48 km northeast of Baker, San Bernardino Co., Cal. (Cu, Ag) ERTS-1 MSS Frame #1106-17495, Fig. 4., southwest quarter	A white anomaly is present where the Goodsprings Dolomite has been metamorphosed, mineralized, and altered along the contacts of quartz monzonite sills.	
Ivanpah district, southern part of Ivanpah Mountains, approximately 12 km north of Cima, San Bernardino Co., Cal. (Cu, Au, Ag, W, F) ERTS-1 MSS Frame #1106-17495, Fig. 4, southwest quarter		A large yellow anomaly is present over the iron-stained Teutonia quartz monzonite of Mesozoic age. Mineralization occurs in quartz veins in the quartz monzonite and in the carbonate country rocks.
Searchlight district, centered at Searchlight, Clark Co., Nev. (Au, Ag) ERTS-1 MSS Frame #1106-17495, Fig. 4, southeast quarter	Light colored argillic and silicic alteration occurs in the Eldorado Mountains east and southeast of Searchlight. The alteration is in Precambrian metamorphic rocks and Tertiary intrusive and extrusive igneous rocks.	A yellow anomaly southwest of the town of Searchlight is due to iron staining associated with alteration in Tertiary felsic volcanic rocks.
Newberry district, Newberry Mountains, located 24 km southeast of Searchlight and 18 km northwest of Davis Dam, southern tip of Clark Co., Nev. (Au, Ag) ERTS-1 MSS Frame #1106-17495, Fig. 4, southeast quarter	Light colored argillic and silicic alteration occurs along Tertiary rhyolite dikes and quartz veins in Precambrian gneisses.	Small yellow-orange anomalies occur over iron-stained Precambrian metamorphic rocks and Tertiary granitic intrusive rocks.
Mocking Bird district, north of Mt. Perkins in the Black Mountains, Mohave Co., Arizona, 10 km east-northeast of Searchlight, Clark Co., Nev. (Au, Ag) ERTS-1 MSS Frame #1106-17495, Fig. 4, east-central part		An orange anomaly in the vicinity of the Great West Mine is due to iron staining in mineralized intermediate to felsic volcanic rocks of Tertiary age.

Color Anomalies Associated with Altered or Mi[illegible]ed Areas (Table 1, cont'd.)

Mining Area and ERTS-1 Frame Number	Argillic, Silicic and Other Light Colored Alteration Recognized in ERTS-1 Imagery	Iron Staining Recognized in ERTS-1 Imagery
Oatman district, west slope of the Black Mountains, centered at Oatman, Mohave Co., Ariz. (Au, Ag, Cu) ERTS-1 MSS Frame #1051-17434, Fig. 10, northwest quarter	An irregular light yellow to buff colored anomaly in the mineralized areas is due to argillic and silicic alteration of Tertiary intrusive and extrusive rocks.	A pale yellow-orange anomaly along the northwestern side of the district is associated with iron staining in altered Tertiary volcanic and shallow intrusive rocks.
Union Pass district, centered west of Union Pass in the Black Mountains, approximately 30 km west of Kingman and 16 km north of Oatman, Mohave Co., Ariz. (Au, Ag) ERTS-1 MSS Frame #1106-17495, Fig. 4, southeast quarter		A yellow anomaly is due to iron staining in shallow Tertiary plugs and dikes and associated felsic volcanic rocks.

3.4.4 Structural Anomalies Associated with Altered or Mineralized Areas:

A variety of structural features or structural intersections are spatially associated with known mineral deposits in the Argus Exploration Company test site. These include the following:

1. Faults
   - Strike-slip faults
   - Thrust faults
   - Normal faults
   - Structural intersections
2. Features associated with volcanic centers and shallow intrusive bodies, such as radial or concentric dikes and faults, shallow intrusive domes and collapse features.
3. Folds

Due to generally low dips and irregular traces, thrust faults are the most difficult of these structures to recognize except where distinctive rock types have been juxtaposed. Table 2 gives examples of prominent structural features expressed in ERTS-1 MSS imagery that are associated with known ore deposits.

An example of a mineralized area closely associated with fault intersections is the Eldorado gold district of Clark County, Nevada (see Table 2). This district is located at the intersection of a major east trending left-lateral fault zone and a system of north striking normal faults (Volborth, 1973). Gold mineralization has been localized along faults having both of these trends. This intersection is clearly expressed in ERTS-1 MSS Frame #1106-17495 (Figure 4, southeast quarter) by the anomalous termination of strands of the north striking normal fault system against the east-west structural trend.

Tertiary intrusive domes and dike swarms are expressed in ERTS-1 MSS imagery over the Newberry Mountains of southern Clark County, Nevada (see Table 2; and ERTS-1 MSS Frame #1106-17495, southeast quarter). Two granitic domes appear as light colored circular anomalies. Dike swarms form a system of north striking lineaments which cross both Precambrian metamorphic rocks and the Tertiary granitic domes. Gold, silver and minor copper mineralization is known to occur within the dike swarms along the faulted western margin of one of the intrusive domes.

Arcuate faults which border the Long Valley caldera and form part of the eastern escarpment of the Sierra Nevada, north of Bishop, California, are expressed in ERTS-1 MSS Frame #1163-18063 (Figure 14, north-central part). A large resurgent dome within the caldera and smaller silicic domes, flows and cones which extend northward from the caldera are also expressed in the ERTS-1 imagery.

Mercury mineralization is associated with hot spring deposits along a fault within the resurgent portion of the caldera (Rinehart and others, 1964).

STRUCTURAL ANOMALIES ASSOCIATED
WITH ALTERED OR MINERALIZED AREAS

TABLE 2

Mining Area and ERTS-1 Frame Number	Primary Structural Anomaly Visible in ERTS-1 Imagery and Notes on Geologic Settings	Secondary Structural Anomalies Visible in ERTS-1 Imagery and Notes on Geologic Settings
Buena Vista district, northern end of White Mountains, approximately 16 km southwest of Basalt, Mineral Co., Nev. (Hg, Au, Ag) ERTS-1 MSS Frame #1163-18063, Fig. 14, northeast quarter	North and northwest striking faults cut Tertiary volcanic rocks at the northern end of the Death Valley-Furnace Creek fault zone. Cinnabar occurs in silicified fault zones in volcaniclastic rocks.	The east-northeast striking fault zone through the Montgomery Pass area appears to terminate the Death Valley-Furnace Creek fault zone in the area where mercury mineralization occurs along faults.
Casa Diablo Hot Springs area, Long Valley caldera, approximately 16 km west of Lake Crowley, Mono Co., Cal. (Hg) ERTS-1 MSS Frame #1163-18063, Fig. 14, north-central part	The elliptical shape of the caldera and the numerous silicic domes and flows in its resurgent western portion form prominent anomalies. A small amount of cinnabar is reported in hot spring deposits located within the resurgent portion of the caldera.	Several faults, including a large graben are recognized within the resurgent dome. Hydrothermal alteration and hot spring activity are associated with these faults.
Darwin district, centered at Darwin, 32 km southeast of Keeler, Inyo Co., Cal. (Pb, Zn, Ag, W) ERTS-1 MSS Frame #1162-18011, Fig. 13, northeast quarter	The left-lateral Darwin tear fault and other strike-slip faults are mineralized along their east-northeast trends.	The richest mineralization is associated with north striking normal faults where they intersect the strike-slip faults.
Ruth, Mohawk, Wild Rose, Mammoth, Star of the West, Sterling Queen and other mines, southern Argus Range, San Bernardino and Inyo Cos., Cal., west and northwest of Trona, Cal. (Au, Ag, Fe, Cu) ERTS-1 MSS Frame #1125-17554, Fig. 12, southwest quarter	Several large faults of uncertain displacement transect the range with west to northwesterly strikes. The most prominent of these is the Wilson Canyon fault. Mines are located in shear zones along these large faults.	North striking normal faults have localized some mineralization.
Slate Range, Inyo and San Bernardino Cos., Cal., east of Trona, Cal. (Au, Ag, Pb, Zn, Cu) ERTS-1 MSS Frame #1125-17554, Fig. 12, southwest quarter	Mines occur witnin a broad, north trending shear zone (the Manly Pass fault) which cuts the margins of a large Mesozoic granitic body. Most movement on the shear zone is thought to have been pre-middle Tertiary in age.	
Shoshone Mines, south end of Nopah Range and in Alexander Hills area, Inyo and San Bernardino Cos., Cal., 10 km east of Tecopa, Cal. (Ag, Au, Pb, Zn, Cu) ERTS-1 MSS Frame #1106-17495, Fig. 4, west-central part	Northwest striking normal faults which transect the southern end of the Nopah Range have localized mineralization.	Northwest striking faults are located along the northeast flank of a northwest trending anticline. Northeast and northwest fault sets occur in the mineralized area.
Bullfrog district, centered at Rhyolite, approximately 8 km west of Beatty, Nye Co., Nev. (Au, Ag, Hg, F) ERTS-1 MSS Frame #1126-18010, Fig. 6, southeast quarter	Gold deposits occur along normal faults which form the rim of a collapsed caldera. Other mines are located near the contact between basement rocks and overlying Tertiary felsic volcanic rocks of the central dome.	The eastern portion of an indistinct east-west trending structural anomaly is formed by the mineralized graben of Fluorspar Canyon. This structure extends westward to Scotty's Castle in the northern part of the Grapevine Mountains, California.
Cactus Range, approximately 32 km east of Goldfield, Nye Co., Nev. (Au, Ag, Cu) ERTS-1 MSS Frame #1126-18010, Fig. 6, northeast quarter	North and northwest trending normal faults have localized mineralization and alteration in many areas within and along the margins of the Cactus Range.	
Mount Helen area, 40 km southeast of Goldfield, Nye Co., Nev. (Ag, Au) ERTS-1 MSS Frame #1126-18010, Fig. 6, northeast quarter	Altered and mineralized areas north of Mount Helen lie along the northern margin of a possible caldera structure. Faults and lithologic contacts follow the northern, eastern and western margins of the caldera.	

Structural Anomalies Associated with Altered or Mineralized Areas (Table 2, cont'd.)

Mining Area and ERTS-1 Frame Number	Primary Structural Anomaly Visible in ERTS-1 Imagery and Notes on Geologic Settings	Secondary Structural Anomalies Visible in ERTS-1 Imagery and Notes on Geologic Settings
Searchlight district and portions of the Eldorado Mountains, centered at Searchlight, Clark Co., Nev. (Au, Ag) ERTS-1 MSS Frame #1106-17495, Fig. 4, southeast quarter	Left-lateral strike-slip faults and felsic dike swarms which trend roughly east-west occur in mineralized areas east and south of Searchlight.	Northerly trending normal faults, felsic dike swarms, and elongate Tertiary granitic plutons are associated with mineralization in the Searchlight district.
Eldorado district, centered at Nelson, Clark Co., Nev. (Au, Ag) ERTS-1 MSS Frame #1106-17495, Fig. 4, southeast quarter	A large left-lateral strike-slip fault which extends roughly east-west through the center of the district has controlled mineralization.	Mineralized north striking normal faults terminate against the east-west, left-lateral fault system.
Newberry district, Newberry Mountains, 24 km southeast of Searchlight and 18 km northwest of Davis Dam, southern tip of Clark Co., Nev. (Au, Ag) ERTS-1 MSS Frame #1106-17495, Fig. 4, southeast quarter	A north striking normal fault along the west side of the Tertiary Spirit Mountain quartz monzonite has localized gold and silver mineralization.	The Tertiary granitic rocks of the Newberry Mountains were intruded as two large nearly circular domes with Precambrian gneiss dipping outward around the margins. Abundant north striking dike swarms cut the domes and the Precambrian country rock. Several of the large rhyolite dikes along the northwest margin of the granitic intrusive complex are altered and mineralized. Mines and prospects are developed in east-west trending quartz veins near the rhyolite dikes.
Templute, Delamar, Pioche, Bristol, Pahranagat, Comet, Highland, Chief, and Don Dale districts, and the Arrowhead mine, Lincoln Co., Nev. (Ag, Pb, Zn, Cu, Au) ERTS-1 MSS Frame #1106-17492, Fig. 7, west half	Northeast and subsidiary northwest striking faults and disruptions of north trending mountain ranges form major structural anomalies. Some of these transverse structures are strike-slip fault zones which have controlled mineralization.	Mineralized veins are localized along northerly trending normal faults and dike swarms where these structures are intersected by northwest or northeast trending strike-slip fault zones. Mineralization in these structural settings is best developed near Tertiary granitic bodies.
Pennsylvania district, Clover Mountains, approximately 20 km south-southeast of Caliente, Lincoln Co., Nev. (Cu, Au) ERTS-1 MSS Frame #1106-17492, Fig. 7, northeast quarter	Northwest striking fault zones extend through a large area east and south of Caliente. These fault zones are larger and more numerous than previously mapped. Mineralization is localized near granitic intrusive bodies along the northwest trending faults.	
Bull Valley-Cove Mountain district, Bull Valley Mountains, 15 km south of Enterprise, Washington Co., Utah. (Fe) ERTS-1 MSS Frame #1051-17425, Fig. 8, west-central part	Many east-west trending faults form the western portion of a major arcuate structure (concave to the northwest). The Iron Springs district is located along the northern part of this structure where the component faults have northerly trends.	Syenite porphyry has been intruded as plutons which are elongate roughly east-west. Iron deposits occur as replacement bodies and along faults in carbonate rocks near the intrusive bodies.
Silver Reef district, near Leeds, approximately 8 km northwest of Hurricane, Washington Co., Utah (Ag) ERTS-1 MSS Frame #1051-17425, Fig. 8, southwest quarter	The Virgin anticline plunges northeast and can be traced for about 18 miles from south of St. George, Utah to northeast of Leeds, Utah. The Silver Reef district is located in the Leeds anticline just north of the hinge of the Virgin anticline. The ores are thought to be of syngenetic depositional origin, although there is some evidence that they may be in part controlled by the folding. The Virgin and Leeds anticlines are prominent features delineated by the Aztec (Navaho) Sandstone which is expressed as a strong yellow anomaly.	

3.4.5 Topographic Expression Associated with Altered or Mineralized Areas:

The synoptic perspective of topographic patterns expressed in ERTS-1 MSS imagery is useful in interpreting a variety of geologic and structural features. Weathering, erosion, and drainage patterns of rock units are frequently controlled by such features as mineralogy, internal rock fabric, jointing, compositional layering, and alteration. Table 3 in this section presents examples of the topographic expression of known altered or mineralized areas in the test site.

Within the southern Basin Range Province, granitic bodies often appear as topographic plateaus or domes having irregular to radial drainage. The margins of such plutons are commonly expressed as arcuate topographic depressions where fracturing, faulting, recrystallization, jointing and hydrothermal alteration have resulted in relatively rapid erosion rates. Many types of mineral deposits, especially gold and silver-lead-zinc, occur along these altered and faulted margins of granitic bodies. An example is the arcuate depression surrounding the Santa Rita Flat pluton approximately 40 km north of Lone Pine, California (Table 3; and ERTS-1 MSS Frame #1126-18010, Figure 6, southwest quarter). This depression is the result of erosion along the faulted, altered and mineralized margin of the pluton (Ross, 1965). Gold-silver, tungsten and iron prospects are located along this arcuate depression.

Volcanic centers generally have physiographic expression characteristic of their composition and depth of erosion. For example, the Long Valley caldera and associated felsic volcanic rocks near Bishop, California contrast markedly with the basaltic flows and cones of the Owens Valley volcanic field near Big Pine, California (see ERTS-1 MSS Frame #1163-18063, Figure 14, north-central and southeast quarters). Throughout the test site, many of the known areas of gold and silver mineralization are genetically associated with volcanic centers of intermediate to felsic composition. Prominent examples expressed in the ERTS-1 imagery are the Bullfrog and Goldfield districts in Nevada and the Oatman district in Arizona.

Faults are expressed topographically both as primary surface breaks and by structurally controlled in-place weathering and erosion. As outlined in Section 3.1, most of the major topographic trends in the southern Basin Range Province are controlled by northerly striking normal faults of Cenozoic age. This deformation is superposed on complex pre-Tertiary structures representing several earlier periods of deformation. The older structural trends are locally reflected in the topography through weathering and erosion.

TOPOGRAPHIC EXPRESSION ASSOCIATED WITH ALTERED OR MINERALIZED AREAS

TABLE 3

Mining Area and ERTS-1 Frame Number	Topographic Expression Recognized in ERTS-1 Imagery
Casa Diablo Hot Springs area, Long Valley caldera, approximately 16 km west of Lake Crowley, Mono Co., Cal. (Hg) ERTS-1 MSS Frame #1163-18063, Fig. 14, north-central part	An elliptical topographic depression with long axis oriented east-west represents the collapsed portion of the Long Valley caldera. A series of hills in the western part of the caldera depression is underlain by the younger resurgent portion of the caldera. The resurgent dome is cut by a large graben valley within which mercury mineralization has been reported.
Santa Rita Flat pluton, approximately 40 km north of Lone Pine, Inyo Co., Cal. (Au, Ag, W) ERTS-1 MSS Frame #1126-18010, Fig. 6, southwest quarter	The granitic Santa Rita Flat pluton underlies a low plateau with arcuate stream canyons along the eastern margin of the pluton. Dikes and faults within the intrusive body appear as linear anomalies. Mines are located in the country rock and within the pluton near its margins.
Buena Vista district, northern end of White Mountains, approximately 16 km southwest of Basalt, Mineral Co., Nev. (Hg, Au, Ag) ERTS-1 MSS Frame #1163-18063, Fig. 14, northeast quarter	Closely spaced faults of diverse trends control drainage and erode to straight stream segments within Tertiary volcanic rocks. The volcanic rocks are generally less dissected than the underlying basement rocks of the White Mountains. Mercury mineralization occurs along faults in these volcanic rocks.
Several mines and prospects north of Deep Springs Valley, White Mountains, approximately 24 km east of Bishop, Inyo Co., Cal. (W, Ag, Pb, Zn, Cu) ERTS-1 MSS Frame #1126-18010, Fig. 6, west-central part	Deep canyons and tributary streams follow the margins of the granitic Birch Creek pluton of Mesozoic age. The pluton itself is expressed as a dissected plateau. The larger Beer Creek pluton underlies an adjacent plateau area to the east and a wedge of north striking lower Paleozoic sedimentary rocks separates the two plutons. The trends of Paleozoic rocks are expressed topographically by Beer Creek and other north trending valleys and intervening ridges. Mineralization is localized near the margins of the granitic bodies.
Nickolaus Eureka mine, Victor Cons mine and other mines, eastern side of Inyo Mountains, north of Joshua Flat and south of Deep Spring Valley, approximately 40 km east-southeast of Bishop, Inyo Co., Cal. (W, Au, Ag, Cu) ERTS-1 MSS Frame #1126-18010, Fig. 6, west-central part	Marked ridges and valleys represent a sequence of Cambrian metasedimentary rocks where it bends around the southern margin of the large Joshua Flat pluton. The Cambrian rocks can be traced in the ERTS-1 composite for a distance of 16 km from the southeast side of Deep Springs Valley toward the southeast and then northward until they are buried by the basin sediments of Eureka Valley. Tungsten, copper and gold prospects are located within the Cambrian rocks and tungsten prospects are found in the Mesozoic granite.
Marble Canyon pluton, eastern Inyo Mountains, approximately 48 km southeast of Bishop, Inyo Co., Cal. (Au) ERTS-1 MSS Frame #1126-18010, Fig. 6, southwest quarter	Marble Canyon is a major topographic feature draining eastward into Eureka Valley along the contact between the granitic Marble Canyon pluton to the north and metasedimentary rocks to the south. Layering in the metasedimentary rocks trends generally parallel to the curvilinear plutonic margin. Mines are located along the margin of the pluton.
Lippincott mine, Panamint Range, 32 km north-northwest of Panamint Springs, Inyo Co., Cal. (Ag, Cu) ERTS-1 MSS Frame #1162-18011, Fig. 13, northeast quarter	A large body of Hunter Mountain quartz monzonite underlies a high plateau with subdued internal topography. The mine is located on an arcuate fault which strikes north and west along the margin of the granitic body. This fault and the margin of the granitic body are expressed as deep canyons.
Hunter Mountain, Panamint Range, north end of Panamint Valley, approximately 24 km north of Panamint Springs, Inyo Co., Cal. (W) ERTS-1 MSS Frame #1162-18011, Fig. 13, northeast quarter	A large body of Hunter Mountain quartz monzonite is expressed topographically as a semi-circular plateau with deep moat-like canyons along its northern margin. Tungsten deposits are located along the margins of the granitic body.
Cactus Range, Trappman Hills, Gold Crater area, approximately 40 km east-southeast of Goldfield, Nye Co., Nev. (Au, Ag) ERTS-1 MSS Frame #1126-18010, Fig. 6, northeast quarter	Subdued topography with isolated and irregular small hills surrounds the main ranges. Many of the isolated hills are underlain by altered and mineralized shallow intrusive and volcanic rocks.
Beck deposits and other mines, north side of Kingston Range, 24 km east-southeast of Tecopa, San Bernardino and Inyo Cos., Cal. (Fe, Pb) ERTS-1 MSS Frame #1106-17495, Fig. 4, west-central part	The roughly circular Kingston Peak quartz monzonite pluton underlies a pronounced topographic highland with irregular to radial drainage controlled in part by faulting. Where unvegetated, the quartz monzonite pluton forms a light yellow anomaly. Deep canyons have developed along the plutonic margins.
Newberry district, Newberry Mountains, 24 km southeast of Searchlight and 18 km northwest of Davis Dam, southern tip of Lincoln Co., Nev. (Au, Ag) ERTS-1 MSS Frame #1106-17495, Fig. 4, southeast quarter	Two nearly circular granitic intrusive domes underlie low topographic domes with major canyons and washes along their margins. Abundant north trending felsic dike swarms appear as linear ridges within a large part of the Newberry Mountains. Mines are located along the margins of the granitic domes near altered felsic dikes.

3.4.6 Rock-Type Associations of Altered or Mineralized Areas:

Several key rock types can be discriminated in ERTS-1 MSS imagery over areas of minimal vegetation cover within the Argus Exploration Company test site. Table 4 lists areas of known mineralization throughout the test site which have characteristic rock-type associations recognizable in the ERTS-1 imagery. These include felsic dikes and plutons, carbonate rocks, felsic to intermediate volcanic rocks, metamorphic rocks, and alluvial and playa sediments. This use of ERTS-1 imagery in reconnaissance exploration is distinct from the interpretation of alteration color anomalies. Although certain rock types or combinations of rock types are favorable for mineralization, mapping of their distribution provides only an indirect guide to potential mineralization.

Several types of mineral deposits within the test site occur in areas where gray carbonate rocks have been bleached and recrystallized to white marble along the margins of granitic intrusives. Examples are the tungsten, copper and silver-lead deposits of the Inyo and Panamint Ranges of California. Both the metamorphosed layered carbonate rocks and the associated plutons can be distinguished by their coloration and characteristic topographic expression (Tables 3 and 4; and ERTS-1 MSS Frames #1163-18063, Figure 14; #1126-18010, Figure 6; and #1162-18011, Figure 13).

ROCK-TYPE ASSOCIATIONS OF ALTERED OR MINERALIZED AREAS TABLE 4

Mining Area and ERTS-1 Frame Number	Rock-Type Association Recognized in ERTS-1 Imagery	Other Associations Recognized in ERTS-1 Imagery
Indian Wells Canyon, southeastern part of Sierra Nevada Range, approximately 24 km west of China Lake, Kern Co., Cal. (Au, W) ERTS-1 MSS Frame #1162-18011, Fig. 13, south-central part	A bluish gray anomaly is present over a metasedimentary roof pendant which trends northwest. Tungsten mineralization is in tactite deposits within the roof pendant.	The granitic rocks of the Sierra Nevada batholith surrounding the roof pendant appear light brown. At higher elevations, rock type discrimination is hampered by heavy vegetation cover.
Several mines and prospects north of Deep Springs Valley, White Mountains, 24 km east of Bishop, Inyo Co., Cal. (W, Ag, Pb, Zn, Cu) ERTS-1 MSS Frame #1126-18010, Fig. 6, west-central part	Paleozoic carbonate rocks which wrap around the Mesozoic Birch Creek pluton appear as a light colored anomaly where they have been contact metamorphosed. Other Paleozoic sedimentary rocks appear dark brown. Mines are present in the metasedimentary rocks around the pluton as well as within the granitic rocks.	The granitic pluton appears light gray and is separated by a dark gray and brown wedge of Paleozoic sedimentary rocks from the Beer Creek pluton to the east. Layering and faulting in the Paleozoic rocks help to distinguish them from the jointed, massive granitic rocks.
Nickolaus Eureka mine, Victor Cons mine, and other mines, eastern Inyo Mountains, approximately 40 km east-southeast of Bishop, Inyo Co., Cal. (Au, Ag, W) ERTS-1 MSS Frame #1126-18010, Fig. 6, southwest quarter	The Bonanza King Formation has been metamorphosed to white marble along the margins of the large Joshua Flat pluton. This white anomaly can be clearly discerned for approximately 11 km along the southern and eastern margins of the Joshua Flat pluton.	Some phases of the Joshua Flat pluton can be distinguished from each other by color differences. The strong layering in the sedimentary and metasedimentary units permits their discrimination from the massive granitic intrusive rocks.
Modoc district and northern Argus Range, 8 km south of Panamint Springs, Inyo Co., Cal. (Au, Pb) ERTS-1 MSS Frame #1162-18011, Fig. 13, northeast quarter	Gray limestones of the Lost Burro Formation form a light colored anomaly where they have been metamorphosed to marble along the northern margin of a granitic intrusive body.	
Lippincott mine, Panamint Range, 32 km north-northwest of Panamint Springs, Inyo Co., Cal. (Ag, Cu) ERTS-1 MSS Frame #1162-18011, Fig. 13, northeast quarter	Gray carbonate rocks have been metamorphosed to white marble within a metasedimentary sequence wedged between two large bodies of Hunter Mountain quartz monzonite. The marble forms an arcuate light colored anomaly where it wraps around the westernmost of the two granitic bodies.	
Lost Burro mine, Panamint Range, 40 km north of Panamint Springs, Inyo Co., Cal. (Au) ERTS-1 MSS Frame #1126-18010, Fig. 6, south-central part	A large light colored anomaly extending southward from the mine is underlain by marble and by small satellitic bodies of the Sally Ann and Hunter Mountain quartz monzonite plutons. The main mass of Sally Ann quartz monzonite to the south appears as a second light colored anomaly. Marble appears white, granitic rocks light gray and unmetamorphosed sedimentary rocks dark gray.	
Slate Range, Inyo and San Bernardino Cos., Cal., east of Trona, Cal. (Au, Ag, Pb, Zn, Cu) ERTS-1 MSS Frame #1125-17554, Fig. 12, southwest quarter	A Mesozoic granitic pluton appears as a white to light yellow anomaly. Mines are located in tactite deposits near the contacts between the granitic rocks and the dark brown Mesozoic and Precambrian rocks to the south and northwest.	
Goldstone district, including the Gold Divide, Rio Hondo and Montana mines, Olympus and Daisy Mountain mines in the Paradise Range and several mines near Williams Well south of Superior Valley, centered approximately 16 km west-southwest of Fort Irwin, San Bernardino Co., Cal. (Au, W, Cu) ERTS-1 MSS Frame #1125-17554, Fig. 12, south-central part	A large Mesozoic granitic mass is recognizable as a light yellow to white anomaly. This light colored anomaly extends into alluvium derived from the granitic rocks. Mines are in granite, along granitic dikes, north trending faults, and in tactite bodies in dark gray and brown Paleozoic rocks near the margins of the granite.	

Rock Type Associations of Altered or Mineralized Areas (Table 4, cont'd.)

Mining Area and ERTS-1 Frame Number	Rock-Type Association Recognized in ERTS-1 Imagery	Other Associations Recognized in ERTS-1 Imagery
Silurian Hills, 24 km north of Baker, San Bernardino Co., Cal. (Ag) ERTS-1 MSS Frame #1106-17495, Fig. 4, southwest quarter	Metamorphosed carbonate rocks form a white anomaly along the northern margins of a granitic body at the east end of the Silurian Hills. The granitic rocks appear light gray and older Precambrian rocks are darker gray or brown.	
Ivanpah district, southern part of Ivanpah Mountains, approximately 12 km north of Cima, San Bernardino Co., Cal. (Cu, Au, Ag, W, F) ERTS-1 MSS Frame #1106-17495, Fig. 4, southwest quarter	Paleozoic carbonate rocks are metamorphosed to marble, bleached and altered along the northern margin of the Teutonia quartz monzonite. A yellow anomaly over the quartz monzonite and a white anomaly over the marble contrast strongly with the dark color of the surrounding unmetamorphosed sedimentary rocks. Mineralization is localized along the margins of the Teutonia quartz monzonite.	
New York Mountains, approximately 16 km east of Cima, San Bernardino Co., Cal. (W, Pb, Ag, Cu) ERTS-1 MSS Frame #1106-17495, Fig. 4, south-central part	A large body of Teutonia quartz monzonite forms a light colored anomaly which is masked by vegetation reflectance at higher elevations in the New York Mountains. This anomaly extends from Cedar Canyon on the south to Slaughterhouse Springs on the north. Large quartz monzonite dike swarms produce white northeast trending linear anomalies within the intrusive body and the surrounding country rocks.	The northern border of the quartz monzonite is intrusive into the Goodsprings Dolomite. A white anomaly is present where the dolomite has been metamorphosed and bleached by the Teutonia quartz monzonite. Several copper and silver-lead mines are located in the dolomite along the intrusive margin. These include the Trio Mine, the Giant Ledge Mine and the Copper King #2 Mine. Several mines are localized along the Clark Mountain fault where it follows part of the intrusive contact.
Devil's Peak, in southern Spring Mountains at south end of the Goodsprings district, approximately 11 km southwest of Jean, Clark Co., Nev. (Ag, Pb, Zn, Au, Cu) ERTS-1 MSS Frame #1106-17495, Fig. 4, southwest quarter	A strong blue gray color anomaly is present over the Tertiary rhyolitic intrusive of Devil's Peak. The blue anomaly extends from the rhyolite plug into the surrounding alluvium for up to 6 km. Several silver mines occur along the northern margin of the rhyolitic plug in gray to brown Paleozoic carbonate rocks.	

3.4.7 Types of Mineralization:

The distribution, geologic settings and characteristic expressions of the nine genetic types of mineralization included in this study are summarized below. The types of mineralization are listed in approximate order of decreasing expression in the ERTS-1 MSS imagery.

1. Gold: Gold is commonly associated with widespread silicic and argillic alteration. Many epithermal gold districts are located in or near silicic igneous centers of Tertiary age and the large Mesozoic granitic plutons in the western part of the test site. A province of quartz-vein gold mineralization is recognized along the Colorado River south of Lake Mead. Deposits within this province are Tertiary in age and are closely associated with shallow granitic plutons which have intruded Precambrian metamorphic and Tertiary volcanic rocks. The structure of the province is dominated by north trending normal faults, elongate plutons, and dike swarms which are believed to represent east-west crustal extension (Liggett and Childs, 1974*). Several of the mining districts are located near transverse faults, some of which have had left-lateral movement. Examples are the gold mining districts of Oatman, Searchlight, and Nelson.

The Bullfrog district at Rhyolite, Nevada, is located in the Bullfrog Hills caldera, and the gold districts of Goldfield and Tonopah, Nevada, are also located within Tertiary volcanic centers. Several other calderas are recognized northeast of the Bullfrog district within the Nye County Volcanic Province (Liggett and Childs, 1974*). Two of these, the Timber Mountain and Black Mountain calderas, are easily distinguished in ERTS-1 MSS Frame #1125-17551, Figure 5, southwest quarter. Recognition of late Tertiary volcanic centers, intrusive bodies and associated alteration using ERTS-1 imagery is a useful guide to areas of potential mineralization.

2. Lead, zinc, and silver: Lead, zinc, and silver deposits in the test site are generally closely associated with granitic intrusive rocks of Tertiary age and their contact metamorphic aureoles. The ore is frequently localized along fault intersections recognizable in ERTS-1 imagery. Lead, zinc and silver deposits associated with shallow granitic plutons in the northern Argus Range, the Darwin Hills, and the Santa Rosa Hills in Inyo County, California, are late Mesozoic to Tertiary in age. The deposits are localized along normal faults which strike generally northward. However, mineralization appears to be best developed where transverse strike-slip faults have transected the normal faults. Examples are the Darwin and Modoc districts in the Darwin Hills and the northern Argus Range, respectively (ERTS-1 MSS Frame #1162-18011, Figure 13, northeast quarter).

Silver-lead-zinc and some gold districts of Lincoln County, Nevada are

---

* Appendix O, this report

localized where northeast or northwest trending transverse structures intersect the northerly striking Basin Range normal faults. Several of the transverse structures have strike-slip movement, a notable example being the left-lateral Pahranagat shear system south of Hiko, Nevada (Liggett and Ehrenspeck, 1974*). The localization of replacement-type ore deposits at or near these structural intersections appears to be due to the intense crushing of the host carbonate rocks, providing access for ore-bearing solutions.

3. Mercury: Mercury deposits are commonly localized along faults in crushed and silicified volcanic rocks of intermediate to silicic composition. This mineralization is often located in or near volcanic centers or hot springs areas. Known mercury deposits in the test site have geologic and structural settings similar to those of Tertiary gold mineralization.

4. Iron: Iron is found primarily in tactite deposits in roof pendants or along the margins of granitic intrusive bodies, especially where faulting has occurred during or just after intrusion. Where vegetation is sparse, these deposits are sometimes characterized by bluish-gray anomalies in the ERTS-1 composites. In the Iron Springs and Bull Valley-Cove Mountain iron districts in southwestern Utah, iron occurs as replacement deposits in Mesozoic sedimentary rocks along the margins of Tertiary granitic bodies. These deposits occur along an arcuate fault system characterized by east-west striking faults in the Bull Valley-Cove Mountain area (ERTS-1 MSS Frame #1051-17425, Figure 8, east-central part) and by northeast striking faults in the Iron Springs area. The Tertiary plutons associated with the ore deposits in the Bull Valley-Cove Mountain area are elongate east-west, parallel with the strikes of many closely spaced faults in this district that appear as linear anomalies in the ERTS-1 imagery. The intrusive bodies in the Iron Springs district are aligned along a northeasterly structural trend expressed topographically in ERTS-1 MSS Frame #1051-17425 (Figure 8, northwest quarter).

5. Copper-molybdenum: The small copper-molybdenum deposits within the test site are difficult to recognize, since they are usually not accompanied by extensive faulting or alteration coloring. Many are pre-Tertiary in age and tend to be obscured by Tertiary sedimentary cover or structural deformation. Copper and molybdenum are found associated with other metals in contact metamorphic deposits and are recognized mainly by rock-type associations and structural setting at the margins of plutonic bodies.

In eastern Lincoln County, southeast of Caliente, Nevada, copper mineralization has been found in association with Tertiary granitic stocks along a northwest striking fault system. These faults are expressed as a pervasive linear trend in the ERTS-1 imagery and are larger and more numerous than has been shown on previous geologic maps of the area (ERTS-1 MSS Frame #1106-17492, Figure 7, northeast quarter).

---

* Appendix L, this report

A major copper-molybdenum province is present along the western margin of the Colorado Plateau in the southeastern portion of the test site. Several of the deposits are of the "porphyry copper" variety including the Ithaca Peak deposit in the Cerbat Mountains and the Bagdad deposit just east of the test site. These deposits are genetically related to late Mesozoic granitic plutons. Vegetation masks possible color expression of the Ithaca Peak deposit, although the pluton, dike system, and fault pattern with which it is associated have topographic expression in ERTS-1 MSS Frame #1069-17432, (Figure 9, southwest quarter).

6. Tungsten: Tungsten deposits, although found throughout the test site, are generally concentrated in a broad belt across the Mesozoic granitic plutons of the Sierra Nevada, White Mountains and Inyo Mountains in eastern California and western Nevada. The largest known tungsten deposit is the Pine Creek Mine near Bishop, California. The deposits are most often developed in quartz veins in granitic rocks or in tactite deposits within roof pendants near intrusive contacts. A useful guide to this mineralization is the bleaching of the carbonate country rocks in contact metamorphic aureoles along the plutonic margins. However, full seasonal ERTS-1 MSS coverage and high quality enhancements of the imagery are necessary to recognize such color anomalies in the heavily vegetated mountain ranges.

7. Fluorite: Fluorite is associated with Tertiary volcanic activity and shallow intrusive rocks, especially where they contact limestone country rocks. Fluorite is also found as gangue in lead-zinc-silver mining areas. Structural control is usually local.

8. Uranium-thorium: The known uranium-thorium deposits in the test site are small in size, generally lack clear structural control, have scattered distribution and occur in a wide variety of host rocks. No characteristic anomalies have been recognized in the ERTS-1 imagery.

9. Rare earth elements: Due to the small size and scattered distribution of these deposits, the problems of identification using satellite data are similar to those encountered with uranium-thorium deposits. No distinctive expression of known rare earth deposits has been recognized in the ERTS-1 imagery.

3.4.8 Conclusions and Recommendations:

This investigation of known mineral deposits within the Argus Exploration Company test site indicates that many geologic and structural features related to mineralization are visible in the ERTS-1 MSS imagery. Although mineral deposits are found to vary in both characteristics and degree of expression, analysis and interpretation of ERTS-1 data can provide a useful guide for reconnaissance mineral exploration.

Approximately 70 percent of the known mining districts in the test site have anomalous expression in the ERTS-1 MSS imagery. The area of these anomalies represents between 10 and 15 percent of the total area of the test site. The use of

ERTS-1 MSS data in reconnaissance exploration can result in the selection of anomalies of a size feasible for economical evaluation using a variety of geologic, geophysical and geochemical survey techniques. Recommendations for application of ERTS-1 MSS imagery in reconnaissance mineral exploration are summarized in Section 4.1 of this report.

The areas discussed below have been selected as regions of interest for mineral exploration on the basis of their geologic settings and expression in ERTS-1 MSS imagery. Although several of these regions have known mineralization, the size of the anomalies and the relatively limited mining activity in the areas suggest that they warrant further exploration.

1. The area between the southern Cactus Range and the Goldfield Hills in southern Nye County and eastern Esmeralda County, Nevada, is believed to be favorable for potential gold and copper mineralization. This area is the site of extensive alteration of middle to late Tertiary volcanic and intrusive rocks, which is expressed in the ERTS-1 imagery as a strong light colored anomaly. Known gold and copper deposits indicate that this alteration was accompanied, at least locally, by mineralization.

2. The region bordering the Colorado River south of Lake Mead, Nevada, is a gold, silver and copper province of Tertiary age controlled by regional structural deformation and synchronous igneous activity (Liggett and Childs, 1974*; Bechtold and others, 1973**). The province contains several known mining areas, which have produced resources valued at over $100 million during the early part of this century. Areas of alteration and potential mineralization are expressed in the ERTS-1 imagery as coloration anomalies located where transverse east striking faults intersect the dominant northerly trend of normal faults and dike swarms in the province. An area warranting further study is that between the Newberry and Searchlight districts west of the Colorado River in Clark County, Nevada. A second area of interest is situated between Union Pass and Eldorado Canyon on the east side of the Colorado River north of Oatman, Arizona.

3. The color, topographic and structural expression in ERTS-1 imagery of known mineral deposits in Lincoln County, Nevada suggests several areas of potential alteration and mineralization. Many of the known lead-zinc-silver deposits in the area are located where the northerly trend of the Basin Range structures is disrupted by transverse faults, several of which are known to have strike-slip displacement. Examples of areas warranting consideration are the northern Sheep Range, the northern Groom Range, the North Pahranagat Range, and the range that bounds the northern end of Pahroc Valley.

4. A pervasive system of northwest striking faults is expressed in

---

* Appendix D, this report

** Appendix E, this report

ERTS-1 imagery over the Clover Mountains in eastern Lincoln County, Nevada. In portions of this area, copper mineralization is located along these faults in the vicinity of Tertiary granitic plutons. The extent of the northwest trending fault system apparent in the ERTS-1 imagery is far greater than that shown on previous geologic maps. The central and eastern Clover Mountains warrant consideration for mineral exploration based on similarities in rock types and structural setting in this area and in mineralized areas to the northwest.

5. The region between the Iron Springs district, Utah, and the Bull Valley-Cove Mountain district to the southwest is considered to be a potential area of iron, copper and other metallic mineralization. Known mineralization in this area is located within an east-west to northeast trending arcuate structural pattern apparent in the ERTS-1 imagery, and shown on geologic maps of portions of the area. The Tertiary granitic plutons in the Bull Valley-Cove Mountain district are elongate roughly east-west, parallel to this structural trend. The iron deposits are replacement bodies adjacent to Tertiary plutons. The structural continuity and the similarities in rock types throughout this region indicate a potential for undiscovered mineralization east and northeast of the Bull Valley-Cove Mountain district.

3.4.9 References Cited in Text:

Bechtold, I.C., Liggett, M.A., and Childs, J.F., March 1973, Regional tectonic control of Tertiary mineralization and Recent faulting in the southern Basin-Range Province: An application of ERTS-1 data, in Freden, S. C., Mercanti, E.P., and Becker, M.A., eds., Symposium on significant results obtained from the Earth Resources Technology Satellite-1: New Carrollton, Maryland, v. 1, sect. A, paper G 21, NASA-SP-327, E73-10824, p. 425-432.

Liggett, M.A., and Ehrenspeck, H.E., January 1974, Pahranagat Shear System, Lincoln County, Nevada: NASA Rept. Inv., NASA-CR-136388, E74-10206, 10 p.

Liggett, M.A., and Childs, J.F., March 1974, Crustal extension and transform faulting in the southern Basin Range Province: NASA Rept. Inv., NASA-CR-137256, E74-10411, 28 p.

Rinehart, C.D., Ross, D.C., and Pakiser, L.C., 1964, Geology and mineral deposits of the Mount Morrison quadrangle, Sierra Nevada, California; With a section on a gravity study of Long Valley: U.S. Geol. Survey Prof. Paper 385, 106 p.

Ross, D.C., 1965, Geology of the Independence quadrangle, Inyo County, California: U.S. Geol. Survey Bull. 1181-0, 64 p.

Volborth, Alexis, 1973, Geology of the granite complex of the Eldorado, Newberry, and northern Dead Mountains, Clark County, Nevada: Nevada Bur. Mines and Geology Bull. 80, 40 p.

3.4.10 References Cited in Plate 4:
(Numbers correspond to numbers on the map)

1) U.S. Geological Survey, Arizona Bureau of Mines, and U.S. Bureau of Reclamation, 1969, Mineral and water resources of Arizona: Arizona Bur. Mines Bull. 180, 638 p.

2) Carr, M.S., and Dutton, C.E., 1959, Iron-ore resources of the United States including Alaska and Puerto Rico, 1955: U.S. Geol. Survey Bull. 1082-C, p. 61-134.

3) Smith, G.I., Troxel, B.W., Gray, C.H., Jr., and von Huene, Roland, 1968, Geologic reconnaissance of the Slate Range, San Bernardino and Inyo Counties, California: California Div. Mines and Geology Spec. Rept. 96, 33 p.

4) Cornwall, H.R., and Kleinhampl, F.J., 1964, Geology of Bullfrog quadrangle and ore deposits related to Bullfrog Hills caldera, Nye County, Nevada and Inyo County, California: U.S. Geol. Survey Prof. Paper 454-J, 25 p.

5) Dale, V.B., 1961, Tungsten deposits of Gila, Yavapai, and Mohave Counties, Arizona: U.S. Bur. Mines Information Circ. 8078, 104 p.

6) Jahns, R.H., ed., 1954, Geology of southern California: California Div. Mines Bull. 170.

7) Koschmann, A.H., and Bergendahl, M.H., 1968, Principal gold-producing districts of the United States: U.S. Geol. Survey Prof. Paper 610, 283 p.

8) Clark, W.B., 1970, Gold districts of California: California Div. Mines and Geology Bull. 193, 186 p.

9) Horton, R.C., 1962, Fluorspar occurrences in Nevada: Nevada Bur. Mines Map 3, scale 1:1,000,000.

10) Bonham, H.F., 1967, Gold-producing districts of Nevada: Nevada Bur. Mines Map 32, scale 1:1,000,000.

11) Bonham, H.F., 1967, Silver-producing districts of Nevada: Nevada Bur. Mines Map 33, scale 1:1,000,000.

12) Horton, R.C., 1962, Iron ore occurrences in Nevada: Nevada Bur. Mines Map 5, 1:1,000,000.

13) Schilling, J.H., 1963, Uranium occurrences in Nevada: Nevada Bur. Mines

Map 19, scale 1:1,000,000.

14) California Division of Mines, 1948, Iron resources of California: California Div. Mines Bull. 129, 304 p.

15) Walker, G.W., Lovering, T.G., and Stephens, H.G., 1956, Radioactive deposits in California: California Div. Mines Spec. Rept. 49, 38 p.

16) Hillier, R.L., 1954, Preliminary report on the uranium occurrence of the Jeep No. 2 claim, Clark Mountain mining district, San Bernardino County, California: U.S. Atomic Energy Comm. Rept. RME-2011, 11 p.

17) Nelson, H.E., and Hillier, R.L., 1954, Preliminary report on the uranium occurrence of the Silver Lady claim, Jaw Bone mining district, Cross Mountain quadrangle, Kern County, California: U.S. Atomic Energy Comm. Rept. RME 2012, 19 p.

18) Eric, J.H., 1948, Tabulation of copper deposits of California, in Copper in California: California Div. Mines Bull. 144, p. 199-429.

19) Goodwin, J.G., 1957, Lead and zinc in California: California Jour. Mines and Geology, v. 53, nos. 3 and 4, p. 353-724.

20) Bailey, E.H., and Phoenix, D.A., 1944, Quicksilver deposits in Nevada: Univ. Nevada Bull., v. 38, no. 5 (Geology and Mining Ser. no. 41), 50 p.

21) MacKevett, E.M., Jr., 1960, Geology and ore deposits of the Kern River uranium area, California: U.S. Geol. Survey Bull. 1087-F, p. 169-222.

22) Morton, P.K., 1965, Geology of the Queen of Sheba lead mine, Death Valley, California: California Div. Mines and Geology Spec. Rept. 88, 18 p.

23) Smith, M.B., Engler, V.L., Lee, D.I., Horn, K.J., and Wayland, R.G., 1971, Reported occurrences of selected minerals in the central third of California: U.S. Geol. Survey Mineral Inv. Resource Map MR-48, scale 1:500,000.

24) Wright, L.A., Stewart, R.M., Gay, T.E., Jr., and Hazenbush, G.C., 1953, Mines and mineral deposits of San Bernardino County, California: California Jour. Mines and Geology, v. 49, nos. 1 and 2, p. 49-192.

25) Rinehart, C.D., Ross, D.C., and Pakiser, L.C., 1964, Geology and mineral deposits of the Mount Morrison quadrangle, Sierra Nevada, California; With a section on a gravity study of Long Valley: U.S. Geol. Survey Prof. Paper 385, 106 p.

26) Pierce, H.W., Keith, S.B., and Wilt, J.C., 1970, Coal, oil, natural gas,

helium, and uranium in Arizona: Arizona Bur. Mines Bull. 182, 274 p.

27) Granger, H.C., and Raup, R.B., 1962, Reconnaissance study of uranium deposits in Arizona: U.S. Geol. Survey Bull. 1147-A, 54 p.

28) Lausen, Carl, and Gardner, E.D., 1927, Quicksilver resources of Arizona: Arizona Bur. Mines Bull. 122, 112 p.

29) Harrer, C.M., 1964, Reconnaissance of iron resources in Arizona: U.S. Bur. Mines Information Circ., IC 8236, 204 p.

30) McCrory, F.J., and O'Haire, R.T., 1961, Map of known nonmetallic mineral occurrences of Arizona: Arizona Bur. Mines Map, scale 1:1,000,000.

31) Beal, L.H., 1965, Geology and mineral deposits of the Bunkerville mining district, Clark County, Nevada: Nevada Bur. Mines Bull. 63, 96 p.

32) Wright, L.A., ed., 1957, Mineral commodities of California: California Div. Mines Bull. 176, 736 p.

33) Crosby, J.W., III, and Hoffman, S.R., 1951, Fluorspar in California: California Jour. Mines and Geology, v. 47, p. 619-638.

34) Lausen, Carl, 1931, Geology and ore deposits of the Oatman and Katherine districts, Arizona: Arizona Bur. Mines Bull. 131, 126 p.

35) U.S. Geological Survey, Utah Geological and Mineralogical Survey, and Utah Water and Power Board, 1964, Mineral and water resources of Utah: Utah Geol. and Mineralog. Survey Bull. 73, 275 p.

36) Olson, J.C., and Adams, J.W., 1962, Thorium and rare earth in the United States exclusive of Alaska and Hawaii: U.S. Geol. Survey Mineral Inv. Resource Map MR-28, scale 1:3,168,000.

37) Carr, M.S., Guild, P.W., and Wright, W.B., 1967, Iron in the United States exclusive of Alaska and Hawaii: U.S. Geol. Survey Mineral Inv. Resource Map MR-51, scale 1:3,168,000.

38) Bailey, E.H., 1962, Mercury in the United States exclusive of Alaska and Hawaii: U.S. Geol. Survey Mineral Inv. Resource Map MR-30, scale 1:3,168,000.

39) Lemmon, D.M., and Tweto, O.L., 1962, Tungsten in the United States exclusive of Alaska and Hawaii: U.S. Geol. Survey Mineral Inv. Resource Map MR-25, scale 1:3,168,000.

40) McKnight, E.T., Newman, W.L., and Heyl, A.V., Jr., 1962, Zinc in the

United States exclusive of Alaska and Hawaii: U.S. Geol. Survey Mineral Inv. Resource Map MR-19, scale 1:3,168,000.

41) McKnight, E. T., Newman, W. L., and Heyl, A. V., Jr., 1962, Lead in the United States exclusive of Alaska and Hawaii: U.S. Geol. Survey Mineral Inv. Resource Map MR-15, scale 1:3,168,000.

42) McKnight, E. T., Newman, W. L., Klemic, Harry, and Heyl, A. V., 1962, Silver in the United States exclusive of Alaska and Hawaii: U.S. Geol. Survey Mineral Inv. Resource Map MR-34, scale 1:3,168,000.

43) Kinkel, A. R., Jr., and Peterson, N. P., 1962, Copper in the United States exclusive of Alaska and Hawaii: U.S. Geol. Survey Mineral Inv. Resource Map MR-13, scale 1:3,168,000.

County Reports

(Mineral deposits compiled from these sources have not been assigned reference numbers on Plate 4)

Goodwin, J. G., 1958, Mines and mineral resources of Tulare County, California: California Jour. Mines and Geology, v. 54, no. 3, p. 317-492.

Longwell, C. R., Pampeyan, E. H., Bowyer, Ben, and Roberts, R. J., 1965, Geology and mineral deposits of Clark County, Nevada: Nevada Bur. Mines Bull. 62, 218 p.

Norman, L. A., Jr., and Stewart, R. M., 1951, Mines and mineral resources of Inyo County: California Jour. Mines and Geology, v. 47, no. 1, p. 17-223.

Ross, D. C., 1961, Geology and mineral deposits of Mineral County, Nevada: Nevada Bur. Mines Bull. 58, 98 p.

Troxel, B. W., and Morton, P. K., 1962, Mines and mineral resources of Kern County, California: California Div. Mines and Geology, County Rept. no. 1, 370 p.

Tschanz, C. M., and Pampeyan, E. H., 1970, Geology and mineral deposits of Lincoln County, Nevada: Nevada Bur. Mines Bull. 73, 187 p.

3.4.11 Supplemental References:

Albers, J.P., and Kleinhampl, F.J., 1970, Spatial relation of mineral deposits to Tertiary volcanic centers in Nevada: U.S. Geol. Survey Prof. Paper 700-C, p. C1-C10.

Anderson, R.E., Ekren, E.B., and Healey, D.L., 1965, Possible buried mineralized areas in Nye and Esmeralda Counties, Nevada: U.S. Geol. Survey Prof. Paper 525-D, p. D144-D150.

Baker, Arthur, III, Archbold, N.L., and Stoll, W.J., 1972, Forecasts for the future-minerals: Nevada Bur. Mines and Geology Bull. 82, 223 p.

Bateman, P.C., 1965, Geology and tungsten mineralization of the Bishop district, California: U.S. Geol. Survey Prof. Paper 470, 208 p.

Bowen, O.E., Jr., 1954, Geology and mineral deposits of Barstow quadrangle, San Bernardino County, California: California Div. Mines Bull. 165, 208 p.

Callaghan, Eugene, 1939, Geology of the Searchlight district, Clark County, Nevada: U.S. Geol. Survey Bull. 906-D, p. 135-185.

Cook, E.F., 1957, Geology of the Pine Valley Mountains, Utah: Utah Geol. and Mineralog. Survey Bull. 58, 111 p.

Cook, E.F., 1960, Geologic atlas of Utah, Washington County: Utah Geol. and Mineralog. Survey Bull. 70, 119 p.

Cornwall, H.R., 1972, Geology and mineral deposits of southern Nye County, Nevada: Nevada Bur. Mines and Geology Bull. 77, 49 p.

Dover, J.H., 1962, Geology of the northern Palmetto Mountains, Esmeralda County, Nevada (M.S. thesis): Seattle, Univ. Washington, 50 p.

Eidel, J.J., 1966, The crystallization and mineralization of a porphyry stock, Ithaca Peak, Mohave County, Arizona (abs.): Econ. Geology, v. 61, p. 1305-1306.

Ekren, E.B., Anderson, R.E., Rogers, C.L., and Noble, D.C., 1971, Geology of northern Nellis Air Force Base Bombing and Gunnery Range, Nye County, Nevada: U.S. Geol. Survey Prof. Paper 651, 91 p.

Gregory, H.E., 1950, Geology of eastern Iron County, Utah: Utah Geol. and Mineralog. Survey Bull. 37, 153 p.

Hall, W.E., and MacKevett, E.M., 1958, Economic geology of the Darwin quad-

rangle, Inyo County, California: California Div. Mines Spec. Rept. 51, 73 p.

Hall, W. E., and Stephens, H. G., 1963, Economic geology of the Panamint Butte quadrangle and Modoc district, Inyo County, California: California Div. Mines and Geology Spec. Rept. 73, 39 p.

Hansen, S. M., 1962, The geology of the Eldorado mining district, Clark County, Nevada (Ph. D. dissert.): Rolla, Univ. Missouri, 262 p.

Hewett, D. F., 1931, Geology and ore deposits of the Goodsprings quadrangle, Nevada: U. S. Geol. Survey Prof. Paper 162, 172 p.

Heylmun, E. B., ed., 1963, Guidebook to the geology of southwestern Utah: Intermountain Assoc. Petroleum Geologists Guidebook 12, Salt Lake City, Utah, 232 p.

Horton, R. C., Bonham, H. F., and Longwill, W. D., 1962, Zinc occurrences in Nevada by district: Nevada Bur. Mines Map 15, scale 1:1,000,000.

Jerome, S. E., and Cook, D. R., 1967, Relation of some metal mining districts in the western United States to regional tectonic environments and igneous activity: Nevada Bur. Mines Bull. 69, 35 p.

Kantor, Tedral, 1961, Geology of the east-central portion of the Nelson quadrangle, Clark County, Nevada (M. S. thesis): Rolla, Univ. Missouri, 80 p.

Kupfer, D. H., 1960, Thrust faulting and chaos structure, Silurian Hills, San Bernardino County, California: Geol. Soc. America Bull., v. 71, p. 181-214.

Lincoln, F. C., 1923, Mining districts and mineral resources of Nevada: Reno, Nevada Newsletter Publishing Co., p. 137-157.

MacGalliard, Wally, and Liggett, M. A., November 1973, False-color compositing of ERTS-1 MSS imagery: NASA Rept. Inv., NASA-CR-135859, E74-10018, 5 p.

McAllister, J. F., 1952, Rocks and structure of the Quartz Spring area, northern Panamint Range, California: California Div. Mines Spec. Rept. 25, 38 p.

McAllister, J. F., 1955, Geology of mineral deposits in the Ubehebe Peak quadrangle, Inyo County, California: California Div. Mines Spec. Rept. 42, 63 p.

McAllister, J. F., 1956, Geology of the Ubehebe Peak quadrangle, California: U. S.

Geol. Survey Geol. Quad. Map GQ-95, scale 1:62,500.

McKee, E. H., and Nelson, C. A., 1967, Geologic map of the Soldier Pass quadrangle, California and Nevada: U.S. Geol. Survey Geol. Quad. Map GQ-654, scale 1:62,500.

McKee, E. H., 1968, Geology of the Magruder Mountain area, Nevada-California: U.S. Geol. Survey Bull. 1251-H, 40 p.

Nelson, C. A., 1966, Geologic map of the Blanco Mountain quadrangle, Inyo and Mono Counties, California: U.S. Geol. Survey Geol. Quad. Map GQ-529, scale 1:62,500.

Nelson, C. A., 1966, Geologic map of the Waucoba Mountain quadrangle, Inyo County, California: U.S. Geol. Survey Geol. Quad. Map GQ-528, scale 1:62,500.

Nelson, C. A., 1971, Geologic map of the Waucoba Spring quadrangle, Inyo County, California: U.S. Geol. Survey Geol. Quad. Map GQ-921, scale 1:62,500.

Park, C. F., Jr., Gemmill, Paul, and Tschanz, C. M., 1958, Geologic map and sections of the Pioche Hills, Lincoln County, Nevada: U.S. Geol. Survey Mineral Inv. Field Studies Map MF-136, scale 1:12,000.

Park, C. F., Jr., MacDiarmid, R. A., 1970, Ore deposits (second ed.): San Francisco, W. H. Freeman and Co., 522 p.

Proctor, P. D., 1953, Geology of the Silver Reef (Harrisburg) mining district, Washington County, Utah: Utah Geol. and Mineralog. Survey Bull. 44, 169 p.

Ransome, F. L., 1909, The geology and ore deposits of Goldfield, Nevada: U.S. Geol. Survey Prof. Paper 66, 258 p.

Ransome, F. L., 1923, Geology of the Oatman gold district, Arizona: A preliminary report: U.S. Geol. Survey Bull. 743, 58 p.

Rinehart, C. D., and Ross, D. C., 1956, Economic geology of the Casa Diablo Mountain quadrangle, California: California Div. Mines Spec. Rept. 48, 17 p.

Ross, D. C., 1967, Generalized geologic map of the Inyo Mountains region, California: U.S. Geol. Survey Misc. Geologic Inv. Map I-506, 1:125,000.

Schrader, F. C., 1909, Mineral deposits of the Cerbat Range, Black Mountains, and Grand Wash Cliffs, Mohave County, Arizona: U.S. Geol. Survey Bull.

397, 226 p.

Searls, Fred, Jr., 1948, A contribution to the published information on the geology and ore deposits of Goldfield, Nevada: Univ. Nevada Bull., v. 42, no. 5 (Geology and Mining Ser. 48), 24 p.

Spurr, J. E., 1905, Geology of the Tonopah mining district: U. S. Geol. Survey Prof. Paper 42, 295 p.

3.5 RADIOMETRIC AGE DATES

Published radiometric age dates of rocks within the Argus Exploration Company test site were compiled to support the regional investigations summarized in the preceding sections of this report and the detailed field studies outlined in the Appendices. The radiometric age data are shown in the map compilation of Plate 6. The map symbols indicate locations, calculated ages, bibliographic references and the rock types used in the radiometric analyses. The bibliographic references cited in Plate 6 are listed by number in Section 3.5.1 below.

The data in Plate 6 have been used extensively in studying the regional age distribution patterns of plutonic and volcanic rocks and related mineralization, geothermal activity and structural deformation within the test site. These data have supported literature research and field investigations.

3.5.1 References Cited in Plate 6:

1) Curtis, G.H., Evernden, J.F., and Lipson, J., 1958, Age determination of some granitic rocks in California by the potassium-argon method: California Div. Mines Spec. Rept. 54, 16 p.

2) Marvin, R.F., 1968, Transcontinental Geophysical Survey (35°-39° N), radiometric age determinations of rocks: U.S. Geol. Survey Misc. Geologic Inv. Map I-537, scale 1:7,500,000.

3) Larsen, E.S., Jr., Gottfried, David, Jaffe, H.W., and Waring, C.L., 1958, Lead-alpha ages of the Mesozoic batholiths of western North America: U.S. Geol. Survey Bull. 1070-B, p. 35-62.

4) Gottfried, David, Jaffe, H.W., and Senftle, F.E., 1959, Evaluation of the lead-alpha (Larsen) method for determining ages of igneous rocks: U.S. Geol. Survey Bull. 1097-A, 63 p.

5) Gilbert, C.M., Christensen, M.N., Al-Rawi, Yehya, and Lajoie, K.R., 1968, Structural and volcanic history of Mono Basin, California-Nevada, in Coats, R.R., Hay, R.L., and Anderson, C.A., eds., Studies in volcanology: Geol. Soc. America Memoir 116, p. 275-329.

6) Robinson, P.T., McKee, E.H., and Moiola, R.J., 1968, Cenozoic volcanism and sedimentation, Silver Peak region, western Nevada and adjacent California, in Coats, R.R., Hay, R.L., and Anderson, C.A., eds., Studies in volcanology: Geol. Soc. America Memoir 116, p. 577-611.

7) Noble, D.C., 1968, Kane Springs Wash volcanic center, Lincoln County, Nevada, in Eckel, E.B., ed., Nevada Test Site: Geol. Soc. America Memoir 110, p. 109-116.

8) Kistler, R.W., 1968, Potassium-Argon ages of volcanic rocks in Nye and Esmeralda Counties, Nevada, in Eckel, E.B., ed., Nevada Test Site: Geol. Soc. America Memoir 110, p. 251-262.

9) Chesterman, C.W., 1968, Volcanic geology of the Bodie Hills, Mono County, California, in Coats, R.R., Hay, R.L., and Anderson, C.A., eds., Studies in volcanology: Geol. Soc. America Memoir 116, p. 45-68.

10) McKee, E.H., 1968, Age and rate of movement of the northern part of the Death Valley-Furnace Creek fault zone, California: Geol. Soc. America Bull., v. 79, p. 509-512.

11) Evernden, J.F., and Kistler, R.W., 1970, Chronology of emplacement of Mesozoic batholithic complexes in California and western Nevada:

U.S. Geol. Survey Prof. Paper 623, 42 p.

12) Jerome, S.E., and Cook, D.R., 1967, Relation of some metal mining districts in the western United States to regional tectonic environments and igneous activity: Nevada Bur. Mines Bull. 69, 35 p.

13) Schilling, J.H., 1965, Isotopic age determinations of Nevada rocks: Nevada Bur. Mines Rept. 10, 79 p.

14) Anderson, R.E., Longwell, C.R., Armstrong, R.L., and Marvin, R.F., 1972, Significance of K-Ar ages of Tertiary rocks from the Lake Mead region, Nevada-Arizona: Geol. Soc. America Bull., v. 83, p. 273-288.

15) Burchfiel, B.C., Pelton, P.J., and Sutter, J., 1970, An early Mesozoic deformation belt in south-central Nevada - southeastern California: Geol. Soc. America Bull., v. 81, p. 211-215.

16) Marvin, R.F., Byers, F.M., Jr., Mehnert, H.H., Orkild, P.P., and Stern, T.W., 1970, Radiometric ages and stratigraphic sequence of volcanic and plutonic rocks, southern Nye and western Lincoln Counties, Nevada: Geol. Soc. America Bull., v. 81, p. 2657-2676.

17) Fleck, R.J., 1970, Age and tectonic significance of volcanic rocks, Death Valley area, California: Geol. Soc. America Bull., v. 81, p. 2807-2816.

18) Krueger, H.W., and Schilling, J.H., 1971, Geochron/Nevada Bureau of Mines K/Ar age determinations - list 1: Isochron/West, no. 1, p. 9-14.

19) Silberman, M.L., and Chesterman, C.W., 1972, K-Ar age of volcanism and mineralization, Bodie mining district and Bodie Hills volcanic field, Mono County, California: Isochron/West, no. 3, p. 13-22.

20) Armstrong, R.L., Dick, Henry, and Vitaliano, C.J., 1972, K-Ar dates and strontium isotope initial ratios of some Cenozoic volcanic rocks from west-central Nevada: Isochron/West, no. 3, p. 23-28.

21) Silberman, M.L., and McKee, E.H., 1972, A summary of radiometric age determinations of Tertiary volcanic rocks from Nevada and eastern California: Part II, western Nevada: Isochron/West, no. 4, p. 7-28.

22) Ashley, R.P., 1973, Fission-track ages for premineralization volcanic and plutonic rocks of the Goldfield mining district, Esmeralda and Nye Counties, Nevada: Isochron/West, no. 8, p. 25-29.

23) Bonham, H.F., Jr., Garside, L.J., and Silberman, M.L., 1972, K-Ar ages of ore deposition at Tonopah, Nevada: Isochron/West, no. 4, p. 5-6.

24) Speed, R.C., and Armstrong, R.L., 1971, Potassium-Argon ages of some minerals from igneous rocks of western Nevada: Isochron/West, no. 1, p. 1-8.

25) Damon, P.E., 1969, Correlation and chronology of ore deposits and volcanic rocks, in Annual progress report no. COO-689-120 to Research Division: U.S. Atomic Energy Comm., 90 p.

26) Damon, P.E., 1968, Correlation and chronology of ore deposits and volcanic rocks, in Annual progress report no. COO-689-100 to Research Division: U.S. Atomic Energy Comm., 75 p.

27) Krieger, M.H., Creasy, S.C., and Marvin, R.F., 1971, Ages of some Tertiary andesitic and latitic volcanic rocks in the Prescott-Jerome area, north-central Arizona: U.S. Geol. Survey Prof. Paper 750-B, p. B157-B160.

28) Hedge, C.E., and Noble, D.C., 1971, Upper Cenozoic basalts with high Sr^{87}/Sr^{86} and Sr/Rb ratios, southern Great Basin, western United States: Geol. Soc. America Bull., v. 82, p. 3503-3510.

29) Armstrong, R.L., 1966, K-Ar dating using neutron activation for Ar analysis: granitic plutons of the eastern Great Basin, Nevada and Utah: Geochimica et Cosmochimica Acta, v. 30, p. 565-600.

30) Sutter, J.F., 1968, Geochronology of major thrusts, southern Great Basin, California (M.S. thesis): Houston, Rice University, 32 p.

31) Anderson, R.E., 1973, Large-magnitude late Tertiary strike-slip faulting north of Lake Mead, Nevada: U.S. Geol. Survey Prof. Paper 794, 18 p.

32) Anderson, C.A., Blacet, P.M., Silver, L.T., and Stern, T.W., 1971, Revision of Precambrian stratigraphy in the Prescott-Jerome area Yavapai County, Arizona: U.S. Geol. Survey Bull. 1324-C, 16 p.

33) Damon, P.E., and Mauger, R.L., 1966, Epeirogeny-orogeny viewed from the Basin and Range Province: Trans. Soc. Mining Engineers, v. 235, p. 99-112.

34) Livingston, D.E., Mauger, R.L., and Damon, P.E., 1966, Geochronology of the emplacement, enrichment and preservation of Arizona porphyry copper deposits: Econ. Geology, v. 63, p. 30-36.

35) Armstrong, R. L., and Suppe, John, 1973, Potassium-Argon geochronometry of Mesozoic igneous rocks in Nevada, Utah, and southern California: Geol. Soc. America Bull., v. 84, p. 1375-1392.

36) Lanphere, M.A., 1964, Geochronologic studies in the eastern Mojave Desert, California: Jour. Geology, v. 72, no. 4, p. 381-399.

37) Stern, T.W., Newell, M.F., and Hunt, C.B., 1966, Uranium-lead and potassium - argon ages of parts of the Amargosa thrust complex, Death Valley, California: U.S. Geol. Survey Prof. Paper 550-B, p. B142-B147.

38) Edwards, George, and McLaughlin, W.A., 1972, Shell list no. 1, K-Ar and Rb-Sr age determinations of California, Nevada, and Utah rocks and minerals: Isochron/West, no. 3, p. 1-7.

39) Noble, D.C., and McKee, E.H., 1972, Description and K-Ar ages of volcanic units of the Caliente volcanic field, Lincoln County, Nevada, and Washington County, Utah: Isochron/West, no. 5, p. 17-24.

40) Armstrong, R.L., 1970, Geochronology of Tertiary igneous rocks, eastern Basin and Range Province, western Utah, eastern Nevada, and vicinity, U.S.A.: Geochimica et Cosmochimica Acta, v. 34, p. 203-232.

41) Armstrong, R.L., and Higgins, R.E., 1973, K-Ar dating of the beginning of Tertiary volcanism in the Mojave Desert, California: Geol. Soc. America Bull., v. 84, p. 1095-1100.

42) Crowder, D.F., McKee, E.H., Ross, D.C., and Krauskopf, K.B., 1973, Granitic rocks of the White Mountains area, California-Nevada: Age and regional significance: Geol. Soc. America Bull., v. 84, p. 285-296.

43) McKee, E.H., and Nash, D.B., 1967, Potassium-Argon ages of granitic rocks in the Inyo batholith, east-central California: Geol. Soc. America Bull., v. 78, p. 669-680.

44) Dalrymple, G.B., 1963, Potassium-argon dates of some Cenozoic volcanic rocks of the Sierra Nevada, California: Geol. Soc. America Bull., v. 74, p. 379-390.

45) Smith, G.I., Troxel, B.W., Gray, C.H., Jr., and von Huene, Roland, 1968, Geologic reconnaissance of the Slate Range, San Bernardino and Inyo Counties, California: California Div. Mines and Geology Spec. Rept. 96, 33 p.

46) Marvin, R. F., Mehnert, H. H., and McKee, E. H., 1973, A summary of radiometric ages of Tertiary volcanic rocks in Nevada and eastern California. Part III: southeastern Nevada: Isochron/West, no. 6, p. 1-30.

Section 4.0

4.0 POTENTIAL APPLICATIONS OF ERTS-1 MSS DATA

The following sections summarize concepts and analytical techniques recommended for application of ERTS-1 MSS imagery to operational programs of natural resource exploration and management. The following four disciplines are considered:

1. Reconnaissance mineral exploration
2. Reconnaissance hydrologic exploration
3. Reconnaissance geothermal exploration
4. Reconnaissance study of geologic hazards

Each of the four report sections defines the applications of the ERTS-1 data, suggests potential users, recommends imagery analysis and interpretation techniques, and presents qualitative and quantitative assessments of the cost-benefit advantages of the ERTS-1 data.

This analysis of potential applications of ERTS-1 data is based on the results of the regional investigations of geologic phenomena summarized in the preceding sections of this report, and on detailed ground based field studies of key geologic and structural anomalies observed in the ERTS-1 imagery. These field studies have been conducted in the varied geologic, topographic and climatic settings within the test site. Although the effectiveness of the ERTS-1 data may vary greatly with local setting , we have attempted to define principles that can be applied to resource exploration and management in other parts of the world.

4.1 RECONNAISSANCE MINERAL EXPLORATION

4.1.1 Introduction:

An investigation of known mineral deposits in the Argus Exploration Company test site is summarized in Section 3.4 of this report. This investigation has demonstrated that a variety of geologic features associated with mineralization are expressed in ERTS-1 MSS imagery. Although these features are often imprecise and variable, the ERTS-1 data can be used as a basis for selection of preliminary exploration anomalies, providing an effective tool for planning and guiding reconnaissance phases of a mineral exploration program.

The information interpreted from ERTS-1 data is in many respects different from, and complementary to, that gained through conventional geologic, geophysical and geochemical exploration techniques. The following discussion outlines concepts and analytical techniques that show promise in effective application of ERTS-1 data to mineral exploration. Comparisons with other reconnaissance exploration methods suggest potential cost savings in excess of 10 to 1.

4.1.2 Applications:

The application of ERTS-1 MSS imagery to reconnaissance mineral exploration is based on the expression of a variety of geologic and structural features at the synoptic scale of the satellite imagery. Many such features are not generally apparent or efficiently studied at the scale of conventional ground based mapping. For this reason, the ERTS-1 data can be effectively used for studying the regional geologic and structural settings of known mineral deposits, and for selecting new areas of potential mineralization.

Geologic and structural features, or signatures, recognized in association with alteration and mineralization in the test site include the following:

1. Structural controls of ore deposits
2. Rock or soil color anomalies
3. Topographic expression of alteration and mineralization
4. Lithologic associations of mineralization

The characteristics and expression of these signatures typically vary with the age, alteration and mineralization chemistry, lithologic hosts, and physiographic and climatic settings of the deposits. At best such signatures provide only indirect evidence of mineralization. However, at the scale of a reconnaissance exploration program, the ERTS-1 imagery can provide a useful tool for selection of preliminary exploration anomalies and for interpretation of regional geologic, geophysical or geochemical data.

In typical applications, exploration anomalies interpreted from ERTS-1 imagery are on the order of a few tens of square miles in size. Such anomalies are

generally too large for economical evaluation by ground based exploration methods. However, ERTS-1 data can provide a basis for selecting from a large area, a series of exploration anomalies that can be economically narrowed by reconnaissance airborne remote sensing or geophysics and evaluated by subsequent ground based geologic, geophysical or geochemical techniques.

Reconnaissance exploration of this nature has not been generally possible using conventional exploration methods. However, because of the size and imprecision of anomalies selected from the ERTS-1 data, it is improbable that an effective exploration program could be conducted without the expert use of geophysical and/or geochemical techniques. The application of ERTS-1 data to mineral exploration is considered operationally feasible only as part of an integrated exploration program.

4.1.3 Analysis and Interpretation Techniques:

Application of a variety of data analysis and interpretation techniques is important for effective use of the ERTS-1 MSS data. The image enhancement techniques cited below are discussed in greater detail in Section 2.4 of this report.

Spectral Information:

Characteristics of surface coloring related to lithology, soils or vegetation can be studied using several enhancement techniques. Additive color viewing has proven valuable for determining the optimum color balance for discrimination of geologic features. High resolution false-color composites (MacGalliard and Liggett, 1973*), which record this optimum color balance, can then be used for detailed laboratory or field analysis. Spectral ratioing techniques show promise for use in enhancing subtle color anomalies in rock, soil or alluvium associated with alteration and mineralization (see Section 2.4.7; Billingsley and Goetz, 1973; Vincent, 1973). The perception of surface color anomalies is best accomplished in areas where masking by vegetation cover is small and exposures of the characteristic rock or soil are large. Masking by vegetation is often seasonally variable, and repetitive coverage of ERTS-1 data is, therefore, a valuable asset. Current research on anomalous vegetation reflectance in mineral-rich soils (see Howard and others, 1971) and the use of "indicator plants" in geochemical exploration show promise for further refinement of interpretation techniques.

Spatial Information:

The use of ERTS-1 imagery for studying the structural and topographic expressions of alteration and mineralization can be aided by a variety of spatial enhancement techniques. These techniques include edge enhancement, gray-level density slicing, directional pattern filtering with the use of Moiré patterns (see Section 2.4.8;

---

* Appendix J, this report

and Cummings and Pohn, 1966), Fourier transform analysis (see Section 2.4.9) and computer processing of spatial information (Billingsley and Goetz, 1973). Sun azimuth and elevation have a strong influence on the expression of topographic information in ERTS-1 data (see for example, Barth, 1974*), and for this reason a full range of seasonal coverage should be studied when available.

4.1.4 Potential Users:

Applications of ERTS-1 data to reconnaissance mineral exploration have an obvious source of potential users in the mineral resource industry. However, several related applications can be made by governmental research organizations, such as the U.S. Geological Survey and the U.S. Bureau of Mines and corresponding state and foreign governmental agencies. The capability for inventory and reconnaissance of priority exploration areas can play an important role in land use planning and related legislative policies for resource development or conservation. The ERTS-1 imagery provides a unique basis for such investigations.

4.1.5 Qualitative Assessment:

The spectral and spatial information recorded in ERTS-1 imagery provides a basis for reconnaissance exploration, previously unavailable except from more costly reconnaissance geologic mapping, color aerial photography, airborne geophysics, or gravity surveys. In addition, the synoptic scale of the ERTS-1 imagery permits the regional synthesis and interpretation of diverse geologic and structural phenomena.

Examples of applications of ERTS-1 data are documented in several studies conducted as part of this research program. Analysis of ERTS-1 imagery over southern Nevada has led to recognition of regional structural control of gold mineralization in a large metallogenic province along the Colorado River south of Lake Mead, Nevada (Liggett and Childs, 1974**; Bechtold and others, 1972***, 1973****). These studies have resulted in a structural model which suggests a genetic interrelationship between six major areas of gold mineralization, each formerly considered to be separate districts. This model provides a valuable tool for guiding exploration for new ore deposits in the province. A similar structural study using ERTS-1 MSS imagery over the northern termination of the Death Valley-Furnace Creek fault zone has revealed probable structural control of mercury mineralization associated with late Tertiary silicic volcanism (Childs, 1974*****).

---

* Appendix N, this report
** Appendix O, this report
*** Appendix A, this report
**** Appendix E, this report
***** Appendix K, this report

The knowledge of structural control of mineralization gained from studies such as these can play a valuable role in the planning and interpretation of geophysical exploration surveys. Geologic reconnaissance of structural anomalies interpreted in ERTS-1 MSS imagery over southern Nevada and eastern California has led to recognition of a major fault system, called the Pahrump fault zone (Liggett and Childs, 1973*). In addition to guiding efficient and economical field work, the ERTS-1 data provided a basis for interpretation of an existing regional gravity survey. Neither the extent of the fault system nor its control of regional gravity patterns had been recognized from earlier geologic mapping in the area.

ERTS-1 imagery can be used in the selection of key exploration anomalies, which can be efficiently and economically evaluated using a variety of conventional exploration techniques. In this application, ERTS-1 data can provide a valuable tool for planning and directing reconnaissance exploration.

4.1.6 Quantitative Assessment:

The geologic information gained from ERTS-1 MSS imagery is not generally equivalent to that obtained from other reconnaissance geologic or geophysical tools. Nevertheless, a comparison of costs for the acquisition and analysis of ERTS-1 data and other exploration techniques will illustrate some of the cost advantages of the satellite imagery.

At an optimum level of study, geologic analysis of ERTS-1 imagery is estimated to cost approximately $10,000 per scene covering roughly 13,200 square miles (33,800 square km), or less than $1.00 per square mile. Such a study would include image enhancement and analysis processing, research and analysis of subsidiary geologic, geophysical, and remote sensing data, ground based reconnaissance of key areas, and related overhead expenses. An investigation of this nature would be expected to result in selection of key exploration anomalies representing less than 5 percent of the original 13,200 square mile area.

The selection of comparable exploration areas, using other reconnaissance techniques, is considerably more expensive. Reconnaissance geologic mapping, comparable in resolution to the ERTS-1 imagery, would probably need to be at the scale of 1:100,000 or 1:200,000. The costs for such reconnaissance mapping in the southwestern United States are estimated at between $60 and $200 per square mile.

The range in costs for acquisition of several alternate types of remote sensing data over the western United States is estimated below. These estimates are based on experience and on data cited by Carter and others (1972).

---

* Appendix H, this report

Black and white aerial photography	$3.00 to $10.00/square mile
Color or multispectral aerial photography	$10.00 to $40.00/square mile
Thermal-infrared imagery	$5.00 to $30.00/square mile
Low resolution aerial magnetometry	$10.00 to $50.00/square mile
Multiple airborne geophysics	$50.00 to $150.00/square mile

These acquisition costs can increase substantially, depending on geographic area, mobilization costs, topography and seasonal logistics. The costs for analysis and interpretation of these data are likewise variable. The higher costs for acquisition of aerial remote sensing data over ERTS-1 MSS data do not ensure greater effectiveness in reconnaissance exploration.

The analysis of ERTS-1 imagery over known ore deposits in the southern Basin Range Province has indicated a variety of spectral and spatial anomalies related to alteration and mineralization. This information is complementary to data from conventional geologic mapping, geophysics and aerial photography. Although the use of ERTS-1 imagery would typically be confined to the reconnaissance phases of an exploration program, its application can result in significant cost savings. Comparisons with other techniques suggest cost savings in excess of 10 to 1 for reconnaissance exploration in the semiarid terrane of the southwestern United States.

4.1.7 References Cited in Text:

Barth, J.W., March 1974, Investigation of a lineament expressed in an oblique Apollo 9 photograph: NASA Rept. Inv., NASA-CR-137255, E74-10410, 7 p.

Bechtold, I.C., Liggett, M.A., and Childs, J.F., November 1972, Structurally controlled dike swarms along the Colorado River, northwestern Arizona and southern Nevada (abs.): NASA Rept. Inv., NASA-CR-128390, E72-10192, 2 p.

Bechtold, I.C., Liggett, M.A., and Childs, J.F., March 1973, Regional tectonic control of Tertiary mineralization and Recent faulting in the southern Basin-Range Province: An application of ERTS-1 data, in Freden, S.C., Mercanti, E.P., and Becker, M.A., eds., Symposium on significant results obtained from the Earth Resources Technology Satellite-1: New Carrollton, Maryland, v. 1, sect. A, paper G21, NASA-SP-327, E73-10824, p. 425-432.

Billingsley, F.C., and Goetz, A.F.H., 1973, Computer techniques used for some enhancements of ERTS images, in Freden, S.C., Mercanti, E.P., and Becker, M.A., eds., Symposium on significant results obtained from the Earth Resources Technology Satellite-1: New Carrollton, Maryland, v. 1, sect. B, paper I9. NASA-SP-327, E73-10824, p. 1159-1168.

Carter, W.D., Hammond, C.W., Barnett, Thomas, Muhm, J.R., Anderson, Richard, Schmer, Fred, Everett, Gordon, Peplies, R.W., Morain, Stanley and Marcus, Paul, 1972, Evaluation of remote sensing by Geology, Hydrology, and Geography Panel, in Seminar on operational remote sensing: Am. Soc. Photogrammetry, p. 269-281.

Childs, J.F., January 1974, Fault pattern at the northern end of the Death Valley - Furnace Creek Fault Zone, California and Nevada: NASA Rept. Inv., NASA-CR-136387, E74-10205, 8 p.

Cummings, David, and Pohn, H.A., 1966, Application of Moiré patterns to lunar mapping, in Astrogeologic studies, Annual Progress Report 1965-66, part A (lunar and planetary investigation): U.S. Geol. Survey, p. 183-187.

Howard, J.A., Watson, R.D., and Hessin, T.D., 1971, Spectral reflectance properties of Pinus ponderosa in relation to copper content of the soil-Malachite Mine, Jefferson County, Colorado, in Proceedings of the seventh international symposium on remote sensing of environment: Inst. Sci. and Technology, Univ. of Michigan, Ann Arbor, Michigan, v. 1, p. 285-297.

Liggett, M.A., and Childs, J.F., July 1973, Evidence of a major fault zone along the California-Nevada state line, 35°30' to 36°30' N. latitude: NASA Rept. Inv., NASA-CR-133140, E73-10773, 10 p.

Liggett, M.A., and Childs, J.F., March 1974, Crustal extension and transform faulting in the southern Basin Range Province: NASA Rept. Inv., NASA-CR-137256, E74-10411, 28 p.

MacGalliard, Waliy, and Liggett, M.A., November 1973, False-color compositing of ERTS-1 MSS imagery: NASA Rept. Inv., NASA-CR-135859, E74-10018, 5 p.

Vincent, R.K., March 1973, Ratio maps of iron ore deposits, Atlantic City District, Wyoming, in Freden, S.C., Mercanti, E.P., and Becker, M.A., eds., Symposium on significant results obtained from the Earth Resources Technology Satellite-1: New Carrollton, Maryland, v. 1, sect. A, paper G16, NASA-SP-327, E73-10824, p. 379-386.

4.2 RECONNAISSANCE HYDROLOGIC EXPLORATION

4.2.1 Introduction:

This report section describes concepts and interpretation techniques for potential applications of ERTS-1 imagery to reconnaissance hydrologic exploration. Our study of regional structural geology using ERTS-1 MSS data has indicated that geologic and structural features associated with hydrologic basin development can be studied efficiently over larger areas than formerly possible using conventional methods. The resolution of the ERTS-1 imagery provides details of fault patterns, vegetation distribution, and rock and soil types sufficient to aid in the selection and subsequent evaluation of areas having high potential for ground water development.

Estimates of the cost advantages gained through the use of ERTS-1 imagery in reconnaissance hydrologic exploration in arid or semiarid areas are on the order of 10 to 1 over conventional techniques.

4.2.2 Applications:

Potential applications of ERTS-1 imagery to hydrologic exploration in the southern Basin Range Province may be classified as follows:

1. Recognition of structural control of basin geometry and structural ground water traps

2. Recognition of vegetation anomalies related to springs, seeps, and intermittent streams

3. Discrimination of rock and soil types

The primary application of the ERTS-1 data to hydrology is in recognizing structural controls of ground water basin geometry and ground water movement within the basins. A secondary application relies on repetitive ERTS-1 coverage for studying the seasonal expression of drainage patterns and phreatophyte plant distribution. Rock and soil discrimination will assume greater importance in hydrologic applications as new imagery enhancement techniques are perfected. Potential applications of rock and soil discrimination involve recognition of aquifers, such as coarse-grained alluvium in basin areas and carbonate units in the bedrock of ranges. Rock-type discrimination can also support interpretation of structural ground water traps, such as faults that have juxtaposed rock types with different reflectance characteristics.

Most of the proven ground water resources in the arid to semiarid terrane of the Argus Exploration Company test site have been found in basin areas. The ERTS-1 MSS imagery has proven to be especially useful for reconnaissance in such basin areas, where structure and topography are simple and vegetation is scarce.

A reconnaissance investigation using ERTS-1 MSS imagery can provide hydrologic information of sufficient detail to outline areas for further study using ground based geochemical, geophysical and geohydrological techniques.

4.2.3 Discussion:

In several studies conducted as part of this investigation, analysis of ERTS-1 imagery has led to recognition of regional structural control of ground water basins. For example, in a study of the Pahranagat shear system in Lincoln County, Nevada, Liggett and Ehrenspeck (1974*) established a model for the interrelationship between Basin Range normal faulting and contemporaneous strike-slip faulting. This model indicates the probable geometry of two structural depressions, which are the sites of the Delamar and Sheep Mountain Dry Lake ground water basins.

Analysis of ERTS-1 MSS imagery over the California-Nevada border west of Las Vegas, Nevada, has led to recognition of a large fault system, named the Pahrump fault zone by Liggett and Childs (1973**). Several strands of this fault system form the steep western sides of Stewart, Pahrump, and Mesquite Valleys and the western termination of the alluvial ground water system. The eastern margin of Pahrump Valley is formed by a tilted block of Paleozoic rocks which dips gently beneath the basin alluvium. In a hydrological study of Pahrump Valley, Malmberg (1967) recognized the eastern margin of the valley to be the major source of ground water recharge. The ground water flows westward in two aquifer systems; an upper alluvial system and a lower system developed in the Paleozoic carbonate bedrock. The ground water in the alluvial aquifer is trapped along the valley floor by strands of the Pahrump fault zone, expressed in the ERTS-1 imagery as linear scarps and alignments of vegetation at springs and seeps (Liggett and Childs, 1973).

The presence of phreatophyte vegetation at springs and seeps along faults in alluvium has been recognized in ERTS-1 imagery over several other basins, including Las Vegas Valley, the Ash Meadows region and Death Valley. In central Death Valley, the springs are recognized not only by their vegetation but also by the white travertine deposits at Keane Springs on the east side of the valley north of Furnace Creek.

Vegetation abundance can also be a guide to the overall ground water budget of the basins. For example, Malmberg (1965, p. 80) calculated that the draft on the Las Vegas ground water basin by phreatophyte plants in 1906 (before artificial development) was approximately 30,000 acre-feet. The average annual natural recharge was estimated at 25,000 acre-feet (Malmberg, 1965, p. 1), suggesting that the phreatophytes were formerly the major draft on the ground water system in the Las Vegas Basin. The repetitive coverage of the ERTS-1 imagery forms a

---

* Appendix L, this report

** Appendix H, this report

useful record of seasonal plant vigor and abundance. Analysis of the distribution and abundance of vegetation can provide a basis for estimating the ground water reserves of a hydrologic basin.

An additional use of ERTS-1 imagery in hydrologic exploration is the discrimination of key soil and rock types based on differences in coloring, vegetation, topographic and drainage characteristics. Such rocks as clay-rich playa sediments, older and younger alluvium, and carbonate, volcanic, metamorphic and granitic rock units can frequently be recognized in ERTS-1 data. In Pahrump Valley, for example, several faults that form ground water traps are expressed in the ERTS-1 imagery by the juxtaposition of sediments of contrasting color (Liggett and Childs, 1973*). Discrimination of key rock types can be useful in estimating the thickness and distribution of alluvial valley fill, the size of potential ground water reservoirs, and in studying the late Cenozoic history of ground water basins.

4.2.4 Analysis and Interpretation Techniques:

Experimentation with the ERTS-1 MSS imagery has shown several enhancement techniques to be effective in applications to hydrologic exploration.

Spectral Information:

High resolution false-color composites of ERTS-1 MSS imagery (MacGalliard and Liggett, 1973**) are a basic tool for studying the reflectance characteristics of rock and vegetation units. The optimum choice of composite band-filter combinations and color balance can be selected using an additive color viewer. False-color compositing and spectral band ratioing (see Sections 2.4.5 and 2.4.7) of ERTS-1 data over Las Vegas, Pahrump and Mesquite Valleys, Nevada, have enhanced subtle differences in playa and alluvial sediments, vegetation and drainage patterns and structural features useful in understanding the geometry and dynamics of the known ground water reservoirs in these basins.

ERTS-1 imagery covering a full seasonal span is valuable for understanding annual changes in the expression of vegetation, intermittent streams and spring flow.

Spatial Information:

Edge enhancement and directional pattern filtering using Moiré patterns have been used to accentuate the expression of faults in alluvial basins, at range fronts, and within the bedrock of ranges (see Sections 2.4.3 and 2.4.8). These techniques have also been used to enhance the topographic expression of drainage patterns. Photographic density slicing has been used to enhance subtle differences in alluvial

---

* Appendix H, this report

** Appendix J, this report

characteristics.

Recognition of fault scarps in alluvium is frequently dependent on the sun azimuth and elevation. For this reason, it is valuable to examine ERTS-1 imagery recorded over a full seasonal span.

4.2.5 Potential Users:

Effective applications of ERTS-1 data can be made by governmental agencies and private organizations in a broad range of reconnaissance hydrologic studies, including ground water exploration, pollution studies, land use planning and agricultural development. The reconnaissance nature, low cost, and usefulness in arid terrane make the ERTS-1 data well suited for potential applications by governments of developing countries.

Potential users in the United States include the U.S. Geological Survey, Bureau of Land Management, Bureau of Reclamation, and Department of Agriculture, along with corresponding state and local agencies.

4.2.6 Qualitative Assessment:

The primary advantage of the ERTS-1 imagery is the ability to conduct reconnaissance hydrologic studies of large areas more economically than with conventional techniques. Use of the ERTS-1 data in a reconnaissance program provides information on basin geometry, vegetation, drainage patterns, soil and rock types, and structural control of ground water distribution. These data can be used to guide investigators to areas of high potential in which more expensive ground based geologic and geophysical techniques can be concentrated for maximum efficiency.

In a three-year hydrologic study of Hualapai and Sacramento Valleys in Mohave County, Arizona, Gillespie and Bentley (1971) produced a geohydrologic map at a scale of 1:125,000. This study concentrated on the alluvial basins and provided information on ground water movement, water table levels and geochemistry that cannot be interpreted from ERTS-1 imagery. However, within this same area, the ERTS-1 imagery provides data on drainage patterns, vegetation distribution and seasonal changes, structural control of basin development, and rock and soil type discrimination which are not shown on the published geohydrologic map. Based on comparison of the ERTS-1 data analysis with other hydrologic studies in the test site, it is estimated that the satellite data is suitable to guide reconnaissance geohydrologic studies at scales of 1:125,000 and possibly larger.

4.2.7 Quantitative Analysis:

The information gained from analysis of ERTS-1 MSS imagery is complementary to data from ground based geohydrologic studies. Based on our work in the southern Basin Range Province, hydrologic reconnaissance using ERTS-1 imagery, including limited ground based study, is estimated to cost approximately $8,000

per scene (13,200 square miles or 33,800 square km). The cost of ground based hydrologic mapping of comparable scale is estimated to be approximately $100 per square mile, excluding detailed geochemical or geophysical surveys. The potential cost savings gained by using ERTS-1 imagery in reconnaissance hydrologic exploration in the arid southwestern United States are estimated to be approximately 10 to 1 over conventional reconnaissance techniques.

4.2.8 References Cited in Text:

Gillespie, J.B., and Bentley, C.B., 1971, Geohydrology of Hualapai and Sacramento Valleys, Mohave County, Arizona: U.S. Geol. Survey Water-Supply Paper 1899-H, 37 p.

Liggett, M.A., and Childs, J.F., July 1973, Evidence of a major fault zone along the California-Nevada state line, 35°30' to 36°30' N. latitude: NASA Rept. Inv., NASA-CR-133140, E73-10773, 10 p.

Liggett, M.A., and Ehrenspeck, H.E., January 1974, Pahranagat Shear System, Lincoln County, Nevada: NASA Rept. Inv., NASA-CR-136388, E74-10206, 10 p.

MacGalliard, Wally, and Liggett, M.A., November 1973, False-color compositing of ERTS-1 MSS imagery: NASA Rept. Inv., NASA-CR-135859, E74-10018, 5 p.

Malmberg, G.T., 1965, Available water supply of the Las Vegas ground-water basin Nevada: U.S. Geol. Survey Water-Supply Paper 178C, 116 p.

Malmberg, G.T., 1967, Hydrology of the valley-fill and carbonate-rock reservoirs, Pahrump Valley, Nevada-California: U.S. Geol. Survey Water-Supply Paper 1832, 47 p.

4.3 RECONNAISSANCE GEOTHERMAL EXPLORATION

4.3.1 Introduction:

This report section describes concepts and techniques for application of ERTS-1 MSS imagery to reconnaissance exploration for geothermal resources. As a part of this investigation we have studied the distributions of known geothermal areas in the Argus Exploration Company test site (see Plate 5) and the relationship of these areas to a variety of geologic and structural features expressed in the ERTS-1 MSS imagery. The ERTS-1 data have provided information complementary to that obtained through conventional geologic, geochemical and geophysical reconnaissance techniques.

The following discussions are restricted to the area of the test site, although the known geothermal potential of surrounding areas to the north and northeast in Nevada and Utah is presently also attractive. The general concepts and techniques summarized here are considered applicable to reconnaissance exploration in many other parts of the world.

4.3.2 Applications:

Applications of ERTS-1 imagery to the search for geothermal resources fall within four broad categories, as follows:

1. Recognition of regional tectonic controls of volcanism, plutonism, and related geothermal activity

2. Identification of volcanic rocks, their shallow plutonic equivalents and related features such as caldera structures

3. Interpretation of the local structural settings of known or potential areas of geothermal activity

4. Identification of vegetation oases, hot spring deposits, and associated hydrothermal alteration

The first three applications noted above utilize the synoptic overview provided by the ERTS-1 MSS imagery. The fourth application relies heavily on the ability to recognize small spectral and topographic anomalies often approaching the limit of ERTS-1 resolution. These applications require interpretation of widely different spatial and spectral anomalies in high resolution color composites and other enhancements of the basic ERTS-1 MSS imagery.

Proper analysis and interpretation of ERTS-1 MSS imagery can provide a useful basis for planning and guiding reconnaissance exploration for potential geothermal heat or steam sources. Such reconnaissance and subsequent evaluation are expected to be most effective when coordinated as part of an integrated exploration program

using other geological, geophysical and geochemical survey techniques.

4.3.3 Discussion:

The four main uses of ERTS-1 imagery in reconnaissance geothermal surveys are discussed in greater detail in the following paragraphs. Specific examples are given to illustrate these applications. Reference should be made to Plate 5 and to the ERTS-1 color composites presented in Section 2.3 of this report.

1. A primary use of ERTS-1 imagery is in analyzing the regional geologic settings of known geothermal areas and in identifying the tectonic controls of the distribution of volcanic and plutonic activity. A comparison between the tectonic map (Plate 1) and the compilation of known geothermal areas (Plate 5) shows that a large proportion of the known hot springs in the test site are located along major tectonic features. Prominent examples of such associations occur along the Kern Canyon fault zone, Owens Valley fault zone, Panamint fault zone, Death Valley fault zone, Pahrump fault zone (Liggett and Childs, 1973*), Las Vegas shear zone (Liggett and Childs, March 1974**), Paymaster fault zone (Childs, November 1973***), and the Hurricane fault zone.

Analysis of ERTS-1 imagery over the southern Basin Range Province has led to a hypothesis of regional tectonic control of Tertiary igneous activity in parts of the province (Liggett and Childs, March 1974**). Several hot springs are located in the volcanic terrane south of Lake Mead, Nevada (ERTS-1 MSS Frame #1106-17495, Figure 4, northeast quarter). This region is characterized by a thick sequence of Tertiary volcanic rocks and epizonal granitic plutons and is inferred to be an area of crustal extension (Liggett and Childs, March 1974**). A second area of inferred crustal extension is located in the volcanic terrane of Nye County, Nevada. This volcanic province contains several late Tertiary volcanic centers including the Bullfrog Hills, Timber Mountain, and Black Mountain calderas near Beatty, Nevada (ERTS-1 MSS Frame #1125-17551, Figure 5, southwest quarter). Although the only active hot spring in this area is along the eastern margin of the Bullfrog Hills caldera, the extensive late Tertiary and Quaternary volcanic activity suggests considerable potential for dry rock geothermal sources at shallow depths. It is probable that dry rock systems will become increasingly important in the future. The remoteness and government control of this area make it attractive for experimental development.

2. Most of the known hot springs in the test site are located within Tertiary or Quaternary volcanic terranes, which can be clearly discriminated in ERTS-1 imagery. In California, the most prominent of these springs are Coso

---

* Appendix H, this report
** Appendix O, this report
*** Appendix I, this report

Hot Springs, located in an intensely faulted volcanic terrane of Cenozoic cinder cones, and lava flows at the southern end of Owens Valley (ERTS-1 MSS Frame #1162-18011, Figure 13, center); Casa Diablo Hot Springs, located in the resurgent portion of the Long Valley caldera, north of Bishop (ERTS-1 MSS Frame #1163-18063, Figure 14, north half); and Grapevine Springs, situated near the Ubehebe Craters and associated basaltic flows in northern Death Valley (ERTS-1 MSS Frame #1126-18010, Figure 6, south-central part).

In Nevada, potential geothermal areas are represented by Hicks Hot Springs, located along the eastern margin of the Bullfrog Hills caldera, near Beatty (ERTS-1 MSS Frame #1125-17551, Figure 5, southwest quarter); hot springs south of Lake Mead located along the margin of the Boulder City pluton of Tertiary age (Anderson, 1969) and near basaltic dikes and flows of Quaternary age (ERTS-1 MSS Frame #1106-17495, Figure 4, northeast quarter); and hot springs in the Caliente depression in Lincoln County, which are centered in a Cenozoic igneous complex of shallow granitic plutons and felsic volcanic rocks (ERTS-1 MSS Frame #1106-17492, Figure 7, northeast quarter). In Grand Canyon, Arizona, Lava Warm Springs is situated on the Toroweap fault at the south end of a large basalt field (ERTS-1 MSS Frame #1069-17432, Figure 9, northeast quarter). Nearly all of the known hot springs in volcanic areas are located where the rocks have been intensely faulted.

Based on field reconnaissance and analysis of ERTS-1 imagery, the following areas are believed to warrant investigation for possible volcanogenic geothermal resources: the Long Valley-Mono area (already designated a Known Geothermal Resource Area by the federal government); the area immediately east and west of Beatty, Nevada, including the western part of the Atomic Energy Commission Nevada Test Site; an area immediately south of Lake Mead along the Colorado River; the Coso Hot Springs area in southern Owens Valley, California; and the Caliente depression of Lincoln County, Nevada (see Plate 5).

3. The ERTS-1 data have proven effective in field investigations of the local structural settings of known geothermal areas. Such a reconnaissance study in central Death Valley (Childs, July 1973*) has indicated that a previously unrecognized fault intersects the Keane Wonder fault at Keane Hot Springs (ERTS-1 MSS Frame #1125-17554, Figure 12, northwest quarter). Interpretation of ERTS-1 imagery and study of published data on the Coso Hot Springs area of southern Owens Valley has indicated the presence of numerous normal faults, which have resulted in the formation of grabens and tilted blocks in the Cenozoic basaltic and andesitic volcanic rocks of the area.

Several north striking faults within the Long Valley caldera that control known hot spring locations, and arcuate faults that rim the caldera structure

---

* Appendix F, this report

are expressed in the ERTS-1 imagery. In the Grapevine Springs area of Death Valley, several faults associated with the hot springs are apparent in ERTS-1 MSS Frame #1126-18010 (Figure 6, southeast quarter). Some of these faults are branches of the northwest striking Death Valley-Furnace Creek fault zone, but others appear to be extensions of a more vague, east-west zone which extends eastward to the Bullfrog Hills caldera.

The known hot springs south of Lake Mead are in an area of Tertiary fault zones, dike swarms and shallow plutons, many of which are expressed in the ERTS-1 imagery and have been studied in the field. Most known hot springs in the Sierra Nevada are located along fault zones in the granitic rocks of the Sierran batholith. Many of these structural lineaments are recognizable in ERTS-1 imagery. For example, the Kern Canyon fault (Liggett and Childs, February 1974*) in the southern Sierra Nevada is believed to have controlled the location of hot springs and related uranium deposits near Kernville, California (ERTS-1 MSS Frame #1162-18011, Figure 13, southwest quarter; and MacKevett, 1960).

4. The ERTS-1 MSS imagery has provided spectral information useful in identifying hot spring sites. Some of the larger hot springs have developed tufa deposits large enough to form color anomalies in the ERTS-1 imagery. An example is the travertine deposit on the east side of Death Valley at Keane Hot Springs, north of Furnace Creek Ranch. The travertine covers an area of approximately 2 square km and is expressed as a strong white anomaly in ERTS-1 MSS Frame #1125-17554 (Figure 12, northwest quarter). In the arid environment of the test site, the ERTS-1 imagery has been used to identify oases of vegetation that are commonly present at springs. Examples are the vegetation anomalies in the Pahrump fault zone along the Nevada-California state line (Liggett and Childs, 1973** ; and ERTS-1 MSS Frame #1106-17495, Figure 4, northwest quarter). Two of these, Pahrump and Manse Springs, are known to be warm, although the temperatures of springs cannot be differentiated in the ERTS-1 imagery. Efficient field reconnaissance can be conducted for image anomalies located in areas having high potential for geothermal sources.

4.3.4 Analysis and Interpretation Techniques:

The image analysis and interpretation techniques found useful in studying the characteristics of known geothermal areas are outlined below. The reader is referred to Section 2.4 for a detailed discussion of these techniques.

Spectral Information:

Spectral information useful in geothermal exploration can be interpreted from

---

* Appendix M, this report

** Appendix H, this report

vegetation, hot spring deposits, hydrothermal alteration of country rocks, and distinctive color anomalies associated with igneous rocks. Many of these spectral anomalies are recognizable in the high resolution color composites used in this study (MacGalliard and Liggett, 1973*). In addition, spectral ratio composites have proven valuable for discriminating vegetation anomalies, hydrothermal alteration zones and hot spring deposits. This technique has been used on ERTS-1 imagery over the Pahrump and Manse Springs to achieve enhanced definition of the vegetation anomalies associated with the Pahrump fault zone.

Spatial Information:

Edge enhancement printing of ERTS-1 MSS imagery and the use of Moiré patterns in image analysis and interpretation have proven useful in studying regional structural patterns. Seasonal changes in sun azimuth and elevation make analysis of multiseasonal imagery advantageous in studying the topographic expression of structural patterns. As a supplement to the ERTS-1 data, SLAR imagery has been used successfully in recognizing subtle fault patterns in the Mono-Long Valley Known Geothermal Resource Area.

4.3.5 Potential Users:

The number of private firms entering the search for geothermal resources is growing rapidly, and ERTS-1 imagery can be a useful component of their exploration programs. Governmental agencies can effectively use ERTS-1 imagery in reconnaissance geothermal resource exploration and related land use planning. Such agencies include the U.S. Geological Survey, Bureau of Mines, Department of Agriculture, and Environmental Protection Agency, as well as corresponding foreign governmental agencies.

4.3.6 Qualitative Assessment:

Most regional geothermal exploration conducted to date has been based on reconnaissance geologic mapping and study of known hot springs or wells. However, several recent exploration programs have experimented with reconnaissance gravity (Rinehart and others, 1964), aeromagnetic (Griscom and Muffler, 1971) and thermal infrared surveys (Carter and others, 1972). Heat flow and resistivity surveys have been applied in more detailed studies of geothermal prospects. The information gathered through these techniques is found to differ greatly, depending on the geologic and structural settings of the geothermal reservoirs.

Proper analysis and interpretation of ERTS-1 MSS imagery are potentially useful in reconnaissance geothermal exploration when used in coordination with other exploration techniques. The key use of ERTS-1 data is in studying the regional

---

* Appendix J, this report

tectonic framework of areas of Cenozoic igneous activity for selection of potential geothermal steam or heat sources at shallow depths. The size of exploration anomalies identified in ERTS-1 data is likely to be a minimum of several tens of square miles. These exploration areas can be more narrowly defined and evaluated using specialized geophysical, geochemical and geologic techniques such as those cited above. However, the ERTS-1 data provide a basis for reconnaissance exploration previously available only with regional geologic or geophysical map compilations of variable accuracy and detail.

4.3.7 Quantitative Assessment:

Analysis and interpretation of ERTS-1 data for application to reconnaissance geothermal exploration is estimated to cost less than $1.00 per square mile (2.5 square km). Such an exploration program would include research of existing geologic and regional geophysical data and field investigations of key geologic and structural anomalies for selection of geothermal exploration targets.

In comparison with the use of ERTS-1 MSS imagery, other reconnaissance techniques applicable to geothermal exploration are considerably more expensive. The costs of geologic mapping at a scale of 1:100,000 or 1:200,000 are estimated to be between $60 and $200 per square mile; aeromagnetic surveys from $10 to $50 per square mile; reconnaissance gravity surveys from $150 to $300 per square mile; and thermal infrared imaging from $5 to $30 per square mile.

The use of ERTS-1 imagery for reconnaissance of potential geothermal sources can significantly reduce the overall size of the area that would need to be surveyed using the more expensive geologic and geophysical techniques cited above. In reconnaissance exploration, the application of ERTS-1 data is believed to provide potential cost savings on the order of 10 to 1.

4.3.8 References Cited in Text:

Anderson, R.E., 1969, Notes on the geology and paleohydrology of the Boulder City pluton, southern Nevada: U.S. Geol. Survey Prof. Paper 650-B, p. B35-B40.

Carter, W.D., Hammond, C.W., Barnett, Thomas, Muhm, J.R., Anderson, Richard, Schmer, Fred, Everett, Gordon, Peplies, R.W., Morain, Stanley and Marcus, Paul, 1972, Evaluation of remote sensing by Geology, Hydrology, and Geography Panel, in Seminar on operational remote sensing: Am. Soc. Photogrammetry, p. 269-281.

Childs, J.F., July 1973, The Salt Creek Fault, Death Valley, California (abs.), in Type II Progress Rept.: NASA-CR-133141, E73-10774, 6 p.

Childs, J.F., November 1973, A major normal fault in Esmeralda County, Nevada (abs.), in Type I Progress Rept.: NASA-CR-135859, E74-10018, 6 p.

Griscom, Andrew, and Muffler, L.J.P., 1971, Aeromagnetic map and interpretation of the Salton Sea geothermal area, California: U.S. Geol. Survey Geophys. Inv. Map GP-754, scale 1:62,500.

Liggett, M.A., and Childs, J.F., July 1973, Evidence of a major fault zone along the California-Nevada state line, 35°30' to 36°30' N. latitude: NASA Rept. Inv., NASA-CR-133140, E73-10773, 10 p.

Liggett, M.A., and Childs, J.F., February 1974, Structural lineaments in the southern Sierra Nevada, California: NASA Rept. Inv., NASA-CR-136665, E74-10279, 9 p.

Liggett, M.A., and Childs, J.F., March 1974, Crustal extension and transform faulting in the southern Basin Range Province: NASA Rept. Inv., NASA-CR-137256, E74-10411, 28 p.

MacGalliard, Wally, and Liggett, M.A., November 1973, False-color compositing of ERTS-1 MSS imagery: NASA Rept. Inv., NASA-CR-135859, E74-10018, 5 p.

MacKevett, E.M., Jr., 1960, Geology and ore deposits of the Kern River uranium area, California: U.S. Geol. Survey Bull. 1087-F, p. 169-222.

Rinehart, C.D., Ross, D.C., and Pakiser, L.C., 1964, Geology and mineral deposits of the Mount Morrison quadrangle, Sierra Nevada, California; With a section on a gravity study of Long Valley: U.S. Geol. Survey Prof. Paper 385, 106 p.

4.4 RECONNAISSANCE STUDY OF GEOLOGIC HAZARDS

4.4.1 Introduction:

This section summarizes concepts and analytical techniques that show promise in the application of ERTS-1 MSS data to reconnaissance investigation of geologic hazards. Such hazards can be related to a variety of geologic, geomorphic, structural and hydrological phenomena observed in ERTS-1 MSS imagery. Since the kinds and magnitudes of geologic hazards in an area may vary with the geologic, climatic and cultural setting, this discussion is focused on potential hazards recognized in the arid to semiarid, sparsely populated terrane of the Argus Exploration Company test site.

The information contained in ERTS-1 imagery is complementary to that from regional geologic mapping, geophysical surveys, and aerial remote sensing techniques commonly used in regional hazard and environmental investigations. The use of ERTS-1 MSS data as part of an integrated geologic hazards investigation can result in substantial cost savings over conventional reconnaissance techniques.

4.4.2 Applications:

Evidence of a variety of geologic hazards can be interpreted from ERTS-1 MSS imagery. Among the most important hazards recognized in the terrane of the test site are active fault systems, seismically unstable soils, areas of potential landslides, areas prone to flash-flooding, and regions of extensive wind erosion or migrating sand dunes. These hazards are indirectly expressed in the ERTS-1 MSS imagery by such features as topography, drainage patterns, vegetation distribution, and rock and soil coloring.

The synoptic scale of the ERTS-1 imagery is suitable for surveying large areas as a preliminary basis for the planning, routing, and engineering of large and continuous structures, such as highway systems, pipelines, aqueducts and power transmission systems. On a more local scale, ERTS-1 data can furnish information on the geologic and structural settings of sites for such developments as dams, nuclear power plants and housing projects.

It is unlikely that ERTS-1 MSS data could be used effectively in a hazards study without the support of detailed geologic and structural information. However, preliminary low risk sites or potential hazards, selected by analysis of ERTS-1 data, can be economically evaluated with the use of a variety of ground based geologic and geophysical survey techniques. Analysis and interpretation of ERTS-1 MSS imagery can be an effective tool when applied as part of an integrated geologic hazards investigation.

4.4.3 Discussion:

Several geologic hazards are associated directly with tectonic and seismic activity.

These include physical displacement along faults, such as the development of fault scarps either by abrupt movement during earthquakes or by gradual creep. In addition, seismic events associated with tectonic activity may trigger such phenomena as the mobilization of topographically or structurally unstable bedrock or surficial materials.

The historical earthquakes and patterns of recorded seismic activity within the test site are compiled in Plate 3 and discussed in Section 3.2 of this report. Within the region of the test site, the key evidence for seismic activity is the abundance of faults that have been mapped cutting alluvium and playa sediments of Quaternary age. Many of these structures are clearly recognizable in ERTS-1 MSS imagery as linear breaks in slope, alignments of vegetation or drainage, and linear contacts between alluvium or soils of contrasting color.

Bechtold and others (1973*) used ERTS-1 imagery in an experimental reconnaissance of faults that cut alluvium in an area of approximately 8,000 square km along the Colorado River between Lake Mead and Lake Havasu, in eastern California, southern southern Nevada, and northwestern Arizona. Interpretation of linear anomalies in the ERTS-1 data was followed by analysis of intermediate scale U-2 photography, SLAR, and by field reconnaissance, in which these anomalies were identified as faults. Similar applications of ERTS-1 data have been made by Liggett and Childs (1973**) in an investigation of the Pahrump fault zone, strands of which cut Quaternary basin deposits along the California-Nevada state line. Other examples of faulting, have been cited by Childs (November 1973***) in Esmeralda County, Nevada, and by Liggett and Ehrenspeck (1974****) in Lincoln County, Nevada. Similar results have been found in the Coast Ranges of California by Abdel-Gawad and Silverstein (1973, p. 439), who concluded that " ... study of ERTS-1 imagery shows that in most areas where earthquake clusters occur, there is usually ample evidence of recent faulting".

The effects of earthquake shaking on rock and soil stability vary greatly. The ERTS-1 MSS imagery has proven useful at the reconnaissance scale for discrimination of playa deposits, clay-rich soils and alluvial sediments, some of which may be subject to subsidence, slumping or flowage. Thixotropic sediments, saturated or partially saturated with ground water, can be a major hazard even in dry climates. Thus, ground water distribution is a major factor affecting the relative structural stability of such sediments. In some areas, proximity of the water table to the ground surface can be inferred in ERTS-1 imagery from the types and abundance of vegetation and the presence of springs or seeps. Examples of near-surface occurrences of ground water are cited in Section 4.2 in a discussion of

---

* Appendix B, this report
** Appendix H, this report
*** Appendix I, this report
**** Appendix L, this report

hydrologic applications of ERTS-1 data.

ERTS-1 imagery can be used to identify potential landslide hazards through reconnaissance of unstable rock and soil types, areas of intense faulting and fracturing, and topographic and drainage patterns characteristic of landslide areas. Examples apparent in ERTS-1 imagery over the test site are the Blackhawk slide on the northern slope of the San Bernardino Mountains of San Bernardino County, California (Shelton, 1966, p. 330-331), and the Tin Mountain slide west of the Panamint Mountains in Inyo County, California (Burchfiel, 1966). Both of these major slides originated in areas of rugged topography and active Quaternary faulting.

Other potential hazards in parts of the test site are flash-floods, mudflows and massive erosion which can result when intermittent storms bring sudden, heavy precipitation. The ability of water to erode rock or soil materials is largely a function of the consolidation of that material. Morrison and Cooley (1973) have successfully used ERTS-1 MSS imagery in determining the locations and types of easily eroded rocks in arid and semiarid regions of southern Arizona. The risk of flash-flooding and massive erosion can also depend on topography, drainage configuration, and the abundance and type of vegetation cover, all of which can be studied at a reconnaissance scale in ERTS-1 data. An example is the recently active Wrightwood mud flow on the northern slope of the San Gabriel Mountains. This area is expressed in ERTS-1 imagery by two large landslide scars, an anomalous drainage configuration and the distinctive rock type exposed on the Wrightwood fan (Childs, January 1973*).

In arid or semiarid regions, large-scale wind erosion of surficial materials and their redeposition as migrating sand bodies constitute an important hazard. In the test site, several large areas of deflation, sand accumulation, and migrating dune fields are recognizable in ERTS-1 imagery by their distinctive color and topographic expressions. The expression of these features permits reconnaissance study of the prevailing direction of transport and relative rates of erosion, migration, and deposition.

4.4.4 Analysis and Interpretation Techniques:

Effective use of ERTS-1 MSS data must be coupled with a variety of data analysis and interpretation techniques. The image enhancement techniques cited below are discussed in greater detail in Section 2.4 of this report.

Spectral Information:

Surface coloring related to vegetation, rock, and soil types has been enhanced in

---

* Appendix D, this report

ERTS-1 imagery using specific techniques. Additive color viewing has been effective in determining the optimum MSS band-filter combinations for enhancing spectral information. High resolution color enlargements have been employed in detailed laboratory and field analysis. Band ratioing techniques have been used for differentiating rock and vegetation anomalies in ERTS-1 imagery over a large area around Las Vegas, Nevada. Where available, ERTS-1 imagery covering a full seasonal cycle should be used to analyze seasonal changes in vegetation vigor and distribution.

Spatial Information:

Faults and drainage patterns in Quaternary alluvium have been enhanced using a variety of image enhancement techniques. Drainage patterns have been accentuated by using gray-level density slicing. Fault patterns in alluvium in a broad area south of Lake Mead, Nevada have been discriminated using edge enhancement printing and directional pattern filtering with Moiré pattern overlays. Sun azimuth and elevation have a strong influence on expression of topographic information in ERTS-1 data and seasonal coverage should thus be studied when available.

4.4.5 Potential Users:

Applications of ERTS-1 data to reconnaissance study of geologic hazards can be made by state and federal agencies and private industry in a broad range of civil engineering and land use planning roles. U.S. governmental agencies include the Bureau of Land Management, Soil Conservation Service, Bureau of Reclamation, Forest Service and Geological Survey.

4.4.6 Qualitative Analysis:

A primary advantage of ERTS-1 MSS data in the study of geologic hazards is the ability to conduct regional reconnaissance of hazard anomalies that can be economically evaluated using a variety of conventional geologic and geophysical survey techniques. This approach can be applied to the study of large areas for the routing and engineering of structures such as pipelines or highways, and for evaluating the regional structural and geologic settings of key construction sites.

In geologic and climatic terrane such as that found in the southwestern United States, ERTS-1 data can be readily applied to the reconnaissance of potentially active fault systems, landslide areas and areas prone to flash-flooding and extensive erosion by wind or water. The synoptic scale and resolution of the ERTS-1 data is estimated to be sufficient to guide investigations at map scales of approximately 1:200,000 or possibly larger.

A reconnaissance investigation using ERTS-1 imagery would result in the recognition and mapping of specific hazards, rather than the generalized classification of areas by "relative risk". Such an inventory of key geologic hazards can form an effective basis for compilation of regional hazard evaluation maps, such as that

prepared by the California Division of Mines for the state of California (see Alfors and others, 1973).

4.4.7 Quantitative Assessment:

The type of information and level of detail resulting from a reconnaissance study of geologic hazards using ERTS-1 MSS imagery differ from data compiled using conventional geologic and geophysical survey techniques. However, a rough comparison of costs can be made based on estimates discussed in Section 4.1 of this report. Reconnaissance study of geologic and structural hazards using ERTS-1 data is estimated to cost approximately $10,000 per scene (13,200 square miles) or less than $1.00 per square mile (2.5 square km). Such an investigation would include imagery enhancement processing, field reconnaissance and literature and map research resulting in selection of key anomalies for more detailed investigation.

Reconnaissance mapping of geologic hazards at a scale of approximately 1:200,000 using conventional mapping techniques is estimated to cost between $25 and $100 per square mile in terrane typical of the western United States. Low altitude color or multispectral aerial photography can cost an additional $40 per square mile. The larger scale of aircraft imagery is not necessarily more effective for recognizing potential hazards, and repetitive seasonal coverage such as that available from ERTS-1 data would be prohibitively expensive in regional airborne surveys. Based on these cost comparisons, the application of ERTS-1 data to reconnaissance study of geologic hazards in the southwestern United States is estimated to permit savings on the order of 10 to 1 over conventional reconnaissance techniques.

4.4.8 References Cited in Text:

Abdel-Gawad, Monem, and Silverstein, Joel, 1973, ERTS applications in earthquake research and mineral exploration in California, in Freden, S. C., Mercanti, E. P., and Becker, M. A., eds., Symposium on significant results obtained from the Earth Resources Technology Satellite-1: New Carrollton, Maryland, v. 1, sect. A, paper G22, NASA-SP-327, E73-10824, p. 433-450.

Alfors, J. T., Burnett, J. L., and Gay, T. E., Jr., 1973, Urban geology master plan for California: California Div. Mines and Geology Bull. 198, 112 p.

Bechtold, I. C., Liggett, M. A., and Childs, J. F., January 1973, Remote sensing reconnaissance of faulting in alluvium, Lake Mead to Lake Havasu, California, Nevada and Arizona: An application of ERTS-1 satellite imagery: NASA Rept. Inv., NASA-CR-130011, E73-10070, 9 p.

Burchfiel, B. C., 1966, Tin Mountain landslide, southeastern California, and the origin of megabreccia: Geol. Soc. America Bull., v. 77, p. 95-100.

Childs, J. F., January 1973, Preliminary investigation of rock type discrimination near Wrightwood, California (abs.), in Type II Progress Rept.: NASA-CR-129969, E73-10028, 1 p.

Childs, J. F., November 1973, A major normal fault in Esmeralda County, Nevada (abs.), in Type I Progress Rept.: NASA-CR-135859, E74-10018, 6 p.

Liggett, M. A., and Childs, J. F., July 1973, Evidence of a major fault zone along the California-Nevada state line, 35°30' to 36°30' N. latitude: NASA Rept. Inv., NASA-CR-133140, E73-10773, 10 p.

Liggett, M. A., and Ehrenspeck, H. E., January 1974, Pahranagat Shear System, Lincoln County, Nevada: NASA Rept. Inv., NASA-CR-136388, E74-10206, 10 p.

Morrison, R. B., and Cooley, M. E., 1973, Application of ERTS-1 multispectral imagery to monitoring the present episode of accelerated erosion in southern Arizona, in Freden, S. C., Mercanti, E. P., and Becker, M. A., eds., Symposium on significant results obtained from the Earth Resources Technology Satellite-1: New Carrollton, Maryland, v. 1, sect. A, paper G7, NASA-SP-327, E73-10824, p. 283-290.

Shelton, J. S., 1966, Geology illustrated: San Francisco, W. H. Freeman and Co., 434 p.

5.0 CONCLUSIONS

The Argus Exploration Company research program has evaluated ERTS-1 MSS imagery and subsidiary remote sensing data in applications to a broad range of geologic and structural problems in the topographically and climatically diverse terranes of the Sierra Nevada, the southern Basin Range Province, and the western Colorado Plateau.

This program has included detailed ground based study of key field areas in order to determine the origins and significance of geologic and structural anomalies visible in the ERTS-1 MSS imagery. At a broader scale the ERTS-1 data has been used to study the interrelationship between regional Cenozoic tectonic patterns and other geologic phenomena in the area of the test site. The results of this program support the following conclusions:

1. The synoptic scale of the ERTS-1 MSS imagery has permitted the recognition of large geologic features, trends and patterns often obscured by detail at the scale of low altitude aerial photography or conventional geologic mapping. These anomalies are expressed in ERTS-1 imagery by such characteristics as surface coloring and texture, topography and vegetation patterns. Ground based reconnaissance of anomalies recognized in ERTS-1 imagery has resulted in identification of previously unreported strike-slip and normal fault systems, structural ground water traps, dike swarms, domal plutonic structures, volcanic centers, and areas of hydrothermal alteration.

2. Using ERTS-1 MSS imagery, the Cenozoic tectonic framework of the test site has been studied at a scale and level of detail not possible using available tectonic map compilations. This study has documented an interrelationship between the Cenozoic tectonics of the southern Basin Range Province and the regional distribution of seismic activity, volcanism, plutonism and related mineralization and geothermal activity. This research has resulted in new concepts of Basin Range tectonics and related structural control of igneous activity and mineralization.

3. Several image enhancement techniques have been developed for effective analysis of the ERTS-1 data. High resolution false color compositing of multispectral imagery, with precise control of image color balance and contrast range, has been a primary tool. Edge enhancement printing has proven useful for studying structural trends expressed by patterns of topography and drainage. False color spectral ratio imaging has been effective for enhancing subtle reflectance differences between rock and soil types, and in studying the distribution and density of vegetation.

4. A primary limitation of the ERTS-1 imagery has been in studying at a local scale, geologic and structural features such as folds, foliation and irregular lithologic contacts. Although large exposures of surface material can often be distinguished by color, texture or erosional morphology, specific rock or soil types cannot generally be identified by composition. Surface coloring and small structural features are easily masked by vegetation.

5. The repetitive ERTS-1 imagery coverage has provided unique information related to seasonal changes of vegetation patterns and varied illumination of topography. Similar repetitive aircraft imagery has not generally been available. However, the scale and resolution of available U-2 photography and SLAR have proven useful for guiding detailed laboratory and field studies of geologic and structural anomalies interpreted in the ERTS-1 data.

6. ERTS-1 MSS imagery can be a valuable tool for reconnaissance exploration of mineral, geothermal and groundwater resources, and for regional study of geologic hazards. Used as part of an integrated exploration or research program, anomalies selected from ERTS-1 data can be economically narrowed and evaluated using a variety of geophysical, geochemical and geologic techniques. Within the geologic and climatic terrane of the test site, the use of ERTS-1 MSS imagery in natural resource exploration and management is estimated to permit cost savings of approximately 10 to 1 over conventional reconnaissance techniques.

The use of satellite remote sensing does not outmode classical techniques of field geology. Many of our investigations have relied heavily on data from previous studies which involved detailed geologic or structural mapping, geochemical sampling and analysis, petrography and geochronology. However, the ERTS-1 MSS imagery has guided analysis and synthesis of these data, resulting in a unique overview of regional geologic patterns and relationships. Refinements in data analysis and interpretation methods show promise for applications of satellite remote sensing to a broad range of geologic research problems, including operational resource exploration and management, in parts of the world where geologic reconnaissance has not been economically feasible in the past.

In discussing the nature and significance of geologic maps, J. M. Harrison (1963, p. 225) has written:

> "A geologic map may be defined as one on which are shown the distribution and structural relations of rocks. As such, it is the product of research undertaken in the geologists' principal laboratory, the earth itself. And because it describes and interprets the earth the map must, in the last analysis, be the source of geological theory."

Because of the limited detail and scope of information that can be recorded on geologic maps, they are often compilations of interpretation rather than fact. In contrast, satellite images record the complex spectral and spatial expressions of the earth's surface, and are, in a sense, a type of geologic map unbiased by the hand of a map maker. The task is to learn to recognize and interpret the geologic phenomena visible for the first time from this new perspective. Satellite remote sensing shows promise in becoming a major source of future geological theory.

5.1 RECOMMENDATIONS

A variety of remote sensing techniques have been employed in gathering data over various parts of the Argus Exploration Company test site. Through analysis and comparison of these data for key field areas, it has been possible to evaluate the effective applications of different imaging techniques.

Summarized below are suggested technical and operational modifications for consideration in future ERTS or other spacecraft remote sensing programs. These recommendations are primarily concerned with applications to reconnaissance geologic and tectonic mapping and related exploration for mineral, hydrologic and geothermal resources. For this reason the following comments are not necessarily optimum for applications in other disciplines.

5.1.1 Data Products and User Services:

To facilitate operational applications of ERTS imagery, it is important that NASA provides consistently high quality in data product reproduction. Rapid data processing and distribution is especially critical for support of research relating to seasonal variation of vegetation, snow cover, sun elevation, and other transient phenomena.

To the extent feasible, NASA and EROS should compile and distribute comprehensive indexes of available subsidiary remote sensing data.

5.1.2 Stereoscopic Coverage:

Stereoscopic imagery coverage would facilitate the use of orbital remote sensing in many applications to terrane analysis, especially structural geology, geomorphology, engineering geology, and related disciplines. Stereoscopic coverage might be achieved by increased sidelap of Multispectral Scanner (MSS) imagery or forward overlap of Return Beam Vidicon (RBV) imagery.

5.1.3 Spectral Range of ERTS Sensors:

Additional spectral bands extending into the thermal infrared would be complementary to the present ERTS-1 MSS spectral range. In addition, narrow-band multispectral imaging could aid discrimination of rock and soil types and support studies of vegetation distribution, vigor and abundance.

5.1.4 Variable Sun Angle Illumination:

The use of remote sensing in terrane analysis could be improved by acquisition of imagery having variation in angle of solar illumination. Such variation would complement stereoscopic analysis and help compensate for the preferential enhancement of topographic trends controlled by direction of illumination. In ERTS-1 MSS imagery, high angles of illumination have generally been found to be optimum for study of surface reflectance, while low angles have proven most useful for structural analysis.

5.1.5 Variable Image Scale and Resolution:

Applications of ERTS-1 MSS imagery have benefited from the use of intermediate scale imagery from near-space X-15 and high altitude U-2 aircraft. Experimental satellite imagery having fields of view both larger and smaller than the ERTS-1 MSS system should also be investigated. Resolution higher than that of the ERTS-1 MSS data would be valuable in certain geologic applications.

5.1.6 Multi-Sensor Space Platforms:

Data from a variety of airborne and spacecraft imaging systems have complemented analysis and interpretation of the ERTS-1 MSS imagery. The Skylab (EREP) program has tested a variety of new sensing techniques. Consideration should be given to future space platforms employing such techniques as multi-frequency synthetic aperture radar (SAR), high resolution thermal infrared sensing, and laser imaging systems. The space shuttle could be an effective platform for testing experimental sensors at variable altitudes and in different orbital configurations.

5.1.7 Enhancement and Analysis Techniques:

Image enhancement and analysis techniques have proven to be an important requirement for effective application of the ERTS-1 MSS data. Further research should be conducted on techniques for independent analysis of spatial and spectral image components. As feasible, such techniques should be operator-interactive to facilitate optimum use of human interpretation skills.

5.1.8 Supporting Research:

More field research and laboratory study is needed to identify the geologic and structural origins and significances of anomalies widely observed in existing spacecraft remote sensing data. An effort should be made to establish consistent descriptive terms for different types of data anomalies.

5.1.9 References Cited in Text:

Harrison, J.M., 1963, Nature and significance of geological maps, in Albritton, C.C., Jr., ed., The fabric of geology: Stanford, California, Freeman, Cooper & Co., p. 225-232.

Appendix A

STRUCTURALLY CONTROLLED DIKE SWARMS ALONG THE COLORADO RIVER, NORTHWESTERN ARIZONA AND SOUTHERN NEVADA
(Abstract)

Argus Exploration Company
555 South Flower Street - Suite 3670
Los Angeles, California 90071

November 1972

Prepared for
GODDARD SPACE FLIGHT CENTER
Greenbelt, Maryland 20771

STRUCTURALLY CONTROLLED DIKE SWARMS ALONG THE COLORADO RIVER, NORTHWESTERN ARIZONA AND SOUTHERN NEVADA (ABS.)

Bechtold, I. C., Liggett, M. A., and Childs, J. F.

An area of anomalous linear topographic grain and color expressions was recognized in Apollo 9 and ERTS-1 satellite imagery along the Colorado River of northwestern Arizona and southern Nevada; 35° to 36° north latitude. Field reconnaissance and analysis of USAF/USGS U-2 photography has shown the anomaly to be a zone of north to north-northwest trending dike swarms and associated granitic plutons. The dikes vary in composition from rhyolite to diabase, with an average composition nearer rhyolite. Dikes range in width from a few feet to over 75 feet, and can be traced along strike for as far as two miles. Most are steeply dipping to vertical, and in portions of the Newberry Mountains, Nevada, closely spaced dikes comprise approximately fifty percent of the rock volume.

In the Eldorado Mountains, Nevada, radiometric age dates from a 15,000 foot sequence of intermediate volcanics range from 18.6 to 13.8 m.y. (Anderson et al, 1972). The dike swarms described here are believed to be feeders for much of this volume. This is supported by the similarity in compositions of the dikes and volcanics, and the scarcity of dikes cutting upper members of the volcanic pile. Dated dikes fall within this age span, and further K-Ar dates for representative dikes are presently being obtained. A maximum age for intrusion is indicated for the dikes that cut a 15.9±0.3 m.y. granite pluton at Spirit Mountain, Nevada (And et al, 1972). Reconnaissance has indicated similar plutons in the Newberry, ado, and Black Mountains that may form a Tertiary aged composite batholi

Shearing and displacement of host rocks along dikes suggest dike emplacement along active fault zones. Post-dike deformation has resulted in shearing and complex normal faulting along a similar north-south trend. Some of these faults form present range-front scarps, and have locally been sites of hydrothermal alteration and mineralization.

The epizonal plutonism and volcanism of this north-south belt appears to represent a structurally controlled volcanogenic province which ends abruptly in the vicinity of Lake Mead at a probable eastern extension of the Las Vegas Shear Zone. Fleck (1971) postulated the Las Vegas Shear Zone as a transform fault separating two areas of crustal spreading. The magnitude and chronology of extensional faulting and plutonism recognized in the north-south zone described here, supports this hypothesis.

References:

Anderson, R.E., Longwell, C.R., Armstrong, R.L., and Marvin, R.F., 1972, Significance of K-Ar ages of Tertiary rocks from the Lake Mead region, Nevada-Arizona: Geol. Soc. America Bull., v. 83, no. 2, p. 273-288.

Fleck, R.J., 1970, Age and possible origin of the Las Vegas Valley Shear Zone, Clark and Nye Counties, Nevada: Geol. Soc. Am. Abs. with Programs (Rocky Mtn. Sec.), v. 2, no. 5, p. 3[illegible]

REMOTE SENSING RECONNAISSANCE OF FAULTING IN ALLUVIUM, LAKE MEAD TO LAKE HAVASU, CALIFORNIA, NEVADA AND ARIZONA

Appendix B

Argus Exploration Company
555 South Flower Street - Suite 3670
Los Angeles, California 90071

January 1973
Report of Investigation

Prepared for
GODDARD SPACE FLIGHT CENTER
Greenbelt, Maryland 20771

REMOTE SENSING RECONNAISSANCE OF FAULTING IN ALLUVIUM, LAKE MEAD TO LAKE HAVASU, CALIFORNIA, NEVADA AND ARIZONA

An Application of ERTS-1 Satellite Imagery

I. C. Bechtold, M. A. Liggett and J. F. Childs
Argus Exploration Company
Newport Beach, California

A B S T R A C T

Analysis of ERTS-1 MSS and other imagery for a 125 x 25 mile area in the southern part of the Basin-Range Province of southeastern California, southern Nevada and northwestern Arizona, indicates the presence of numerous color and contrast anomalies in alluvium. Field work guided by high altitude U-2 and Side Looking Aerial Radar imagery confirmed that these anomalies are fault zones, many of which are believed to be of Recent age. Few faults in alluvium have been reported from previous ground based geologic studies in the area.

Some faults occur along range fronts where they have been traced along strike into bedrock but more often they are found out from the range fronts in the intermontane alluvial sediments. The faults strike generally northward and have predominantly dip slip displacement. Many bound grabens suggesting an east-west direction of extension. Major extension occurred in this area during a mid-Tertiary episode of plutonism, volcanism and normal faulting.

ERTS imagery provides a synoptic perspective previously unavailable for regional geologic studies. The ability to conduct rapid and inexpensive reconnaissance of Recent faulting has important applications to land use planning, ground water exploration, geologic hazards study and the siting and design of engineering projects.

INTRODUCTION

Analysis of Earth Resources Technology Satellite (ERTS-1) multispectral scanner (MSS) imagery and subsequent field study indicates the presence of numerous faults cutting alluvium in an area approximately 125 miles long and 25 miles wide (Fig. 1). The area lies between 34°15' N to 36°45' N and 114°W to 115°W in the southern part of the Basin-Range Province.

Method:

The widespread development of normal faults in Late Tertiary and Quaternary alluvium was recognized by study of anomalies present in ERTS and Apollo space imagery. Details and individual breaks were mapped using available color infrared and black and white U-2 imagery and SLAR. Another important tool in directing field study was the use of 35mm color transparencies taken during low altitude fixed wing reconnaissance. Imagery used in this study is listed below:

ERTS-1 MSS
12 September 1972, Frame 1069-17432
5 November 1972, Frame 1105-17443
6 November 1973, Frame 1106-17495

Apollo 9
Frames AS 9-20-3135 and AS 9-20-3136

Side Looking Aerial Radar, Westinghouse AN/APQ 97 XE-1,
NASA Mission 103, 5 November 1965

U-2 High Altitude Photography, USAF-USGS (Black and White):

Mission 018V, 10 July 1968, Frames 211 through 214
Mission 018L, 10 July 1968, Frames 214 through 217
Mission 059V, 17 July 1968, Frames 169 through 174, 177, and 178
Mission 059R, 17 July 1968, Frames 164 through 178
Mission 374V, 6 September 1968, Frames 209, 211 212, 213 and 214
Mission 374L, 6 September 1968, Frames 208 and 209.

NASA U-2 High Altitude Color IR Photography, Mission 189.

Background:

Some faults in alluvium, not shown in our illustrations, have been mapped by previous workers. Willis Lee (1908) shows an extension of the Grand Wash Fault for a short distance into alluvium in Hualpai Valley east of Detrital Valley.

Longwell (1936) shows two faults which extend through volcanics and for short distances into alluvium near Echo Wash in an area now covered by the Overton Arm of Lake Mead. Another fault mapped by Longwell cuts recent gravel and wash deposits about four miles north of Hoover Dam at the south end of Lake Mead. In a later paper, Longwell (1963) describes a basin in which alluvium was being deposited while the basin was lowered along the Horse Thief Fault two miles east of Hoover Dam. Longwell also mapped several faults in alluvium along the Colorado River south of Lake Mead, the largest of which is now covered by Lake Mojave. Hansen (1962) shows a small normal fault which strikes approximately north-south along the west side of the Colorado River about 15 miles north of Lake Mojave. The abundance of late Quaternary faulting has not been generally recognized.

RESEARCH

General Characteristics:

Fault scarps recognized in our investigation are shown in Figures 2 and 3. Some faults occupying range front positions have been traced from breaks in alluvium into bedrock. Most faults, however, occur well out from the range fronts in the alluvium. These faults are generally characterized by long, sharp, linear breaks in slope, parallel alignment, and frequent juxtaposition of contrasting alluvial sediments. The youngest faults disrupt the drainage texture and are only beginning to be incised by intermittent streams. The traces of older faults are frequently apparent as a contrast in alluvial rock type of drainage texture, although their original topographic expression may have become indistinguishable. No evidence of landslide morphology is recognized, associated with the scarps.

Fault Description:

In ERTS imagery, a light colored zone in alluvium extends from the bend in the Colorado River near Bullhead City, Arizona south-southeast toward Topock, Arizona. Field study indicates that this zone is made up of light colored sandy sediments, bound on the west by a west dipping escarpment 15-25 feet high, which we interpret as a normal fault (Figure 2). South of Topock and along the east shore of Lake Havasu, a possible extension of this fault has been recognized. The fault is thought to extend northward into bedrock in the Newberry Mountains west of Bullhead City where it has been mapped independently by one of the authors and by Alexis Volborth (personal communication). Here this fault cuts Precambrian augen gneiss and Tertiary granitic rocks along an intensely brecciated zone up to one half mile wide (Figure 2).

The largest number of faults in alluvium were found west of Gold Butte and east of the Overton Arm of Lake Mead (Figure 3). Field study guided by color infrared

U-2 imagery provided detail on the system of scarps in this area. Several well developed grabens bound by normal faults are present in the alluvium, as well as other generally north trending normal faults. These faults indicate structural extension in an east-west direction. Dikes south of Lake Mead which cut Quaternary alluvium follow this northerly trend, as do the major range front scarps in the region. Two weakly defined faults may extend in an anomalous northeast direction in this area with possible left lateral offset of washes along them.

Regional Significance:

The area between Lake Mead and Lake Havasu was the site of extensive mid-Tertiary volcanism and related plutonism. Dike swarms elongated plutons, and penecontemporaneous normal faulting all maintain a generally northerly trend (Bechtold and Others, 1972). These phenomena are believed to represent crustal extension on the order of several tens of miles. The mechanisms of crustal extension are well documented for key areas within this province. Anderson (1971) describes complex systems of low angle normal faults in the Nelson area, Nevada, which he believes resulted during distension of thick volcanic cover during rifting and emplacement of plutons at depth. Volborth (personal communication, 1972) describes mid-Tertiary extensional emplacement of plutons and dike swarms in the Newberry and Eldorado Mountains west of the Colorado River and south of Lake Mead.

The orientation and abundance of normal faults cutting alluvium shown in Figures 2 and 3 suggest that regional structural extension has occurred during late Pleistocene and Recent Time. Similar extensional normal faulting has been recognized in other parts of the Basin-Range Province. (Stewart, 1971, Thompson, 1967).

Implications:

The ERTS-1 multispectral scanner imagery has provided an effective tool for geologic reconnaissance of fault breaks in unconsolidated alluvium over an area of several thousand square miles. Intermediate scale U-2 photography and side looking aerial radar guided field study and provided detail for mapping, but most fault zones could be distinguished as contrast or color anomalies in ERTS-MSS imagery. Few of these faults have been reported on the basis of previous conventional geologic mapping, nor would the regional extent and consistent orientation have been obvious from maps of small sub-areas.

The ability to conduct low cost regional surveys of recent faulting has several important applications. The distribution of recent fault breaks should be seriously considered in regional land use planning. This is especially significant in determining the location and engineering design of installations such as dams, highway

systems, and nuclear generating stations. We are presently corresponding with other workers studying microseismic activity in the Lake Mead area in order to compare surface break distribution with present and historical earthquake activity.

Many alluvial fault breaks form suitable traps for ground water. Reconnaissance mapping of faults guided by ERTS imagery may provide an important tool for hydrologic exploration in arid terrain.

REFERENCES

Anderson, R. E., 1971, Thin Skin Distension in Tertiary Rocks of Southeastern Nevada: Geol. Soc. America Bull., v. 82, p 43-58.

Bechtold, I. C., Liggett, M. A., and Childs, J. F., 1972, Structurally Controlled Dike Swarms Along the Colorado River, Northwestern Arizona and Southern Nevada (ABS): NASA-CR-128290, E72-10192.

Hansen, S. M., 1962, The Geology of the Eldorado Mining District, Clark County, Nevada: Ph.D. Thesis, University of Missouri, Rolla, Missouri.

Lee, W. T., 1908, Geologic Reconnaissance of a Part of Western Arizona: U.S. Geol. Survey Bull. 352, 96 p.

Longwell, C. R., 1936, Geology of the Boulder Reservoir Floor, Arizona-Nevada: Geol. Soc. America Bull., Vol. 47, p. 1393-1476.

Longwell, C. R., 1963, Reconnaissance Geology Between Lake Mead and Davis Dam, Arizona-Nevada: U.S. Geol. Survey Prof. Paper 374.E, 51 p.

Stewart, J. H., 1971, Basin and Range Structure: A System of Horsts and Grabens Produced by Deep-Seated Extension: Geol. Soc. America Bull., v. 82, p 1019-1044.

Thompson, G. A., 1967, Background and Results: in Geophysical Study of Basin-Range Structure, Dixie Valley Region, Nevada (G. A. Thompson and Others), U.S. Air Force, Cambridge Res. Labs., Final Rep.

Volborth, A., 1972. Personal Communication
Nevada Bureau of Mines, Reno, Nevada.

Figure 1

Index map of the area from Lake Mead to Lake Havasu in southeastern California, northwestern Arizona and southern Nevada. Bedrock areas are shaded.

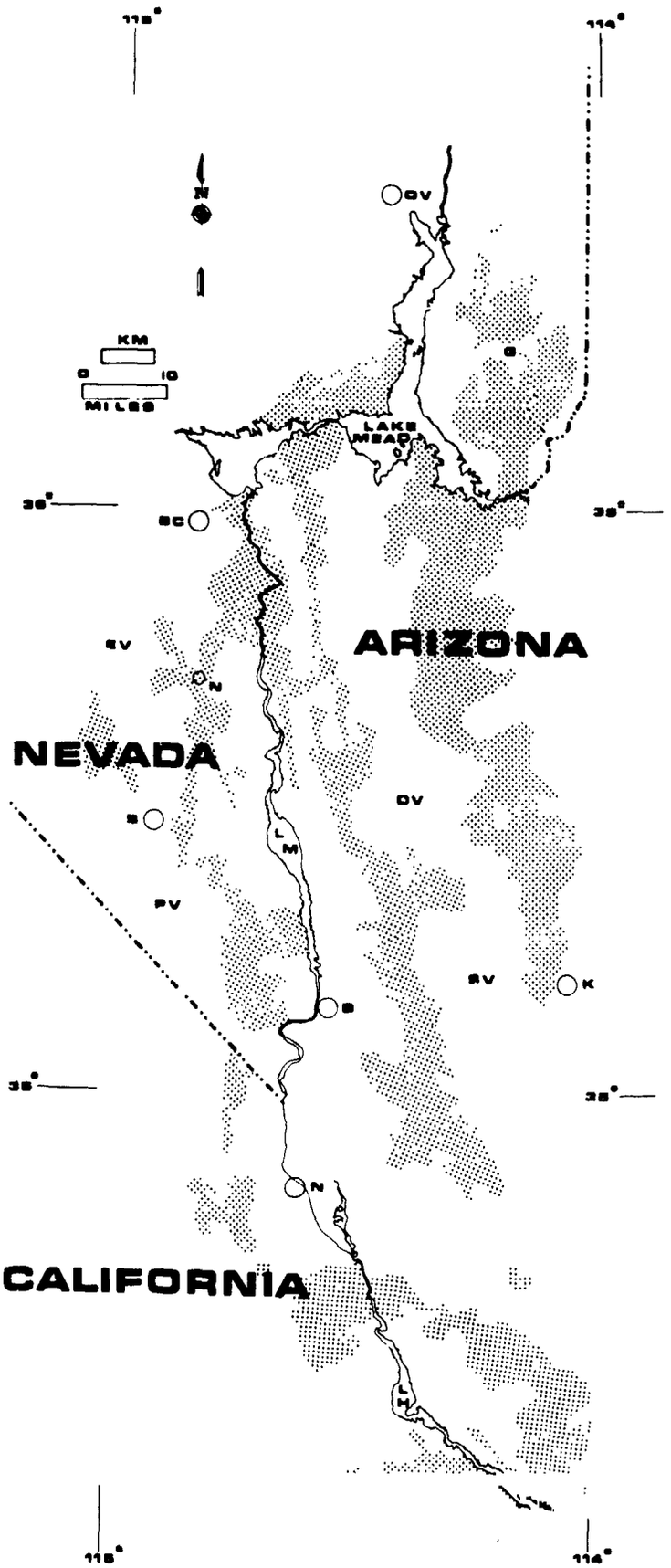

Location Index

B	Bullhead City, Ariz.
BC	Boulder City, Nev.
DV	Detrital Valley, Ariz.
EV	Eldorado Valley, Nev.
G	Gold Butte, Nev.
K	Kingman, Ariz.
LH	Lake Havasu
LM	Lake Mojave
OV	Overton, Nev.
N	Needles, Calif.
N	Nelson, Nev.
PV	Piute Valley, Calif.-Nev.
S	Searchlight, Nev.
SV	Sacramento Valley, Ariz.

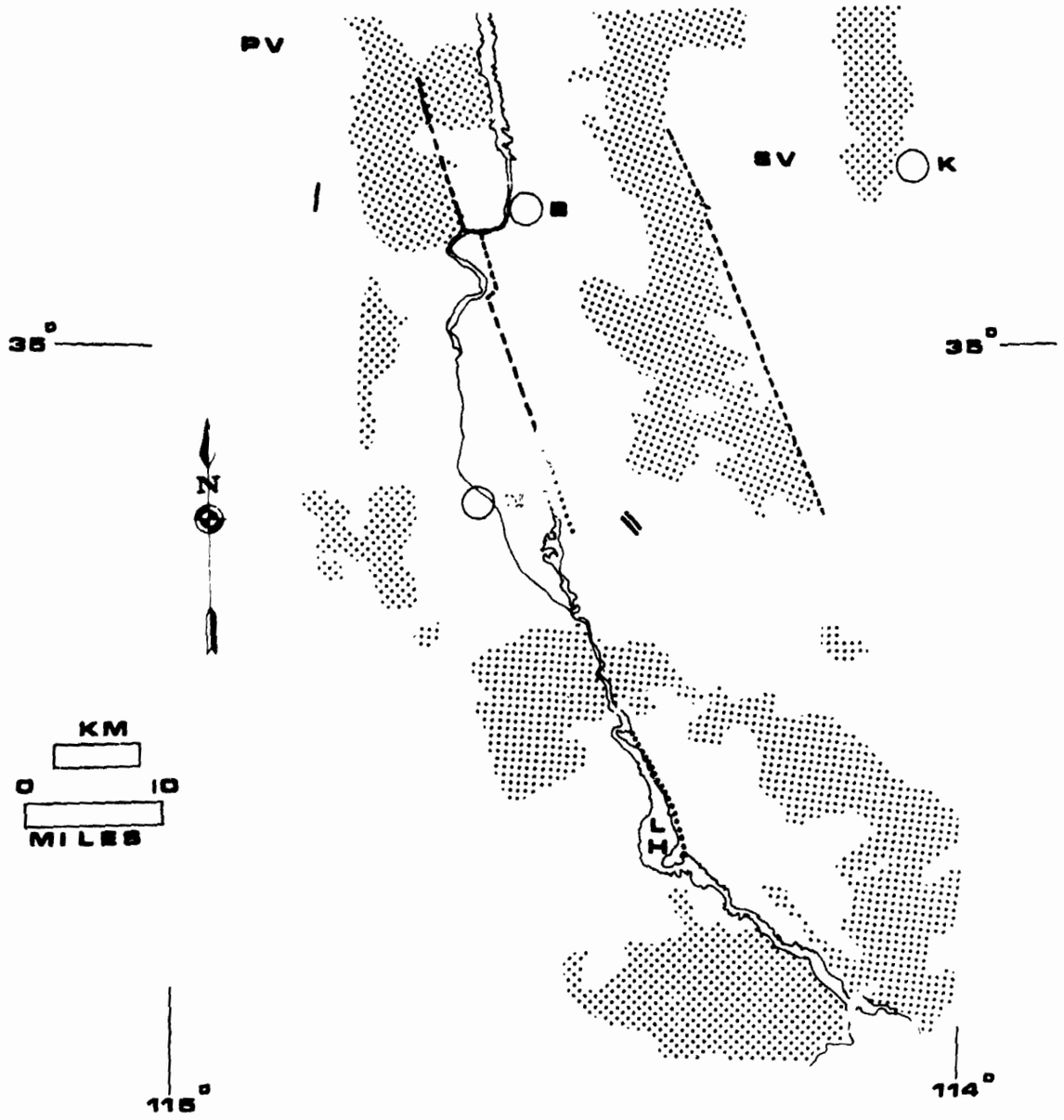

Figure 2 Previously unreported faults cutting alluvium in the southern half of area in Figure 1. Faults are dashed or dotted where indefinite or inferred. Bedrock areas are shaded. Location names as in Figure 1.

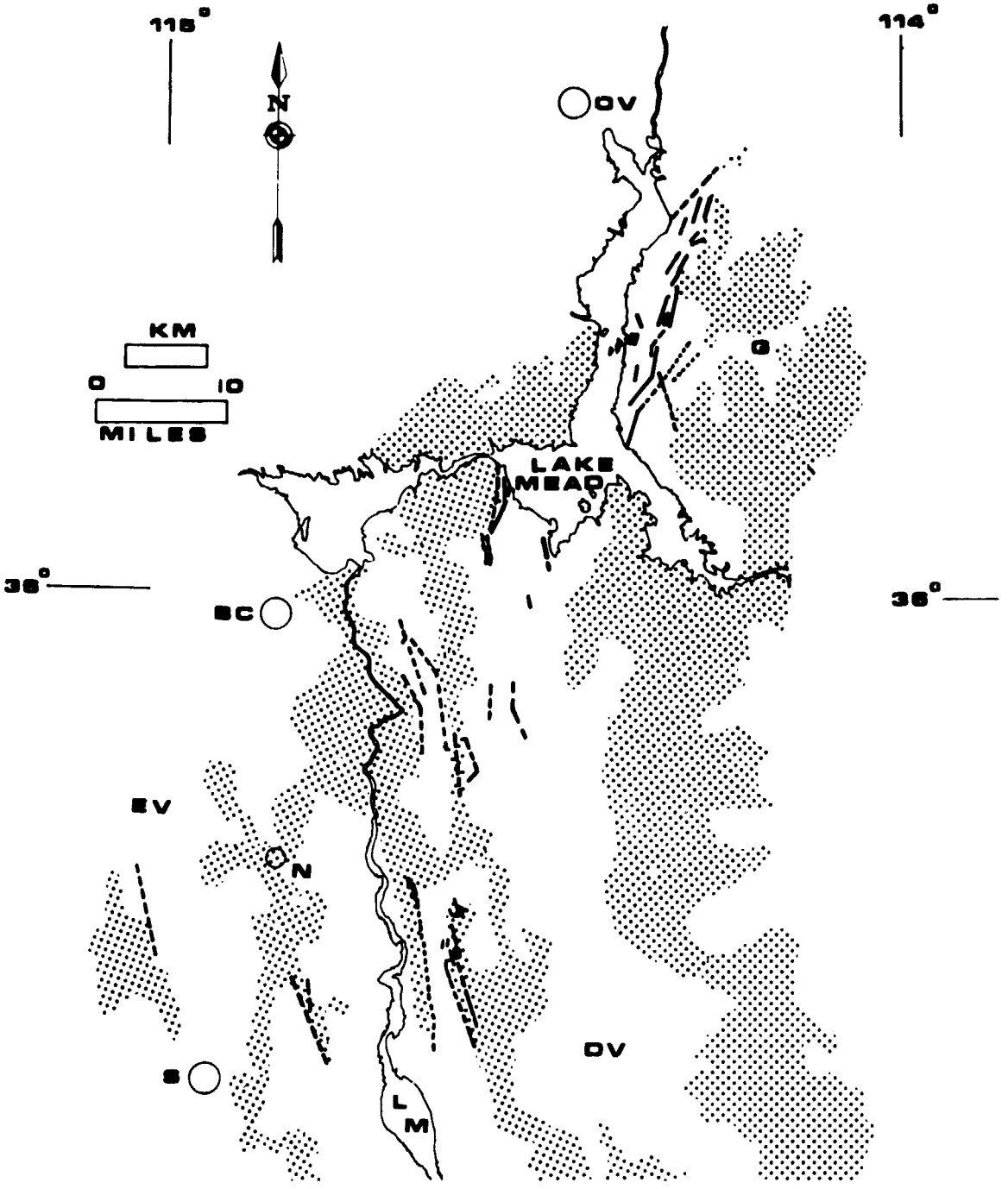

Figure 3 Previously unreported faults cutting alluvium in the northern half of area in Figure 1. Faults are dashed or dotted where indefinite or inferred. Bedrock areas are shaded. Location names as in Figure 1.

PSEUDO-RELIEF ENHANCEMENT OF COLOR IMAGERY
(Abstract)

Argus Exploration Company
555 South Flower Street - Suite 3670
Los Angeles, California 90071

Appendix C

January 1973

Prepared for
GODDARD SPACE FLIGHT CENTER
Greenbelt, Maryland 20771

PSEUDO-RELIEF ENHANCEMENT OF COLOR IMAGERY (ABS.)

I. C. Bechtold, M. A. Liggett, & J. F. Childs

A planoconvex Fresnel lens can be used for pseudo-relief enhancement of composite ERTS-1 imagery. The three-dimensional perception may be due in part to chromatic aberation of the lens which causes separation of focal planes for different colors in the imagery. Because focal length is inversely proportional to wave length, red areas appear raised above yellow, green and blue areas respectively. Magnification by the lens may have an additional psychological effect on perception.

Best results are obtained viewing rear-projected color composites with red hues assigned to areas of highest topography. The projection screen is viewed from a distance of 10 to 20 inches with the Fresnel lens held 2 to 6 inches from the screen. The technique may be applied to any color imagery.

A similar pseudo-relief effect is described by McLeroy and Vaughan (1970) using a more complex optical system for viewing small color transparencies. Short (1972) discussed a related effect achieved by viewing a pair of identical ERTS images in a standard stereoscopic viewer.

A variety of inexpensive Fresnel lenses are available through Edmund Scientific Company, Barrington, New Jersey. The lens described here is an 11-inch square Fresnel lens, focal length 16 inches, Stock No. 70533.

References:

McLeroy, D. F., and Vaughan, O. H., Jr., 1970, Enhancement and application of space photographs for earth resources studies with special emphasis on regional geologic investigations; NASA-ASEE Summer Faculty Fellowship, Marshall Space Flight Center, Grant No. NGT-01-003-45.

Short, N. M., (discussion): ERTS-1 Users Conference, October 1972, NASA-Goddard Space Flight Center, Greenbelt, Maryland.

PRELIMINARY INVESTIGATION OF ROCK TYPE DISCRIMINATION NEAR WRIGHTWOOD, CALIFORNIA
(Abstract)

Argus Exploration Com
555 South Flower Street - S .670
Los Angeles, California 9

January 1973

Appendix D

Prepared for
GODDARD SPACE FLIGHT CENTER
Greenbelt, Maryland 20771

PRELIMINARY INVESTIGATION OF ROCK TYPE DISCRIMINATION NEAR WRIGHTWOOD, CALIFORNIA (ABS.)

A large alluvial fan, 18 miles in axial dimension, near Wrightwood, California shows a pronounced dark anomaly in Apollo photography and ERTS multispectral imagery. Preliminary field work indicates that the dark coloring of the fan is caused by a sharp change in alluvial rock type from the surrounding alluvium onto the fan. The fan alluvium is composed predominantly of Pelona schist, while the surrounding alluvium is mostly granitic material. Petrography on schist boulders from the fan shows them to be high in Fe and Ca rich minerals such as epidote, tremolite-actinolite and chlorite. These minerals are known to have reflectance minimal in the near infrared portion of the spectrum and it is the near infrared bands of ERTS imagery that show the highest contrast difference between fan and surrounding alluvium.

Our reconnaissance study has indicated an increase in abundance of California Juniper and Joshua Trees on the fan, compared with surrounding alluvium. We suspect that this vegetation change is related to rock type. Vegetation on the fan is generally scarce and the effects of ground water and vegetation in producing the image anomaly are thought to be minimal.

REGIONAL TECTONIC CONTROL OF TERTIARY MINERALIZATION AND RECENT FAULTING IN THE SOUTHERN BASIN-RANGE PROVINCE

Argus Exploration Company
555 South Flower Street - Suite 3670
Los Angeles, California 90071

March 1973
Report of Investigation

Prepared for
GODDARD SPACE FLIGHT CENTER
Greenbelt, Maryland 20771

REGIONAL TECTONIC CONTROL OF TERTIARY MINERALIZATION AND RECENT FAULTING IN THE SOUTHERN BASIN-RANGE PROVINCE
An Application of ERTS-1 Data

I. C. Bechtold, M. A. Liggett and J. F. Childs
Argus Exploration Company
Newport Beach, California

ABSTRACT

Research based on ERTS-1 MSS imagery and field work in the southern Basin-Range Province of California, Nevada and Arizona has shown regional tectonic control of volcanism, plutonism, mineralization and faulting. This paper covers an area centered on the Colorado River between 34°15' N and 36°45' N. During the mid-Tertiary, the area was the site of plutonism and genetically related volcanism fed by fissure systems now exposed as dike swarms. Dikes, elongate plutons, and coeval normal faults trend generally northward and are believed to have resulted from east-west crustal extension. In the extensional province, gold and silver mineralization is closely related to Tertiary igneous activity. Similarities in ore, structural setting, and rock types define a metallogenic district of high potential for exploration. The ERTS imagery also provides a basis for regional inventory of small faults which cut alluvium. This capability for efficient regional surveys of Recent faulting should be considered in land use planning, geologic hazards study, civil engineering and hydrology.

INTRODUCTION: This report summarizes a portion of a NASA funded investigation intended to test the application of ERTS-1 imagery to studies of regional tectonics. The region discussed in this paper occupies a belt approximately 25 miles wide and 125 miles long aligned along the Colorado River between 34°15' and 36°34' N latitude in the Basin-Range province of southern Nevada, southeastern California and northwestern Arizona. This area is shown in Figure 1.

The primary tool used in the investigation is additive color enhancement of ERTS-1 MSS imagery. The synoptic perspective gained in ERTS imagery permits investigation of regional geologic phenomena at a scale not feasible using conventional aerial photography. As a complement to ERTS data, intermediate scale remote sensing imagery and low altitude aerial reconnaissance has proven valuable in guiding efficient and economical ground based geologic reconnaissance. The primary data used in this study includes:

NASA ERTS-1 MSS	12 September 1972, Frame 1069-17432
	5 November 1972, Frame 1105-17443
	6 November 1972, Frame 1106-17495

NASA Apollo 9 Ektachrome Frames AS9-20-3135; 3136

NASA SLAR AN/APQ 97, 5 November 1965 Mission 103

USAF-USGS U-2 Black and White Photography

10 July 1968	Mission 018
17 July 1968	Mission 059
6 Sept. 1968	Mission 374

NASA U-2 Color Infrared Photography

11 Oct. 1971	Mission 189

REGIONAL TECTONICS: In the ERTS-1 image of Figure 1, a belt of anomalous north-south topographic, textural and color expression is visible along the Colorado River. Structural analysis of this imagery and related literature research and ground based reconnaissance has led to a hypothesis integrating many aspects of the regional geology previously considered as isolated phenomena.

We believe the anomalous north-south structural pattern is the result of east-west crustal extension of at least 30 km which occurred during an episode of Miocene plutonism and genetically related volcanism. The bulk of igneous activity occurred in an interval from 10 to 15 million years B.P. (Anderson & Others, 1972) and was synchronous with major strike-slip displacement on the Las Vegas Shear Zone (Fleck, 1970). We believe the Las Vegas Shear Zone extends eastward just north of Lake Mead, and forms the northern boundary of the extensional province. This tectonic relationship is illustrated in the simplified model of Figure 2. Here the strike-slip fault zone (X-Y) is a transform fault bounding two areas of crustal extension (braided patterns). The southern extensional province corresponds to the area described in this paper; a sister province is believed to exist in the vicinity of the AEC Nevada test site, 75 miles north-west of Lake Mead.

A diagrammatic section across an area of crustal extension is shown in Figure 3. Normal faults related to extension, shown in Figure 3, are believed to decrease in dip downward and give way at depth to a zone of plastic deformation (Stewart, 1971). Extension by low dipping normal faults in a thick Tertiary volcanic sequence near Nelson, Nevada has been described by Anderson (1971). Another mechanism of crustal extension is the addition of new crust by plutonism and related volcanism: in part along extensional fault zones (Bechtold et al, 1972). Figure 4 shows the distribution of Tertiary granitic plutons and related dike swarms in the area of investigation. Dings (1951) describes numerous large rhyolite dikes in the Wallapai Mining District north of Kingman, Arizona. Petrographic and chemical similarities among the volcanics, dikes and larger plutonic bodies have been demonstrated by Volborth (personal communication, 1972) for the Newberry Mountains area, Nevada. Temporal and genetic relationships between plutonic and volcanic rocks within the area have been cited by Volborth (personal correspondence 1972), Lausen (1931), Ransome (1923), Bechtold et al, (1972), Callaghan (1939), and Anderson et al, (1972).

MINERALIZATION: The shallow granitic plutons and dike swarms of Figure 4 are closely related to extensive gold, silver and lesser copper-molybdenum mineralization. Figure 5 shows the distribution of known mining areas in the region. Longwell et al (1965) briefly discuss many Nevada mining districts, and Ransome (1923), Callaghan (1939) and others describe some of the larger mining areas in detail. Review of the literature and geologic reconnaissance has revealed marked similarities in the structural setting, ore and gangue mineral assemblages, and rock type associations among mining areas. The gold-silver deposits along the Colorado River are part of a north-trending metallogenic province genetically related to the Tertiary extensional deformation. This regional structural control of mineralization has not been previously reported. The value of ore recovered in this province (based upon 1973 metal prices) exceeds 100 million dollars. Although mining activity is largely inactive at present, the new understanding of the area made possible by ERTS data merits consideration in future mineral exploration programs.

RECENT FAULTING: In addition to regional tectonic syntheses, ERTS data has provided a basis for efficient geological reconnaissance of relatively small faults which cut alluvium. Most of the faults cut alluvium of probable Recent age.

Figure 6 shows the distribution of these faults identified in ERTS and intermediate scale imagery and confirmed during subsequent reconnaissance and detailed field mapping. Faults previously reported (Longwell, 1963) and confirmed by our imagery analysis are distinguished from newly recognized faults. Displacement is mainly dip slip, and in several instances the faults form small grabens (Bechtold et al, 1973). Many of the faults occur out from the range fronts in intermontane alluvial sediments where they are difficult to recognize in ground-based mapping. The faults trend generally northward and probably represent late-Tertiary to Recent east-west extension similar to that recognized elsewhere in the Basin-Range Province (Thompson, 1967).

The use of ERTS-1 imagery for efficient reconnaissance of Recent faulting over large areas of semi-arid terrain can have important applications in the planning and design of engineering projects such as dams, highways and nuclear power generating stations. Related applications can also be made in regional geologic hazard studies and in the search for increasingly valuable ground water sources.

CONCLUSIONS: ERTS-1 MSS imagery is a unique tool for a broad range of geologic investigations, some of which are discussed above. Analysis of ERTS data coordinated with the use of other remote sensing techniques has permitted efficient and economical ground-based reconnaissance. At a regional scale, the application of ERTS to tectonics shows promise in reconnaissance mineral exploration. In addition, the resolution of the ERTS-MSS imagery is sufficient for surveys of relatively small faults which cut alluvium. This capability should be considered in land-use planning, geologic hazards study, and civil engineering.

REFERENCES

Anderson, R.E., 1971, Thin Skin Distension in Tertiary Rocks of Southeastern Nevada: Geol. Soc. America Bull., v. 82, p 43-58.

Anderson, R.E., Longwell, C.R., Armstrong, R.L., and Marvin, R.F., 1972, Significance of K-Ar Ages of Tertiary Rocks from the Lake Mead region, Nevada-Arizona: Geol. Soc. America Bull., v. 83, No. 2, p 273-288.

Bechtold, I.C., Liggett, M.A., and Childs, J.F., 1972, Structurally Controlled Dike Swarms Along the Colorado River, Northwestern Arizona and Southern Nevada (ABS): NASA-CR-128290, E72-10192.

Bechtold, I.C., Liggett, M.A., Childs, J.F., 1973, Remote Sensing Reconnaissance of Faulting in Alluvium, Lake Mead to Lake Havasu, California, Nevada and Arizona: NASA Report of Investigation, Goddard Space Flight Center, Greenbelt, Maryland.

Callaghan, E., 1939, Geology of the Searchlight District, Clark County, Nevada: U.S. Geological Survey Bulletin 906-D, p 165-185.

Dings, G., 1951, The Wallapai Mining District, Cerbat Mountains, Mojave County, Arizona: U.S. Geol. Survey Bull. 978-E, 39 p.

Fleck, R.J., 1970, Age and possible Origin of the Las Vegas Shear Zone, Clark and Nye Counties, Nevada: Geol. Soc., America Abs. with Programs (Rocky Mountain Sec.), v. 2, No. 5, p 333.

Lausen, G., 1931, Geology and Ore Deposits of the Oatman and Katherine Districts, Arizona: Arizona Bur. Mines Bulletin 131, Geol. Ser. 6, (Univ. Bull., v 2, No. 2), 126 p.

Longwell, C.R., 1963, Reconnaissance Geology Between Lake Mead and Davis Dam, Arizona-Nevada: U.S. Geol. Survey Prof. Paper 374-E, 51 p.

Longwell, C.R., Pampeyan, E.H., Bowyer, B., and Roberts, R.J., 1965, Geology and Mineral Deposits of Clark County, Nevada: Nevada Bur. Mines Bull. 62, 218 p.

Ransome, F.L., 1923, Geology of the Oatman District, Arizona, A Preliminary Report: U.S. Geol. Survey Bull. 743, 58 p.

Stewart, J.H., 1971, Basin and Range Structure: A System of Horsts and Grabens Produced by Deep-Seated Extension: Geol. Soc. America Bull., v. 82, p 1019-1044.

Thompson, G. A., Meister, L. T., Herring, A. T., Smith, T. E., Burke, D. B., Kovach, R. L., Burford, R. O., Salehi, A., and Wood, M. D., 1967. Geophysical Study of Basin-Range Structure, Dixie Valley Region, Nevada: U. S. Air Force Cambridge Research Labs. Spec. Rept. 66, 848 p.

Volborth, A., 1972. Personal Communication. Nevada Bureau of Mines, Reno, Nevada.

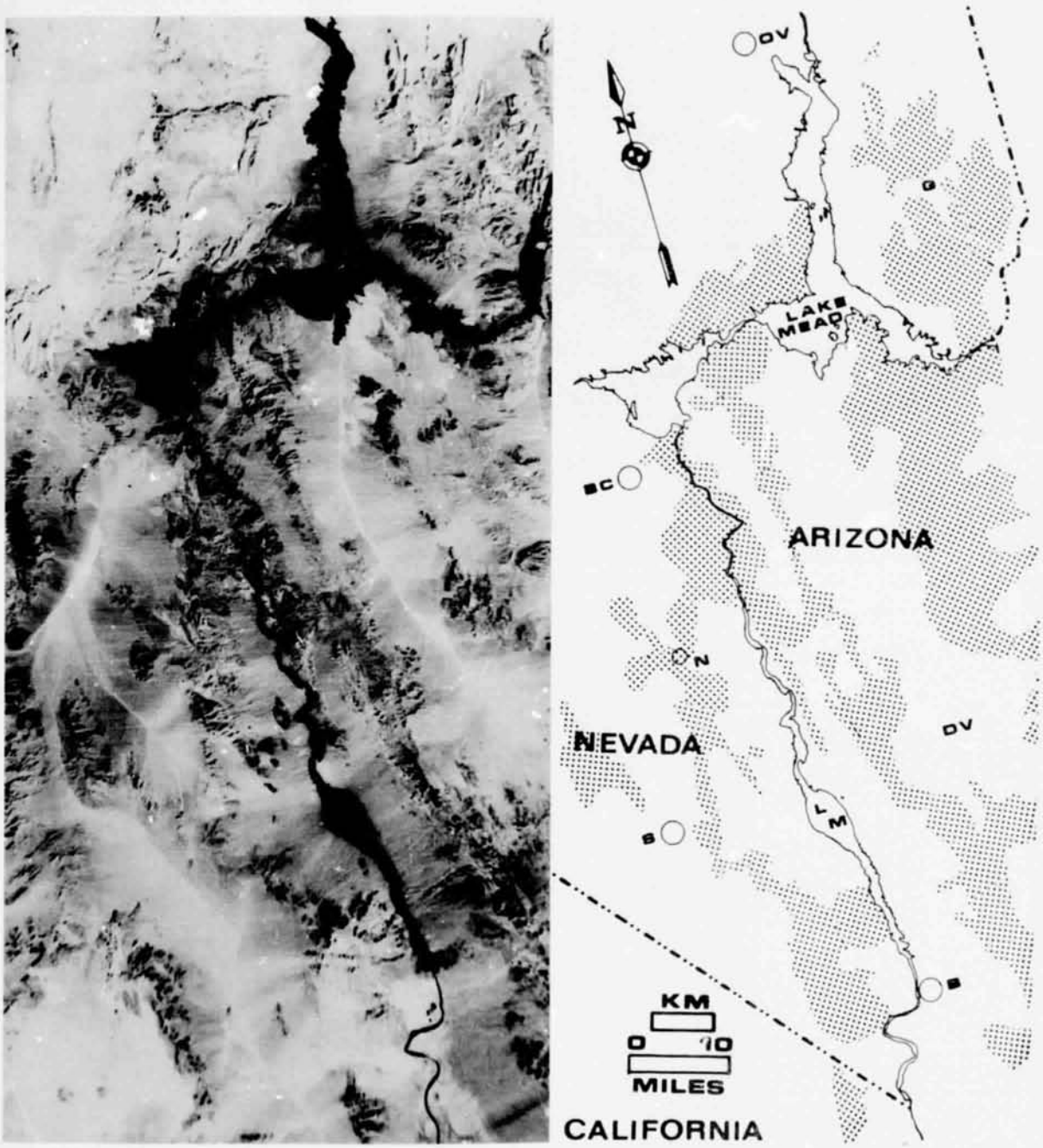

Figure 1: Portion of ERTS-1 MSS image 1106-17495-7 and index map of the study area. Location names are as follows:

B	-	Bullhead City, Ariz	LM	-	Lake Mojave
BC	-	Boulder City, Nev	N	-	Nelson, Nev
DV	-	Detrital Valley, Ariz	OV	-	Overton, Nev
G	-	Gold Butte, Nev	S	-	Searchlight, Nev

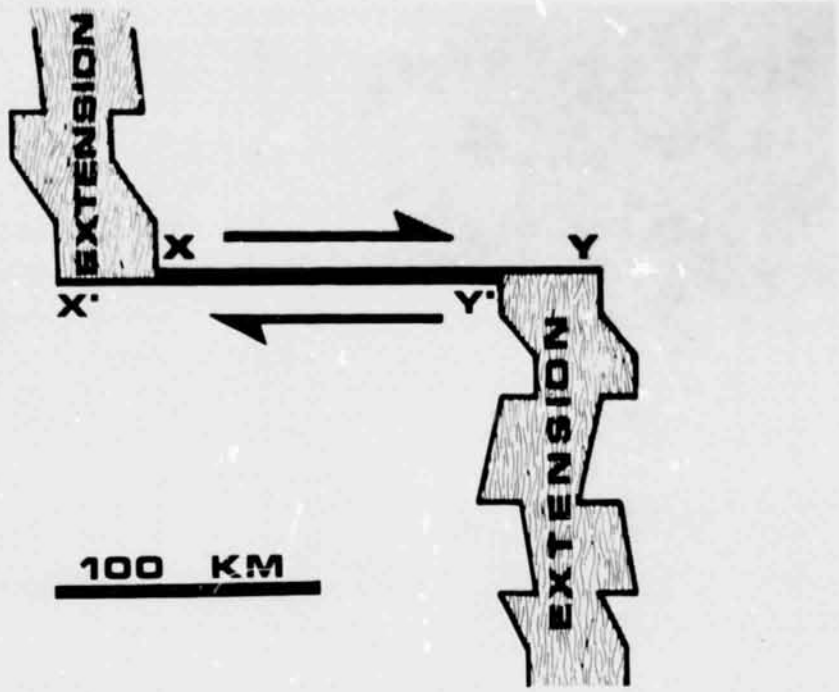

Figure 2.
Simplified tectonic diagram of a transform fault (X-Y) separating two areas of crustal extension (braided patterns). The shaded and white areas represent two crustal "plates". The Las Vegas shear zone is believed to be the transform fault which forms the northern boundary of an extensional province along the Colorado River.

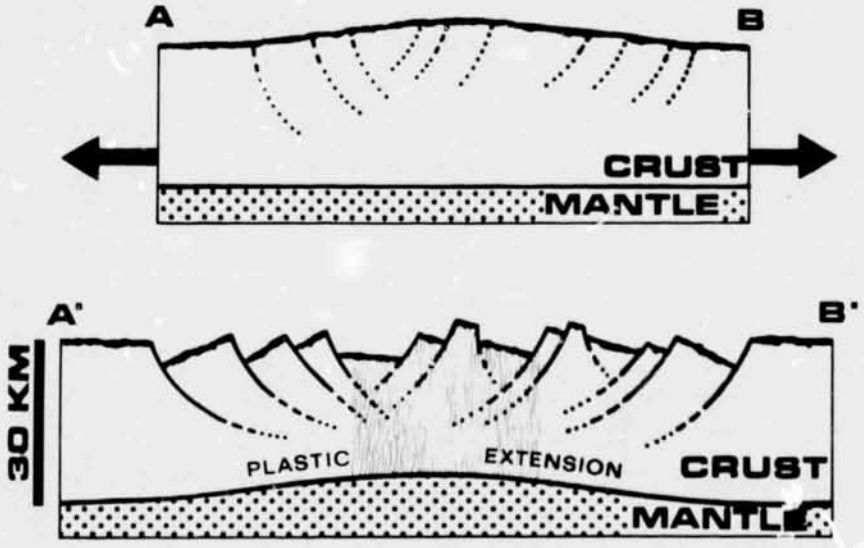

Figure 3.
Vertical sections of a region before and after crustal extension. Mechanisms of extension are normal faulting, plastic extension in the lower crust, and formation of new crust by volcanism and plutonism (braided pattern).

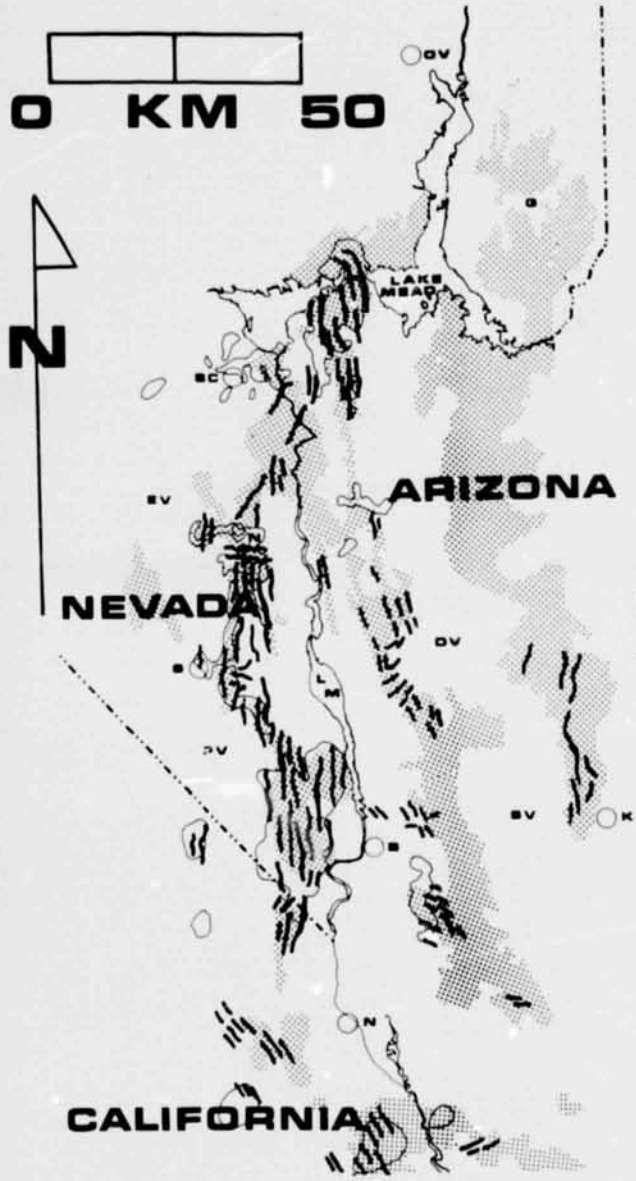

Figure 4. Distribution of Tertiary intrusive rocks, believed emplaced during crustal extension. Granitic plutons are outlined, and dike swarms are shown with heavy lines. Stippled areas are generalized bedrock exposures. Location names are as in Figures 1 and 6.

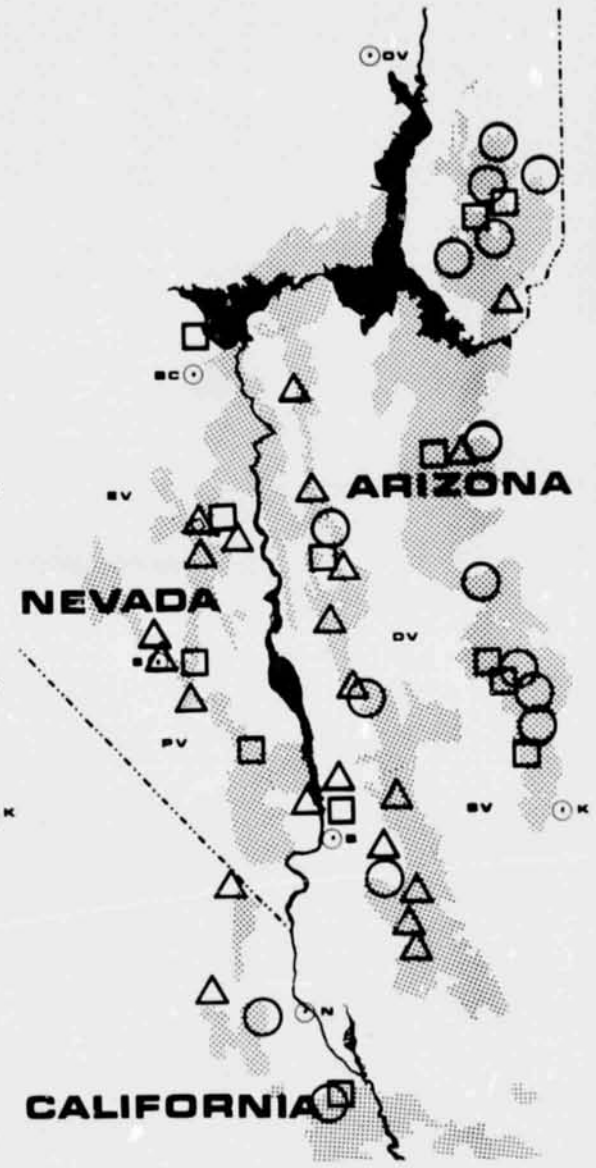

Figure 5. Distributions of known mineral deposits are indicated by triangles for gold; squares for lead, zinc, and silver; and circles for copper and molybdenum. Stippled areas are generalized bedrock exposures. Location names are as in Figures 1 and 6.

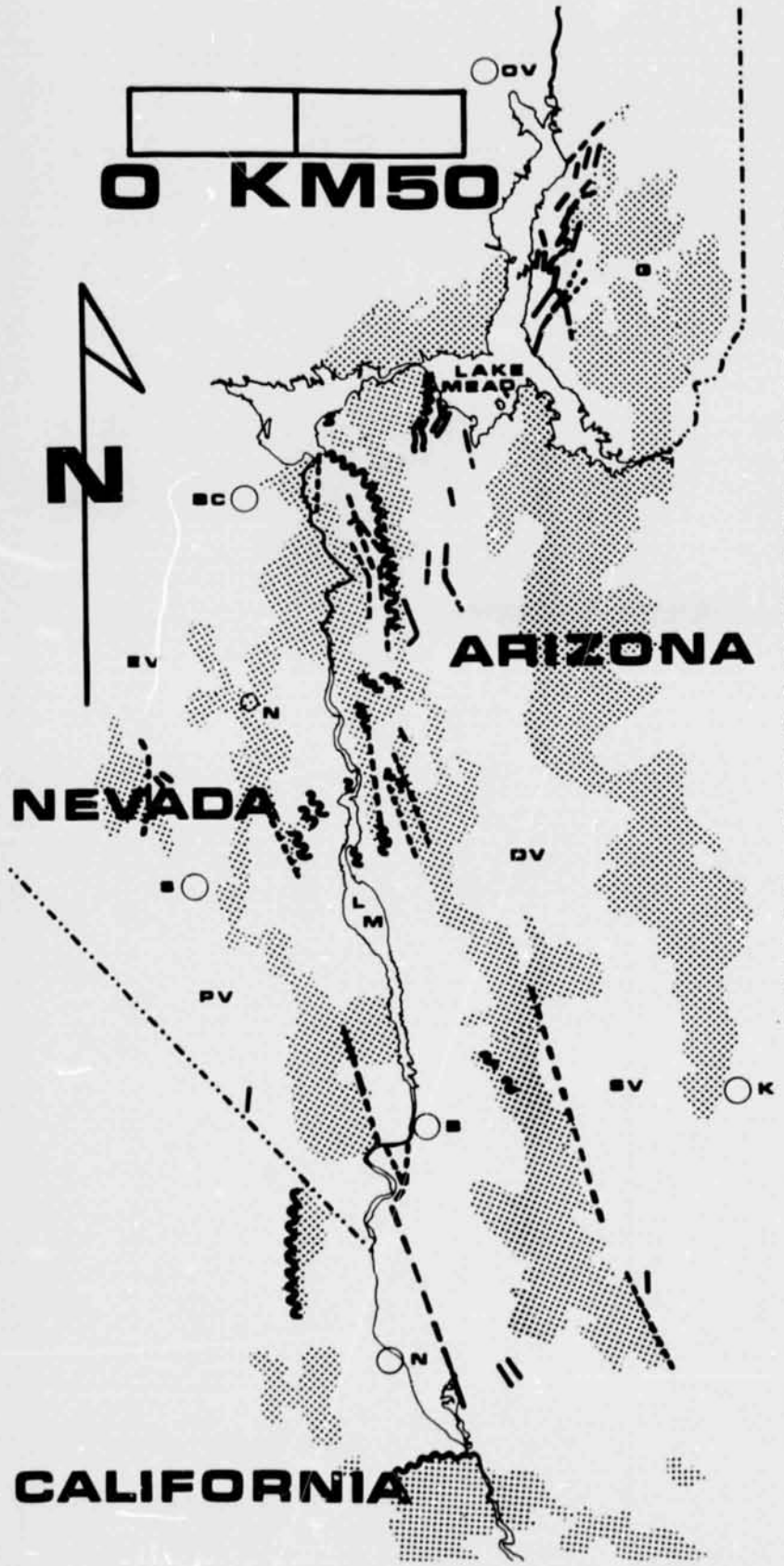

Figure 6. Newly recognized faults which cut alluvium are shown with solid lines where distinct; dashed lines where indefinite. Previously reported faults in alluvium, also apparent in ERTS imagery, are shown with wiggled lines. Faults cutting bedrock have been excluded. Stippled areas are generalized bedrock exposures. Locations names are as in Figure 1, with the following additions:

EV - Eldorado Valley
K - Kingman, Ariz.
N - Needles, Calif.
PV - Piute Valley
SV - Sacramento Valley

THE SALT CREEK FAULT, DEATH VALLEY, CALIFORNIA
(Abstract)

Argus Exploration Company
555 South Flower Street - Suite 3670
Los Angeles, California 90071

July 1973

Prepared for
GODDARD SPACE FLIGHT CENTER
Greenbelt, Maryland 20771

THE SALT CREEK FAULT, DEATH VALLEY, CALIFORNIA (ABS.)

By John F. Childs

In the central part of Death Valley, California, (Figure 1) several subtle linear anomalies, trending about N 15°E, were recognized in ERTS-1 MSS imagery. The most prominent of these features (see Figure 2) was singled out for study because it appears to extend undeflected across several strands of the Death Valley-Furnace Creek Fault Zone. Subsequent field work, using high altitude U-2 photography, confirmed this feature as a high-angle, oblique-slip fault, referred to as the Salt Creek Fault (Figure 3). Along its northern end, the Salt Creek Fault cuts Recent travertine deposits and has uplifted Miocene (?) and Oligocene (?) sediments on its southeast side. Southward, it crosses the Death Valley-Furnace Creek Fault Zone at an angle of approximately 60°. Near its southern end, the fault bifurcates and appears to terminate in the Paleozoic bedrock of Tucki Mountain. In a study of the geology of Death Valley, Hunt & Mabey (1966) infer a 2-1/2 mile segment of the Salt Creek Fault, but they show it terminating against strands of the Death Valley Fault Zone. (Hunt & Mabey, 1966, Geologic Map).

Structural measurements taken at the localities shown in Figure 3 are plotted on equal area nets in Figure 4. The scatter in fault plane orientation (Figure 4A) is probably due to interference of northwest trending faults, possibly related to the Death Valley-Furnace Creek Fault Zone, with the predominant northeast trends of the Salt Creek Fault.

The data in Figure 4B suggests that some of the faults measured have essentially down dip movement, but most have a strong component of strike slip. Although the data shows considerable scatter, over half of the low plunging slickensides trend northeast. This northeast plunge, combined with field evidence that the east side of the fault is uplifted indicates a possible component of right lateral slip.

Burchfiel and Stewart (1966) proposed a "pull apart" origin for the central part of Death Valley by which the valley opened between two northwest trending strike slip faults; the Death Valley-Furnace Creek Fault Zone on the north and the Death Valley Fault Zone on the south. The lack of apparent offset of the Salt Creek Fault where it crosses the Death Valley-Furnace Creek Fault Zone may be explained as the result of synchronous movement on the two faults or a temporary transfer of active movement to the Salt Creek Fault. Some of the discrepancies in estimates of displacement across the Death Valley-Furnace Creek Fault Zone (Wright and Troxel, 1967; Stewart and others, 1968) may be explained by taking into account the movement on northeast trending oblique slip faults such as the Salt Creek Fault.

References

Burchfiel, B. C., and Stewart, J. H., 1966, "Pull-Apart" Origin of the Central Segment of Death Valley, California: Geol. Soc. Amer. Bull., v. 77, p. 439-442.

Hunt, C. B. and Mabey, D. R., 1966, Stratigraphy and Structure, Death Valley, California: U. S. Geol. Survey Prof. Paper 494-A, 162 p.

Stewart, J. H., Albers, J. P., and Poole, F. G., 1968, Summary of Regional Evidence for Right-Lateral Displacement in the Western Great Basin: Geol. Soc. Amer. Bull., v. 79, p. 1407-1414.

Wright, L. A., and Troxel, B. W., 1967, Limitations on Right-Lateral, Strike-slip Displacement, Death Valley and Furnace Creek Fault Zones, California: Geol. Soc. Amer. Bull., v. 78, p. 933-950.

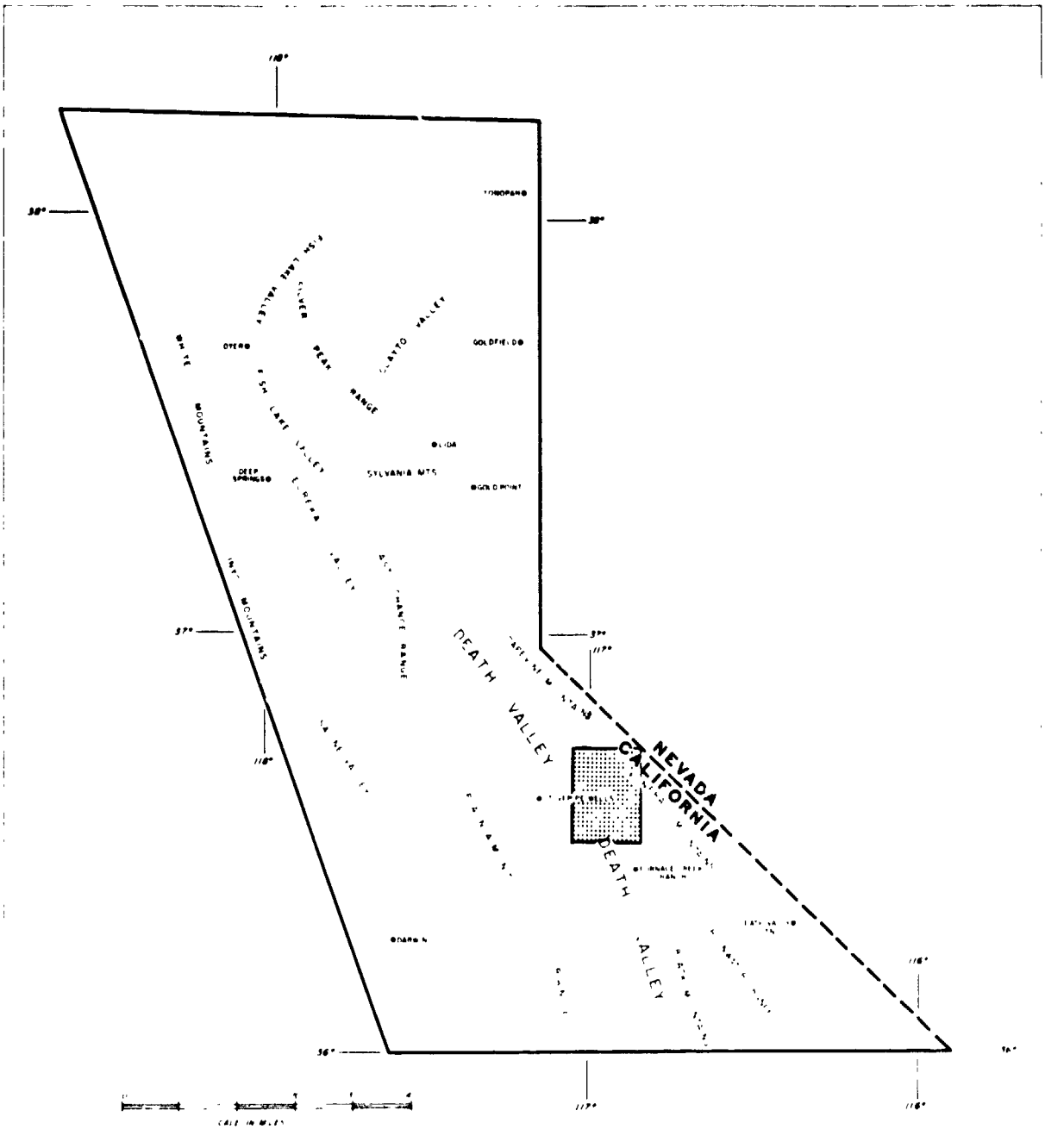

Figure 1 - Index map showing location of study area (shaded) in the central part of Death Valley, California

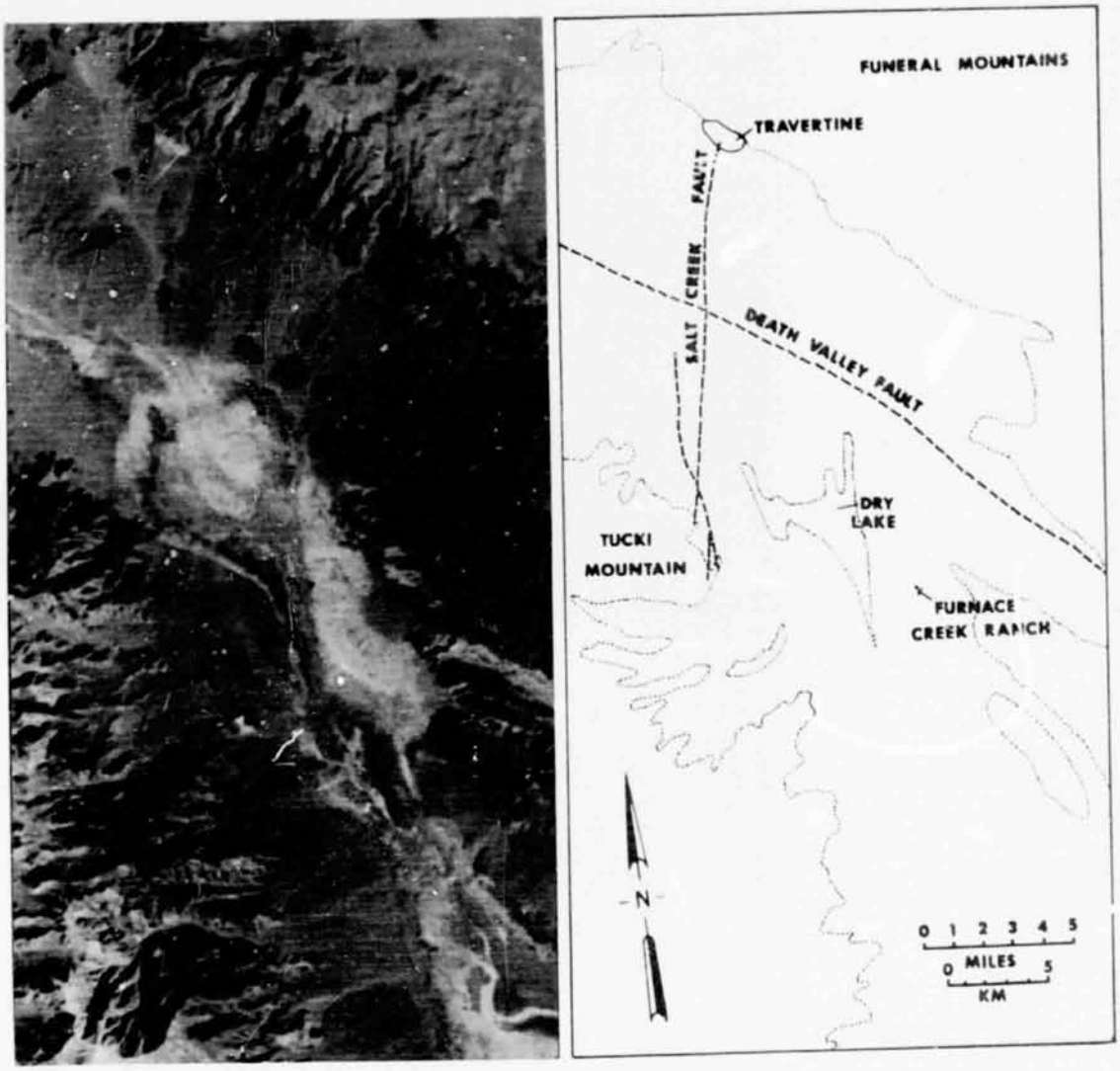

Figure 2 - Enlarged portion of ERTS-1 MSS Frame 1125-17554, 25 Nov. 1972 and corresponding index map. The Salt Creek Fault, described in the text, is shown in relation to the most prominent of several strands of the Death Valley-Furnace Creek Fault Zone.

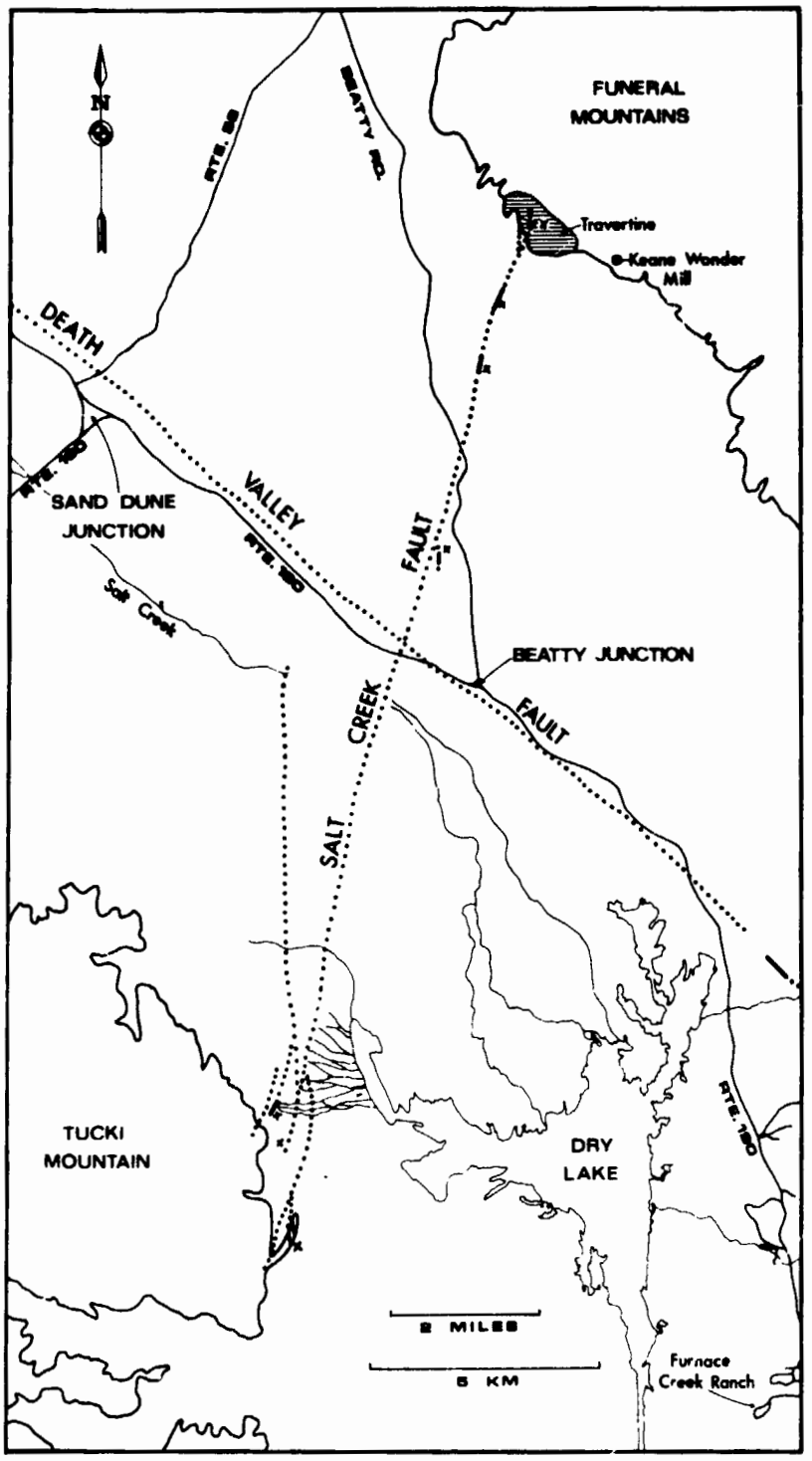

Figure 3 - Map showing the Salt Creek Fault and a prominent strand of the Death Valley-Furnace Creek Fault Zone. Topographic base maps used are the Chloride Cliff, Emigrant Canyon, Furnace Creek and Stovepipe Wells 15' Quadrangles. Localities where structural measurements were made are shown as Xs.

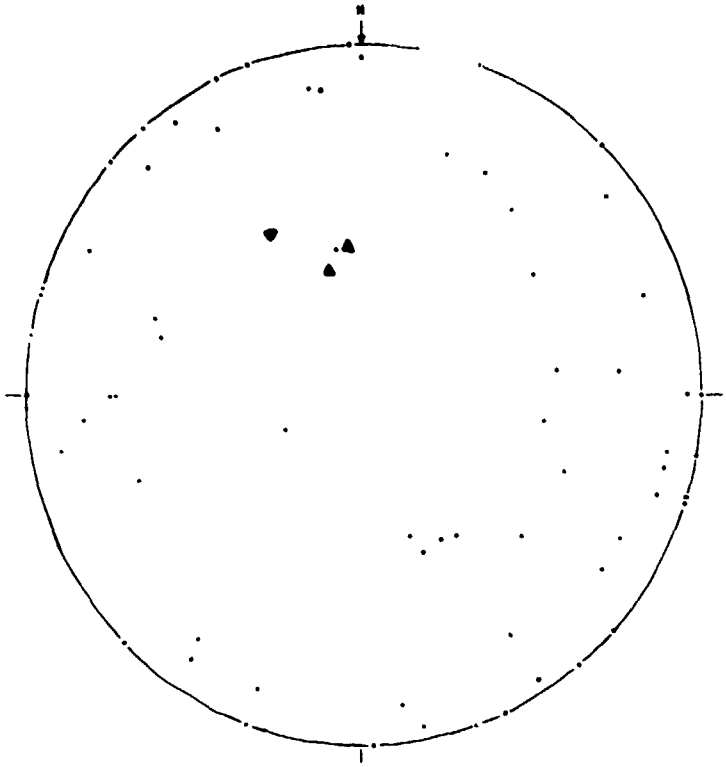

Figure 4 A -

Lower hemisphere equal area projection of 55 poles to fault planes (dots) and three poles to bedding (triangles) from localities shown in Figure 3 along the Salt Creek Faut.

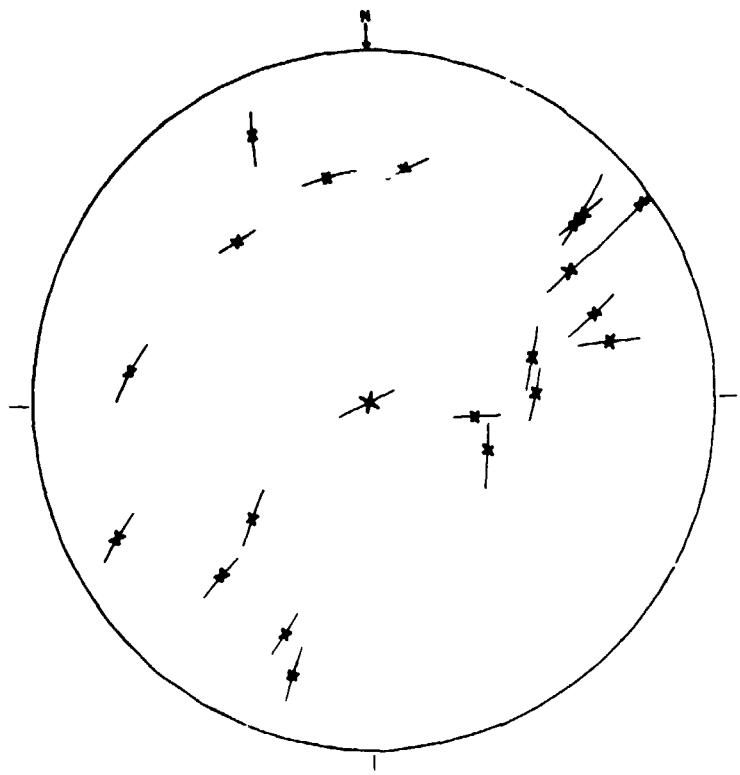

F ,,are 4 B -

Equal area projection of slickensides (crosses) and the fault planes on which they lie (arcs). Localities same as in Figure 4 A.

STRUCTURE AND VOLCANISM
UBEHEBE CRATERS, DEATH VALLEY, CALIFORNIA
(Abstract)

Argus Exploration Company
555 South Flower Street - Suite 3670
Los Angeles, California 90071

July 1973

Prepared for
GODDARD SPACE FLIGHT CENTER
Greenbelt, Maryland 20771

STRUCTURE AND VOLCANISM, UBEHEBE CRATERS, DEATH VALLEY, CALIFORNIA

John F. Childs and Mark A. Liggett

ABSTRACT

The Ubehebe Craters in northern Death Valley, California, are a cluster of Pleistocene or Recent (?) maar volcanoes located at the intersection of two faults recognized as major lineaments in ERTS-1 imagery. These north trending faults have not been previously mapped in the craters area. Field reconnaissance and mapping suggest an alignment of structural trends with volcanic features in the Ubehebe Craters area. Similar alignments of basaltic vents along subparallel faults in the vicinity suggest that northerly trending faults may have served as conduits for basaltic magma.

The Ubehebe Craters (Figure 1) are a cluster of shallow volcanoes of Pleistocene or Recent (?) age (Crowe and Fisher, 1973) which are aligned on north-south and east-west trends (Figures 2 and 3). In a study of the sedimentary structures of the volcanic ejecta, Crowe and Fisher (1973) concluded that the craters are maar volcanoes formed primarily by phreatic eruptions of basaltic magma.

The Ubehebe Craters appear to be located at the intersection of two prominent lineaments in ERTS-1 imagery (see Figure 2). The purpose of this study was twofold; to document the nature of the ERTS-1 lineaments in the craters area, and to investigate possible correlation of tectonic and volcanic features.

The intersecting ERTS-1 lineaments were confirmed as normal faults at several localities and are referred to here as the East and West Faults (see Figure 3). The East Fault can be followed in ERTS-1 imagery from north of the craters southward into the Panamint Range, a distance of 25 miles. The West Fault extends from just south of the craters for at least 20 miles along the west side of the Panamint Range. Displacement on the East Fault is probably on the order of tens or hundreds of feet, based on offset of lithologic units. Several thousand feet of displacement on the West Fault is suggested by the relief of the steep western face of the Panamint Range. The faults are thought to be Pleistocene to Recent in age since they cut Pliocene-Pleistocene (?) fanglomerates and possibly Recent alluvium. Although segments of both faults appear on the newly revised Death Valley Geologic Sheet (Streitz, 1973, written communication), and parts of the East Fault were mapped by McAllister (1952), these faults have not been previously mapped into the vicinity of the craters.

An alignment of volcanic features and faults is suggested by evidence from our field work, imagery analysis and previous geologic studies (Crowe and Fisher, 1973; Von Engeln, 1932). Faults in and adjacent to the Ubehebe Craters have trends similar to the East and West Faults in addition to a less pronounced east-west trend. The East Fault can be traced through the crater area except where it is deeply buried by volcanic debris near the eruptive center. The West Fault can be traced to within half a mile of the craters. Several north trending faults are mapped near the craters and others are inferred from topographic expression where the maar deposits have obscured the underlying geology (Figure 3).

The outline of the main Ubehebe crater is nearly circular except for a straight, slumped section along the western side. The slumping and asymmetry may be fault controlled. Von Engeln (1932) describes a fault which cuts through the center of the main crater and continues to the north but unfortunately his report does not include a map.

Basalt dikes found in the craters area, although few in number, have orientations similar to the north-trending faults. Dikes are thought to have fed basalt flows and spatter cones which preceded the main phreatic eruptive activity.

Pleistocene or Recent (?) basalt flows found along the Death Valley-Furnace Creek Fault Zone five miles to the east of Ubehebe Craters were erupted along fissures parallel to and within the fault zone, and are nearly identical petrographically to the basalts at Ubehebe Craters (Crowe, 1973, personal communication).

The frequent occurrence of basaltic volcanism along north trending faults in the Death Valley area suggests possible regional structural controls of basaltic magma sources. If faults in the Ubehebe Craters area acted to localize ground water as well as serving as conduits for rising basaltic magma, phreatic eruptions such as those which produced the craters may have occurred as the magma and water came into contact at shallow depth.

Acknowledgements

Bruce Crowe, University of California at Santa Barbara, generously made available a number of oblique and enlarged low altitude aerial photos for use in this study. He also gave freely of his time and of his detailed knowledge of the Ubehebe Craters area, making many helpful suggestions. However, the authors are fully responsible for the contents of this study.

References

Crowe, Bruce M., 1973, Oral Communication: University of California, Santa Barbara, California

Crowe, Bruce M., and Fisher, R. V., 1973, Sedimentary Structures in the Base-Surge Deposits with Special Reference to Cross-Bedding, Ubehebe Craters, Death Valley, California: Geol. Soc. Amer. Bull., v. 84, p. 663-682.

Von Engeln, O. D., 1932, The Ubehebe Craters and Explosion Breccias in Death Valley, California: Journ. of Geol., v. 15, no. 8, p. 726-734.

McAllister, James F., 1952, Rocks and Structure of the Quartz Spring Area, Northern Panamint Range, California: Calif. Div. Mines Special Report No. 25, 38 pp.

Streitz, Robert, 1973, Written communication: California Division of Mines and Geology, Sacramento, California.

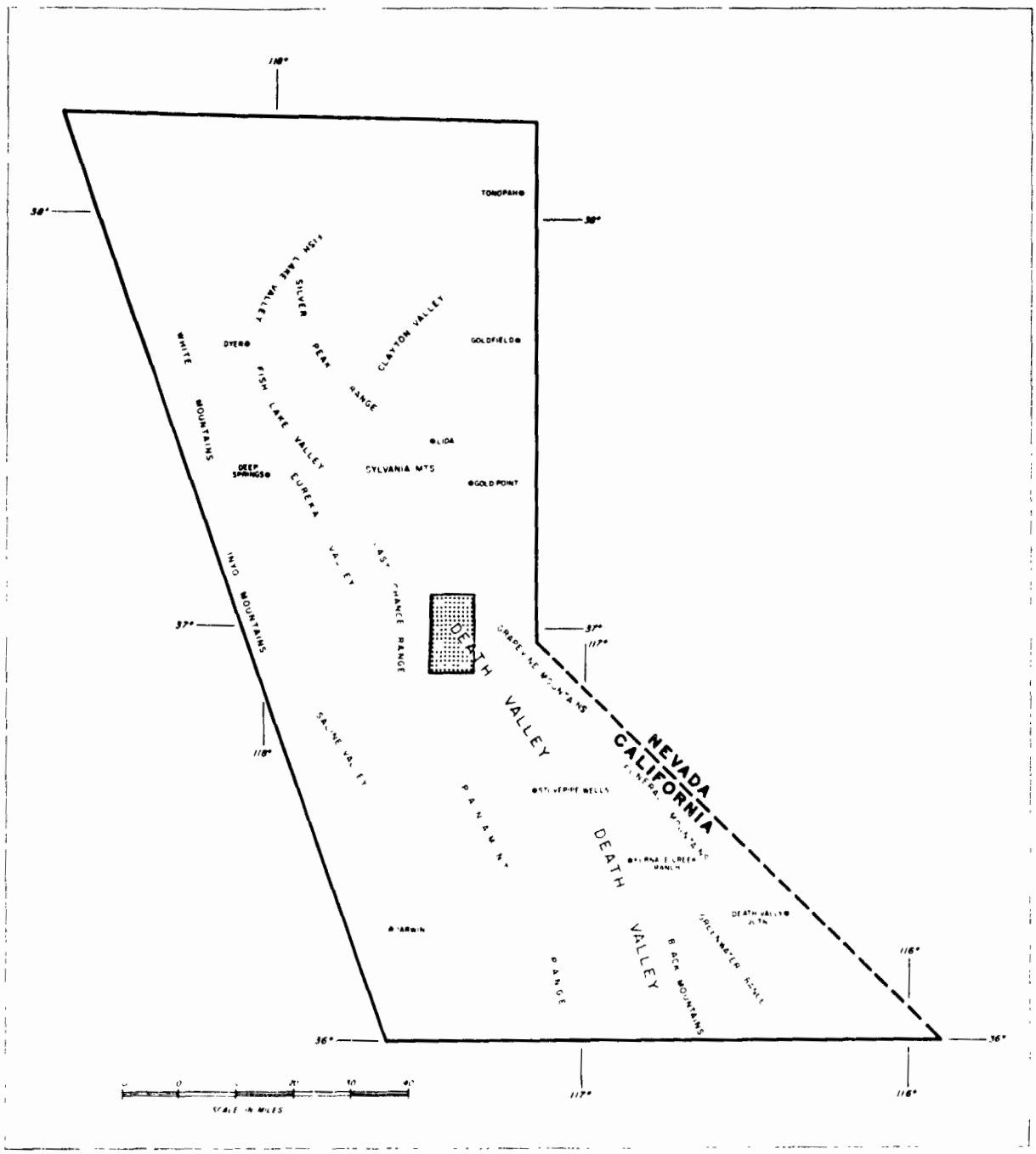

Figure 1 - Index map showing location of study area (shaded) in north-central Death Valley, California.

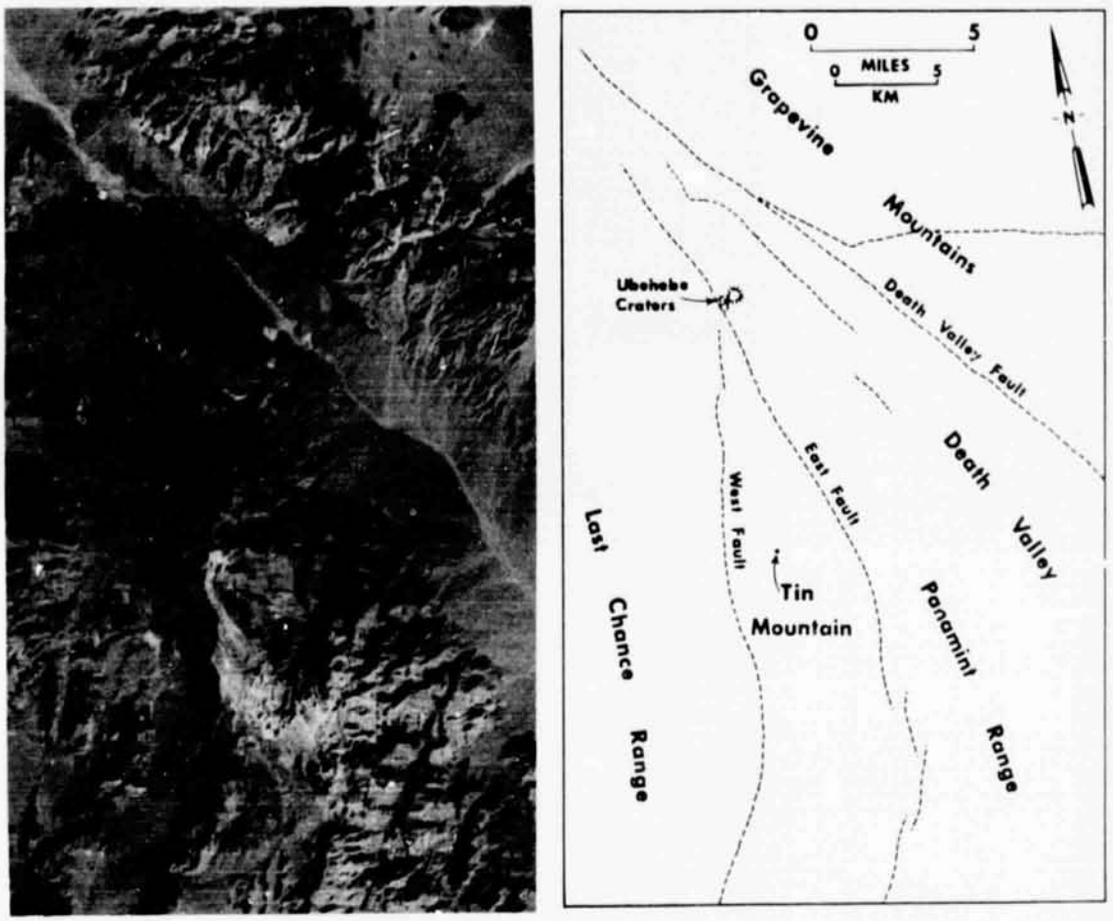

Figure 2 - Enlarged portion of ERTS-1 MSS Frame 1126-18010, 26 Nov. 1972, Band 7 and corresponding index map. The main structural features discussed in the text are shown in relation to Ubehebe Craters. The maar deposits surrounding Ubehebe Craters appear dark in the ERTS image. Basalts along the Death Valley-Furnace Creek Fault Zone appear dark grey.

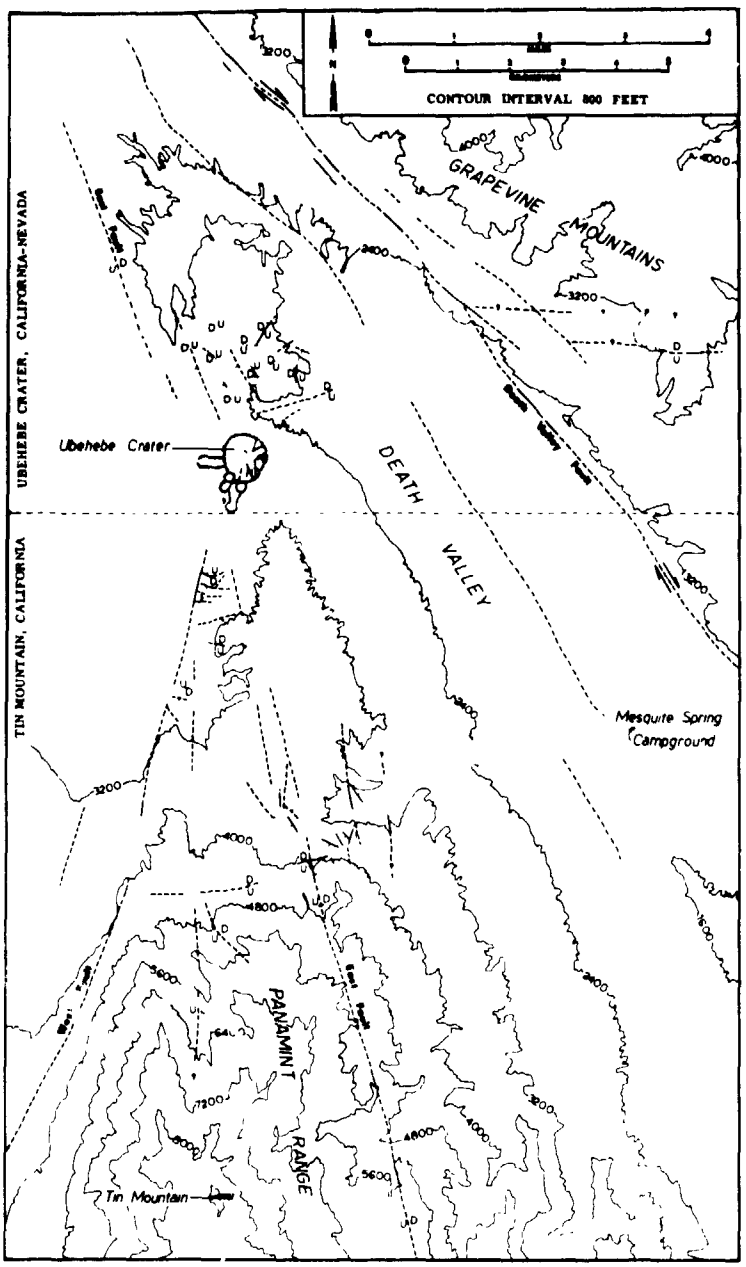

Figure 3 - Structural map of the Ubehebe Craters area based upon field work and analysis of ERTS-1 imagery and low altitude aerial photographs. Topographic base maps used are the Ubehebe Craters and the Tin Mountain Quadrangles. Faults dashed where approximate and dotted where inferred.

Appendix H

EVIDENCE OF A MAJOR FAULT ZONE ALONG THE CALIFORNIA-NEVADA STATE LINE, 35°30' TO 36°30' N. LATITUDE

Argus Exploration Company
555 South Flower Street - Suite 3670
Los Angeles, California 90071

July 1973
Report of Investigation

Prepared for
GODDARD SPACE FLIGHT CENTER
Greenbelt, Maryland 20771

EVIDENCE OF A MAJOR FAULT ZONE ALONG THE CALIFORNIA-NEVADA STATE LINE, 35°30' TO 36°30' N. LATITUDE

An Application of ERTS-1 Satellite Imagery

Mark A. Liggett, and John F. Childs
Argus Exploration Company
Los Angeles, California

ABSTRACT

Geologic reconnaissance guided by analysis of ERTS-1 and Apollo 9 satellite imagery and intermediate scale photography from X-15 and U-2 aircraft has confirmed the presence of a major fault zone along the California-Nevada state line, between 35°30' and 36°30' north latitude. We suggest the name Pahrump Fault Zone for this feature after the valley in which it is best exposed. Field reconnaissance has indicated the existence of previously unreported faults cutting bedrock along range fronts, and displacing Tertiary and Quaternary basin sediments. Gravity data support the interpretation of regional structural discontinuity along this zone. Individual fault traces within the Pahrump Fault Zone form generally left-stepping en echelon patterns These fault patterns, the apparent offset of a Laramide age thrust fault, and possible drag folding along a major fault break suggest a component of right lateral displacement. The trend and postulated movement of the Pahrump Fault Zone are similar to the adjacent Las Vegas Shear Zone and Death Valley-Furnace Creek Faults, which are parts of a regional strike slip system in the southern Basin-Range Province.

Introduction:

This report summarizes a result of research being conducted for the National Aeronautics and Space Administration on geologic applications of Earth Resources Technology Satellite (ERTS-1) imagery. The work was performed under NASA contract NAS5-21809.

The area of study was selected on the basis of the strong linear expression of Pahrump and Mesquite Valleys visible in oblique Apollo 9 satellite imagery. Although first recognized in the Apollo photography, the present investigation was guided primarily by data from ERTS-1 Multispectral Scanner (MSS) imagery. Analysis of this data has included additive color viewing and production of high resolution color composite imagery (MacGalliard & Liggett, in preparation). Research and analysis of additional satellite and aerial remote sensing data was conducted to evaluate the relative utility of various sensors and imagery scales. This research was coordinated with a program of ground-based geologic reconnaissance and mapping to evaluate imagery interpretation.

The following table lists imagery used in this investigation:

ERTS-1 NASA:	Multispectral Scanner Imagery (MSS)	
	13 September 1972	Frame 1052-17484
	14 September 1972	Frame 1053-17542
	6 November 1972	Frame 1106-17495
	25 November 1972	Frame 1125-17554
Apollo-9 Satellite, NASA:	Color Ektachrome Photography	
	Approximate altitude 148 miles	
	12 March 1969	Frame AS9-20-3135
NIMBUS-1, NASA:	Advanced Vidicon Camera System (AVCS)	
	5 September 1964	Orbit 124
X-15 Experimental Spacecraft, NASA-USAF:	Black and White Photography	
	Approximate altitude 130,000 feet	
	9 October 1962	Frames 081 thru 086
		Frames 089 thru 093
		Frames 095 thru 105
U-2 High Altitude Aircraft, USAF-USGS:	Black and White Photography	
Mission 018V	10 July 1968	Frames 200 thru 204
Mission 018L	10 July 1968	Frames 193 thru 201
Mission 018R	10 July 1968	Frame 204
Mission 374V	6 September 1968	Frames 201 thru 204
Mission 374L	6 September 1968	Frames 194 thru 202
Mission 744V	29 November 1967	Frame 079

Regional Geology and Previous Work:

The area of study is located in the southern Basin-Range Province of southern Nevada and eastern California. A mosaic of ERTS-1 MSS frames 1125-17554, 1053-17542, 1052-17484 and 1106-17495 which cover this region is shown in Figure 1. Geographic locations within this mosaic and major structural features (Carlson & Willden, 1968) discussed in the text are shown in Figure 2.

Pahrump and Mesquite Valleys form a narrow closed basin bordered on the east and west by generally north-trending mountain ranges typical of the Basin-Range Province. Topographic relief in the area is large with elevations ranging from 2,600 feet on the valley floor to over 11,900 feet in the adjacent ranges. Climate is semi-arid and vegetation cover is sparse at lower elevations, providing excellent outcrop exposure. Geologic mapping in the vicinity of the Pahrump Fault Zone has been conducted in a number of investigations. Although several fault breaks, which form parts of the zone, have been previously mapped, the extent of faulting and its regional continuity have not previously been reported.

Longwell and others (1965) mapped the eastern portion of the Pahrump area in their study of Clark County, Nevada. They recognize a belt of thrust faults trending generally north-northeast and high angle faults trending generally northwest in the Spring Mountains east of Pahrump Valley. The thrust faults are part of a major Laramide thrust belt which can be traced the length of the western Cordillera.

Cornwall (1972) mapped the geology of Nye County, Nevada, which includes the northeastern part of Figures 1 and 2. Fleck (1967 and 1970) worked in the northern Spring Mountains where he constructed isopach maps for the Eureka Quartzite and the Laketown Dolomite and described the geometry and style of deformation of thrust faults there and elsewhere in the zone of thrusting.

Hewett (1956) mapped the Ivanpah one degree quadrangle which includes the southern portion of Figures 1 and 2. He shows several northwest trending normal faults; two of these, the Stateline and the Ivanpah Faults, are extrapolated across alluvium from south of Sandy, Nevada toward Nipton, California. These may be parts of the Pahrump Fault Zone. Clary (1967) remapped part of the Ivanpah Fault south of Sandy in the eastern Clark Mountains.

G. T. Malmberg (1967), in a study of the hydrology of the Pahrump Valley mapped a 16 mile portion of the fault break shown on our Figure 2 along the California-Nevada state line.

Burchfiel and Davis (1971) have worked extensively in the western part of the study area where they have mapped components of the Laramide thrust belt mentioned above. Burchfiel (1965) has mapped normal and strike slip faults in the Specter

Range east of Lathrop Wells, Nevada. Several smaller mapping projects and topical studies have been conducted in and near the Pahrump area. Discussion of these is beyond the scope of this paper.

Pahrump Fault Zone:

The basin formed by Pahrump, Mesquite and Stewart Valleys is an asymmetrical graben typical of much of the Basin-Range Province. Along the west side of the graben, fault scarps form the steep fronts of the Ivanpah, Kingston, Mesquite and Nopah Ranges. The Ivanpah fault of Hewett (1956) is one of these range front faults, but the extent of faulting along the ranges has not previously been reported.

Within the Tertiary and Quaternary basin sediments of Pahrump Valley, a set of two subparallel fault scarps form an essentially continuous break which can be traced for approximately 25 miles. These faults are shown as a single dashed line trending north-northwest in Figure 2. Malmberg (1967) mapped a 16 mile portion of this fault, and stated that it could be traced for 23 miles along the valley floor. He estimated the vertical displacement to be approximately 1,000 feet, west side down, based on displacement of lithologic units in the sedimentary basin deposits. The geomorphology of the fault scarps and the age of the youngest rocks cut by the faults suggest a late Quaternary or Recent Age.

Possible right lateral displacement of streams along the 25 mile long break in Pahrump Valley has been recognized, but evidence of recent lateral fault displacement is ambiguous. Similar, though less pronounced lines of springs and vegetation found in Mesquite Valley, Stewart Valley and north of Stewart Valley are also believed to be fault traces.

Strike Slip Displacement:

Several lines of evidence suggest a right lateral component of strike slip along the Pahrump Fault Zone. In the eastern Clark Mountains, south of Sandy, Nevada, Clary (1967) has mapped a syncline which plunges moderately northwestward. The syncline is in Paleozoic sedimentary rocks immediately east of the Ivanpah Fault trace, and may be the result of drag caused by right lateral strike slip on the Ivanpah Fault.

Fleck (1971) suggested that offset in exposures of the Keystone Thrust from the southern Spring Mountains to the northern Clark Mountains may be the result of large scale drag folding about a steep axis, analogous to the flexure of the ranges adjacent to the Las Vegas Shear Zone. Davis and Burchfiel (1971) attribute this offset in the thrust to folding on a gently plunging northwest trending axis. Although Fleck did not propose a "state line shear zone" he suggested that based on available evidence, such an alternate hypothesis was reasonable.

Cornwall (1972) has mapped a right lateral strike slip fault in the mountains just east of Stewart Valley. This fault trends northwest at an oblique angle to Stewart Valley (Figure 2) and may be part of the larger strike slip system.

The Montgomery Thrust Fault, approximately 10 miles northwest of Pahrump, Nevada (Figure 2), was mapped by Hamill (1966). He postulated this fault to be the equivalent of the Wheeler Pass Thrust which occupies an equivalent structural-stratigraphic position 8 miles to the southeast in the Spring Mountains. The Wheeler Pass Thrust is extrapolated southwestward for 3 miles into the alluvium of Pahrump Valley by Longwell and others (1965). If these two thrust faults are equivalents, an offset of about 8 miles on a north trending right lateral strike slip fault is required in the northeast part of Pahrump Valley. Cornwall (1972) has mapped a number of north trending faults in alluvium between the ends of the two thrusts.

Fault scarps along the western margin of Pahrump Valley, form a generally left stepping en echelon pattern as shown in Figure 2. En echelon patterns are also recognized for faults within the basin alluvium. This is particularly well shown in oblique X-15 photography which looks southward along Pahrump Valley and in U-2 photography looking northeast across the valley. These en echelon faults south and west of the town of Pahrump are too small to be shown as individual breaks at the scale of Figure 2.

Although the graben structure of Pahrump Valley indicates east-west extension, the en echelon alignment of fault scarps suggests a right lateral component of stress. Similar patterns of surface faulting were reported by Gianella and Callaghan (1934) resulting from right lateral strike slip on the Cedar Valley Fault, Nevada, and by Brown (1970) for scarps along an active portion of the San Andreas Fault, California. This geometric orientation of faults can be shown in theory to be perpendicular to the direction of extension in a dextral stress system. (See for example, Billings, 1954, p. 196f.)

Figure 3 shows the structural features of Figure 2 superposed on a regional Bouguer gravity survey (USAF, 1968). The trace of the Pahrump Fault Zone coincides with a pattern of aligned low gravity anomalies. This correlation supports the interpretation of structural control of basin development which permitted the accumulation of a thick sequence of Cenozoic sediments less dense than the underlying bedrock. Similar gravity patterns are apparent along the Las Vegas Shear Zone and the Garlock Fault. The gravity pattern along the Death Valley-Furnace Creek Fault Zone is more complex, but the coincidence of gravity trends with the fault zone indicates structural control of subsurface mass.

Regional Implications and Conclusions:

The Pahrump Fault Zone is similar in trend and postulated displacement to the Death Valley-Furnace Creek Fault Zone to the west and the Las Vegas Shear Zone to the east. There is some evidence that these three fault zones may have branches in common but more detailed field work will be required to establish such interrelationships with certainty. The three fault zones form part of a larger northwest-southeast system of right lateral strike slip known as the Walker Lane. Cumulative displacement of 80 to 120 miles within the Walker Lane has been estimated based on displacement of regional isopachs, geologic structures and sedimentary facies, as well as flexure of adjacent mountain ranges (Stewart and others, 1968).

Right lateral movement within the Walker Lane is at least in part coeval with Basin-Range normal faulting and extensive andesitic to rhyolitic volcanism centered east and northeast of Beatty, Nevada (Fleck, 1967; Kistler, 1968). The stress pattern responsible for large scale right lateral movement and possible genetic relationships between faulting and igneous activity are poorly understood. However, recognition of new strands in the strike slip system, such as the Pahrump Fault Zone, may help solve these problems by adding to our knowledge of the regional geometry of faulting.

The Pahrump Fault Zone as described in this report is a system of numerous separate fault breaks which cut both bedrock and unconsolidated alluvium. Much of the zone has subtle expression best studied by a combination of remote sensing and ground based methods. Much of the data cited in this report has come from the work of other investigators which has involved detailed ground based mapping and stratigraphy. The ERTS-1 imagery does not replace these techniques. However, it provides a unique basis for studying the regional patterns of faulting not obvious from the perspective of conventional ground based mapping. We feel the results of this study illustrate the significant applications that orbital remote sensing can have to structural geology.

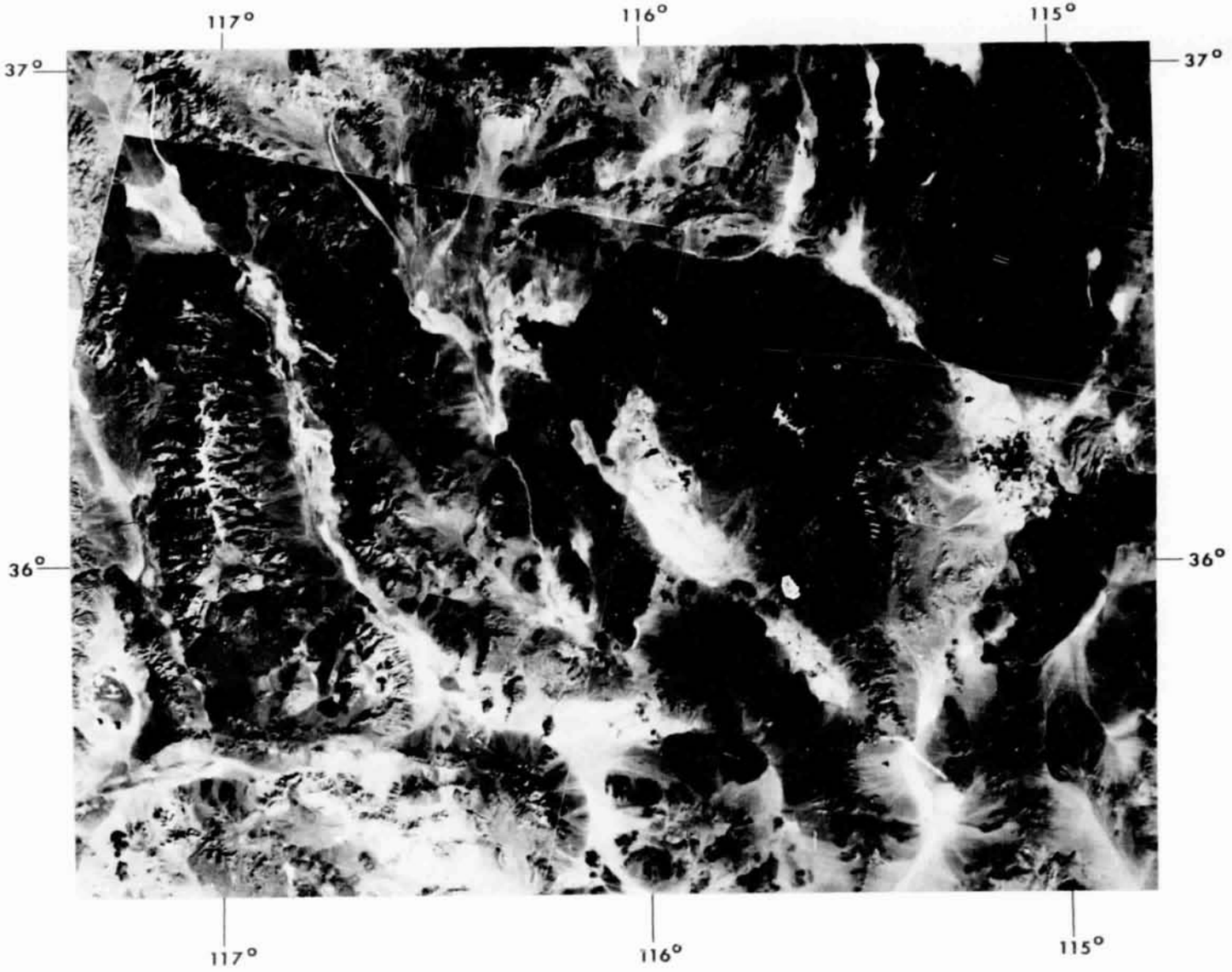

Figure 1. Mosaic of ERTS-1 MSS frames over southern Nevada and eastern California.
(Frame I.D. nos. 1052-17484, 1053-17542, 1106-17495, 1125-17554)

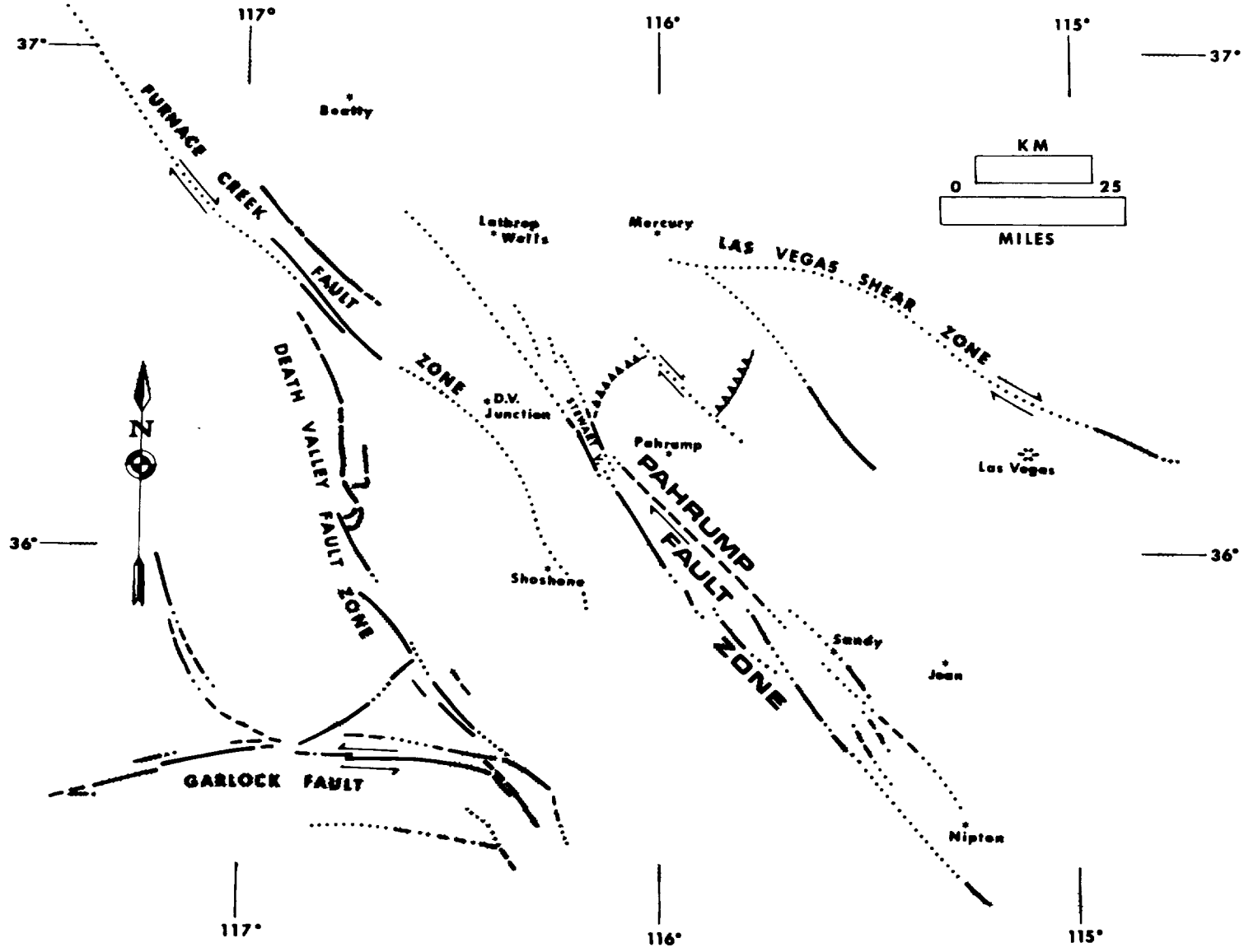

Figure 2. Major fault zones and geographic locations in the area of figure 1. Faults are dashed or dotted where approximate or inferred. Mountainous areas are shaded.

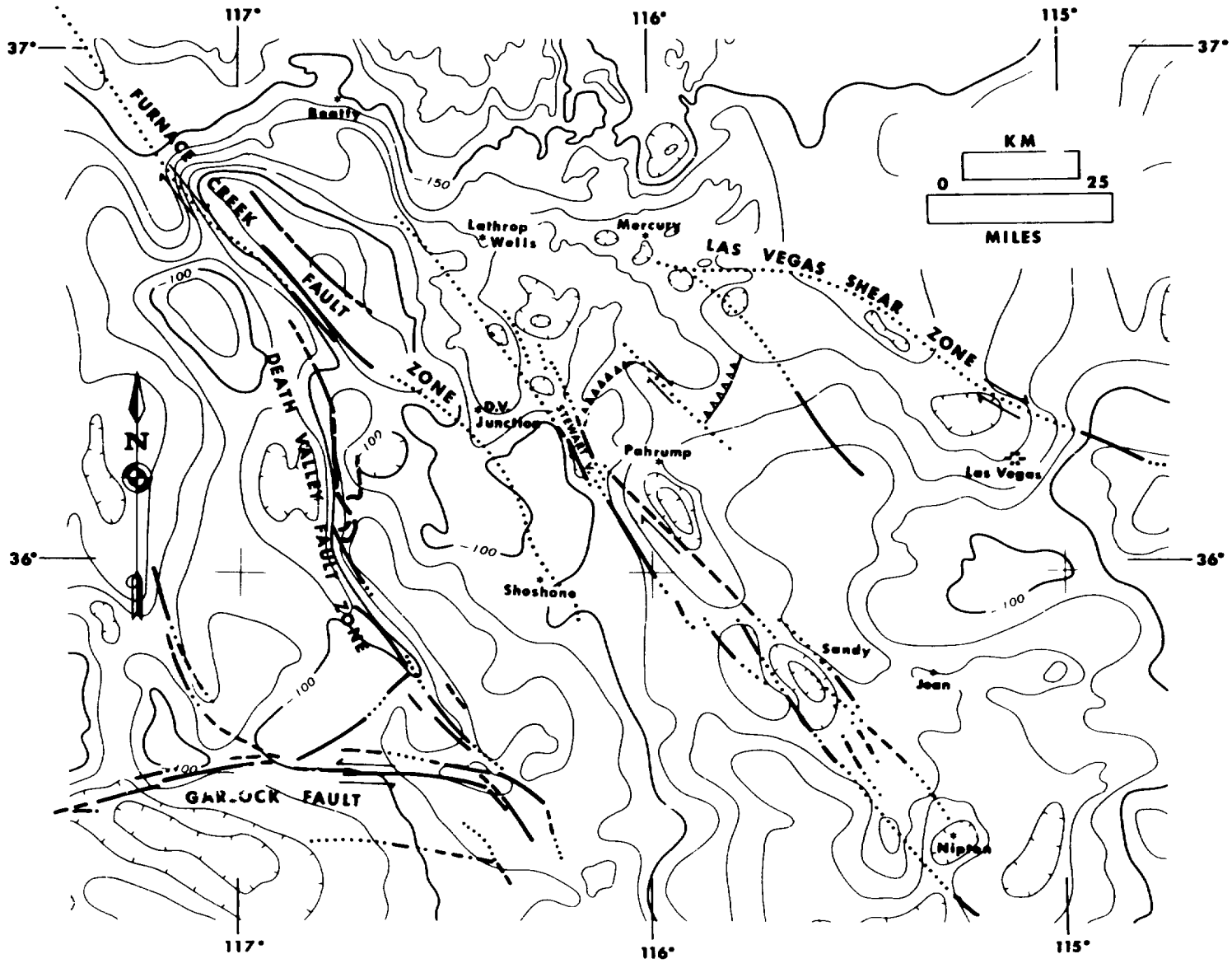

Figure 3. Fault zones of figure 2 superimposed on a regional Bouguer gravity map (USAF, 1968). Gravity contour interval is 10 milligals.

References:

Billings, M. P., 1954, Structural Geology: Prentice-Hall, Inc., Englewood Cliffs, N. J., 514 pp.

Brown, R. D., Jr., 1970, Map Showing Recently Active Breaks Along the San Andreas and Related Faults Between the Northern Gabilan Range and Cholame Valley, California: U. S. Geological Survey Misc. Geol. Investigations Map I-575.

Burchfiel, B. C., 1965, Structural Geology of the Specter Range Quadrangle, Nevada, and its Regional Significance: Geol. Soc. America Bulletin, Vol. 76, p. 175-192.

Burchfiel, B. C., and Davis, G. A., 1971, Clark Mountain Thrust Complex in the Cordillera of Southeastern California, in Geological Excursions in Southern California: Guidebook for Geol. Soc. America Cordilleran Section Meeting, Riverside, California, p. 1-30.

Carlson, J. E. and Willden, R., 1968. Transcontinental Geophysical Survey (35°39° N) Geologic Map from 112° W. to the Coast of California: U. S. Geol. Survey, Misc. Geol. Invest. Map I-532-C.

Clary, M. R., 1967, Geology of the Eastern Part of the Clark Mountain Range, San Bernardino County, California: California Division of Mines and Geology, Map Sheet 6.

Cornwall, H. R., 1972, Geology and Mineral Deposits of Southern Nye County, Nevada: Nevada Bureau of Mines and Geology, Bulletin 77, 49 pp.

Davis, G. A., and Burchfiel, B. C., 1971, Tectonic Style, Magnitude and Age of Deformation in the Sevier Orogenic Belt in Southern Nevada and Eastern California: Discussion: Geol. Soc. Amer. Bull., V. 82, p. 1433-1436.

Fleck, R. J., 1967, The Magnitude, Sequence and Style of Deformation in Southern Nevada and Eastern California: Ph.D. Thesis, University of California, Berkeley, California, 93 pp.

Fleck, R. J., 1970, Tectonic Style, Magnitude, and Age of Deformation in the Sevier Orogenic Belt in Southern Nevada and Eastern California: Geol. Soc. Amer. Bull., V. 81, p. 1705-1720.

Fleck, R. J., 1971, Tectonic Style, Magnitude and Age of Deformation in the Sevier Orogenic Belt in Southern Nevada and Eastern California: Reply: Geol. Soc. Amer. Bull., V. 82, p. 1437-1440.

Gianella, V. P., and Callaghan, E., 1934, The Earthquake of December 20, 1932 at Cedar Mountain, Nevada and Its Bearing on the Genesis of Basin Range Structure: Journal of Geology, Vol. 42, No. 1, p. 1-22.

Hamill, G. S., IV, 1966, Structure and Stratigraphy of the Mt. Shader Quadrangle, Nye County, Nevada-Inyo County, California: Ph. D. Thesis, Rice University, Houston, Texas, 83 pp.

Hewett, D. F., 1956, Geology and Mineral Resources of the Ivanpah Quadrangle California and Nevada: U. S. Geol. Survey Prof. Paper 275, 172 pp.

Kistler, 1968, Potassium Argon Ages of Volcanic Rocks in Nye and Esmeralda Counties, Nevada, in Nevada Test Site: Geol. Soc. America Memoir 110, p. 251- 263.

Longwell, C. R., Pampeyan, E. H., Bowyer, B., and Roberts, R. J., 1965, Geology and Mineral Deposits of Clark County, Nevada: Nevada Bureau of Mines, Bulletin 62, 218 pp.

MacGalliard, W., & Liggett, M., 1973, A Photographic Technique for Producing High Resolution Color Composites of ERTS-1 MSS Imagery: NASA Report of Investigation. In preparation.

Malmberg, G. T., 1967, Hydrology of the Valley-Fill and Carbonate-Rock Reservoirs, Pahrump Valley, Nevada - California: U. S. Geological Survey Water Supply Paper 1832, 47 pp.

Stewart, J. H., Albers, J. P., and Poole, F. G., 1968, Summary of Regional Evidence for Right-Lateral Displacement in the Western Great Basin: Geol. Soc. America Bulletin, Vol. 79, p. 1407-1414.

U. S. A. F. Aeronautical Chart and Information Center, 1968, Transcontinental Geophysical Survey (35°-39° N), Bouguer Gravity Map from 112° W. to the Coast of California: U. S. Geological Survey, Misc. Geol. Invest. Map I-532 B.

A MAJOR NORMAL FAULT IN ESMERALDA COUNTY, NEVADA
(Abstract)

Argus Exploration Company
555 South Flower Street - Suite 3670
Los Angeles, California 90071

Appendix I

November 1973

Prepared for
GODDARD SPACE FLIGHT CENTER
Greenbelt, Maryland 20771

A MAJOR NORMAL FAULT IN ESMERALDA COUNTY, NEVADA

John F. Childs
Argus Exploration Company
Los Angeles, California 90071

ABSTRACT

A 50 mile north-trending linear anomaly recognized in ERTS-1 MSS imagery west of Goldfield, Nevada has been confirmed as a steeply west-dipping normal fault, here termed the Paymaster Fault. This structure trends southward from the General Thomas Hills along Paymaster Valley and the east side of Clayton Valley into the Palmetto Mountains. There, it terminates against a less pronounced east-trending transverse anomaly which is also believed to be fault controlled. The Paymaster Fault is the most prominent of several large normal faults which terminate southward against this transverse anomaly.

DISCUSSION

The Paymaster Fault in southwestern Nevada is a prominent linear feature in ERTS-1 imagery extending approximately north-south for 50 miles (Figures 2 and 3). The fault is shown on the preliminary map of Esmeralda County (Albers & Stewart, 1965) in a generalized tectonic inset map but is not included in the geological map. The inset map shows the Paymaster Fault extending southward along Paymaster Valley into Clayton Valley and from there turning westward toward the Silver Peak Range. ERTS-1 and U-2 imagery of the area suggests that the Paymaster Fault, rather than turning westward, continues southward along the east side of Clayton Valley and along Lida Wash into the Palmetto Mountains northwest of the town of Lida, Nevada (Figures 2 and 3). This interpretation was confirmed by field reconnaissance.

The Paymaster Fault is a steeply west-dipping to vertical normal fault, with probable vertical displacement of at least 1000 feet along some segments. Scarps in alluvium northwest of the General Thomas Hills suggest a Quaternary age for at least some of the movement. A large, nearly vertical east-trending fault intersects the Paymaster Fault in the General Thomas Hills. This fault is probably older than the Paymaster Fault because it does not cut Recent alluvium and appears to be offset by the Paymaster Fault.

The Paymaster Fault is extrapolated southward along the east side of Clayton Valley (Figure 3). Several escarpments, thought to be paleo-shorelines occur in the alluvium along this segment. However, bedded alluvium east of these features is tilted eastward, suggesting that the straight paleoshorelines may be fault controlled.

Range front faulting is evident along the eastern side of Clayton Valley. Numerous faults cutting Tertiary pumice breccias and the underlying granitic rocks were studied in detail in the area indicated by an arrow in Figure 3. The results of this study are summarized in Figure 4. This fault zone can be traced in the ERTS-1 imagery southward along the west face of Clayton Ridge. From the south end of Clayton Ridge, the zone is extrapolated 1/2 mile across alluvium into an andesite sequence near the mouth of Lida Wash. The total amount of movement on individual strands of the fault zone in the andesites is small. Strands of the zone continue along the walls of Lida Wash Canyon for approximately four miles southward into the Palmetto Mountains, where evidence of faulting is found in the offset of lithologic units across the canyon, and in discontinuous zones of faulting and alteration within the canyon.

The Paymaster Fault appears on the ground and in ERTS-1 imagery to terminate southward against a broad east-west trending topographic depression which is probably fault controlled (Figure 2). This transverse zone, here called the Palmetto Zone, extends discontinuously westward from Mount Jackson Ridge to Fish Lake Valley, a distance of approximately 30 miles. The Palmetto Zone appears to be an important structural feature of this region since it also forms the southern terminus of several large normal faults in the Goldfield Hills southeast of Goldfield, Nevada.

CONCLUSIONS

The Paymaster Fault is clearly apparent in ERTS-1 MSS imagery as a prominent north-trending lineament. This fault, unlike most Basin-Range normal faults, is not restricted to a single range and can be traced for 50 miles as a sharp, straight zone along or within three ranges.

REFERENCES

Albers, John P. and Stewart, John H., 1965, Preliminary Geologic Map of Esmeralda County, Nevada: U. S. Geol. Surv. Mineral Investigations Field Studies Map MF-298.

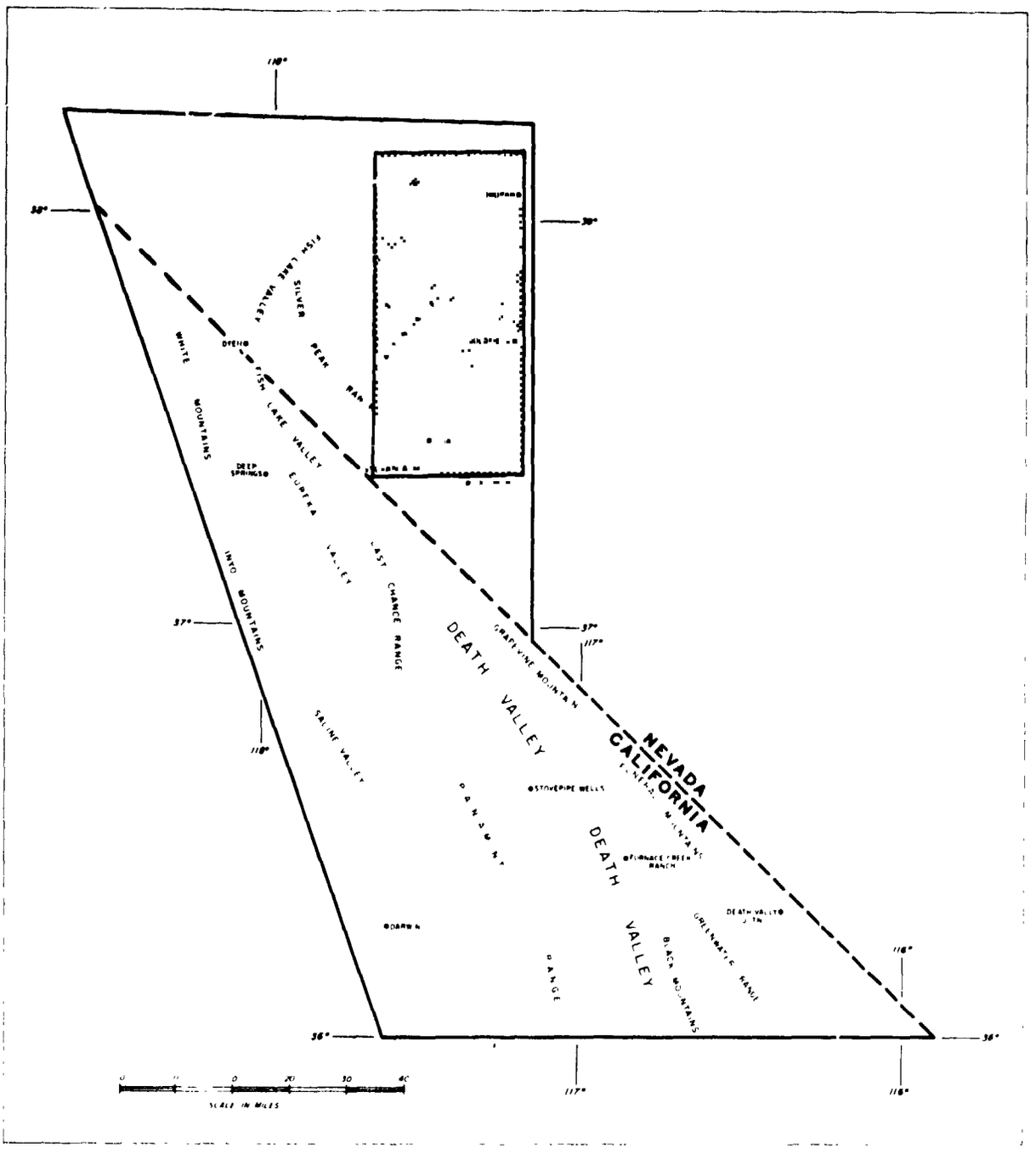

Figure 1 - Index map of the study area in southwestern Nevada. The area covered in Figure 3 is shaded.

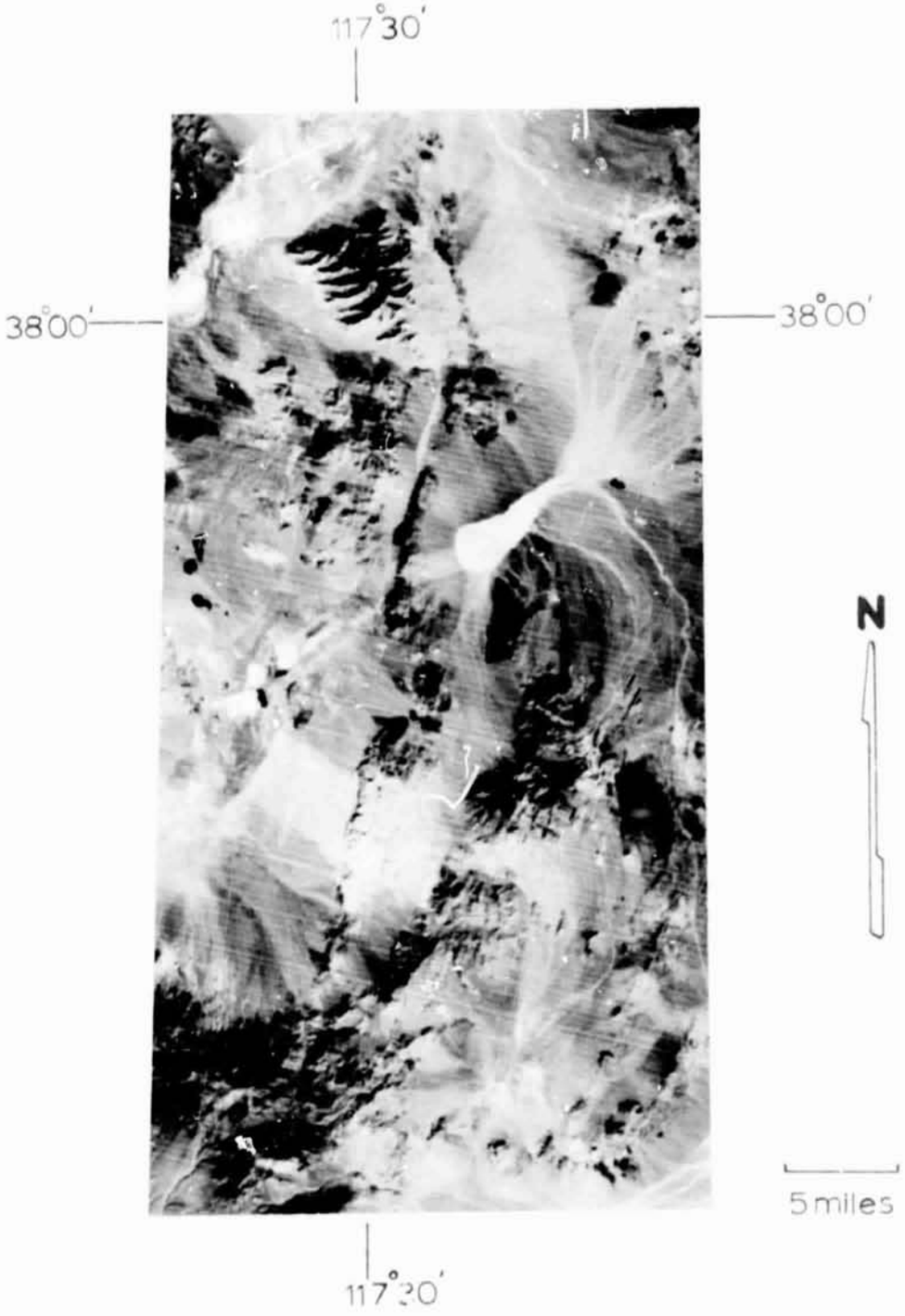

Figure 2 - Enlarged portion of ERTS-1 MSS Frame 1144-18010, Band 7, 14 December 1972. The area covered in this enlargement is approximately the same as in Figure 3.

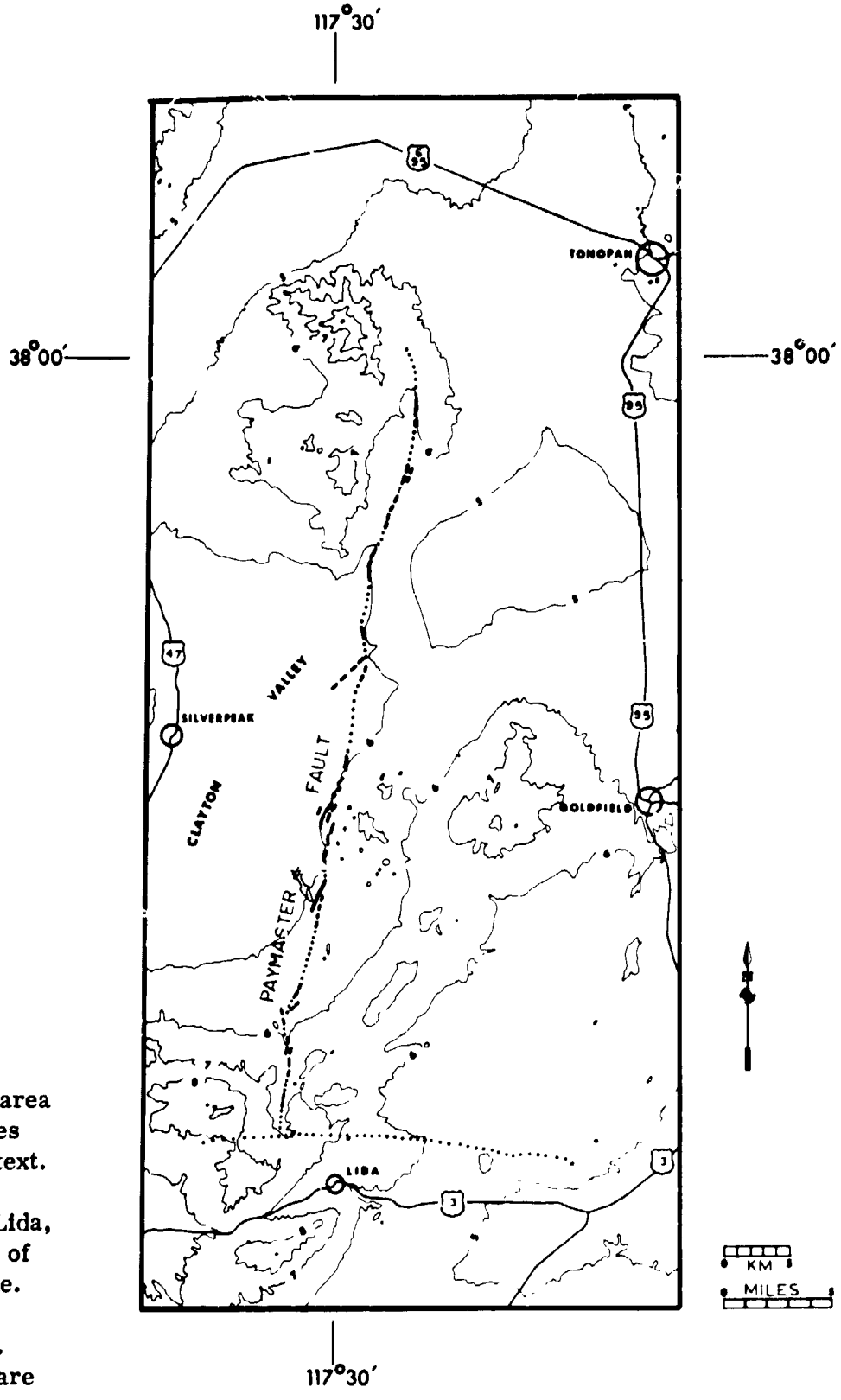

Figure 3 -

Map of the study area showing structures described in the text. Dotted east-west feature north of Lida, Nev. is a portion of the Palmetto Zone. Contours are in thousands of feet. Base maps used are the Goldfield and Tonopah 1:250,000 topographic maps.

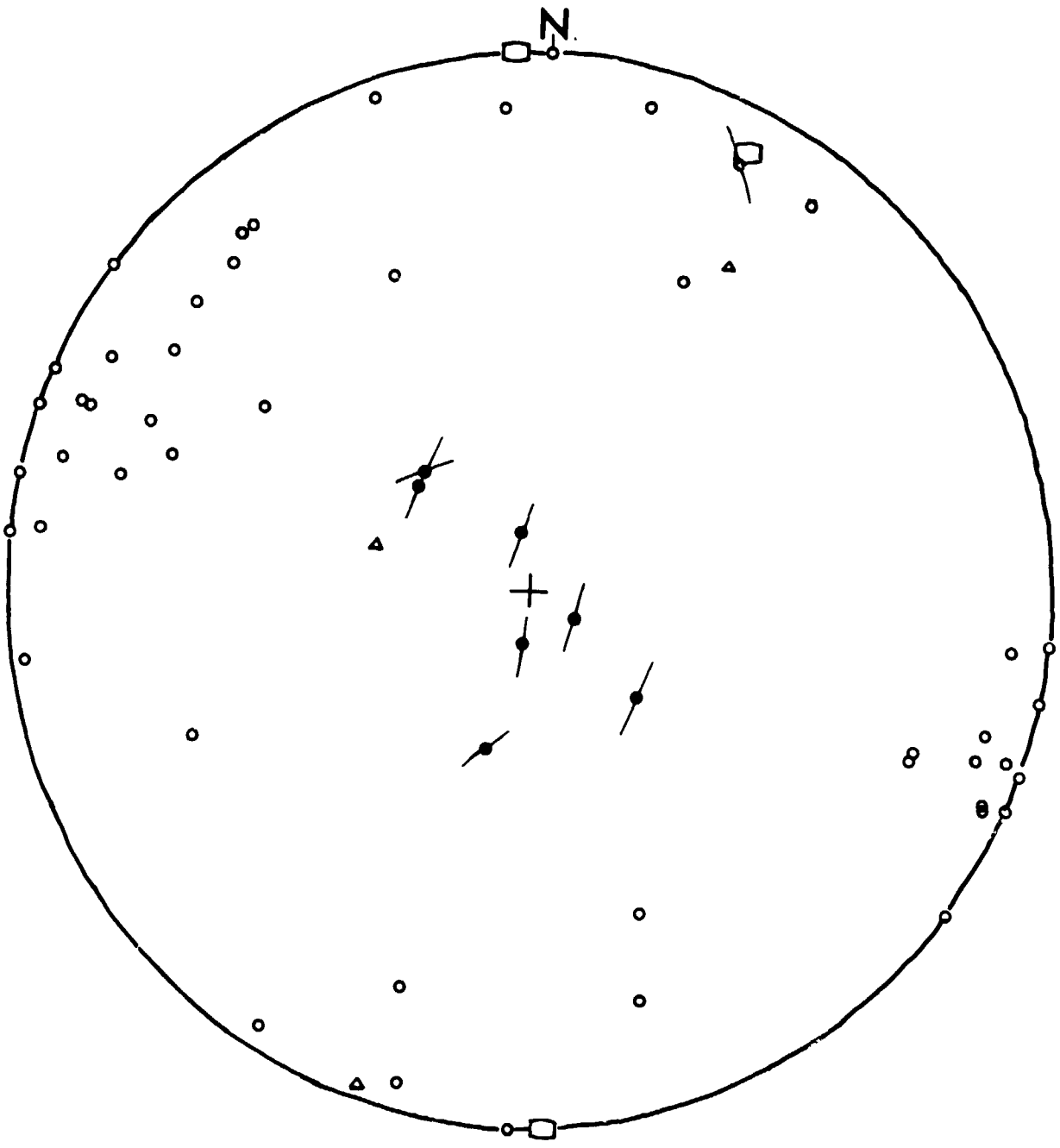

Figure 4 - Equal area lower hemisphere projection of slickensides (closed circles) and part of fault planes on which they lie (arcs), faults (open circles), bedding (triangles) and dikes (rectangles). Structural data from area indicated by arrow in Figure 3.

FALSE-COLOR COMPOSITING OF ERTS-1 MSS IMAGERY

Argus Exploration Company
555 South Flower Street - Suite 3670
Los Angeles, California 90071

November 1973
Report of Investigation

Appendix J

Prepared for
GODDARD SPACE FLIGHT CENTER
Greenbelt, Maryland 20771

False-Color Compositing of ERTS-1 MSS Imagery

Wally MacGalliard* and Mark Liggett
Argus Exploration Company
Los Angeles, California 90071

ABSTRACT

An operational technique for producing high-resolution false-color composites of ERTS-1 Multispectral Scanner (MSS) imagery has been developed for use in a typical photographic laboratory equipped for color processing and printing. The technique uses standard NASA (NDPF) or EROS black/white data products, and permits a broad range of control on composite color balance and contrast range. The use of an additive color viewer has proven valuable for determining the optimum color balance of composites for effective interpretation. The compositing technique is adaptable to data from a variety of multispectral imaging systems, including multi-seasonal and multi-polarization data.

* MacGalliard Colorprints
North Hollywood, California 91602

INTRODUCTION

The following technique was developed as part of an investigation of geologic applications of ERTS-1 Multispectral Scanner (MSS) imagery. An important advantage of multispectral imaging is the ability to study the varied information recorded in each spectral band of the imaging system. These variations are due primarily to differences in the reflectance characteristics of features such as rock or soil units, and vegetation types, vigor or seasonal variation.

In the ERTS-1 MSS system, four images are recorded over the following spectral ranges:

ERTS-1 Band No.	Spectral Range	Description
4	.5-.6 microns	Green and yellow
5	.6-.7 microns	Red
6	.7-.8 microns	Near-infrared
7	.8-1.1 microns	Near-infrared

An important tool for analysis and interpretation of multispectral imagery is additive color viewing, which permits reconstruction of "natural" or "false" color images by combining the spectral bands, each with an appropriate color filter. Additive color viewing also allows the "real time" manipulation of color balance by variation of the band/filter combinations and illumination intensities for each channel. This flexibility in color balance permits more effective interpretation of the multispectral imagery than is possible with the fixed color balance of polyemulsion films or standardized multispectral composites. The principles of additive color imaging are outlined in a number of publications, for example Yost and Wenderoth (1968), and Ross (1973).

In order to most effectively use the ERTS-1 MSS imagery, the following technique was developed for reproducing the optimum color balance as determined by analysis of the MSS imagery on an additive color viewer. The compositing procedure uses standard 70mm or 9" x 9" ERTS-1 MSS positive transparencies as distributed by the NASA Data Processing Facility (NDPF), Goddard Space Flight Center, Greenbelt, Maryland and the EROS Data Center, Sioux Falls, South Dakota.

REGISTRATION

Registration equipment consists of a Master film punch[1] and 1/4" diameter Berkey pins[2]. The pins are positioned on a light table, a negative carrier and a vacuum

[1]Master Products Manufacturing Co., 3481 E. 14th St., Los Angeles, Calif. 90023
[2]Berkey-Alldis Register Products, Berkey Technical Companies, Inc., 25-15 50th St., Woodside, Long Island, N.Y. 11377

printing easel. They are set on 3 1/2" centers for projecting 70mm transparencies onto 5" film, and 7" centers for contact printing 9" x 9" transparencies onto 10" film.

To prepare three 9" x 9" multispectral positive transparencies for contact exposure, the transparencies are first rough registered on a light table, one over the other, and one edge of the set cut uniformly with a straight-edge and mat knife. This facilitates butt taping of the transparencies to leader strips without overlap. The leader strips are 1 1/4" x 9" pre-punched blank films of the same thickness as the positive transparencies.

The first leader is placed over the pins on the light table and a 9" x 9" transparency taped to it, emulsion side down. The tape used is Scotch Brand Polyester Film Tape No. 850. The second leader is then placed on the pins over the first transparency and a second transparency is manually registered with the first. This is done by placing a thin glass plate over the pair to insure image contact, and viewing the corner cross-hairs and edge-identification through a 5X achromatic magnifier. When perfect registration has been achieved, the second transparency is taped to its leader and removed from the pins. Successive positive transparencies are registered and taped in the same manner. In order to facilitate this task, it is often most effective to use the highest contrast transparency, generally Bands 6 or 7, as the master against which the other bands are registered.

The registration procedure for a set of 70mm is the same, except for the smaller size which makes the visual work more tedious. Frequently, however, the ERTS-1 MSS 70mm transparencies surpass the 9" x 9" transparencies in resolution, and are well worth the extra effort required for registration.

TRI-COLOR EXPOSURE

An 8" x 10" Durst Condenser enlarger[3] is used as a light source to produce internegatives by either contact printing or projection. It is equipped with a 500 watt Opal bulb, a filter wheel containing the standard Wratten tri-filter set (Red No. 29, Green No. 61, and Blue No. 47b, process type lenses, and a vacuum easel fitted with pins for registration of various film sizes.

To contact print a set of 9" x 9" transparencies, a sheet of Ektacolor Internegative film, Type 6110, is first punched in the dark and placed on the pins of the vacuum easel, emulsion up. A pre-punched transparency is registered over the film, emulsion down, and exposed using the suitable tri-color filter. It is then removed, replaced by the second transparency and exposed using a second tri-color filter, and so on.

To project a set of 70mm transparencies, the procedure is the same, except that the smaller transparencies are pin registered within a glass negative carrier and projected to the desired size on the easel.

[3]Durst (U.S.A.) Inc., 623 Stewart Ave., Garden City, N.Y. 11533

For each set of MSS transparencies, the proper tri-color exposures are determined by test. The objective is to retain as much of the original image density range as possible, and to duplicate the desired color balance. The color balance is controlled as a function of the relative differences in exposure times for the separate MSS bands. However, several other variables should also be considered in test exposures, including differences in density range between and sometimes within sets of MSS transparencies, and filter factors required for different batches of inter-negative stock. The actual exposures will, therefore, differ between photographic labs. The exposure times currently in use at this facility are: Red-12 seconds, Green-40 seconds, and Blue-18 seconds. Lense apertures are typically varied between f:11 and f:16 as determined by densitometer readings of the MSS transparencies.

Exposure values can be split between two bands if necessary; for instance, Bands 6 and 7 may be combined in a composite both with red illumination. Other variations in exposure intensity and time can be made within the reciprocity range of the internegative film.

DEVELOPMENT

Ektacolor inter-negative films are developed to normal gamma using standard Eastman Kodak C-22 chemistry.

PRINTING

Inter-negatives are printed on Ektacolor RC paper, N surface. Prints up to 16" x 20" are processed by batch in a Calumet processor, using Ektaprint 3-sol. chemistry. Prints to 30" x 40" are processed one at a time in a Kodak 30 A processor.

When using a balanced inter-negative, a test print should have a neutral gray scale, extending from off-white to black. This then is a technically accurate composite, which is normally the objective of color separation work. However, in printing false-color composites for maximum interpretive value, subjective judgments take priority and the gray scale is typically shifted from neutral toward a yellow, orange or red balance by 10 to 20 units of filtration. By test printing with varied filtration, subtle shifts in color balance can be precisely controlled.

CONCLUSION

Because of the broad control of composite color balance and contrast range, the procedure outlined above has proven effective for detailed analysis and interpretation of ERTS-1 MSS imagery. Enlargements having excellent resolution up to 30" x 30" have been made from the standard NASA data products.

The details of equipment and development processes outlined here are intended only as a guide for initial experimentation. Specific procedures can be easily modified depending upon available laboratory equipment and final imagery requirements. A

variety of image enhancement procedures can be performed at various steps during compositing. Some procedures, such as manipulation of image contrast range, highlight masking, or density slicing can be most easily performed on the individual black/white MSS transparencies prior to color compositing. These enhanced transparencies can be analysed by additive color viewing to guide optimum choice of color balance.

In addition to false color analysis of conventional multispectral imagery, the technique can be applied to a wide range of multiple imaging systems as long as suitable registration can be achieved. Examples are multi-seasonal ERTS-1 imagery, cross-polarized SLAR imagery, and diurnal variation of thermal infrared data.

References

Ross, Donald S., 1973, Simple multispectral photography and additive color viewing: Photogrammetric Engineering, Journal of the American Society of Photogrammetry, Vol. XXXIX, No. 6, pp. 583-591.

Yost, Edward, and Wenderoth, Sondra, 1968, Additive color aerial photography: in Manual of Color Aerial Photography, J. T. Smith, Jr., and D. Anson, Editors, American Society of Photogrammetry, Falls Church, Virginia, pp. 451-471.

FAULT PATTERN AT THE NORTHERN END OF THE DEATH VALLEY-FURNACE CREEK FAULT ZONE, CALIFORNIA AND NEVADA

Argus Exploration Company
555 South Flower Street - Suite 3670
Los Angeles, California 90071

January 1974
Report of Investigation

Prepared for
GODDARD SPACE FLIGHT CENTER
Greenbelt, Maryland 20771

FAULT PATTERN AT THE NORTHERN END OF THE DEATH VALLEY-FURNACE CREEK FAULT ZONE, CALIFORNIA AND NEVADA

An Application of ERTS-1 MSS Imagery

John F. Childs
Argus Exploration Company
Los Angeles, California 90071

ABSTRACT

The pattern of faulting associated with the termination of the Death Valley-Furnace Creek Fault Zone in northern Fish Lake Valley, Nevada was studied in ERTS-1 MSS color composite imagery and color IR U-2 photography. Imagery analysis was supported by field reconnaissance and low altitude aerial photography. The northwest-trending right-lateral Death Valley-Furnace Creek Fault Zone changes northward to a complex pattern of discontinuous dip slip and strike slip faults. This fault pattern terminates to the north against an east-northeast trending zone herein called the Montgomery Fault Zone. No evidence for continuation of the Death Valley-Furnace Creek Fault Zone is recognized north of the Montgomery Fault Zone. Penecontemporaneous displacement in the Death Valley-Furnace Creek Fault Zone, the complex transitional zone and the Montgomery Fault Zone suggests that the systems are genetically related.

Mercury mineralization appears to have been localized along faults recognizable in ERTS imagery within the transitional zone and the Montgomery Fault Zone.

INTRODUCTION

The Death Valley-Furnace Creek Fault Zone of eastern California is one of several major right-lateral strike slip fault systems in the southwestern Basin-Range Province. About thirty miles of post-Jurassic displacement and 0.6 miles of post-Pliocene displacement have been estimated (McKee, 1968) on the Death Valley-Furnace Creek

Fault Zone at the south end of Fish Lake Valley (lower right corner of Figure 1). Although detailed studies of portions of the Death Valley-Furnace Creek Fault Zone have been conducted, little attention has been directed to its apparent termination in the northwestern end of Fish Lake Valley, Nevada. For this reason, literature research and field reconnaissance was conducted for the area of Figure 2 to confirm structural interpretation of the ERTS-1 MSS imagery, and to determine possible structural controls of local volcanism and mercury mineralization.

The area of this report (Figure 2) is underlain by Paleozoic sedimentary and volcanic rocks which have been intruded and metamorphosed by Mesozoic granitic rocks of the White Mountains Batholith. Anderson (1933) made a detailed study of an extensive sequence of Oligocene and Miocene andesites, rhyolite flows and tuffs, and Pliocene to Recent basalts which unconformably overlie the Mesozoic and Paleozoic basement. Many of the ignimbrite units within this volcanic sequence may be derived from distant sources such as Silver Peak or the Mono Basin. Other flow units appear to have local sources and restricted areal distribution. For convenience in discussion, this eruptive sequence will be referred to as the Mustang volcanics after the large canyon located near the center of the volcanic terrane (Figure 2).

METHOD

The northern end of Fish Lake Valley was first investigated using color composites of ERTS-1 MSS frame 1126-18010, 26 November 1972, and black and white ERTS MSS frames 1163-18060, 2 January 1973, and 1307-18064, 26 May 1973. Details of the fault pattern were studied in USAF-USGS high altitude U-2 black and white photography and NASA high altitude U-2 color IR photography:

Flight	Frames	Date
USAF-USGS 374L	169-172	6 September 1968
USAF-USGS 744V	003-005	29 November 1968
NASA-PEIS 72-100		15 June 1972

This data was used to guide detailed field reconnaissance supported by color and color infrared photography taken from a low altitude aircraft. Large faults were plotted in the field directly on an ERTS-1 9" x 9" color composite with detail plotted on 15' and 7-1/2' topographic quadrangles.

TRANSITIONAL FAULT PATTERN AT THE NORTH END OF DEATH VALLEY - FURNACE CREEK FAULT ZONE

A progressive change in the pattern of faulting across the study area is shown in the structural map of Figure 2. In the southern portion of the map area, northwest-trending faults of the Death Valley-Furnace Creek Fault Zone predominate. Strands of this zone can be projected northward for short distances into the Mustang volcanics (Figure 2).

Within the volcanic terrane, the fault pattern becomes more complex and two additional fault trends, namely north, and approximately east-west are recognized. The diverse fault system of this region is interpreted to be transitional to the Montgomery Fault Zone.

Anderson (1933) mapped three large northwest-trending normal faults within the Mustang volcanics. Albers and Stewart (1965) recognized three additional northeast trending faults, and Crowder et al (1972) show a large northeast-trending fault and several north-trending faults. In addition, range-front faults, some of which cut Recent alluvium along the eastern side of the White Mountains, have been cited by Anderson (1933), Bryson (1941) and Albers and Stewart (1965). Many of these faults are apparent in the ERTS-1 imagery. Scarps cutting alluvium are not as evident in the Mustang volcanic area as they are farther south, supporting Anderson's (1933) conclusion that Quaternary movement may decrease in magnitude northward.

Vertical displacement across the transitional fault pattern in the Mustang volcanics is estimated to be on the order of 2000 feet, east side down, based on correlation of similar volcanic units near the crest of the White Mountains and in Sand Spring Canyon. Strike slip movement on a north-south fault in Sand Spring Canyon is suggested by a pervasive set of subhorizontal slickensides. Minor strike slip movement is probable on other ERTS-recognized faults to the east and south. The small magnitude of strike slip displacement apparent in the transitional zone contrasts with the large displacements recognized farther south along the Death Valley-Furnace Creek Fault Zone. An analogous northward decrease in strike slip on the nearby, subparallel Owens Valley fault system is suggested by the negligible strike-slip noted by Gilbert (1968) near its northern end.

Many of the larger northwest and north-south faults in the Mustang volcanics have strong topographic expression and produce conspicuous anomalies in the ERTS-1 imagery (Figure 1). A north-south fault in Sand Spring Canyon demonstrates rough synchroneity of at least some of the faulting and volcanism, because the fault offsets a layered sequence of pumice breccias and is itself draped by overlying rhyolite flows. In general, the east-trending faults appear to crosscut and postdate movement on the faults trending north and northwest.

Fault control of mercury mineralization in the area is mentioned by Lincoln (1923) and by Bailey et al (1941) and was confirmed by the author. The two largest mercury mines in the area, the Wild Rose and the B and B, are located on ERTS anomalies identified in the field as fault zones along which Tertiary pumice breccias have been fractured, silicified, and mineralized. The pumice breccias and their altered equivalents appear as white anomalies in the ERTS-1 imagery.

MONTGOMERY FAULT ZONE

The complex pattern of faulting in the Mustang volcanics appears to be terminated on the north by faults of the east-northeast trending Montgomery Fault Zone. Several

earlier workers in the region have disagreed as to the pattern and position of faults [see for instance Anderson (1933), Gilbert (1941), Ross (1961) and Crowder et al (1972)]. In the present study, three main faults are recognized in the Montgomery Fault Zone. These faults are arranged in a general right stepping en echelon pattern which is evident in ERTS-1 MSS and color infrared U-2 imagery and has been confirmed by field work (Figure 2). The westernmost of the three faults, located northwest of Montgomery, Nevada, is shown in part by Crowder et al (1972), Ross (1961) and Gilbert (1941). Based on offset of lithologic units, this fault has apparent dip slip displacement, north side down, and borders the depression occupied by Truman Meadows north of Queen Valley (Figure 2). The middle fault, suggested by Anderson (1933) and mapped in part by Crowder et al (1972), extends from Mount Montgomery on the west to a diatomite mine southeast of Basalt, Nevada (Figure 2). The sense of vertical displacement on this middle strand appears to change along strike.

The third, and easternmost fault has a component of dip slip, north side down, and forms the northern boundary of an extensive sequence of basalt underlying the Volcanic Hills (Figure 2). This fault and a number of parallel subsidiary faults to the south are shown in Figure 2.

Gilbert (1968) describes faults along the north side of Queen Valley on which slickensides plunge eastward at low angles. Because these faults dip steeply southward and are found on a steep south facing escarpment, Gilbert postulates that they have had left lateral movement. The faults described by Gilbert are part of the east-northeast trending Montgomery Fault Zone described here.

L-shaped faults in alluvium concave to the southeast have been recognized in Fish Lake Valley south of the study area (Albers and Stewart, 1965) and at the southern margin of Queen Valley (Figure 2). The Queen Valley faults and other L-shaped faults near Adobe Valley (Figure 1) are considered to be pull apart structures (Gilbert, 1968, 1973) formed southeast of the intersection of the left lateral northeast-trending Mono-Excelsior Zone and right-lateral north-trending faults in Owens Valley. A similar explanation for the L-shaped faults in alluvium in Fish Lake Valley appears to be consistent with their sense of displacement eastside down, and their position southeast of the intersection formed by the right-lateral Death Valley-Furnace Creek Fault Zone and a left-lateral Montgomery Fault Zone.

The sequence of Quaternary basalt south of the easternmost strand of the Montgomery Fault Zone is petrographically similar to basalt found north of the fault zone near Montgomery Pass. These basalt flows may be equivalents which have been offset left-laterally. As cited by Gilbert (1968), recognition of strike slip displacement in the low dipping volcanic rocks of the area is difficult; however, several indirect lines of evidence suggest strike slip movement on the Montgomery Fault Zone. The general right stepping en echelon arrangement of the three main strands, the straight trench-like character of the faults, the apparent reversal in sense of vertical displacement, and parallelism of the fault zone with the left-lateral Mono-Excelsior Zone 35 miles

to the north are all permissive for strike slip displacement. It is, therefore, likely that left-lateral strike slip movement has taken place along the Montgomery Fault Zone, although the total displacement is probably small.

Two lines of evidence suggest approximately synchronous movement in the transitional zone and the Montgomery Fault Zone. First, the western and middle faults forming the Montgomery Fault Zone bend or splay into northerly trending normal faults. The western fault bends northward at its eastward termination and the middle fault splays southward into a normal fault of the transition zone near Basalt, Nevada (Figure 2). Also, both of the fault systems cut Quaternary olivine basalts in the study area.

The complex pattern of faulting in the Mustang volcanics at the northern end of the Death Valley-Furnace Creek Fault Zone does not appear to extend north of the Montgomery Fault Zone within the study area. Several north trending faults within the complex transitional zone terminate against strands of the Montgomery Fault Zone south of Basalt, Nevada [Figure 2; Albers and Stewart, 1965; Crowder et al, 1972]. This termination does not imply that the Montgomery Fault Zone is the younger of the two. Rather, the close temporal relationship and the tendency for one system to bend into the other suggests that they are cogenetic.

CONCLUSIONS

ERTS-1 MSS imagery has proven to be a valuable tool in studying the anomalous structural pattern associated with the northern termination of the Death Valley-Furnace Creek Fault Zone. Field reconnaissance conducted to support interpretation of the ERTS-1 MSS and subsidiary imagery has confirmed a complex transitional pattern of faulting between the Death Valley-Furnace Creek Fault Zone and the Montgomery Fault Zone of probable left-lateral displacement. Movement in the transitional zone and the interconnected Montgomery Fault Zone appears to have been roughly synchronous, suggesting a cogenetic origin. Although faulting and volcanism are spatially and temporally associated, clear structural control of local volcanism has not yet been demonstrated.

Several faults within the transitional zone and the Montgomery Fault Zone which have expression in the ERTS-1 imagery appear to have localized mercury mineralization.

References

Albers, J. P. and Stewart, J. H., 1965, Preliminary Geologic Map of Esmeralda Co., Nevada, 1:200,000: U.S. Geol. Survey Mineral Inv. Field Studies Map MF-298.

Anderson, G. H., 1933, Geology of the North Half of the White Mountain Quadrangle, California-Nevada, Ph.D., California Institute of Technology.

Bailey, E. H. and Phoenix, D. A., 1944, Quicksilver Deposits in Nevada: Nevada University Bull., V. 38, No. 5, Geology and Mining Ser. No. 41.

Bryson, R. P., 1937, Faulted Fanglomerates at the Mouth of Perry Aiken Creek, Northern Inyo Range, California/Nevada, 1:20,000, M. S., California Institute of Technology.

Crowder, D. F., Robinson, P. F., and Harris, D. L., 1972, Geologic Map of the Benton Quadrangle, Mono County, California and Esmeralda and Mineral Counties, Nevada: U.S. Geol. Survey Map, GQ-1013.

Gilbert, C. M., 1941, Late Tertiary Geology Southeast of Mono Lake California: Geol. Soc. America Bull., V. 52, p. 781-815.

Gilbert, C. M., Christensen, M. N., Al-Rawi, Y. T., and Lajoie, K. R., 1968, Structural and Volcanic History of Mono Basin, California-Nevada: Geol. Soc. America Mem. 116, p. 275-329.

Gilbert, C. M. and Reynolds, M. W., 1973, Character and Chronology of Basin Development, Western Margin of the Basin and Range Province: Geol.Soc. America Bull., V. 84, No. 8, p. 2489-2510.

Lincoln, F. C., 1923, Mining Districts and Mineral Resources of Nevada: Reno, Nevada Newsletter Publishing Co., p. 137-157.

McKee, E. H., 1968, Age and Rate of Movement of the Northern Part of the Death Valley-Furnace Creek Fault Zone, California: Geol. Soc. America Bull., V. 79, p. 509-512.

Ross, D. C., 1961, Geology and Mineral Deposits of Mineral Co., Nevada: Nevada Bureau of Mines, Bull. 58, 98 pp.

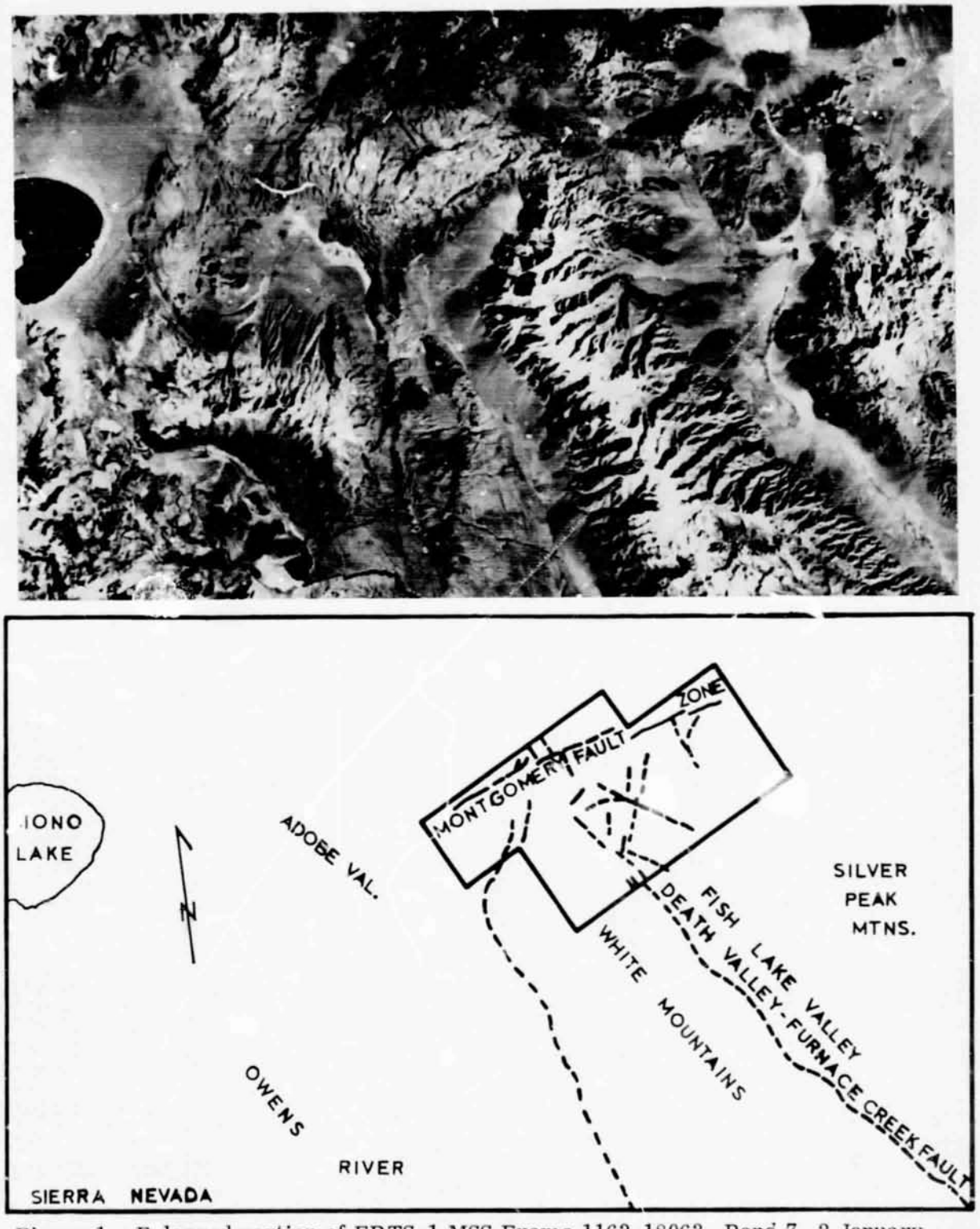

Figure 1 - Enlarged portion of ERTS-1 MSS Frame 1163-18063, Band 7, 2 January 1973, and corresponding index map. The study area shown in Figure 2 is outlined and some of the important structural and geographic features are indicated.

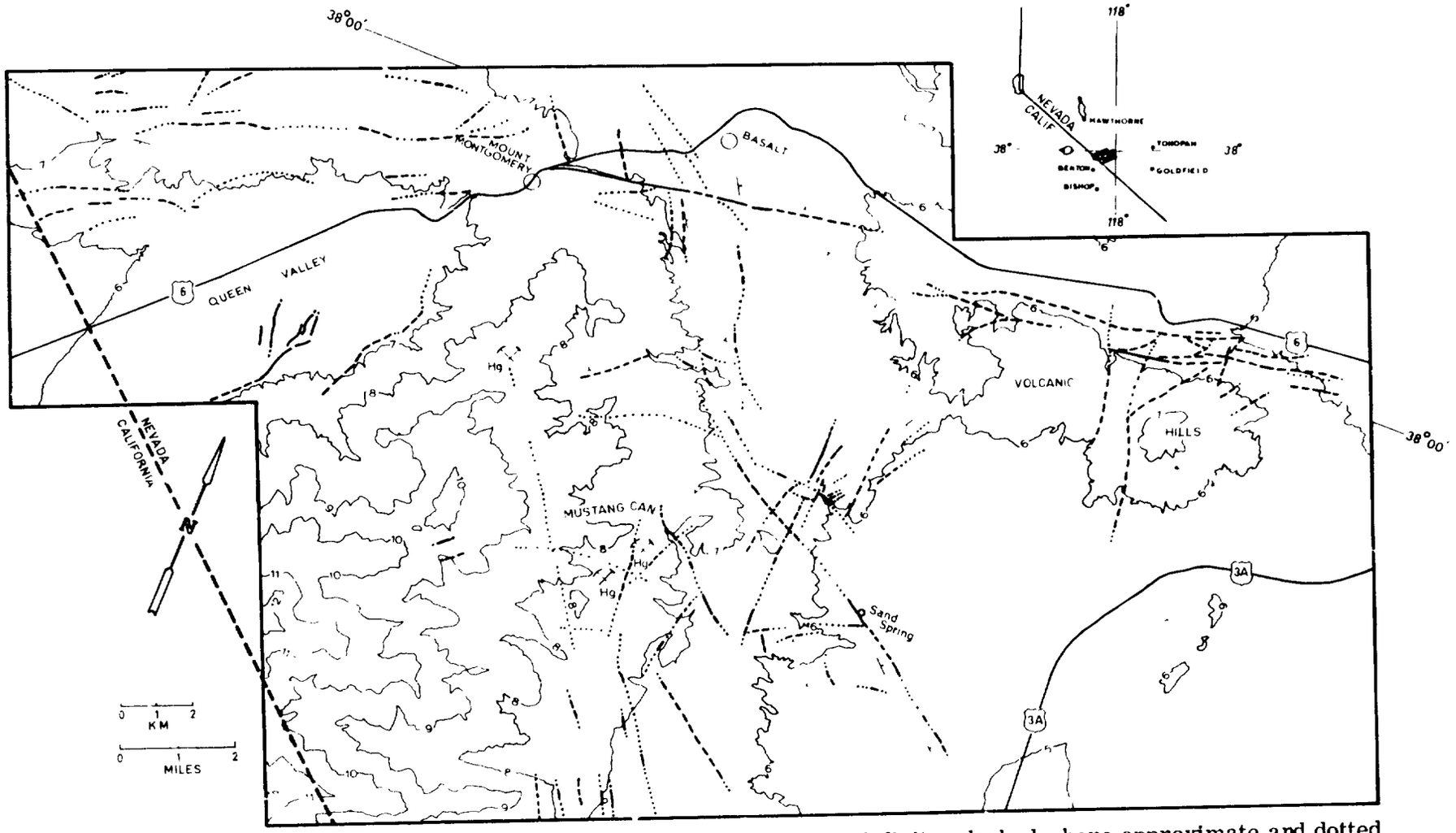

Figure 2 - Structural map of the study area. Faults solid where definite, dashed where approximate and dotted where inferred. Contour interval in thousands of feet. Base maps used are the Benton and Davis Mountain 15' and the Jacks Spring, Basalt, Miller Mountain, and Columbus 7-1/2' topographic quadrangles. Index map is in upper right hand corner.

PAHRANAGAT SHEAR SYSTEM
LINCOLN COUNTY, NEVADA

Argus Exploration Company
555 South Flower Street - Suite 3670
Los Angeles, California 90071

January 1974
Report of Investigation

Prepared for
GODDARD SPACE FLIGHT CENTER
Greenbelt, Maryland 20771

Appendix L

PAHRANAGAT SHEAR SYSTEM, LINCOLN COUNTY, NEVADA

Mark A. Liggett and Helmut E. Ehrenspeck
Argus Exploration Company
Los Angeles, California

ABSTRACT

A structural model which relates strike-slip deformation to Basin Range extensional tectonics was formulated on the basis of analysis and interpretation of ERTS-1 MSS imagery over southern Lincoln County, Nevada. Study of published geologic data and field reconnaissance of key areas has been conducted to support the ERTS-1 data interpretation. The structural model suggests that a left-lateral strike-slip fault zone, called the Pahranagat Shear System, formed as a transform fault separating two areas of east-west structural extension.

Introduction:

This investigation was conducted in order to evaluate an anomalous structural pattern observed in ERTS-1 MSS imagery over a portion of the southern Basin Range Province of Lincoln County, Nevada.

A portion of ERTS-1 MSS frame 1106-17492 over the area of study is shown in Figure 1, and a corresponding structural map in Figure 2. The anomalous northeast strike of the Pahranagat Shear System and its apparently abrupt termination within the north trending valleys focused attention on the genetic origin and tectonic significance of the local fault pattern.

Based on analysis of the ERTS-1 data, a structural model was formulated which suggests that left-lateral strike-slip displacement on the Pahranagat Shear System has resulted from differential east-west extension on Basin Range normal faults. A schematic diagram of this structural model is illustrated in Figure 4. Detailed study of the available published geologic data, and field reconnaissance of key areas was conducted in order to evaluate this hypothesis.

This study was supported by the National Aeronautics and Space Administration and Cyprus Mines Corporation as part of an investigation on applications of ERTS-1 MSS imagery to study of Basin Range tectonics and related resource exploration.

Pahranagat Shear System:

The Pahranagat Shear System was first mapped by Tschanz and Pampeyan (1961) in a regional geologic survey of Lincoln County. The geologic map and its interpretation was considered in greater detail in their County Report (Tschanz and Pampeyan, 1970). This report described three northeast-striking faults which are collectively termed the Pahranagat Shear System. Tschanz and Pampeyan (1970, p. 84, 109) believed the system to have undergone approximately 9 to 16 km of left-lateral strike-slip displacement based on the offset of a distinctive ignimbrite unit. This ignimbrite has been correlated with the Hiko Tuff of middle Miocene age (Noble and McKee, 1972).

Based on possible correlations of lithology and structural features in the Spotted and Pahranagat Ranges, Tschanz and Pampeyan (1970) postulated the existence of an antecedent, right-lateral shear zone of Laramide age along the same trend as the Pahranagat Shear System. However, evidence for this earlier fault system is ambiguous and inconclusive. Although Tschanz and Pampeyan (1970) discussed possible genetic origins for the hypothetical Laramide fault zone, none was considered for the post-Miocene Pahranagat Shear System.

In a discussion of the regional importance of strike-slip faulting in the Basin Range Province, Shawe (1965) cited the Pahranagat area as an example. Shawe interpreted the geologic map of Tschanz and Pampeyan (1961) in support of a temporal and spatial association of late Tertiary and Recent normal and strike-slip faulting. On a regional scale, Shawe concluded that Basin Range structure may have formed en echelon with, and in response to a deep-seated, conjugate system of strike-slip deformation. However, such a causal relationship between strike-slip and normal faulting was not documented in the Pahranagat area.

Tectonic Model:

The structural model for the Pahranagat Shear System proposed here is based largely on the detailed mapping of Tschanz and Pampeyan (1970). However, in key areas this mapping has been amended and supplemented by field reconnaissance guided by analysis of enhanced ERTS-1 MSS data.

A simplified structural diagram is shown in Figure 4 which illustrates a left-lateral strike-slip fault zone formed by differential crustal extension within two structural grabens. This model is believed to be mechanically similar to the tectonics of the Pahranagat Shear System. In contrast to the regional interpretation of Shawe (1965), we propose that the Pahranagat Shear System developed as a response to differential east-west crustal extension. Most of this extension is represented by the complex normal faulting which forms the structural basin of Delamar Valley northeast of the shear system, and a corresponding area of normal faulting adjacent to Desert Valley southwest of the shear system (see Figure 2).

Like the mechanical analogue in plate tectonics, the Pahranagat Shear System may have formed as a transform fault, joining two areas of simultaneous crustal spreading (Wilson, 1965; Dennis, 1967). Similar concepts of intracontinental transform faulting have recently been applied to other areas of the Basin Range Province in explanation of displacement on the Garlock Fault (Davis and Burchfiel, 1973) and the Las Vegas Shear Zone (Fleck, 1970; Bechtold and others, 1973).

Supporting Evidence:

Geologic field evidence and published data corroborate the geometric and temporal requirements of this genetic model. Guided by ERTS-1 imagery, field work along both sides of Delamar Valley has located several large and previously unrecognized north-striking normal faults, which form parts of a complex structural basin in that area. As shown in Figures 1 and 2, north-striking faults on both sides of the Pahranagat Shear System appear to terminate at the zone without being displaced along it. Likewise, strands of the shear system typically end by turning abruptly in strike to merge with north-striking range-front faults. This geometric relationship between dip-slip and strike-slip faulting requires synchronous movement and suggests that displacement on both sets has occurred in response to a common cause.

In the field, strike-slip movement is indicated by abundant subhorizontal slickensides found along east and northeast-striking strands of the Pahranagat Shear System in the vicinity of Maynard Lake in the South Pahroc Range. The estimate by Tschanz and Pampeyan (1970, p. 84, 109) of 9 to 16 km of left-lateral displacement on the Pahranagat Shear System was based on the apparent separation across the fault system of an eastward dipping unit of volcanic ignimbrites. This apparent separation could be caused in part by vertical displacement. For this reason, our estimates of strike-slip movement are based on the displacement of a generally north-south linear trend defined by the angular unconformity between west-dipping sedimentary units of Devonian through Ordovician age, and the overlying east-dipping Miocene volcanic cover (Tschanz and Pampeyan, 1970, geologic map, T9S-R62E, T9S-R61E, T8S-R61F). Although the Paleozoic basement is highly deformed and the regional continuity of structural trends is uncertain, this data suggests post-volcanic strike-slip displacement of approximately 9 to 14 km.

Within the scale limitations of the mapped geology, interpretive structural sections were constructed across the structural basins northeast and southwest of the Pahranagat Shear System. These are shown in Figure 3. For simplicity, these structure sections were constructed assuming an average dip of 45 degrees on the range front faults. As discussed below, this generalization of fault plane dip is based on publisned data as well as field observations.

Gilluly (1928) estimated 40^{o}-80^{o} dips for typical Basin Range normal faults. Stewart (1971, p. 1035) and other recent workers (Hamilton and Myers, 1966; Thompson, 1966) have used a value of approximately 60^{o} as an average for the Basin Range Province.

However, the dips of normal faults in the Pahranagat area appear to be unusually shallow. Along one well-exposed scarp north of Delamar Lake, the dip of the fault is estimated to be less than 45°. Geologic mapping (Longwell, 1945) in the Desert Range south of the Pahranagat Shear System, indicated 15-20° dips on most normal faults. In addition, Longwell's mapping indicated that these faults are concave upward, and hence flatten at depth. Thus, the assumption of an average 45° dip on the range front faults in the Pahranagat area is reasonable, and perhaps conservative.

Analysis of the interpretive structural sections shown in Figure 3 suggests net crustal extension on both normal fault systems of approximately 8-11 km. This figure represents crustal extension of less than 25% in these areas, which is moderate compared with many regional estimates for the Basin Range Province (Davis and Burchfiel, 1973, p. 1416). The amount of extension within the structural basins northeast and southwest of the Pahranagat Shear System is large enough to account for most of the postulated 9-14 km of post-Miocene strike-slip displacement on the shear system.

Conclusion:

Analysis of the ERTS-1 imagery, and field reconnaissance in key areas in the Pahranagat region indicate that eastern portions of the shear system terminate against the north-striking normal faults of the Delamar Range front. Major eastward continuations of the Pahranagat Shear System as suggested by Shawe (1965) and Tschanz and Pampeyan (1970) are unlikely. For this reason, at least in the Pahranagat area, a regional strike-slip stress system does not seem to be a probable driving force for generation of Basin Range structure. Rather, the strike-slip deformation seems to be a normal consequence of differential rates or amounts of regional crustal extension.

Several recently active faults are evident in the Pahranagat area. These include a frontal fault along the east side of Delamar Valley which cuts alluvium for more than 15 km. (Tschanz and Pampeyan, 1970) and similar faults along both sides of the Sheep Range (Longwell, 1930; Tschanz and Pampeyan, 1970, p. 85). The strong topographic expression of both normal and strike-slip faults in the Pahranagat area suggests that both Basin Range extension and the Pahranagat Shear System may be presently active.

The ERTS-1 MSS imagery has proven to be a valuable tool for efficiently studying regional patterns of Tertiary faulting, and for guiding geologic field reconnaissance to evaluate and confirm interpretations.

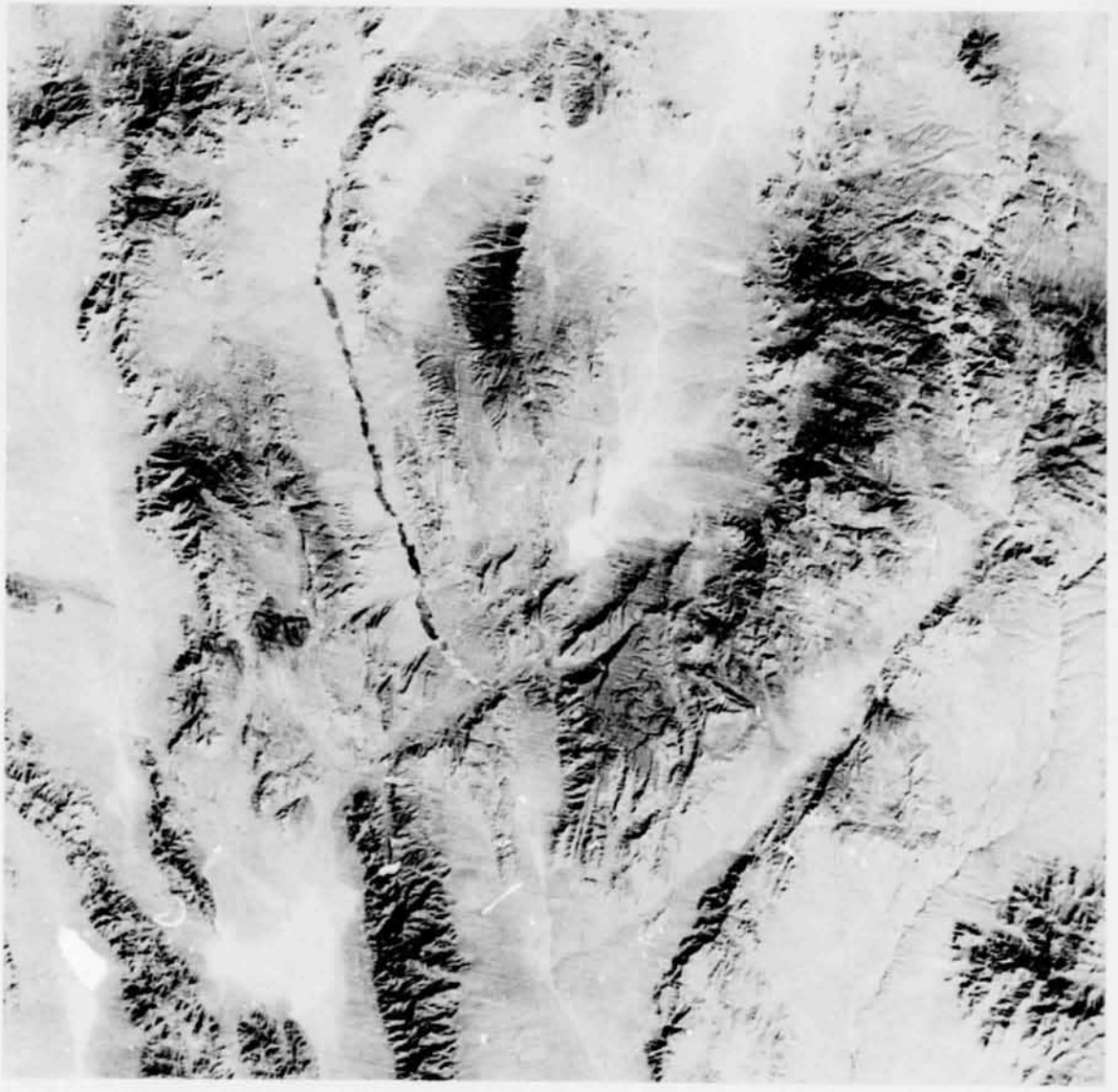

Figure 1: Enlarged portion of ERTS-1 MSS frame 1106-17492 Band 5, over the Pahranagat Shear System of Lincoln County, Nevada. A corresponding structural map is shown at the same scale in Figure 2.

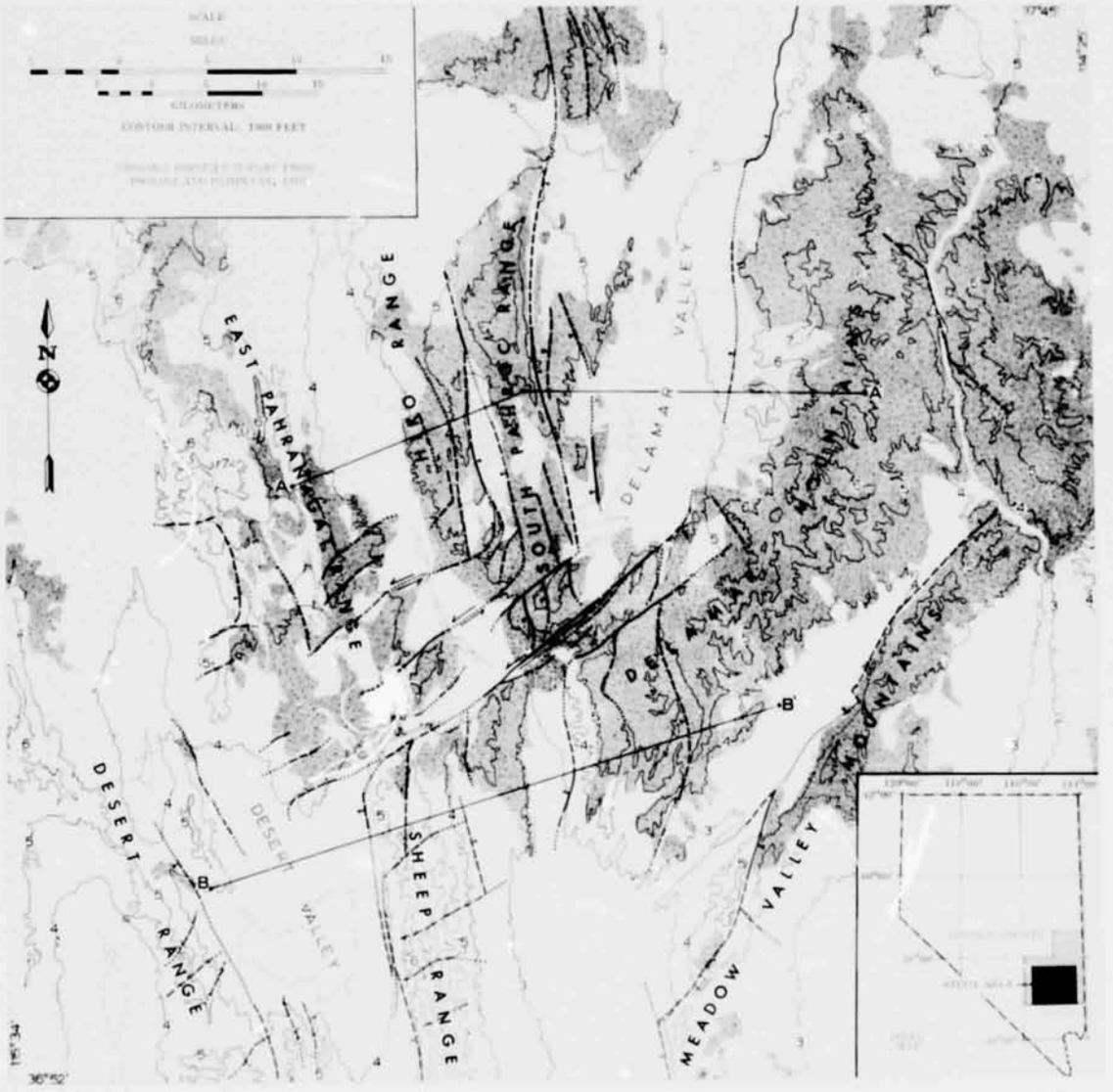

Figure 2: Structural map of the Pahranagat Shear System and surrounding terrain illustrated in Figure 1. Shaded areas represent Tertiary volcanic rocks. Faults are solid where well exposed, and dashed or dotted where approximately located or inferred. Interpretive structural sections along A-A' and B-B' are shown in Figure 3.

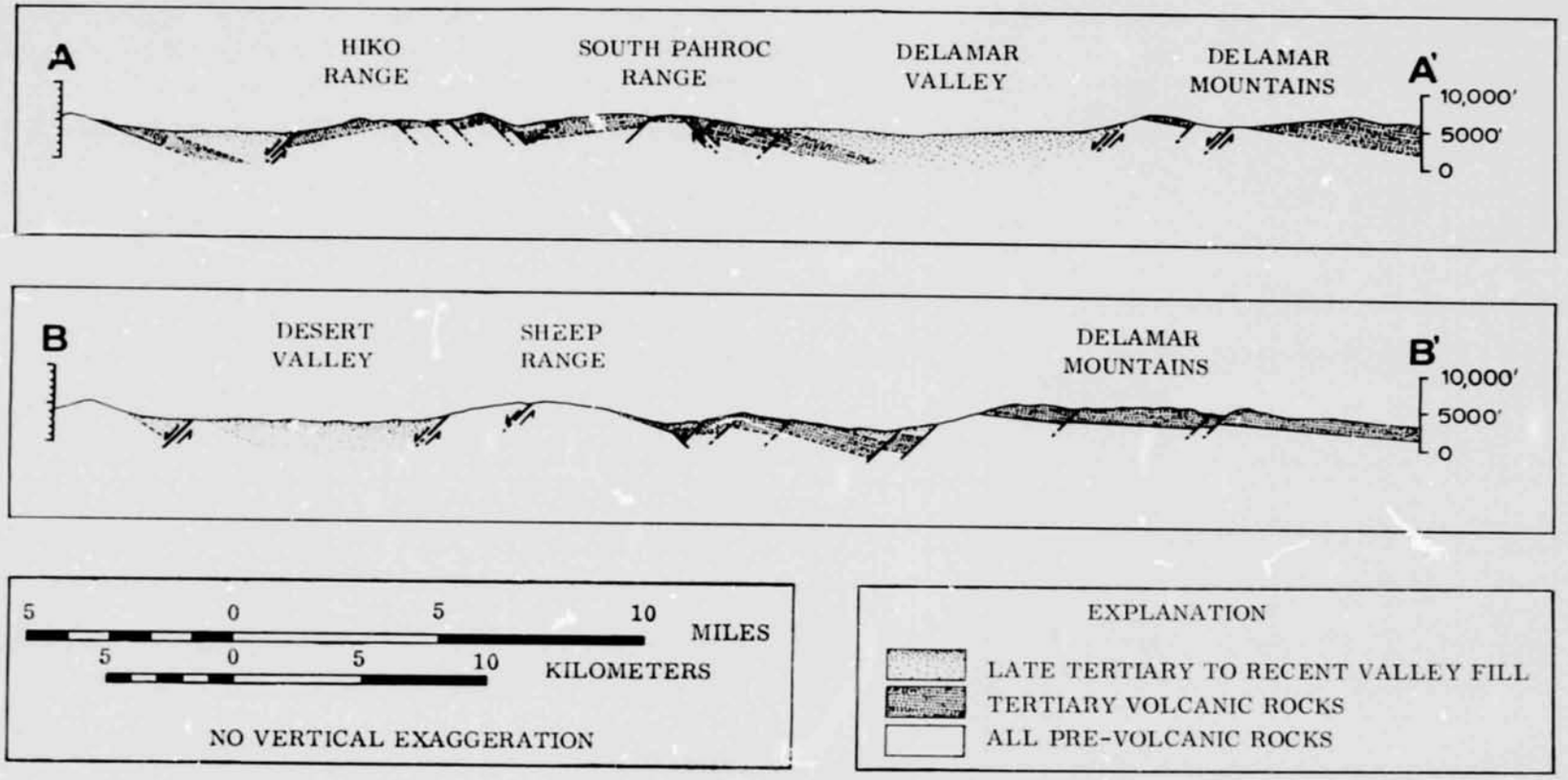

Figure 3: **Interpretive structural sections A-A' and B-B' at locations shown in Figure 2. The complex normal faulting in the areas traversed by these sections is believed to have resulted in crustal extension of from 8 to 11 km. See text for discussion.**

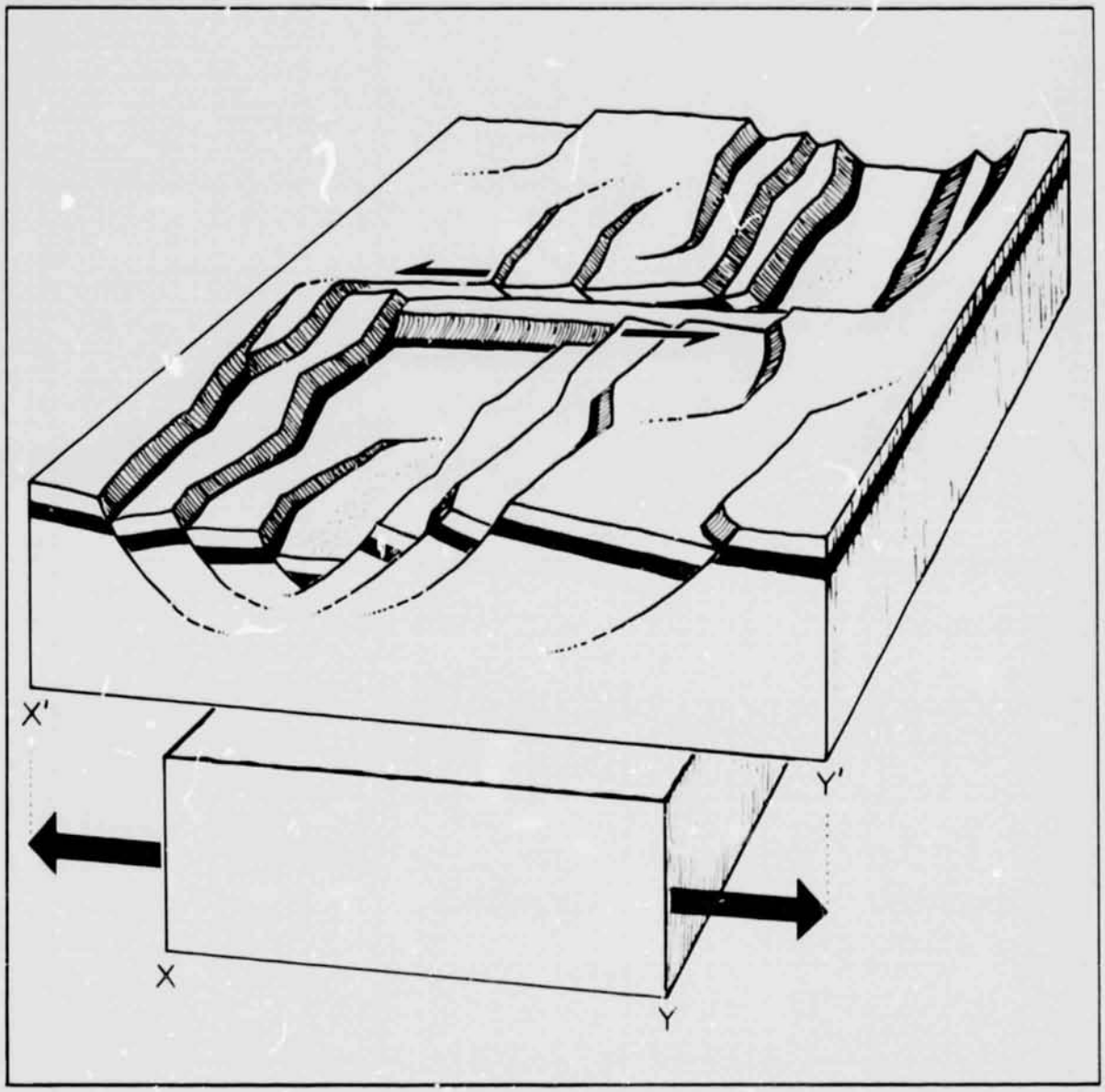

Figure 4: Diagrammatic model illustrating a left-lateral strike-slip fault zone formed by differential crustal extension within the two graben basins. The amount of extension is indicated by the increase in width of block X-Y to X'-Y'. This model is believed to be mechanically similar to the tectonics of the Pahranagat Shear System.

References:

Bechtold, I.C., Liggett, M.A., and Childs, J.F., 1973, Regional tectonic control of Tertiary mineralization and Recent faulting in the southern Basin Range Province: in Symposium on Significant Results Obtained from ERTS-1: NASA S.P. 327, V. 1, Section A, p. 425-432.

Davis, G.A., and Burchfiel, B.C., 1973, Garlock Fault: An intracontinental transform structure, southern California: Geol. Soc. Amer. Bull. V. 84, p. 1407-1422.

Dennis, J.G., 1967, International Tectonic Dictionary, English terminology: Amer. Assoc. Petroleum Geologists, Memoir 7, 196 p.

Fleck, R.J., 1970, Age and possible origin of the Las Vegas Valley Shear Zone, Clark and Nye Counties, Nevada (ABS): Geol. Soc. Amer., Abstracts with Programs, V. 2, No. 5, p. 333.

Gilluly, James, 1928, Basin Range faulting along the Oquirrh Range, Utah: Geol. Soc. Amer. Bull. V. 39, p. 1103-1130.

Hamilton, Warren, and Myers, W.B., 1966, Cenozoic tectonics of the western U.S.: Reviews of Geophysics, V. 4, p. 509-549.

Longwell, C.R., 1930, Faulted fans west of the Sheep Range, southern Nevada: Amer. Jour. Sci., 5th series, V. 20, p. 1-13.

_____, 1945, Low-angle normal faults in the Basin Range Province: Transactions, Amer. Geophys. Union V. 26, p. 107-118.

Noble, D.C., and McKee, E.H., 1972, Description and K-Ar ages of volcanic units of the Caliente volcanic field, Lincoln County, Nevada, and Washington County, Utah: Isochron/West No. 5, p. 17-24.

Shawe, D.R., 1965, Strike-slip control of Basin Range structure indicated by historical faults in western Nevada: Geol. Soc. Amer. Bull., V. 76, p. 1361-1378.

Stewart, J.H., 1971, Basin and range structure: A system of horsts and grabens produced by deep-seated extension: Geol. Soc. Amer. Bull. V. 82, p. 1019-1044.

Thompson, G.A., 1966, The rift system of the western U.S., in The World Rift System, International Upper Mantle Commission Symposium, Ottawa 1965: Can. Geol. Survey Paper 66-14, p. 280-290.

Tschanz, C.M., and Pampeyan, E.H., 1961, Preliminary geologic map of Lincoln County, Nevada: U.S. Geological Survey Mineral Investigation Field Studies Map MF-206.

_____ _, 1970, Geology and mineral deposits of Lincoln County, Nevada: Nevada Bureau of Mines Bull. 73, 187 p.

Wilson, Tuzo, 1965, A new class of faults and their bearing on continental drift: Nature, V. 207, p. 343-347.

STRUCTURAL LINEAMENTS IN THE SOUTHERN SIERRA NEVADA, CALIFORNIA

Argus Exploration Company
555 South Flower Street - Suite 3670
Los Angeles, California 90071

February 1974
Report of Investigation

Prepared for
GODDARD SPACE FLIGHT CENTER
Greenbelt, Maryland 20771

STRUCTURAL LINEAMENTS IN THE SOUTHERN SIERRA NEVADA, CALIFORNIA

Mark A. Liggett and John F. Childs
Argus Exploration Company
Los Angeles, California

ABSTRACT

Several lineaments observed in ERTS-1 MSS imagery over the southern Sierra Nevada of California have been studied in the field in an attempt to explain their geologic origins and significance. The lineaments are expressed topographically as alignments of linear valleys, elongate ridges, breaks in slope or combinations of these. The lineaments are typically less than 1 km wide, and several can be traced in the ERTS-1 imagery for over 30 km. Natural outcrop exposures along them are characteristically poor.

Two lineaments were found to align with foliated metamorphic roof pendants and screens within granitic country rocks. Along other lineaments, the most consistent correlations were found to be alignments of diabase dikes of Cretaceous age, and younger cataclastic shear zones and minor faults. Deep roadcut exposures in several key areas suggest that dikes and shear zones have controlled in-place weathering and erosion along the lineament trends. No evidence was found for hydrothermal alteration or Recent faulting.

The location of several Pliocene and Pleistocene volcanic centers at or near lineament intersections suggests that the lineaments may represent zones of crustal weakness which have provided conduits for rising magma.

Introduction:

ERTS-1 MSS imagery over the southern Sierra Nevada Range of eastern California has revealed a pattern of straight, narrow lineaments, some of which can be traced in the imagery for over 30 kilometers. Most of these features have not been mapped previously. Geologic reconnaissance along several of the lineaments was conducted by the authors in order to identify their geologic origins and significance.

The area of study is located on the Boreal Plateau (Webb, 1946) in parts of Tulare and Inyo Counties (Index Map, figure 2). Topographic relief on this portion of the plateau is moderate, with elevations ranging from 2,000 to 3,000 meters. Vegetation cover is moderate to extensive. Meadows and meandering stream valleys support lush growth

of grass, and the higher elevations are covered by chaparell and stands of pine, fir, and aspen trees.

The dominant rock types in the study area are plutonic, ranging in composition from quartz diorite to granite. In some areas, dike swarms are abundant. These dikes are predominately fine-grained diabase and porphyritic gabbro, although rhyolites, aplites and pegmatites are found locally (Miller and Webb, 1940).

Large, irregular roof pendants of foliated metamorphic rock are mapped in many parts of the study area (Miller and Webb, 1940; Matthews and Burnett, 1966; Smith, 1965). Small pendants and screens of similar metamorphic rock are also widespread, although most of these do not appear at the scale of existing geologic maps.

ERTS-1 MSS Imagery:

Figure 1 shows an enlarged portion of ERTS-1 MSS frame #1162-18011, Band 5. A corresponding topographic map showing the positions of lineaments interpreted from the imagery is illustrated in Figure 2.

ERTS-1 scenes recorded over a 12-month period were studied in this investigation. Seasonal variation of sun angle and snow cover were found to change the expression of some lineaments; however, each of the lineaments shown in Figures 1 and 2 were visible throughout the seasonal span. Seasonal variation of vegetation was not observed to affect expression of the lineaments.

ERTS-1 MSS frames having low to moderate cloud coverage are as follows:

15 September 1972	Frame #1054-18003
21 October 1972	1090-18010
14 December 1972	1144-18012
1 January 1973	1162-18011
12 June 1973	1324-18011
30 June 1973	1324-18010

The ERTS-1 MSS imagery was studied with a Spectral Data Corporation model 61 additive color viewer to determine optimum band/filter combinations and color balance for enhancement of geologic detail. High resolution color composites (MacGalliard and Liggett, 1973) were produced at the scale of 1:500,000 for detailed analysis and interpretation. The positions of key structural anomalies observed in this imagery were transferred to 1:250,000 and 1:62,500 scale topographic quadrangles to facilitate field reconnaissance.

Lineaments:

The lineaments are expressed topographically as alignments of linear valleys, elongate ridges, breaks in slope or combinations of these. Several lineaments can be traced in

the ERTS-1 imagery for over 30 km, and are typically less than 1 km wide.

The dominant trend of the lineaments in the area is slightly east of north. This system is crossed by less numerous lineaments which strike toward the northeast as shown in Figures 1 and 2. The Kern Canyon Fault Zone (Webb, 1955) is the only major structural feature mapped in the area of study. Only small portions of three other lineaments have been previously mapped as faults (see Smith, 1965; Matthews and Burnett, 1966).

In a structural reconnaissance of the southern Sierra Nevada, Mayo (1947) recognized several pervasive structural patterns which he attributed to such phenomena as igneous "flow structure" and post batholithic "joint swarms" and "fissures". The orientation of these features closely parallel the three directional trends apparent in Figures 1 and 2.

During field reconnaissance, two lineaments were found to align with the foliation or compositional layering of metamorphic rocks. Lineament Y-Y shown in Figure 2 is located within a large roof pendant in which the foliation and layering parallels the west-northwest strike of the lineament. Similar exposures along lineament X-X reveal a thin, elongate screen of metamorphic rock in which the foliation and compositional layering align with the lineament. No faulting was recognized along the traces of these lineaments, and their topographic expression as elongate ridges and valleys appears to have been controlled by preferential weathering and erosion of the foliated rock.

The north-south striking lineaments are found to have characteristically vague expression in natural outcrop exposures. Within the areas studied, these lineaments cross varied plutonic country rocks and are confined to valleys or breaks in slope. Sparse outcroppings are found even where lineaments cross topographic saddles.

For these reasons, close study was made of available exposures. Where feasible, measurements were made of such features as igneous foliation, cataclastic foliation, metamorphic foliation or compositional layering, dikes, shear zones, slickensides, epidotized joints, and the dominant trends of these features inferred within each outcrop area in the field.

Dikes:

The dikes indicated in Figure 3 are hornblende diabase, similar in composition and texture throughout the study area. The dikes generally range in width from 0.5 to 5.0 m and are nearly vertical in dip. In areas of good exposure along lineaments, the dikes are spaced at intervals of less than 2 m. Dikes within a swarm typically strike within 10^{0} of each other, although frequently two trends intersecting at a high angle are found within a local area. This bimodal pattern is apparent in the orientation diagrams of Figure 3.

The mafic dikes cut both plutonic and metamorphic country rocks, and are themselves cut only rarely by rhyolite dikes. A K-Ar age date from a north 20° east-striking dike at Station C in Figure 3 (specimen 73L31) yielded an apparent mid-Cretaceous age of 105 ± 5 m.y.

Structures:

Structural features included in the trend diagrams of Figure 3 include cataclastic foliation, slickensided joints and faults. These structures cut across the diabase dikes and are, therefore, younger. Epidotized joints or fractures lacking evidence of movement were not included in the diagrams.

Shears cutting the plutonic country rocks typically appear as planes or zones 1 to 2 cm wide in which the granitic texture of the host is cataclastically foliated. Where well exposed, these planes are found to be subparallel in strike, nearly vertical in dip, and spaced at intervals of a few centimeters to about 1 m.

Within the shear zones, movement is indicated by slickensides, many with sub-horizontal plunges. Slickensides are best preserved on joints or shears which have been epidotized. As shown in the trend diagrams of Figure 3, the strike of shears, joints and fault planes, like the diabase dikes is frequently bimodal.

Discussion:

The continuity of dike swarms and cataclastic shearing along the entire lengths of the lineaments is not documented because of the characteristically poor exposures. However, in several key areas where roadcuts have exposed the deeply weathered granitic rocks along lineaments, slickensided joints and diabase dikes are apparent in far greater abundance than in the adjacent natural outcrop exposures. Examples of this are visible in roadcuts at Station F shown in Figure 3. This selective exposure is believed to be the result of lithologic and structural control of in-place weathering and erosion.

The glassy groundmass, mafic mineralogy and closely spaced jointing of the diabase dikes make them prone to rapid chemical and mechanical weathering. As a result, the positions of former dikes are frequently expressed in outcrops as linear debris-filled depressions. Similar expression is observed in the selective weathering of granitic rocks along shear zones or closely spaced joints, where large surface areas are exposed to chemical and mechanical weathering processes (Thornbury, 1954). These processes favor preservation of natural outcrop exposures which have the fewest shear zones, faults or dikes.

At the reconnaissance scale of this study, no direct evidence was found supporting major displacement of lithologic units across the lineaments. Although some faulting and shearing may be Recent in age, the topographic expression of the lineaments is due to selective weathering and erosion, and not primary topographic displacement.

Mayo (1947) suggested possible structural control of several late Tertiary and Quaternary volcanic centers in the area of this report. These volcanic centers appear to be located at or near the intersection of the lineament systems shown in Figure 2. However, little field evidence was found to confirm structural control. Radiometric ages from a basalt field along the Kern River south of Angora Mountain indicate a late Pliocene age (Matthews and Burnett, 1966). Olivine basalt cinder cones and flows along Golden Trout Creek east of the Kern River are believed to be of Quaternary or Recent age (Webb, 1950).

Monache and Templeton Mountains are large volcanic domes composed of aphanitic latite (Webb, 1950) and considered to be of probable late Tertiary or Quaternary age. Possible structural control of the Monache Mountain dome is suggested by the existence of numerous felsic dikes intruded along fractures adjacent to older diabase dikes in exposures surrounding Monache Meadows.

Conclusions:

At regional scale, the lineament systems discussed in this report, appear to control much of the topography in the southern Sierra Nevada. The origin of these features is uncertain. Their apparent correlations with faulting, jointing, dike swarms and volcanic centers suggest that they may represent steeply-dipping zones of crustal weakness within the Sierra Nevada Batholith. These zones appear to have existed at the time of intrusion of the mid Cretaceous diabase dikes, and may have been reactivated during Tertiary and Quaternary orogenic and volcanic events.

It is hoped that future, detailed studies will help determine the age, precise origins and geological implications of these features.

Although the lineaments are perhaps the largest post-batholithic structural features in the southern Sierra Nevada, they have not been generally recognized on the basis of previous geologic mapping. The ERTS-1 MSS data has proved to be an effective tool for recognition of these large-scale structural anomalies, and for guiding reconnaissance in the field.

Figure 1: Enlarged portion of ERTS-1 MSS frame #1162-18011 Band 5 over the southern Sierra Nevada, California. A corresponding topographic map is shown in Figure 2.

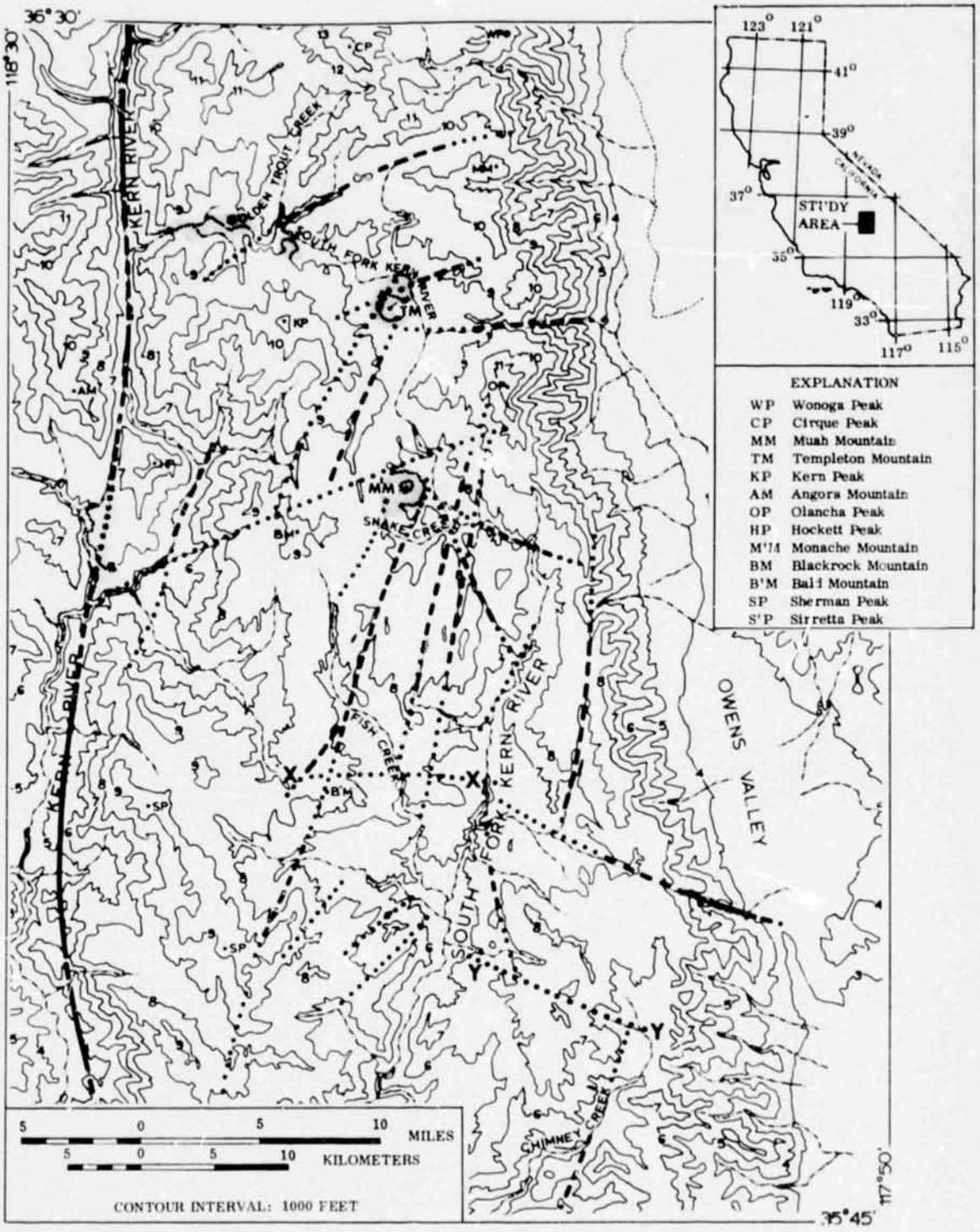

Figure 2: Interpretation of major lineament systems visible in the ERTS-1 image of Figure 1. Location names follow the code shown at right. Topography is from the AMS Fresno and Bakersfield 1^{o} x 2^{o} quadrangles. See text for more detailed discussion.

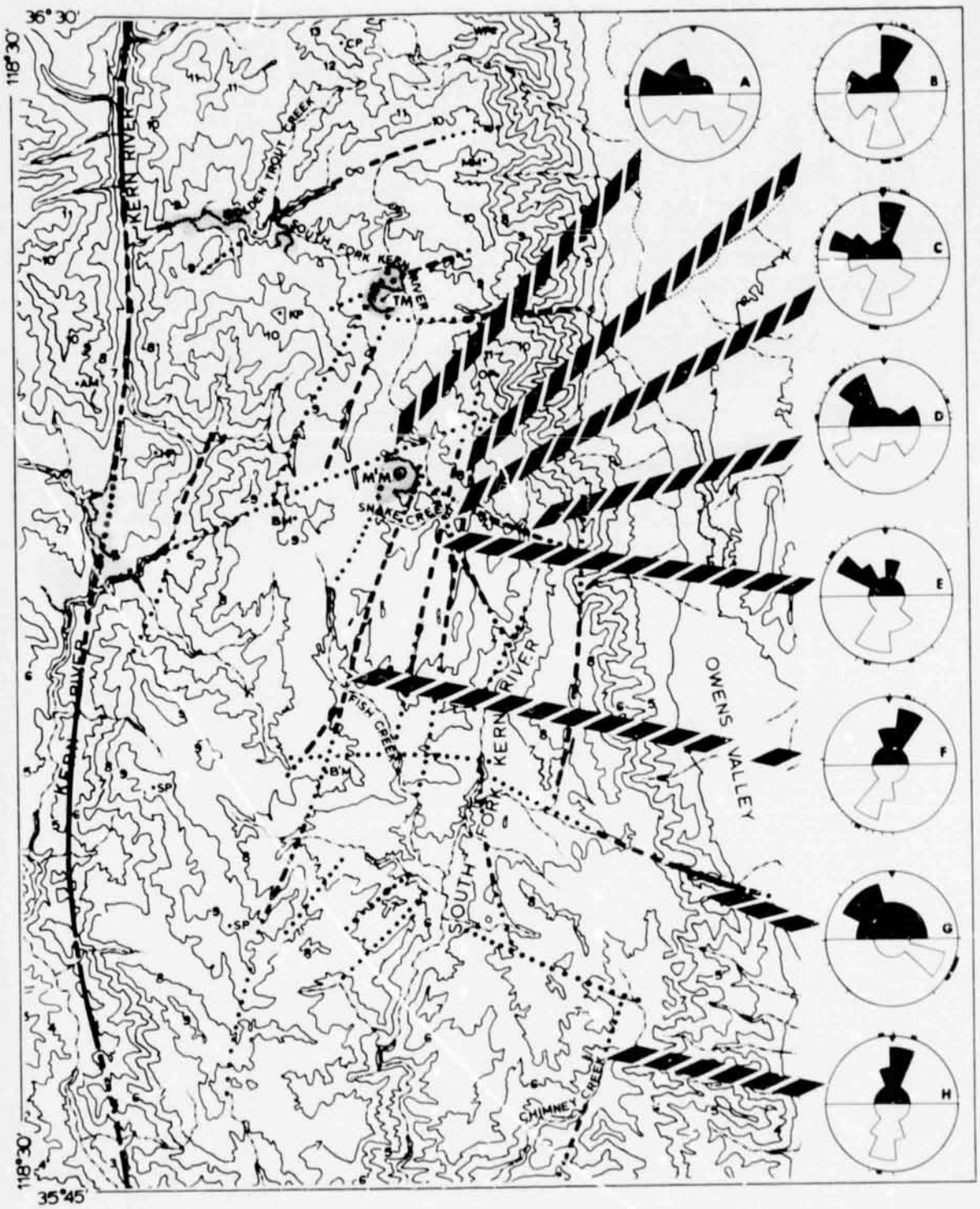

Figure 3: Orientation diagrams for steeply dipping diabase dikes (upper half circle) and faults, slickensided joints and cataclastic foliation (lower half circle). Tick marks on the circumference indicate measured strikes. The generalized rose diagrams illustrate inferred patterns; the outer radius contains over 50% of local strikes, middle radius approximately 30%, and short radius less than 20%.

References:

MacGalliard, W. and Liggett, M.A., 1973, False-color compositing of ERTS-1 MSS imagery: NASA Report of Investigation, 7 pp.

Matthews, R.A. and Burnett, J.L., 1966, Geologic map of California, Fresno Sheet (Olaf P. Jenkins Edition): Calif. Div. of Mines and Geology, Scale 1:250,000.

Mayo, E.B., 1947, Structure plan of the southern Sierra Nevada, California: Geol. Soc. Amer. Bull. v. 58, pp. 495-504.

Miller, W.J. and Webb, R.W., 1940, Descriptive geology of the Kernville Quadrangle, California: In Calif. Jour. of Mines and Geology, v. 36, No. 4, pp. 343-378.

Smith, A.R., 1965, Geologic map of California, Bakersfield Sheet (Olaf P. Jenkins Edition): Calif. Div. of Mines and Geology, Scale 1:250,000.

Thornbury, W.D., 1954, Principles of geomorphology: John Wiley & Sons, Inc., New York, 618 p.

Webb, R.W., 1946, Geomorphology of the middle Kern River Basin, southern Sierra Nevada, California: Geol. Soc. Amer., Bull. v. 57, pp. 355-382.

Webb, R.W., 1950, Volcanic geology of Toowa Valley, southern Sierra Nevada, California: Geol. Soc. Amer. Bull., v. 61, pp. 349-357.

Webb, R.W., 1955, Kern Canyon lineament, in Earthquakes in Kern County, California during 1952: Calif. Div. of Mines and Geology Bull. 171, pp. 35-36.

INVESTIGATION OF A LINEAMENT EXPRESSED IN AN OBLIQUE APOLLO 9 PHOTOGRAPH

Appendix N

Argus Exploration Company
555 South Flower Street - Suite 3670
Los Angeles, California 90071

March 1974

Prepared for
GODDARD SPACE FLIGHT CENTER
Greenbelt, Maryland 20771

INVESTIGATION OF A LINEAMENT EXPRESSED IN AN OBLIQUE APOLLO 9 PHOTOGRAPH

Jack W. Barth
Argus Exploration Company
Los Angeles, California

ABSTRACT

A linear topographic feature, referred to here as the New York Mountains lineament, was recognized in an oblique Apollo 9 photograph to extend from the Providence Mountains of California to near Lake Mead, Arizona. In subsequent vertical ERTS-1 imagery this feature was found to have vague and indistinct expression. A study has been conducted to determine the possible geologic origin(s) of the lineament and to explain its anomalous expression in the Apollo 9 photograph. The results of this study suggest that the apparent expression of the lineament is due to a combination of the oblique view of the Apollo photograph, low sun angle illumination of southeast facing slopes, shadowing of northwest facing slopes, and a linear snow line along the southeastern flank of the New York Mountains. No geologic or structural causes for the lineament have been found.

Introduction:

A narrow topographic lineament is apparent for a distance of approximately 180 km in an oblique Apollo 9 photograph recorded over southeastern California, southern Nevada and northwestern Arizona on 12 March 1969 (Figure 1). The lineament, referred to here as the New York Mountains lineament, is expressed in the Apollo 9 photograph as a discrete northeast trending alignment of ridges, hills, and snow lines.

In vertical multi-seasonal ERTS-1 MSS imagery recorded over the area of the Apollo 9 photograph, the New York Mountains lineament has been found to have vague and indistinct expression. The following study was conducted in order to determine the possible geologic origin(s) of the lineament, and to explain its anomalous expression in the Apollo 9 photograph.

The region traversed by the New York Mountains lineament lies within the southern Basin Range Province, in an area of moderate topographic relief and arid to semi-arid climate. A northeast trending group of ranges including the New York Mountains, Mid Hills and Providence Mountains is aligned along the southwestern

trace of the lineament. The ranges traversed by the northeastern trace of the lineament are the Eldorado and Black Mountains east and west of the Colorado River. The Eldorado and Black Mountains have a northerly trend (Figure 2) controlled by normal faulting, dike-swarms, and elongate plutons of late Cenozoic age (Liggett and Childs, 1974).

The geology along portions of the New York Mountains lineament has been mapped at a variety of scales. This data has aided imagery analysis and guided field reconnaissance by members of the Argus Exploration Company research staff. Reconnaissance geologic maps used in this investigation cover Clark Co., Nevada (Longwell and others, 1965), San Bernardino Co., California (Jennings, 1972), an area bordering the Colorado River (Longwell, 1963), and Mohave Co., Arizona (Wilson and others, 1969). More detailed studies conducted along portions of the New York Mountains lineament include mapping in the vicinity of Nelson, Nevada by R. E. Anderson (1971) and Volborth (1973), the Highland Spring Range by Bingler and Bonham (1973), the Vanderbilt area in the central New York Mountains by Haskell (1959), and the Ivanpah 1^{o}x 2^{o} quadrangle by Hewett (1956).

New York Mountains Lineament:

In the Apollo 9 Ektachrome photograph AS9-20-3135 taken on 12 March 1969, the New York Mountains lineament is most clearly expressed in the northern Eldorado Mountains and on the southeastern slope of the New York Mountains (see Figure 1). In the Eldorado Mountains, near Nelson, Nevada, the lineament appears as an alignment of ridges and hills which are shadowed on the northwest slopes and illuminated on the southeastern slopes by an early morning sun elevation of approx 41°. In the New York Mountains east of Cima, California, the lineament is expressed by the anomalous northeasterly trend of the range and a nearly linear snowline which generally follows a topographic contour along the southeastern flank of the range. In the Providence Mountains, the lineament is expressed by the illumination of southeast facing ridges in the center of the range.

In the multi-seasonal ERTS-1 MSS imagery, the lineament observed on the Apollo 9 photography is poorly expressed. In the Eldorado Mountains a general alignment of hills and ridges shows illumination effects similar to those observed on the Apollo 9 photograph. Analysis of ERTS-1 MSS imagery recorded during several seasons has shown this alignment of topographic features to be most distinct in winter when the solar elevation is at a minimum of approximately 26^{o} above the horizon.

The ERTS-1 MSS imagery and topographic maps of the Providence Mountains show this range to have a more northerly trend than is apparent in the Apollo 9 photograph. This geometric distortion is believed to be the result of the oblique look angle of the Apollo 9 photograph, which has a bearing of N 6^{o}W, and is estimated to be approximately 55^{o} from vertical.

No consistent geologic or structural features which might account for the New York Mountains lineament have been recognized along its trace in either the mapped geology, or field reconnaissance by members of the Argus Exploration Company staff. Detailed analysis of the terrain along the lineament has been conducted using a variety of high altitude imagery including USGS-USAF black and white U-2 photographs, and NASA Pre-ERTS Investigator Support (PEIS) U-2 multispectral, and infrared Aerographic and Aerochrome photography. This supporting data is listed in the imagery reference portion of this report.

In the vicinity of Nelson, Nevada, and east of the Colorado River along the western flank of the Black Mountains in Arizona, late Tertiary and Quaternary dikes and normal faults occur along the northeast trending trace of the New York Mountains lineament. However, most of these features have northerly strikes and it is considered improbable that the few geologic features aligned parallel with the lineament in this region have controlled its apparent topographic expression.

The structure of the New York and Providence Mountains is essentially that of a tilted block raised on the northwestern range front by a system of northeast striking normal faults. Within these ranges Precambrian granitic rocks are overlain by Tertiary volcanic rocks which have been tilted with the range and dip toward the southeast beneath the basin alluvium of Lanfair Valley. Several felsic dikes of probable Cretaceous or younger age (Hewett, 1956) strike parallel to the frontal fault of the New York Mountains but do not align with the trace of the New York Mountains lineament.

Conclusions:

The New York Mountains lineament appears as a prominent linear alignment of ridges, hills, and other geomorphic features in the Apollo 9 oblique photograph, but does not appear as a distinct feature in the multi-seasonal ERTS-1 imagery.

No geologic or structural causes for the New York Mountains lineament in the Apollo 9 photograph have been recognized. The vertical ERTS-1 MSS imagery has shown that the apparent alignment of the New York Mountains, Mid Hills, and Providence Mountains, in the Apollo photograph is incorrect. The apparent alignment of these ranges in the Apollo 9 photograph is due in large part to the oblique look angle of the photograph which has produced a foreshortening of the field of view. The oblique northerly view in the Apollo 9 photograph, in combination with the low sun elevation in the southeast, produced a strong expression of southeasterly facing slopes. This effect is enhanced by the presence of a linear snow line on the southeastern flank of the New York Mountains.

This study emphasizes the value of vertical, repetitive and multi-seasonal ERTS-1 imagery for analysis and evaluation of topographic features, especially in applications to structural geology and geomorphology.

Figure 1 Apollo 9 oblique photograph number AS9-20-3135 over southeastern California, southern Nevada, and northwestern Arizona. The trace of the New York Mountains lineament is shown on the index map, Figure 2.

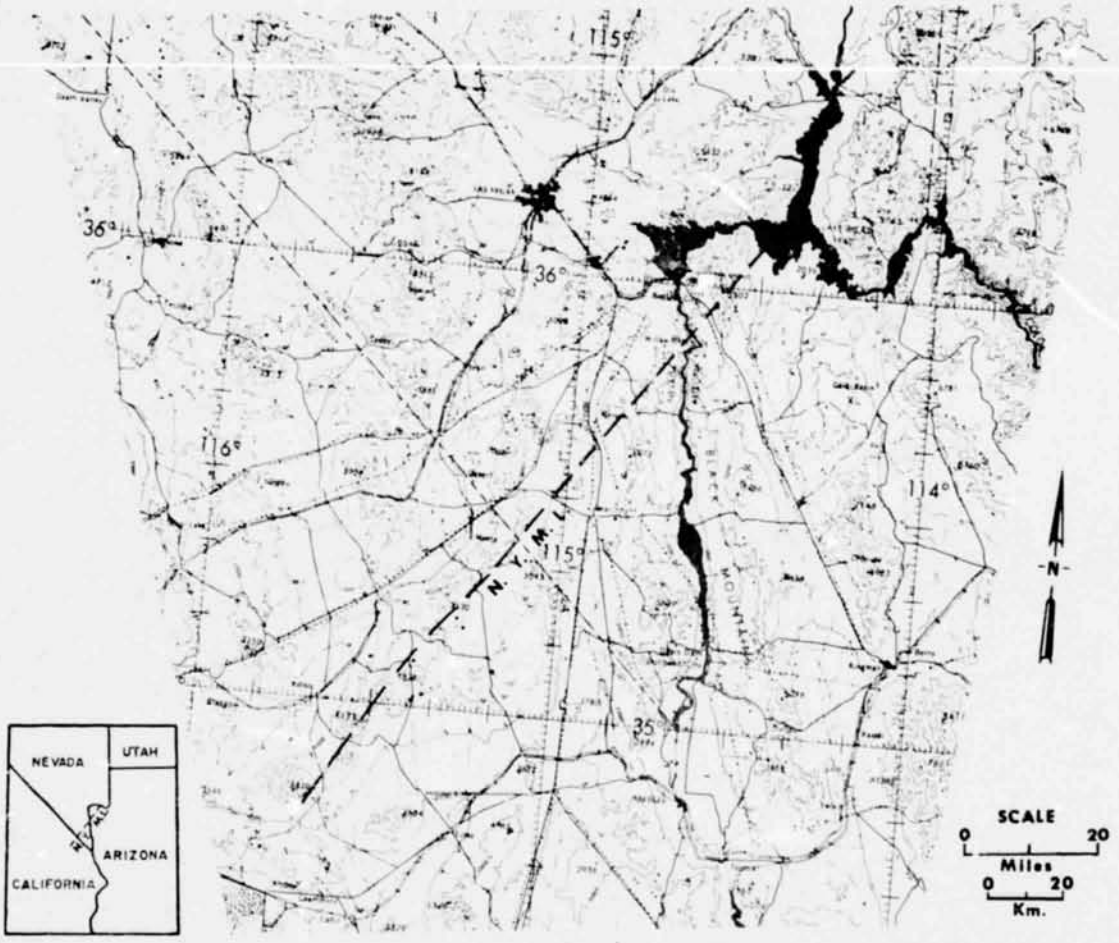

Figure 2 Index map showing the trace of the New York Mountains lineament as expressed on the Apollo 9 oblique photograph. The lineament is notated as N. Y. M. L. The area covered in the index map is the same as shown in the lower two-thirds of the Apollo 9 photograph.

Imagery References:

ERTS-1 multispectral scanner imagery

Date	Frame
13 September 1972	1052-17490
6 November 1972	1106-17495
30 March 1973	1250-17501
17 April 1973	1268-17501
23 May 1973	1304-17495
10 June 1973	1322-17494
28 June 1973	1340-17493

Apollo 9 space photographs

12 March 1969	AS9-20-3135
12 March 1969	AS9-20-3136

NASA Pre-ERTS Investigator Support (PEIS) imagery

Flight No.	Accession No.
72-059	00285
72-077	00345
72-077	00346 Frames 049-049 0058-0061 0065-0067 0072-0073

USGS-USAF high altitude black and white U-2 photography

Flight No.	Frames	Date
018V	207-209	10 July 1968
059V	171-173	17 July 1969
059L	169-171	17 July 1968
059R	173-178	17 July 1968
374V	208-209	6 September 1968
374L	206-209	6 September 1968
374R	207-209	6 September 1968
774R	079b-079e	29 November 1967

Literature References:

Anderson, R. E., 1971, Thin skin distension in Tertiary rocks of southeastern Nevada: Geol. Soc. America Bull., v. 82, p. 43-58.

Bingler, E. C., and Bonham, H. F., Jr., 1973, Reconnaissance geologic map of the McCullough Range and adjacent areas Clark County, Nevada: Nevada Bur. Mines and Geology Map 45, scale 1:125,000.

Haskell, B. S., 1959, The geology of a portion of the New York Mountains and Lanfair Valley (AM. thesis): Los Angeles, Univ. Southern California.

Hewett, D. F., 1956, Geology and mineral resources of the Ivanpah quadrangle California and Nevada: U.S. Geol. Survey Prof. Paper 275, 172 p.

Jennings, C. W., 1972, Geologic map of California; south half (preliminary): California Div. Mines and Geology, scale 1:750,000

Liggett, M. A., and Childs, J. F., March 1974, Crustal extension and transform faulting in the southern Basin Range province: NASA Rept. Inv., 28 p.

Longwell, C. R., 1963, Reconnaissance geology between Lake Mead and Davis Dam Arizona-Nevada: U.S. Geol. Survey Prof. Paper 374-E, 51 p.

Longwell, C. R., Pampeyan, E. H., Bowyer, Ben, and Roberts, R. J., 1965, Geology and mineral deposits of Clark County, Nevada: Nevada Bur. Mines, Bull. 62, 218 p.

Wilson, E. D., Moore, R. T., and Cooper, J. R., 1969, Geologic map of Arizona: U.S. Geol. Survey, and Arizona Bur. Mines, scale 1:500,000.

Volborth, Alexis, 1973, Geology of the granite complex of the Eldorado, Newberry, and northern Dead Mountains, Clark County, Nevada: Nevada Bur. Mines and Geology Bull. 80, 40 p.

CRUSTAL EXTENSION AND TRANSFORM FAULTING IN THE SOUTHERN BASIN RANGE PROVINCE

Argus Exploration Company
555 South Flower Street - Suite 3670
Los Angeles, California 90071

Appendix C

March 1974
Report of Investigation

Prepared for
GODDARD SPACE FLIGHT CENTER
Greenbelt, Maryland 20771

CRUSTAL EXTENSION AND TRANSFORM FAULTING IN THE SOUTHERN BASIN RANGE PROVINCE

Mark A. Liggett and John F. Childs
Argus Exploration Company
Los Angeles, California

ABSTRACT

Field reconnaissance and study of geologic literature guided by analysis of ERTS-1 MSS imagery have led to a hypothesis of tectonic control of Miocene volcanism, plutonism, and related mineralization in part of the Basin Range Province of southern Nevada and northwestern Arizona.

The easterly trending right-lateral Las Vegas Shear Zone separates two volcanic provinces believed to represent areas of major east-west crustal extension. One volcanic province is aligned along the Colorado River south of the eastern termination of the Las Vegas Shear Zone. This province is dominated by large granitic plutons and related silicic to intermediate volcanics of Miocene age. Dike swarms, elongated plutons, and normal faults of major displacement are oriented with northerly trends. The second volcanic province is located north of the western termination of the Las Vegas Shear Zone in southern Nye County, Nevada. This area is characterized by silicic to intermediate volcanics, plutons, dikes, and northerly striking normal faults similar to those in the volcanic province southeast of the Las Vegas Shear Zone.

Geochronology and field evidence indicate that strike-slip movement on the Las Vegas Shear Zone was synchronous with igneous activity and normal faulting in both volcanic provinces. These relationships suggest that the Las Vegas Shear Zone may have formed in response to crustal extension in the two volcanic provinces in a manner similar to the formation of a ridge-ridge transform fault, as recognized in ocean floor tectonics.

Introduction:

Analysis of synoptic imagery from the Earth Resources Technology Satellite (ERTS-1) has guided a regional investigation of tectonic patterns in the Basin Range Province of southern Nevada, eastern California and northwestern Arizona. The area of study is shown in the index map of Figure 1.

A program of literature research and field reconnaissance has been conducted in order to confirm interpretation of the satellite imagery. This synthesis of data has resulted in a tectonic model which relates major strike-slip deformation on the Las Vegas Shear Zone to Basin Range normal faulting, epizonal plutonism, volcanism, and related alteration and mineralization.

Critical parts of this hypothesis were first suggested in an abstract by Fleck (1970), and have since been discussed in greater detail by Anderson and others (1972) and Davis and Burchfiel (1973). The data and concepts presented here draw heavily on the results of studies by other workers in the Basin Range Province. This paper is intended as a synthesis of this work, with the hope of defining problems for further evaluation of the proposed model and its regional genetic implications.

Regional Geology:

Much of the Great Basin is underlain by a crystalline basement of Precambrian age. Throughout most of the province the basement is mantled by Precambrian, Paleozoic and Mesozoic sediments of the Cordilleran geosyncline, deformed during several orogenies of Paleozoic and Mesozoic age (Armstrong, 1968).

The Mesozoic deformation culminated in late Cretaceous time in a belt of eastward overthrusting and related folding, which extends along the eastern margin of the Great Basin from southeastern California to Idaho. West of the frontal zone of thrusting, the Jurassic and Cretaceous orogenies are expressed by scattered plutonism and associated metamorphism. The Sierra Nevada batholith is thought to represent an Andean type volcanic - plutonic arc of Mesozoic age which formed above a subduction zone near the western continental margin (Burchfiel and Davis, 1972).

Following a 60-million year period of relative stability, formation of the Basin Range Province began in mid-Tertiary time with the onset of block faulting and silicic volcanism. The Basin Range structure is characterized by north trending systems of complex grabens, horsts, and tilted blocks bound by moderately dipping normal faults (Stewart, 1971). The province forms a distinctive physiographic terrane, which can be traced from southern Oregon into northern Mexico.

Systems of both right- and left-lateral strike-slip faults have been recognized within the Basin Range Province, generally striking at high angles to the northerly trend of the ranges. Movement on several of these strike-slip fault systems is known to have been synchronous with Basin Range normal faulting. Examples are the right-lateral Las Vegas Shear Zone and Death Valley-Furnace Creek Fault Zone and the left-lateral Garlock Fault Zone, Pahranagat Shear System, and Hamblin Bay Fault (Anderson, 1973). The pattern of major Cenozoic faulting in the southern Basin Range Province is shown in Plate 1.

Cenozoic volcanism throughout the Basin Range Province is dominated by voluminous ignimbrites and flows, generally rhyolitic to dacitic in composition. In

many areas erosion has exposed plutonic bodies chemically equivalent to the associated felsic volcanic rocks. This igneous activity was closely related temporally and spatially to Basin Range structural development. The distribution of Cenozoic volcanic and intrusive rocks in the southern Basin Range Province is shown in Plate 2.

Over the last 100 years various theories have been proposed for the origin of Basin Range structure. These theories are discussed in excellent summaries by Nolan (1943), Gilluly (1963), Roberts (1968), and Stewart (1971). Most concepts can be separated into the following three categories:

1. Basin Range structure has resulted from the collapse of the upper crust caused by such mechanisms as lateral transfer of lower crustal material (Gilluly, 1963) or eruption of huge volumes of volcanic magma (Le Conte, 1889; Mackin, 1960).

2. Basin Range structure has formed en echelon to deep seated, conjugate sets of right- and left-lateral strike-slip (Shawe, 1965; Sales, 1966).

3. Basin Range structure is the result of regional crustal extension in a roughly east-west direction (Hamilton and Myers, 1966; Cook, 1966; Roberts, 1968; Stewart, 1971). This process is thought to have occurred through plastic flow of the mantle and lower crust, sometimes accompanied by intrusion of plutons beneath Basin Range grabens (Thompson, 1960). The net amount of crustal extension has been estimated to be as great as 300 km, or approximately 100 percent (Hamilton and Myers, 1966).

Most current theories of Basin Range structure are based on models which presume net crustal extension within the province during late Cenozoic time. Although the amounts, mechanisms and causes of extension in the Basin Range Province remain controversial, evidence of extension is well documented by recent geologic mapping and geophysical studies in the province.

Tectonic Model:

The tectonic model proposed here was developed in an attempt to synthesize several diverse geologic and structural characteristics of the southern Basin Range Province. We propose that right-lateral strike-slip movement on the Las Vegas Shear Zone may have formed in response to east-west crustal extension in two northerly trending provinces of silicic volcanism, plutonism, and major normal faulting. A generalized structural diagram which illustrates this mechanism is shown in Figure 2.

One area of inferred crustal extension is a volcanic and plutonic province approximately 100 km wide, which is aligned along the Colorado River south of the eastern termination of the Las Vegas Shear Zone. This province is referred to in

this paper as the Black Mountains Volcanic Province. The second area of inferred crustal extension, referred to as the Nye County Volcanic Province, is located north of the western termination of the Las Vegas Shear Zone. The geologic characteristics and chronological development of the Las Vegas Shear Zone and the two volcanic provinces believed to be areas of crustal extension, are summarized below.

Las Vegas Shear Zone:

A major zone of right-lateral strike-slip movement passing through Las Vegas Valley (Plate 1) was first postulated by Gianella and Callaghan (1934) in their study of the regional implications of the Cedar Mountain earthquake of 1932. The existence of this fault zone was supported by detailed mapping and named the Las Vegas Valley Shear Zone by Longwell (1960). Although direct evidence of the shear zone is not exposed, indirect evidence cited by several workers, suggests more than 40 km of right-lateral strike-slip. These estimates have been based on displacements of stratigraphic isopachs and sedimentary facies (Longwell and others, 1965; Fleck, 1967; Stewart and others, 1968) and offset of distinctive thrust faults of the Sevier orogenic belt (Longwell and others, 1965; Fleck, 1967).

At the scale of the ERTS-1 MSS imagery, the most impressive evidence for the existence of the shear zone is the flexure in the range trends immediately north and south of the zone. This phenomenon was termed "oroflexure" by Albers (1967). Compensating for the effect of oroflexural drag along the shear zone, Fleck (1967) estimated a total of approximately 70 km of right-lateral strike-slip displacement of features across the deformed belt bordering the shear zone. Of this total displacement, a net slip of 30 km was estimated for features along the trace of the shear zone.

The Las Vegas Shear Zone was mapped by Longwell and others (1965) from near Lake Mead northwestward to the Spector Range, a distance of approximately 120 km. Detailed mapping in the Spector Range by Burchfiel (1965) yielded only indirect evidence of major strike-slip. Burchfiel concluded, however, that deformation within the area was the result of strike-slip movement in the basement, producing rotation and a mosaic of complex faults in the less competent sedimentary cover. Burchfiel did not map a westward continuation of the Las Vegas Shear Zone but suggested possible continuation westward in the form of discontinuous displacements along several faults, including the northwest trending Furnace Creek Fault.

The eastern termination of the Las Vegas Shear Zone is believed to be in the area north of Lake Mead where major right-lateral slip on the shear zone is replaced by a system of faults having apparent left-lateral movement. In this area Anderson (1973) mapped two halves of a Miocene stratovolcano displaced left-laterally a distance of approximately 19 km along a northeast striking fault zone. This structure, which Anderson has named the Hamblin Bay Fault, strikes at a low angle to the easternmost mapped branch of the Las Vegas Shear Zone, which passes north

of Frenchman Mountain (Plate 1).

East of the Hamblin Bay Fault, the Gold Butte and Lime Ridge Faults of Longwell and others (1965) are considered by Anderson (1973) to be possible left-lateral strike-slip faults. Although field evidence is ambiguous, this hypothesis is supported by the flexure of hogback ridges observed adjacent to these faults in ERTS-1 imagery. Sixteen km to the east of the Gold Butte area, Paleozoic and Mesozoic strata of the Colorado Plateau are uplifted on the northerly striking Grand Wash Fault, east of which no evidence of transverse strike-slip faulting is known (see Plate 1).

The duration of movement on the Las Vegas Shear Zone was estimated by Fleck (1967) from radiometric age determinations of rock units along its trace. A radiometric age date of 15 million years from deformed beds of the Gale Hills Formation indicates that major displacement has occurred on the shear zone since that time. Undeformed basalts of the Muddy Creek Formation have been dated at 10.7 million years. From these dates and field evidence Fleck (1967) concluded that most strike-slip movement on the Las Vegas Shear Zone probably occurred during the period from 17 to 10 million years ago.

Black Mountains Volcanic Province:

An elongate area extending southward along the Colorado River from Lake Mead, Nevada to near Parker, Arizona is a distinct igneous and structural province, referred to here as the Black Mountains Volcanic Province (see Figure 1 and Plate 2). Reconnaissance maps of portions of this region have been published by Longwell (1963), Longwell and others (1965), Wilson and others (1969), and Volborth (1973). Detailed studies of mining districts within the province have been published by Schrader (1917), Ransome (1923), Callaghan (1939), Anderson (1971), and Thorson (1971).

The Black Mountains Volcanic Province is characterized by thick deposits of ignimbrites, flows and volcanic clastic sediments, generally ranging in composition from andesite to rhyolite. Thin basalt flows are locally widespread in the province. In the area near Nelson, Nevada the composite thickness of the Miocene volcanic sequence is estimated to be over 5 km (Anderson and others, 1972).

The volcanics were deposited on an erosional surface developed on a crystalline basement of Precambrian gneiss and rapakivi granite. In parts of the province, the Precambrian basement may have been subjected to metamorphism during a Jurassic orogeny (Volborth, 1973). Both the pre-Tertiary crystalline basement and the Tertiary volcanics have been intruded by granitic plutons of Miocene age (Anderson and others, 1972; Volborth, 1973). The distribution of these Tertiary volcanic and plutonic units is shown in Plate 2. The plutons are generally elongate north-south, and range in composition from leucocratic granite to gabbro, although granite, quartz monzonite, and quartz diorite predominate (Anderson and others, 1972).

Structurally controlled, northerly striking dikes of rhyolite, andesite and diabase are exposed throughout much of the province, cutting both the crystalline basement and the volcanic cover. In the Newberry Mountains of southern Clark County, Nevada a massive swarm of dikes is especially well exposed, forming a belt over 10 km wide. These dikes are bimodal in composition, consisting of porphyritic rhyolite and hornblende diabase. Near Nelson, Nevada dikes of similar compositions are exposed in the lower portions of the volcanic cover, generally decreasing in number upward in the stratigraphic section. It is probable that these dike swarms fed much of the volcanic cover, and were in part synchronous with plutonism (Lausen, 1931; Bechtold and others, 1972; Volborth, 1973).

A close genetic relationship between plutonism and chemically equivalent volcanic facies was suggested as early as 1923 by Ransome in a reconnaissance study of the Oatman mining district, Arizona. This conclusion has been supported by more recent mapping and geochemical studies in this district (Thorson, 1971).

Callaghan (1939) suggested a similar relationship for an intrusive body and adjacent volcanic units in the Searchlight district, Nevada. Through detailed geochemistry and radiometric age date analysis, Volborth (1973) has documented the genetic interrelationship of plutonism, hypabyssal dike emplacement and volcanism over much of the province between Nelson and the Newberry Mountains. Most of the Cenozoic volcanic and hypabyssal intrusive rocks within the province range in age from about 18 to 10 million years before present (Thorson, 1971; Anderson and others, 1972; Volborth, 1973).

Throughout the province the structural deformation is dominated by northerly striking normal faults. In several areas the normal faults dip at angles as low as 10 to 20 degrees, resulting in complex rotation of the volcanic cover. This style of deformation has been mapped in detail near Nelson, Nevada, by Anderson (1971) who attributed the low-angle faulting to extreme east-west distension of the upper crust.

Several normal faults within the Black Mountains Volcanic Province are known to have displacements approaching 2 km (Anderson, 1971; Anderson and others, 1972). Because of the frequency of major normal faults throughout the province, large vertical displacements have occurred between adjacent blocks. Within uplifted blocks, erosion has removed the volcanic cover, and the crystalline basement is commonly juxtaposed against thick sequences of late-Tertiary volcanic rocks.

Although there is insufficient stratigraphic evidence on which to base estimates of net dip-slip on most of the faults in the Black Mountains Volcanic Province, we estimate that crustal extension caused by normal faulting may have exceeded 100 percent. Estimates of similar magnitude have been made in other portions of the Basin Range Province by Hamilton and Myers (1966); Proffett (1971); and Davis and Burchfiel (1973).

Based on a seismic refraction profile across the Las Vegas Shear Zone from near Kingman, Arizona to north of the Las Vegas Shear Zone, Roller (1964) has suggested that an anomalously thin crust of 27 km underlies the Black Mountains Volcanic Province. Just north of the Las Vegas Shear Zone, the crust increases to a more normal thickness of 32 km. This pattern is supported by the existence of a northerly trending Bouguer gravity high (USAF, 1968) which is aligned with the Black Mountains Volcanic Province, suggesting an upward bulge of the mantle beneath this area. This mantle bulge may be the result of isostatic compensation for thin, distended crust in the Black Mountains Volcanic Province. The high gravity anomaly, like the volcanic province, terminates north of Lake Mead along the Las Vegas Shear Zone and the Hamblin Bay Fault.

The southern end of the Black Mountains Volcanic Province is complex and indefinite. The pattern of volcanism, plutonism and normal faulting appears to terminate in the vicinity of Parker, Arizona, against a broad zone of southeast striking faults. Although this fault system is poorly mapped, field reconnaissance along portions of the system near Vicksburg, Arizona has revealed abundant slickensides having moderate plunges, suggesting probable components of strike-slip displacement. The amount and sense of displacement along the entire zone are unknown.

Nye County Volcanic Province:

A sister area of Miocene volcanism, plutonism and extensional normal faulting lies northwest of the Las Vegas Shear Zone in southern Nye County, Nevada. This area is referred to here as the Nye County Volcanic Province (see Figure 1 and Plate 2). This province is a northerly trending area of ten known volcanic centers, at least five of which are believed to be caldera collapse structures (Ekren, 1968). Within the province detailed geologic studies have been conducted in several mining areas associated with Tertiary volcanism at Rhyolite, Beatty (Cornwall and Kleinhampl, 1964), and Goldfield, Nevada (Ransome, 1909; Cornwall, 1972). Detailed mapping, stratigraphic and geophysical studies were conducted by the U. S. Geological Survey in the area of the Atomic Energy Commission's Southern Nevada Test Site (see Eckel, 1968).

The Tertiary ignimbrites and volcanic flows recognized within the Nye County Volcanic Province are estimated to have a composite thickness of approximately 9 km, and a volume estimated to be over 11,000 km^3 (Ekren, 1968). Most of these rocks range in composition from dacite to rhyolite, although andesite and basalt flows are locally abundant (Anderson and Ekren, 1968; Ekren, 1968). The volcanic units uncomformably overlie a basement of Paleozoic carbonate rocks, which were folded, thrust faulted and metamorphosed during Mesozoic time. Several Mesozoic plutons have intruded this Paleozoic basement.

Numerous small plugs, domes and dikes ranging in composition from rhyolite to andesite with minor basalt have intruded the Tertiary volcanic cover. These in-

trusives are similar in composition to the volcanics and are believed to be feeders (Ekren and others, 1971). Larger Tertiary plutons may exist beneath the volcanic cover, but have not been exposed by erosion. Most of the volcanism and plutonism within the province was synchronous with Basin Range normal faulting in a time span from approximately 26.5 to 11 million years ago (Ekren and others, 1968).

Tertiary structural deformation within the Nye County Volcanic Province is dominated by northerly striking normal faults and by caldera subsidence, doming and radial faulting related to the volcanic centers. Known displacements on individual faults which form the complex horst and graben structure of the province exceed 900 meters (Cornwall, 1972). Arcuate faults that rim subsident structures have displacements estimated on the basis of gravity anomalies and drill data to be as great as 2,000 meters (Orkild and others, 1968). However, much of the Basin Range structure is masked by the youngest volcanic rock and the full extent of normal faulting is unknown. On the basis of gravity data several basins are estimated to be filled with as much as 4.8 km of volcanic rock (Healey, 1968). Structural control of these basins is suggested by the strong north trending grain of the gravity anomaly patterns.

The Nye County Volcanic Province terminates southward against the northwestern end of the Las Vegas Shear Zone. This complex structural intersection involves a westward flexure of the ranges immediately north of the Las Vegas Shear Zone, and includes several short northeast striking faults believed to have undergone left-lateral strike-slip movement of between 3 and 5 km (Ekren, 1968). This complex pattern of deformation is similar to that of the eastern end of the Las Vegas Shear Zone north of Lake Mead, Nevada. No definite continuation of the Las Vegas Shear Zone has been recognized west of the Nye County Volcanic Province.

Discussion:

Chronology:

The structural model proposed here for the late Tertiary deformation in the southern Basin Range Province is supported by the synchronism of strike-slip movement on the Las Vegas Shear Zone and volcanism, plutonism, and normal faulting in the two areas of inferred crustal extension.

The folding and thrust faulting of the Sevier orogeny within the southern Basin Range Province is believed to have been confined to a relatively brief time span of from 90 to 75 million years ago (Fleck, 1970b). This orogenic episode is reflected in several deposits of Cretaceous continental clastic sediments in the area north and west of Lake Mead (Longwell and others, 1965). The Sevier orogeny appears to have been followed by a long period of relative stability and moderate erosion which resulted in a broad terrane of subdued topography.

During mid-Tertiary time the area south of Lake Mead appears to have formed a broad arch, which shed arkosic conglomerates and fanglomerates containing fragments of Precambrian rock toward the northeast. These sediments overlie an erosional surface cut in the Paleozoic rock of the western Colorado Plateau northeast of Kingman, Arizona. The sediments are conformably overlain by the Peach Springs Tuff, variously dated at 18.3± 0.6 million years (Lucchitta, 1972) and 16.9± 0.4 million years (Young and Brennan, 1974). These relationships indicate that by Miocene time, erosion had unroofed Precambrian basement in the arch south of Lake Mead, and that major normal faulting had not yet occurred to separate depositional areas on the Colorado Plateau from source areas in the ancestral Basin Range Province (Lucchitta, 1972). Following deposition of the Peach Springs Tuff, Basin Range faulting disrupted the northeast flowing drainage, leading to formation of a new pattern of isolated structural depressions filled by basin deposits (Lucchitta, 1972).

In the Black Mountains Volcanic Province the oldest volcanic rocks overlying the Precambrian crystalline basement are tuff units from the Patsy Mine volcanics believed to be 18.6 million years old (Anderson and others, 1972). Dates from the upper Patsy Mine volcanics indicate an age of about 14.5 million years. This range in dates suggests that 13,000 feet of volcanic rock were erupted over a period of approximately 4 million years. The youngest volcanic units of volumetric significance in the area consist of tuffs and flows dated at 12.7 million years (Anderson and others, 1972). Most of the epizonal plutonic rocks in the Black Mountains Volcanic Province range in age from 18 to 10 million years.

In the area of the Nye County Volcanic Province, the chronology of volcanism and structural deformation is similar. A subdued erosional surface developed on the folded and thrust faulted Paleozoic basement in early Tertiary time. This surface was overlain by a widespread welded tuff dated at 26.5 million years (Ekren and others, 1968). Normal faults striking toward the northeast and northwest developed shortly after the eruption of this tuff unit. Typical north trending Basin Range faults first began to form in the area sometime after deposition of a tuff breccia dated at 17.8 million years, and continued to form synchronously with the eruption of subsequent volcanic units. Much of the normal faulting followed eruption of the Timber Mountain caldera 11 million years ago; however, the present mountain ranges are believed to have been well defined prior to extrusion of the Thirsty Canyon Tuff dated at 7 million years (Ekren and others, 1968).

In summary, the first Tertiary volcanism and Basin Range normal faulting began in the Black Mountains and Nye County Volcanic Provinces approximately 20 million years ago. Strike-slip deformation on the Las Vegas Shear Zone appears to have begun about 17 million years ago and to have continued synchronously with igneous activity and extensional normal faulting in

both provinces. Major strike-slip movement, and silicic volcanism and plutonism ended by approximately 10 million years ago.

Mineralization:

Gold, silver, and minor copper mineralization within the Black Mountains and Nye County Volcanic Provinces is believed to be genetically related to the unique igneous and structural settings of these areas of inferred crustal extension.

Within the Black Mountains Volcanic Province major gold and silver deposits have been mined in the Eldorado and Searchlight districts in Clark County, Nevada, and in the Catherine and Oatman districts east of the Colorado River in Arizona. Small mine workings and prospects for gold, silver and copper are found throughout the province. The known ore deposits are spatially associated with the silicic intrusive bodies of Miocene age that have intruded the Precambrian basement and volcanic cover within the province (Bechtold and others, 1973). The ore bodies typically occur as veins having quartz, calcite and adularia gangue; disseminated sulphide mineralization is generally rare. The mineralized veins are localized along the northerly striking normal faults which dominate the structure of the province, and along transverse faults, some of which are known to have had strike-slip movement. Several of the richer districts appear to be located in areas where this transverse structural trend is well developed (see Volborth, 1973). Formation of the mineralized veins postdated the bulk of volcanism and plutonism in the Black Mountains Volcanic Province, but probably occurred synchronously with late normal faulting and dike intrusion. Mineralized veins frequently show several generations of fracturing and deposition of quartz and calcite (see Ransome, 1923, p. 35).

In the Nye County Volcanic Province gold, silver and minor copper deposits have been mined in many areas, including the Goldfield, Tonopah and Bullfrog districts. These districts are spatially associated with Tertiary volcanic centers and are similar to the deposits of the Black Mountains Volcanic Province in ore and gangue mineralogy, and structural settings. The veins are generally aligned along northerly striking normal faults or fracture zones within the Tertiary intrusive rocks and volcanics. In the Bullfrog district most of the known mineralized veins are along normal faults that are believed to be boundary faults for the Bullfrog Hills caldera (Cornwall and Kleinhampl, 1964).

The distributions and ages of known mineralization within parts of the Nye County Volcanic Province have been summarized by Albers and Kleinhampl (1970). The mineralization in different parts of the province is believed to have followed the bulk of local volcanism and plutonism. Mineralization in the Bullfrog district is thought to be less than 11 million years old; mineralization at Goldfield is believed to have occurred approximately 21 million years

ago and at Tonopah, between 22 and 17.5 million years ago.

Conclusions:

The diagrammatic structural model illustrated in Figure 2 unifies many of the temporal and spatial relationships between strike-slip movement on the Las Vegas Shear Zone and normal faulting, volcanism, plutonism, and mineralization in the Black Mountains and Nye County Volcanic Provinces. The Las Vegas Shear Zone is believed to have functioned as a transform fault, separating two areas of simultaneous crustal extension and formation of new crust by volcanism and plutonism.

As shown in Figure 2, the Las Vegas Shear Zone is mechanically similar to a ridge-ridge transform fault described by Wilson (1965, p. 343) as a type of fault for which " .... the horizontal shear motion along the fault ends abruptly by being changed into an expanding tensional motion across the ridge or rift with a [corresponding] change of seismicity." Wilson (1965, p. 343) describes transform faults as " .... a separate class of horizontal shear faults .... which terminate abruptly at both ends, but which nevertheless may show great displacements." Wilson's distinction between transform faults and other strike-slip faults has been challenged by Garfunkel (1972, p. 3491), who argues that " .... all [strike-slip faults] must terminate on structures in which surface area is increased or decreased. This is a direct consequence of the occurrence of strike-slips on these faults." Garfunkel considers ridge-ridge transform faults to be a type of strike-slip fault that cuts and displaces oceanic crust formed in part synchronously with fault movement. We believe that the Las Vegas Shear Zone is a continental analogue of such a structure.

In a less restricted use of the term, the concept of intracontinental transform faulting has been proposed for other structures in the southern Basin Range Province. The left-lateral displacement on the Garlock Fault Zone of eastern California is believed to be the result of westward crustal extension on Basin Range normal faults north of the fault zone (Hamilton and Myers, 1966; Elders and others, 1970; Davis and Burchfiel, 1973). Left-lateral displacement on the Pahranagat Shear System in southern Lincoln County, Nevada is postulated to have resulted from differential amounts of extension on Basin Range normal faults northeast and southwest of the shear system (Liggett and Ehrenspeck, 1974).

The tectonic model proposed here for the Las Vegas Shear Zone is largely mechanical, and does not explain the driving mechanisms for crustal extension or the physicochemical controls of magma genesis and mineralization in the areas of inferred crustal extension. It is hoped that this model will provide a basis for future investigations of these intriguing problems.

This investigation has benefited greatly from the detailed work of many other geologists in the southern Basin Range Province. In addition, the synthesis of data presented here was facilitated by analysis and interpretation of synoptic

imagery from the ERTS-1 satellite. The ERTS-1 imagery has provided an effective tool for the study of regional tectonic patterns and for guiding research to confirm interpretation.

Acknowledgements:

We wish to thank H. E. Ehrenspeck for his aid in preparation of the map compilations of Plates 1 and 2, and A. K. Baird for his constructive criticism and suggestions.

This investigation was supported by the National Aeronautics and Space Administration and Cyprus Mines Corporation as part of a program investigating the use of ERTS-1 MSS imagery for the study of regional tectonics and related resource exploration.

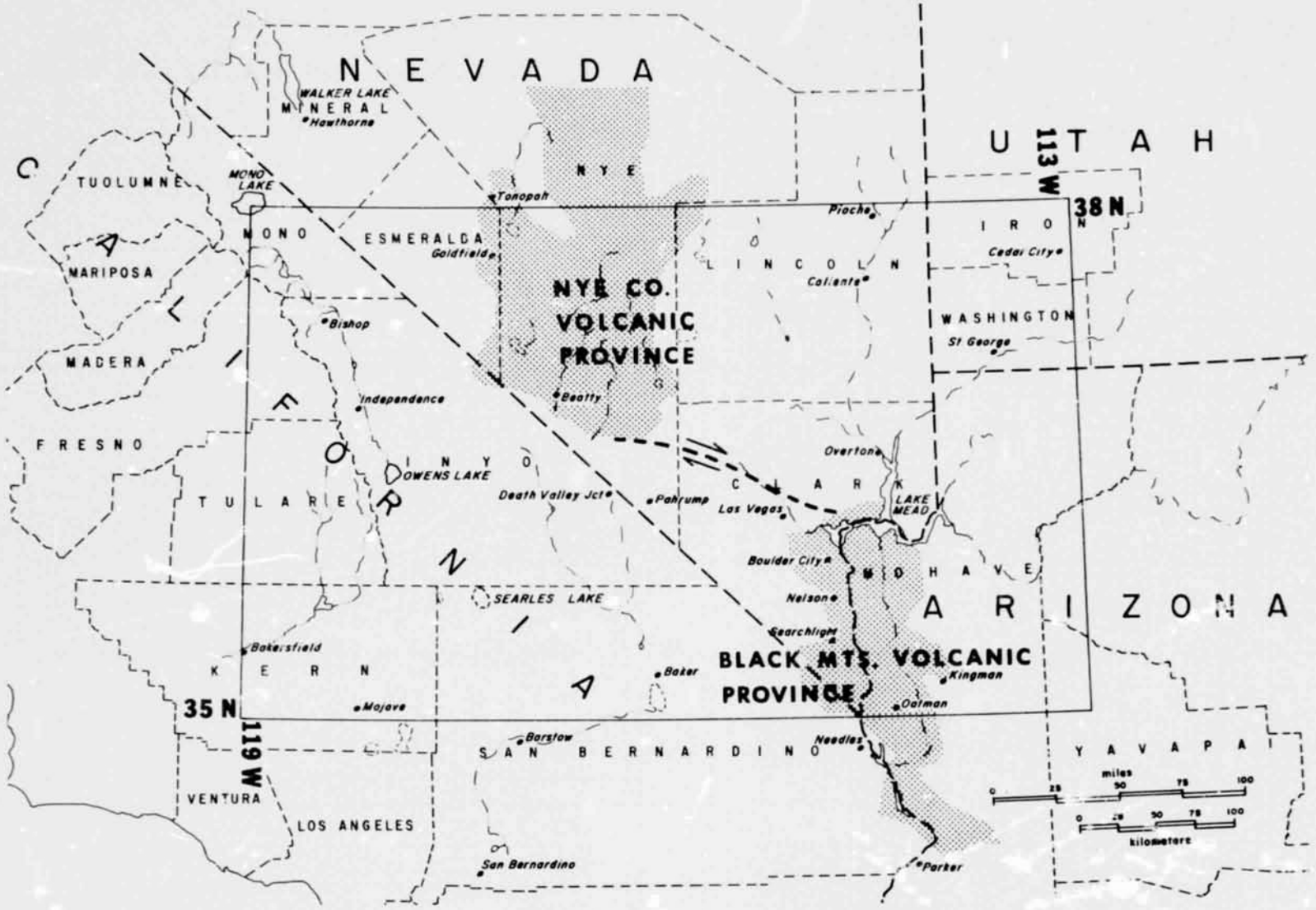

Figure 1: Location map for the area of study. The generalized positions of the Nye County and Black Mountains Volcanic Provinces are indicated with the stippled pattern. The trace of the Las Vegas Shear Zone is shown between these two areas.

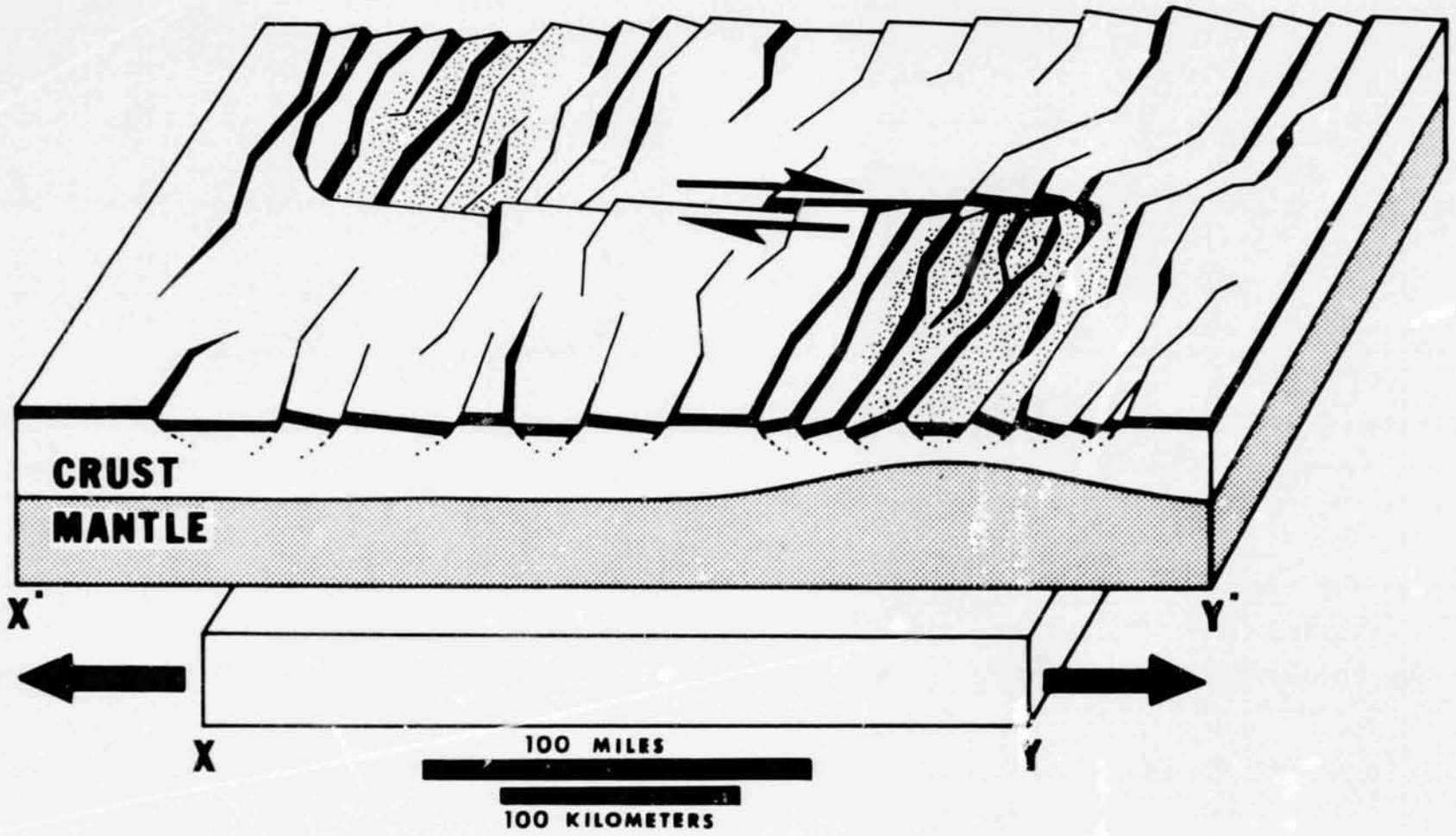

Figure 2: Diagrammatic model of the Las Vegas Shear Zone, separating two areas of crustal extension. Right-lateral strike-slip movement on the Las Vegas Shear Zone is believed to have occurred in response to extension by dip-slip faulting, and formation of new crust by plutonism and volcanism (stippled pattern). The upward bulge of the mantle is believed to be the result of isostatic compensation for the thin, distended crust. The amount of extension is represented by the increase in length of X - Y to X' - Y'.

References Cited in Text:

Albers, J.P., 1967, Belt of sigmoidal bending and right-lateral faulting in the western Great Basin: Geol. Soc. America Bull., v. 78, p. 143-156.

Albers, J.P., and Kleinhampl, F.J., 1970, Spatial relation of mineral deposits to Tertiary volcanic centers in Nevada: U.S. Geol. Survey Prof. Paper 700-C, p. C1-C10.

Anderson, R.E., and Ekren, E.B., 1968, Widespread Miocene igneous rocks of intermediate composition, southern Nye County, Nevada: in Eckel, E.B., ed., Nevada Test Site: Geol. Soc. America Memoir 110, p. 57-63.

Anderson, R.E., 1971, Thin skin distension in Tertiary rocks of southeastern Nevada: Geol. Soc. America Bull., v. 82, p. 43-58.

Anderson, R.E., Longwell, C.R., Armstrong, R.L., and Marvin, R.F., 1972, Significance of K-Ar ages of Tertiary rocks from the Lake Mead region, Nevada-Arizona: Geol. Soc. America Bull., v. 83, p. 273-288.

Anderson, R.E., 1973, Large-magnitude late Tertiary strike-slip faulting north of Lake Mead, Nevada: U.S. Geol. Survey Prof. Paper 794, 18 p.

Armstrong, R.L., 1968, Sevier orogenic belt in Nevada and Utah: Geol. Soc. America Bull., v. 79, p. 429-458.

Bechtold, I.C., Liggett, M.A., and Childs, J.F., November 1972, Structurally controlled dike swarms along the Colorado River, northwestern Arizona and southern Nevada (abs): NASA Rept. Inv., NASA-CR-128390, E72-10192, 2 p.

Bechtold, I.C., Liggett, M.A., and Childs, J.F., March 1973, Regional tectonic control of Tertiary mineralization and recent faulting in the southern Basin-Range Province, an application of ERTS-1 data: Symposium on significant results obtained from the Earth Resources Technology Satellite-1, New Carrollton, Maryland, v. 1, sect. A, NASA-SP-327, E73-10824, p. 425-432.

Burchfiel, B.C., 1965, Structural geology of the Specter Range quadrangle, Nevada, and its regional significance: Geol. Soc. America Bull., v. 76, p. 175-192.

Burchfiel, B.C., and Davis, G.A., 1972, Structural framework and evolution of the southern part of the Cordilleran orogen, western United States: Am. Jour. Sci., v. 272, p. 97-118.

Callaghan, E., 1939, Geology of the Searchlight district, Clark County, Nevada: U.S. Geol. Survey Bull. 906 D, p. 135-185.

Cook, K.L., 1966, Rift system in the Basin and Range province, in The world rift system: Canada Geol. Survey Paper 66-14, p. 246-279.

Cornwall, H.R., and Kleinhampl, F.J., 1964, Geology of Bullfrog quadrangle and ore deposits related to Bullfrog Hills caldera, Nye County, Nevada and Inyo County, California: U.S. Geol. Survey Prof. Paper 454-J, 25 p.

Cornwall, H.R., 1972, Geology and mineral deposits of southern Nye County, Nevada: Nevada Bur. Mines and Geology Bull. 77, 49 p.

Davis, G.A., and Burchfiel, B.C., 1973, Garlock fault: An intracontinental transform structure, southern California: Geol. Soc. America Bull., v. 84, p. 1407-1422.

Eckel, E.B., ed., 1968, Nevada Test Site: Geol. Soc. America Memoir 110, 290 p.

Ekren, E.B., 1968, Geologic setting of the Nevada Test Site and Nellis Air Force Range: in Eckel, E.B., ed., Nevada Test Site: Geol. Soc. America Memoir 110, p. 11-20.

Ekren, E.B., Rogers, C.L., Anderson, R.E., and Orkild, P.P., 1968, Age of Basin and Range normal faults in Nevada Test Site and Nellis Air Force Range, Nevada: in Eckel, E.B., ed., Nevada Test Site: Geol. Soc. America Memoir 110, p. 247-250.

Ekren, E.B., Anderson, R.E., Rogers, C.L., and Noble, D.C., 1971, Geology of northern Nellis Air Force Base Bombing and Gunnery Range, Nye County, Nevada: U.S. Geol. Survey. Prof. Paper 651, 91 p.

Elders, W.A., Rex, R.W., Meidav, T., Robinson, P.T., 1970, Crustal spreading in southern California, The Imperial Valley of California is a product of oceanic spreading centers acting on a continental plate: Institute Geophysics and Planetary Physics, Riverside, Univ. California, 11 p.

Fleck, R.J., 1967, The magnitude, sequence, and style of deformation in southern Nevada and eastern California (Ph.D. thesis): Berkeley, Univ. California, 92 p.

Fleck, R.J., 1970a, Age and possible origin of the Las Vegas shear zone, Clark and Nye Counties, Nevada: Geol. Soc. America, Abs. with Programs (Rocky Mtn. sect.), v. 2, no. 5, p. 333.

Fleck, R.J., 1970b, Tectonic style, magnitude, and age of deformation in the Sevier orogenic belt in southern Nevada and eastern California: Geol. Soc. America Bull., v. 81, p. 1705-1720.

Garfunkel, Z., 1972, Transcurrent and transform faults: A problem of terminology: Geol. Soc. America Bull., v. 83, p. 3491-3496.

Gianella, V.P., and Callaghan, E., 1934, The earthquake of December 20, 1932, at Cedar Mountain, Nevada and its bearing on the genesis of Basin Range structure: Jour. Geology, v. 42, no. 1, p. 1-22.

Gilluly, J., 1963, The tectonic evolution of the western United States: Geol. Soc. London Quart. Jour., v. 119, p. 133-174.

Hamilton, W., and Myers, W.B., 1966, Cenozoic tectonics of the western United States: Rev. Geophysics, v. 4, no. 4, p. 509-549.

Healey, D.L., 1968, Application of gravity data to geologic problems at Nevada Test Site: in Eckel, E.B., ed., Nevada Test Site: Geol. Soc. America Memoir 110, p. 147-156.

Lausen, Carl., 1931, Geology and ore deposits of the Oatman and Katherine districts, Arizona: Arizona Bur. Mines and Geol. Series no. 6, Bull. 131, 126 p.

Le Conte, J., 1889, On the origin of normal faults and of the structure of the Basin region: Am. Jour. Sci., Third series, v. 38, no. 226, p. 257-263.

Liggett, M.A., and Ehrenspeck, H.E., January 1974, Pahranagat shear system, Lincoln County, Nevada: NASA Rept. Inv., 10 p.

Longwell, C. R., 1960, Possible explanation of diverse structural patterns in southern Nevada: Am. Jour. Sci. (Bradley Volume), v. 258-A, p. 192-203.

Longwell, C.R., 1963, Reconnaissance geology between Lake Mead and Davis Dam, Arizona-Nevada: U.S. Geol. Survey Prof. Paper 374-E. p. E1-E51.

Longwell, C.R., Pampeyan, E.H., Bowyer, B., and Roberts, R.J., 1965, Geology and mineral deposits of Clark County, Nevada: Nevada Bur. Mines and Geology Bull. 62, 218 p.

Lucchitta, I., 1972, Early history of the Colorado River in the Basin and Range province: Geol. Soc. America Bull., v. 83, p. 1933-1948.

Mackin. J.H., 1960, Structural significance of Tertiary volcanic rocks in southwestern Utah: Am. Jour. Sci., v. 258, p. 81-131.

Nolan, T.B., 1943, The Basin and Range province in Utah, Nevada and California: U.S. Geol. Survey Prof. Paper 197-D, p. 141-196.

Orkild, P.P., Byers, F.M., Jr., Hoover, D.L., and Sargent, K.A., 1968, Subsurface geology of Silent Canyon caldera, Nevada Test Site, Nevada: in Eckel, E.B., ed., Nevada Test Site: Geol. Soc. America Memoir 110, p. 77-86.

Proffett, J.M., Jr., 1971, Late Cenozoic structure in the Yerington district, Nevada and the origin of the Great Basin: Geol.Soc. America, Abs. with Programs (Cordilleran sect.), v. 3, no. 2, p. 181.

Ransome, F.L., 1909, The geology and ore deposits of Goldfield, Nevada: U.S. Geol. Survey Prof. Paper 66, 258 p.

Ransome, F.L., 1923, Geology of the Oatman gold district, Arizona; A preliminary report: U.S. Geol. Survey Bull. 743, 58 p.

Roberts, R.J., 1968, Tectonic framework of the Great Basin: Rolla, Univ. Missouri Res. Jour., no. 1, p. 101-119.

Roller, J.C., 1964, Crustal structure in the vicinity of Las Vegas, Nevada, from seismic and gravity observations: U.S. Geol. Survey Prof. Paper 475-D, p. D108-D111.

Sales, J.K., 1966, Structural analysis of the Basin Range province in terms of wrench faulting (Ph.D. dissert.): Reno, Univ. Nevada, 289 p.

Schrader, F.C., 1917. Geology and ore deposits of Mohave County, Arizona: Trans. Amer. Inst. Min. Engineers, v. 56, p. 195-236.

Shawe, D.R., 1965, Strike-slip control of Basin-Range structure indicated by historical faults in western Nevada: Geol. Soc. America Bull., v. 76, p. 1361-1378.

Stewart, J.H., Albers, J.P., and Poole, F.G., 1968, Summary of regional evidence for right-lateral displacement in the western Great Basin: Geol. Soc. America Bull., v. 79, p. 1407-1414.

Stewart, J.H., 1971, Basin and Range structure: A system of horsts and grabens produced by deep-seated extension: Geol. Soc. America Bull., v. 82, p. 1019-1044.

Thompson, G.A., 1960, Problem of late Cenozoic structure of the Basin Ranges: International Geol. Congress, session 21, part 18, p. 62-68.

Thompson, G.A., 1966, The rift system of the western United States, in The world rift system: Canada Geol. Survey Paper 66-14, p. 280-290.

Thorson, J.P., 1971, Igneous petrology of the Oatman district, Mohave County, Arizona (Ph.D. dissert.): Santa Barbara, Univ. California, 173 p.

U.S. Air Force Aeronautical Chart and Information Center, 1968, Transcontinental Geophysical Survey (35°-39°N) Bouguer gravity map from 112° W. Longitude to the coast of California: U.S. Geol. Survey, Misc. Geologic Inv. Map I-532-B.

Volborth, Alexis, 1973, Geology of the granite complex of the Eldorado, Newberry and northern Dead Mountains, Clark County, Nevada: Nevada Bur. Mines and Geology Bull. 80, 40 p.

Wilson, E.D., Moore, R.T., and Cooper, T.R., 1969, Geologic map of Arizona: U.S. Geol. Survey, scale 1:500,000.

Wilson, J.T., 1965, A new class of faults and their bearing on continental drift: Nature, v. 207, p. 343-347.

Young, R.A., and Brennan, W.J., 1974, Peach Springs Tuff: Its bearing on structural evolution of the Colorado Plateau and development of Cenozoic drainage in Mohave County, Arizona: Geol. Soc. America Bull., v. 85, p. 83-90.

References Used in Compiling Plate 1:

Albers, J. P., and Stewart, J. H., 1972, Geology and mineral deposits of Esmeralda County, Nevada: Nevada Bur. Mines and Geology Bull. 78, 80 p.

Anderson, R. E., 1971, Thin skin distension in Tertiary rocks of southeastern Nevada: Geol. Soc. America Bull., v. 82, p. 43-58.

Anderson, R. E., 1973, Large-magnitude late Tertiary strike-slip faulting north of Lake Mead, Nevada: U. S. Geol. Survey Prof. Paper 794, 18 p.

Bassett, A. M., and Kupfer, D. H., 1964, A geologic reconnaissance in the southeastern Mojave Desert, California: California Div. Mines and Geol., Spec. Rept. 83, 43 p.

Bateman, P. C., 1965, Geologic map of the Blackcap Mountain quadrangle, Fresno County, California: U. S. Geol. Survey Map GQ-428, scale 1:62,500.

Bateman, P. C., and Moore, J. G., 1965, Geologic map of the Mount Goddard quadrangle, Fresno and Inyo Counties, California: U. S. Geol. Survey Map GQ-429, scale 1:62,500.

Bechtold, I. C., Liggett, M. A., Childs, J. F., March 1973, Regional tectonic control of Tertiary mineralization and Recent faulting in the southern Basin-Range Province: An application of ERTS-1 data: in Freden, S. C., Mercanti, E. P., and Becker, M. A., eds., Symposium on significant results obtained from ERTS-1, New Carrollton, Maryland, v. 1, sect. A, paper G-21, NASA-SP-327, E73-10824, p. 425-432.

Bishop, C. C., 1963, Geologic map of California, Needles sheet, Olaf P. Jenkins edition: California Div. Mines and Geology, scale 1:250,000.

Bowen, O. E., Jr., 1954, Geology and mineral deposits of Barstow quadrangle, San Bernardino County, California: California Div. Mines and Geology Bull. 165, 208 p.

Callaghan, Eugene, 1939, Geology of the Searchlight district, Clark County, Nevada: U. S. Geol. Survey Bull. 906-D, p. 135-185.

Childs, J. F., July 1973, The Salt Creek Fault, Death Valley, California (abs.): NASA Rept. Inv., NASA-CR-133141, E73-10774, 6 p.

Childs, J. F., November 1973, A major normal fault in Esmeralda County, Nevada (abs.): NASA Rept. Inv., 6 p.

Childs, J. F., January 1974, Fault pattern at the northern end of the Death Valley-Furnace Creek Fault Zone, California and Nevada: NASA Rept. Inv., 8 p.

Clary, M. R., 1967, Geology of the eastern part of the Clark Mountains Range, San Bernardino County, California: California Div. Mines and Geology Map Sheet 6.

Cook, E. F., 1957, Geology of the Pine Valley Mountains, Utah: Utah Geol. and Mineralog. Survey Bull. 58, 111 p.

Cook, E. F., 1960, Geologic atlas of Utah, Washington County: Utah Geol. and Mineralog. Survey Bull. 70, 124 p.

Cornwall, H. R., 1972, Geology and mineral deposits of southern Nye County, Nevada: Nevada Bur. Mines and Geology Bull. 77, 49 p.

Crowder, D. F., Robinson, P. F., and Harris, D. L., 1972, Geologic map of the Benton quadrangle, Mono County, California and Esmeralda and Mineral Counties, Nevada: U. S. Geol. Survey Map GQ-1013, scale 1:62,500.

Ekren, E. B., Anderson, R. E., Rogers, C. L., and Noble, D. C., 1971, Geology of northern Nellis Air Force Base Bombing and Gunnery Range, Nye County, Nevada: U. S. Geol. Survey Prof. Paper 651, 91 p.

Gilbert, C. M., Christensen, M. N., Al-Rawi, Y., and Lajoie, K. L., 1968, Structural and volcanic history of Mono Basin, California-Nevada, in Coats, R. R., Hay, R. L., and Anderson, C. A., eds., Studies in volcanology: Geol. Soc. America Memoir 116, p. 275-329.

Gillespie, J. B., and Bentley, C. B., 1971, Geohydrology of Hualapai and Sacramento Valleys, Mohave County, Arizona: U. S. Geol. Survey Water-Supply Paper 1899-H, p. H1-H37.

Goodwin, J. C., 1958, Mines and mineral resources of Tulare County, California: California Jour. Mines and Geology, v. 54, no. 3, p. 317-492.

Gregory, H. E., 1950, Geology of eastern Iron County, Utah: Utah Geol. and Mineralog. Survey Bull. 37, 153 p.

Hall, W. E., and Mackevett, E. M., 1958, Economic geology of the Darwin quadrangle, Inyo County, California: California Div. Mines and Geology Spec. Rept. 51, 73 p.

Hall, W.E., and Stephens, H.G., 1963, Economic geology of the Panamint Butte quadrangle and Modoc district, Inyo County, California: California Div. Mines and Geology, Spec. Rept. 73, 39 p.

Hamblin, W.K., 1970, Structure of the western Grand Canyon region, in Hamblin, W.K., and Best, M.G., eds., Guidebook to the geology of Utah: Utah Geol. Soc. no. 23, p. 3-20.

Hansen, S.M., 1962, The geology of the Eldorado mining district, Clark County, Nevada (Ph.D. thesis): Rolla, Univ. Missouri, 262 p.

Hewett, D.F., 1931, Geology and ore deposits of the Goodsprings quadrangle, Nevada: U.S. Geol. Survey Prof. Paper 162, 172 p.

Heylmun, E.B., ed., 1963, Guidebook to the geology of southwestern Utah: Intermountain Assoc. Petroleum Geologists, 12th Annual Field Conference, Salt Lake City, Utah, 232 p.

Hintze, L.F., 1963, Geologic map of southwestern Utah: Utah Geol. and Mineralog. Survey, scale 1:250,000.

Huber, N.K., and Rinehart, C.D., 1965, Geologic map of the Devils Postpile quadrangle, Sierra Nevada, California: U.S. Geol. Survey Map GQ-437, scale 1:62,500.

Jahns, R.H., ed., 1954, Geology of southern California: California Div. Mines and Geology Bull. 170.

Jennings, C.W., 1958, Geologic map of California, Death Valley sheet, Olaf P. Jenkins edition: California Div. Mines and Geology, scale 1:250,000.

Jennings, C.W., 1961, Geologic map of California, Kingman sheet, Olaf P. Jenkins edition: California Div. Mines and Geology, scale 1:250,000.

Jennings, C.W., 1972, Geologic map of California, south half (preliminary): California Div. Mines and Geology, scale 1:750,000.

Jennings, C.W., Burnett, J.L., and Troxel, B.W., 1962, Geologic map of California, Trona sheet, Olaf P. Jenkins edition: California Div. Mines and Geology, scale 1:250,000.

Jennings, C.W., and Strand, R.G., 1969, Geologic map of California, Los Angeles sheet, Olaf P. Jenkins edition: California Div. Mines and Geology, scale 1:250,000.

Koenig, J.B., 1963, Geologic map of California, Walker Lake sheet, Olaf P. Jenkins edition: California Div. Mines and Geology, scale 1:250,000.

Krauskopf, K.B., 1971, Geologic map of the Mt. Barcroft quadrangle, California-Nevada: U.S. Geol. Survey Map GQ-960, scale 1:62,500.

Kupfer, D.H., 1960, Thrust faulting and chaos structure, Silurian Hills, San Bernardino County, California: Geol. Soc. America Bull., v. 71, p. 181-214.

Liggett, M.A., and Childs, J.F., July 1973, Evidence of a major fault zone along the California-Nevada state line 35°30'-36°30' N. latitude. An application of ERTS-1 satellite imagery: NASA Rept. Inv., 10 p.

Liggett, M.A., and Childs, J.F., February 1974, Structural lineaments in the southern Sierra Nevada, California: NASA Rept. of Inv., 9 p.

Liggett, M.A., and Ehrenspeck, H.E., January 1974, Pahranagat Shear System, Lincoln County, Nevada: NASA Rept. Inv., 10 p.

Longwell, C.R., Pampeyan, E.H., Bowyer, B., and Roberts, R.J., 1965, Geology and mineral deposits of Clark County, Nevada: Nevada Bur. Mines and Geology Bull. 62, 218 p.

Malmberg, G.T., 1967, Hydrology of the valley-fill and carbonate-rock reservoirs, Pahrump Valley, Nevada-California: U.S. Geol. Survey Water Supply Paper 1832, 47 p.

Matthews, R.A., and Burnett, J.L., 1965, Geologic map of California, Fresno sheet, Olaf. P. Jenkins edition: California Div. Mines and Geology, scale 1:250,000.

Maxey, G.B., and Jameson, C.H., 1948, Geology and water resources of L Vegas, Pahrump, and Indian Spring Valleys, Clark and Nye Counties, Nevada: Nevada Water Resources Bull. 5, 121 p.

McAllister, J.F., 1952, Rocks and structure of the Quartz Spring area, northern Panamint Range, California: California Div. Mines and Geology Spec. Rept. 25, 38 p.

McAllister, J. F., 1955, Geology of mineral deposits in the Ubehebe Peak quadrangle, Inyo County, California: California Div. Mines and Geology Spec. Rept. 42, 63 p.

McAllister, J. F., 1956, Geology of the Ubehebe Peak quadrangle, California: U.S. Geol. Survey Map GQ-95, scale 1:62,500.

McAllister, J.F., 1970, Geology of the Furnace Creek borate area, Death Valley, Inyo County, California: California Div. Mines and Geology Map Sheet 14, scale 1:24,000.

McKee, E.H., and Nelson, C.A., 1967, Geologic map of the Soldier Pass quadrangle, California and Nevada: U.S. Geol. Survey Map GQ-654, scale 1:62,500.

McKee, E.H., 1968, Geology of the Magruder Mountain area, Nevada-California: U.S. Geol. Survey Bull. 1251-H, 40 p.

McKee, E.H., 1968, Age and rate of movement of the northern part of the Death Valley-Furnace Creek fault zone, California: Geol. Soc. America Bull. v. 79, p. 509-512.

Nelson, C.A., 1966, Geologic map of the Blanco Mountain quadrangle, Inyo and Mono Counties, California: U.S. Geol. Survey Map GQ-529, scale 1:62,500.

Nelson, C.A., 1966, Geologic map of the Waucoba Mountain quadrangle, Inyo Co., California: U.S. Geol. Survey Map GQ-528, scale 1:62,500.

Nelson, C.A., 1971, Geologic map of the Waucoba Spring quadrangle, Inyo Co., California: U.S. Geol. Survey Map GQ-921, scale 1:62,500.

Noble, D.C., 1968, Kane Springs Wash volcanic center, Lincoln County, Nevada, in Eckel, E.B., ed., Nevada Test Site: Geol. Soc. America Memoir 110, p. 109-116.

Norman, L.A., Jr., and Stewart, R.M., 1951, Mines and mineral resources of Inyo County: California Jour. Mines and Geology, v. 47, p. 17-223.

Ransome, F.L., 1909, The geology and ore deposits of Goldfield, Nevada: U.S. Geol. Survey Prof. Paper 66, 258 p.

Ransome, F.L., 1923, Geology of the Oatman gold district, Arizona: A preliminary report: U.S. Geol. Survey Bull. 743, 58 p.

Rinehart, C.D., and Ross, D.C., 1956, Economic geology of the Casa Diablo Mountain quadrangle, California: California Div. Mines Spec. Rept. 48, 17 p.

Rinehart, C.D., Ross, D.C., and Pakiser, L.C., 1964, Geology and mineral deposits of the Mount Morrison quadrangle Sierra Nevada, California; With a section on a gravity study of Long Valley: U.S. Geol. Survey Prof. Paper 385, 106 p.

Robinson, P.T., McKee, E.H., and Moiola, R.J., 1968, Cenozoic volcanism and sedimentation, Silver Peak region, western Nevada and adjacent California, in Coats, R.R., Hay, R.L., and Anderson, C.A., eds., Studies in volcanology: Geol. Soc. America Memoir 116, p. 577-611.

Rogers, T.H., 1967, Geologic map of California, San Bernardino sheet, Olaf P. Jenkins edition: California Div. Mines and Geology, scale 1:250,000.

Ross, D.C., 1961, Geology and mineral deposits of Mineral County, Nevada: Nevada Bur. Mines and Geology Bull. 58, 98 p.

Ross, D.C., 1965, Geology of the Independence quadrangle, Inyo County, California: U.S. Geol. Survey Bull. 1181-O, 64 p.

Ross, D.C., 1967, Geologic map of the Waucoba Wash quadrangle, Inyo County, California: U.S. Geol. Survey Map GQ-612, scale 1:62,500.

Ross, D.C., 1967, Generalized geologic map of the Inyo Mountains region, California: U.S. Geol. Survey Map I-506, scale 1:125,000.

Ross, D.C., 1970, Pegmatitic trachyandesite plugs and associated volcanic rocks in the Saline Range-Inyo Mountains region, California: U.S. Geol. Survey Prof. Paper 614-D, 29 p.

Schrader, F.C., 1909, Mineral deposits of the Cerbat Range, Black Mountains, and Grand Wash Cliffs, Mohave Co., Arizona: U.S. Geol. Survey Bull. 397, 226 p.

Smith, A.R., 1964, Geologic map of California, Bakersfield sheet, Olaf P. Jenkins edition: California Div. Mines and Geology, scale 1:250,000.

Smith, G.I., Troxel, B.W., Gray, C.H., and von Huene, Roland, 1968, Geologic reconnaissance of the Slate Range, San Bernardino and Inyo Counties, California: California Div. Mines and Geol. Spec. Rept. 96, 33 p.

Stokes, W.L., and Heylmun, E.B., 1963, Tectonic history of southwestern Utah, in Heylmun, E.B., ed., Guidebook to the geology of southwestern Utah: Intermountain Assoc. Petroleum Geologists Guidebook 12, p. 19-25.

Strand, R.G., 1967, Geologic map of California, Mariposa sheet, Olaf P. Jenkins edition: California Div. Mines and Geology, scale 1:250,000.

Threet, R. L., 1963, Structure of the Colorado Plateau margin near Cedar City, Utah, in Heylmun E. B., ed., Guidebook to the geology of southwestern Utah: Intermountain Assoc. Petroleum Geologists Guidebook 12, p. 104-117.

Troxel, B. W., and Morton, P. K., 1962, Mines and mineral resources of Kern County, California: California Div. Mines and Geology, County Rept. no. 1, 370 p.

Tschanz, C. M., and Pampeyan, E. H., 1970, Geology and mineral deposits of Lincoln County, Nevada: Nevada Bur. Mines and Geology Bull. 73, 187 p.

Volborth, Alexis, 1973, Geology of the granite complex of the Eldorado, Newberry, and northern Dead Mountains, Clark County, Nevada: Nevada Bur. Mines and Geology Bull. 80, 40 p.

Wilson, E. D., Moore, R. T., and Cooper, T. R., 1969, Geologic map of Arizona: U. S. Geol. Survey, scale 1:500,000.

Young, R. A., and Brennan, W. J., 1974, Peach Springs Tuff: Its bearing on structural evolution of the Colorado Plateau and development of Cenozoic drainage in Mohave County, Arizona: Geol. Soc. America Bull., v. 85, p. 83-90.

References Used in Compiling Plate 2:

Albers, J. P., and Kleinhampl, F. J., 1970, Spatial relation of mineral deposits to Tertiary volcanic centers in Nevada: U. S. Geol. Survey Prof. Paper 700-C, p. C1-C10.

Albers, J. P., and Stewart, J. H., 1972, Geology and mineral deposits of Esmeralda County, Nevada: Nevada Bur. Mines and Geology Bull. 78, 80 p.

Anderson, R. E., 1969, Notes on the geology and paleohydrology of the Boulder City pluton, southern Nevada: U. S. Geol. Survey Prof. Paper 650-B, p. B35-B40.

Anderson, R. E., 1973, Large-magnitude late Tertiary strike-slip faulting north of Lake Mead, Nevada: U. S. Geol. Survey Prof. Paper 794, 18 p.

Bassett, A.M., and Kupfer, D.H., 1964, A geologic reconnaissance in the southeastern Mojave Desert, California: California Div. Mines and Geol. Spec. Rept. 83, 43 p.

Bayly, Brian, 1968, Introduction to petrology: Englewood Cliffs, New Jersey, Prentice-Hall Inc., 371 p.

Bishop, C.C., 1963, Geologic map of California, Needles sheet, Olaf P. Jenkins edition: California Div. Mines and Geology, scale 1:250,000.

Carlson, J.E., and Willden, Ronald, 1968, Transcontinental Geophysical Survey (35^{o}-39^{o} N) geologic map from 112^{o} W longitude to the coast of California: U.S. Geol. Survey Misc. Geologic Inv. Map I-532-C, scale 1:1,000,000.

Cook, E.F., 1960, Geologic atlas of Utah, Washington County: Utah Geol. and Mineralog. Survey Bull. 70, 124 p.

Cornwall, H.R., 1972, Geology and mineral deposits of southern Nye County, Nevada: Nevada Bur. Mines and Geology Bull. 77, 49 p.

Davis, G.A., February 1974, unpub. mapping.

Dibblee, T.W., Jr., 1967, Areal geology of the western Mojave Desert, California: U.S. Geol. Survey Prof. Paper 522, 153 p.

Ekren, E.B., Anderson, R.E., Rogers, C.L., and Noble, D.C., 1971, Geology of northern Nellis Air Force Base Bombing and Gunnery Range, Nye County, Nevada: U.S. Geol. Survey Prof. Paper 651, 91 p.

Gilbert, C.M., Christensen, M.N., Al-Rawi, Yehya, and Lajoie, K.R., 1968, Structural and volcanic history of Mono Basin, California-Nevada, in Coats, R.R., Hay, R.L., and Anderson, C.A., eds., Studies in volcanology: Geol. Soc. America Memoir 116, p. 275-329.

Hintze, L.F., 1963, Geologic map of southwestern Utah: Utah Geol. and Mineralog. Survey, scale 1:250,000.

Jennings, C.W., 1958, Geologic map of California, Death Valley sheet, Olaf P. Jenkins edition: California Div. Mines and Geology, scale 1:250,000.

Jennings, C.W., 1961, Geologic map of California, Kingman sheet, Olaf P. Jenkins edition: California Div. Mines and Geology, scale 1:250,000.

Jennings, C.W., Burnett, J.L., and Troxel, B.W., 1962, Geologic map of California, Trona sheet, Olaf P. Jenkins edition: California Div. Mines and Geology, scale 1:250,000.

Jennings, C.W., and Strand, R.G., 1969, Geologic map of California, Los Angeles sheet, Olaf P. Jenkins edition: California Div. Mines and Geology, scale 1:250,000.

Koenig, J.B., 1963, Geologic map of California, Walker Lake sheet, Olaf P. Jenkins edition: California Div. Mines and Geology, scale 1:250,000.

Longwell, C.R., Pampeyan, E.H., Bowyer, B., and Roberts, R.J., 1965, Geology and mineral deposits of Clark County, Nevada: Nevada Bur. Mines and Geology Bull. 62, 218 p.

Matthews, R.A., and Burnett, J.L., 1965, Geologic map of California, Fresno sheet, Olaf P. Jenkins edition: California Div. Mines and Geology, scale 1:250,000.

Noble, D.C., 1968, Kane Springs Wash volcanic center, Lincoln County, Nevada in Eckel, E.B., ed., Nevada Test Site: Geol. Soc. America Memoir 110, p. 109-116.

Robinson, P.T., McKee, E.H., and Moiola, R.J., 1968, Cenozoic volcanism and sedimentation, Silver Peak region, western Nevada and adjacent California, in Coats, R.R., Hay, R.L., and Anderson, C.A., eds., Studies in volcanology, p. 577-611.

Rogers, T.H., 1967, Geologic map of California, San Bernardino sheet, Olaf P. Jenkins edition: California Div. Mines and Geology, scale 1:250,000.

Smith, A.R., 1964, Geologic map of California, Bakersfield sheet, Olaf P. Jenkins edition: California Div. Mines and Geology, scale 1:250,000.

Strand, R.G., 1967, Geologic map of California, Mariposa sheet, Olaf P. Jenkins edition: California Div. Mines and Geology, scale 1:250,000.

Tschanz, C.M., and Pampeyan, E.H., 1970, Geology and mineral deposits of Lincoln County, Nevada: Nevada Bur. Mines and Geology Bull. 73, 187 p.

Volborth, Alexis, 1973, Geology of the granite complex of the Eldorado, Newberry, and northern Dead Mountains, Clark County, Nevada: Nevada Bur. Mines and Geology Bull. 80, 40 p.

Wilson, E.D., Moore, R.T., and Cooper, T.R., 1969, Geologic map of Arizona: U.S. Geol. Survey, scale 1:500,000.

SUBSIDIARY REMOTE SENSING DATA OVER THE ARGUS EXPLORATION COMPANY TEST SITE

Argus Exploration Company
555 South Flower Street - Suite 3670
Los Angeles, California 90071

Appendix P

Prepared for
GODDARD SPACE FLIGHT CENTER
Greenbelt, Maryland 20771

SUBSIDIARY REMOTE SENSING DATA OVER THE ARGUS EXPLORATION COMPANY TEST SITE

The subsidiary NASA remote sensing data and USGS-USAF high altitude photographic coverage of the Argus Exploration Company test site are indexed in the following reference Tables and Plates. The remote sensing data used in this investigation was acquired through the following programs:

NASA Pre-ERTS Investigator Support (PEIS) Data

The Pre-ERTS Investigator Support (PEIS) program was operated by the NASA-Ames Research Center, Moffett Field, California. The imagery was recorded from U-2 aircraft flying at altitudes of approximately 65,000 feet. Sensors include the Vinten and Wild RC-10 cameras and the GSFC ERTS simulation multispectral scanner system. The films used were black and white Plus X-2402, Aerographic infrared 2424, and Aerochrome infrared 2443.

Plate 7 shows the geographic position of the PEIS program flight lines over the Argus Exploration Company test site. These flights are also indexed by county in the tables which include the PEIS flight numbers, sensing systems, film types, spectral bands, assession numbers and dates. Plate 7 and the accompanying Tables are designed to enable the interested reader to identify available coverage over specific areas. The data can be obtained through the EROS Data Center, Sioux Falls, South Dakota, 57198.

NASA Earth Observation Aircraft Program

The NASA Earth Observation Aircraft Program was flown by the NASA-L.B. Johnson Space Center, Houston, using both low and high altitude aircraft. The data were recorded at a variety of scales with sensors which recorded in ultraviolet, visible, near infrared and radar portions of the spectrum.

Imagery recorded in this program is indexed in the following Tables by county, with a listing of the AMS 1:250,000 map sheets in which the NASA test site occurs, NASA test site numbers, NASA mission numbers, sensor types, film types, formats, assession numbers, and dates.

Due to the small area covered by many of the sensors, the available imagery has not been plotted on the index maps.

USGS/USAF High Altitude U-2 Photography

Flight tracks showing the geographic areas covered by USGS-USAF U-2 photography are presented on a topographic base map in Plate 8. This plate indicates the geo-

graphic positions of key, consecutively numbered frames along each numbered flight line. These flights are not included in the accompanying Tables. The photographs were taken from approximately 65,000 feet using panchromatic black and white film with vertical, left oblique and right oblique look directions. The photography is available in 9 x 9 inch format from the EROS Data Center. In addition to the subsidiary remote sensing data discussed above, low altitude black and white aerial photography is available over the entire test site. Index maps showing this coverage and referencing the agencies from which the coverage is available may be obtained from:

Map Information Office - Stop 507
U. S. Geological Survey National Center
Reston, Virginia 22092

CLARK COUNTY, NEVADA
Pre-ERTS Investigator Support (PEIS) Data

Airborne Science Office
Ames Research Center
Moffett Field, California

High altitude U-2 flight tracks shown in Plate 7

PEIS Flight No.	Sensor	Film	Spectral Band	PEIS Accession No.	Date
72-059	Vinten	Plus-X, 2402	475-575 NM	00282	14 Apr. 72
	Vinten	Plus-X, 2402	580-680 NM	00283	14 Apr. 72
	Vinten	Aerographic infrared 2424	690-760 NM	00284	14 Apr. 72
	Vinten	Aerochrome infrared 2443	510-900 NM	00285	14 Apr. 72
72-064	Vinten	Plus-X, 2402	580-680 NM	00298	20 Apr. 72
	Vinten	Plus-X, 2402	475-575 NM	00299	20 Apr. 72
	Vinten	Aerographic infrared 2424	690-760 NM	00300	20 Apr. 72
	Vinten	Aerochrome infrared 2443	510-900 NM	00301	20 Apr. 72
72-071	Vinten	Plus-X, 2402	475-575 NM	00314	3 May 72
	Vinten	Plus-X, 2402	580-680 NM	00315	3 May 72
	Vinten	Aerographic infrared 2424	690-760 NM	00316	3 May 72
	Vinten	Aerochrome infrared 2443	510-900 NM	00317	3 May 72
	Multispectral scanner		500-1100 NM	00318	3 May 72
72-077	Vinten	Plus-X, 2402	475-575 NM	00342	12 May 72
	Vinten	Plus-X, 2402	580-680 NM	00343	12 May 72
	Vinten	Aerographic infrared 2424	690-760 NM	00344	12 May 72
	Vinten	Aerochrome infrared 2443	510-900 NM	00345	12 May 72

CLARK COUNTY, NEVADA
Pre-ERTS Investigator Support (PEIS) Data (cont'd.)

PEIS Flight No.	Sensor	Film	Spectral Band	PEIS Accession No.	Date
	Wild RC-10	Plus X, 2402	510-900 NM	00346	12 May 72
72-098	Vinten	Plus-X, 2402	580-680 NM	00422	14 June 72
	Vinten	Aerographic infrared 2424	690-760 NM	00443	14 June 72
	Vinten	Aerochrome infrared 2443	510-900 NM	00444	14 June 72
	RC-10	Panatomic X, 3400	510-700 NM	00445	14 June 72
72-100	Vinten	Plus-X, 2402	475-575 NM	00451	15 June 72
	Vinten	Plus-X, 2402	580-680 NM	00452	15 June 72
	Vinten	Aerographic infrared 2424	690-760 NM	00453	15 June 72
	Vinten	Aerochrome infrared 2443	510-900 NM	00454	15 June 72
	RC-10	Aerochrome infrared 244	510-900 NM	00455	15 June 72

CLARK COUNTY, NEVADA
Earth Observation Aircraft Program Data

Earth Resources Research Data Facility
National Aeronautics and Space Administration
Lyndon B. Johnson Space Center
Houston, Texas

AMS Map Sheet 1/250,000	Geographical area	NASA Test Site No
Las Vegas	Las Vegas and Lake Mead, Nevada	291

Sensor	Site No.	Mission	Film	Format	Accession No.	Date
RC-8/4L	291	189	50-397	9-1/2"		11 Oct. 71
RC-8/4R	291	189	Aerochrome infrared 2443	9-1/2"		11 Oct. 71
Zeiss	291	189	Aerochrome infrared 2443	9-1/2"		11 Oct. 71
Hasselblad	291	189	Plus-X, 2402	70 mm		11 Oct. 71
Hasselblad	291	189	Aerographic infrared 2424	70 mm		11 Oct. 71
Hasselblad	291	189	Aerochrome infrared 2443	70 mm		11 Oct. 71
Hasselblad	291	189	50-356	70 mm		11 Oct. 71
RS-7 IR Sensor	291	189		70 mm		11 Oct. 71

ESMERALDA COUNTY, NEVADA
Pre-ERTS Investigator Support (PEIS) Data

Airborne Science Office
Ames Research Center
Moffett Field, California

High altitude U-2 flight tracks shown in Plate 7

PEIS Flight No.	Sensor	Film	Spectral Band	PEIS Accession No.	Date
72-059	Vinten	Plus X, 2402	475-575 NM	00282	14 Sept. 72
	Vinten	Plus X, 2402	580-680 NM	00283	14 Apr. 72
	Vinten	Aerographic infrared 2424	690-760 NM	00284	14 Apr. 72
	Vinten	Aerochrome infrared 2443	510-900 NM	00285	14 Apr. 72
72-077	Vinten	Plus X, 2402	475-575NM	00343	12 May 72
	Vinten	Plus X, 2402	580-680 NM	00343	12 May 72
	Vinten	Aerographic infrared 2424	690-760 NM	00344	12 May 72
	Vinten	Aerochrome infrared 2443	510-900 NM	00345	12 May 72
	Wild RC-10	Plus X, 2402	510-700 NM	00346	12 May 72

ESMERALDA COUNTY, NEVADA
Earth Observation Aircraft Program Data

Earth Resources Research Data Facility
National Aeronautics and Space Administration
Lyndon B. Johnson Space Center
Houston, Texas

AMS Map Sheet 1/250,000	Geographical area	NASA Test Site No.
Mariposa	Volcanic Hills, Nevada	74

Sensor	Site No.	Mission	Film	Format	Accession No.	Date
APQ-97 SLAR (Westinghouse)	074	100W	Radar	9-1/2"	NR-33-EJ-074-00060	1 Nov. 65

FRESNO COUNTY, CALIFORNIA
Pre-ERTS Investigator Support (PEIS) Data

Airborne Science Office
Ames Research Center
Moffett Field, California

High altitude U-2 flight tracks shown in Plate 7

PEIS Flight No.	Sensor	Film	Spectral Band	PEIS Accession No.	Date
72-098	RC-10	Panatomic X	510-700 NM	00445	14 June 72

INYO COUNTY, CALIFORNIA
Pre-ERTS Investigator Support (PEIS) Data

Airborne Science Office
Ames Research Center
Moffett Field, California

High altitude U-2 flight tracks shown in Plate 7

PEIS Flight No.	Sensor	Film	Spectral Band	PEIS Accession No.	Date
72-077	Vinten	Plus-X, 2402	475-575 NM	00342	12 May 72
	Vinten	Plus-X, 2402	580-680 NM	00343	12 May 72
	Vinten	Aerographic infrared 2424	690-760 NM	00344	12 May 72
	Vinten	Aerochrome infrared 2443	510-900 NM	00345	12 May 72
	Wild RC-10	Plus-X, 2402	510-700 NM	00346	12 May 72
72-098	Wild RC-10	Panatomic	510-700 NM	00445	14 June 72

INYO COUNTY, CALIFORNIA
Earth Observation Aircraft Program Data

Earth Resources Research Data Facility
National Aeronautics and Space Administration
Lyndon B. Johnson Space Center
Houston, Texas

AMS Sheet 1/250,000	Geographical area	NASA Test Site No.
Death Valley	Rose Valley and Coso Hot Springs, Calif.	72
Fresno	East flank of the Sierra Nevada Mtn., Calif.	72
Fresno	Inyo Mountains, Owens Valley	140

Sensor	Site No.	Mission	Film	Format	Accession No.	Date
RC-8 camera	072	73	8442	9-1/2"	NR-22-EJ-072-00234	25-27 May 68
Wild-Heerbrugg	072	73	8443	9-1/2"	NR-22-EJ-072-00240	25-27 May 68
Reconofax IV IR Scanner (HRB Singer)	072	73	TRI-X	70 mm	NR-23-EJ-072-00137	26 May 68
AAS-5 UV camera (HRB Singer)	072	73	TRI-X	35 mm	NR-24-EJ-072-00062	26 May 68
Nikon K-17 camera	072	73	Plus-X	35 mm	NR-25-EJ-072-00136	21-28 May 68

LINCOLN COUNTY, NEVADA
Pre-ERTS Investigator Support (PEIS) Data

Airborne Science Office
Ames Research Center
Moffett Field, California

High altitude U-2 flight tracks shown in Plate 7

PEIS Flight No.	Sensor	Film	Spectral Band	PEIS Accession No.	Date
72-064	Vinten	Plus-X, 2402	580-680 NM	00298	20 Apr. 72
	Vinten	Plus-X, 2402	475-575 NM	00299	20 Apr. 72
	Vinten	Aerographic infrared 2424	690-760 NM	00300	20 Apr. 72
	Vinten	Aerochrome infrared 2443	510-900 NM	00301	20 Apr. 72
72-071	Vinten	Plus-X, 2402	475-575 NM	00314	3 May 72
	Vinten	Plus-X, 2402	580-680 NM	00315	3 May 72
	Vinten	Aerographic infrared 2424	690-760 NM	00316	3 May 72
	Vinten	Aerochrome infrared 2443	510-900 NM	00317	3 May 72
	Multispectral scanner		500-1100 NM	00318	3 May 72
72-098	Vinten	Plus-X, 2402	580-680 NM	00422	14 June 72
	Vinten	Aerographic infrared 2424	690-760 NM	00443	14 June 72
	Vinten	Aerochrome infrared 2443	510-900 NM	00444	14 June 72
	RC-10	Panatomic X, 3400	510-700 NM	00445	14 June 72

MINERAL COUNTY, NEVADA
Pre-ERTS Investigator Support (PEIS) Data

Airborne Science Office
Ames Research Center
Moffett Field, California

High altitude U-2 flight tracks shown in Plate 7

PEIS Flight No.	Sensor	Film	Spectral Band	PEIS Accession No.	Date
72-059	Vinten	Plus-X, 2402	475-575 NM	00282	14 Apr. 72
	Vinten	Plus-X, 2402	580-680 NM	00283	14 Apr. 72
	Vinten	Aerographic infrared 2424	690-760 NM	00284	14 Apr. 72
	Vinten	Aerochrome infrared 2443	510-900 NM	00285	14 Apr. 72
72-077	Vinten	Plus-X, 2402	475-575 NM	00342	12 May 72
	Vinten	Plus-X, 2402	580-680 NM	00343	12 May 72
	Vinten	Aerographic infrared 2424	690-760 NM	00344	12 May 72
	Vinten	Aerochrome infrared 2443	510-900 NM	00345	21 May 72

MINERAL COUNTY, NEVADA
Earth Observation Aircraft Program Data

Earth Resources Research Data Facility
National Aeronautics and Space Administration
Lyndon B. Johnson Space Center
Houston, Texas

AMS Map Sheet 1/250,000	Geographical area	NASA Test Site No.
Mariposa	Volcanic Hills, Nevada	074

Sensor	Site No.	Mission	Film	Format	Accession No.	Date
APQ-97 SLAR (Westinghouse)	074	100W	Radar	9-1/2"	NR-33-EJ-074-00060	1 Nov. 65

MOHAVE COUNTY, ARIZONA
Earth Observation Aircraft Program Data

Earth Resources Research Data Facility
National Aeronautics and Space Administration
Lyndon B. Johnson Space Center
Houston, Texas

AMS Sheet 1/250,000	Geographical area	NASA Test Site No.
Grand Canyon	Mesquite, Nevada, Virgin Mountains, Nevada and Arizona	51
Kingman	Black Mountains, Sacramento Valley, Ariz.	29

Sensor	Site No.	Mission	Film	Format	Accession No.	Date
RC-8 camera Wild-Heerbrugg	051	59	Ektachrome	9-1/2"	NR-22-EJ-051-00172	17-18 Oct. 67
Reconofax IV IR Scanner (HRB Singer)	051	18		70 mm	NR-23-EJ-051-00038	12 Jan. 66
	051	44	TX-415	70 mm	NR-23-EJ-051-00083	24 Mar. 67
	051	59	TRI-X	70 mm	NR-23-EJ-051-00104	17-21 Oct. 67
AAS-5 UV camera (HRB Singer)	051	44	TX-417	35 mm	NR-24-EJ-051-00029	24 Mar. 67
Nikon k-17 camera	051	44	Plus-X	35 mm	NR-25-EJ-051-00079	21-24 Mar. 67
	051	59	Plus-X	35 mm	NR-25-EJ-051-00103	7-21 Oct. 67
T-11 camera (Fairchild)	051	44	Dup. Pas.	9-1/2"	NR-26-EJ-051-00002	9 Jan. 65
	051	59	5424 B/W IR	9-1/2"	NR-26-EJ-051-00027	20 Oct. 67
	051	59	Plus-X, 5401	9-1/2"	NR-26-EJ-051-00028	20-21 Oct. 67

MOHAVE COUNTY, ARIZONA
Earth Observation Aircraft Program (cont'd.)

Sensor	Site No.	Mission	Film	Format	Accession No.	Date
APQ-97 SLAR	051	103W	Radar	9-1/2"	NR-33-EJ-051-00073	5 Nov. 65
(Westinghouse)	29	104W	Radar	9-1/2"	NR-33-EJ-029-00075	8 Nov. 65

MONO COUNTY, CALIFORNIA
Pre-ERTS Investigator Support (PEIS) Data

Airborne Science Office
Ames Research Center
Moffett Field, California

High altitude U-2 flight tracks shown in Plate 7

PEIS Flight No.	Sensor	Film	Spectral Band	PEIS Accession No.	Date
72-059	Vinten	Plus-X, 2402	475-575 NM	00282	14 Apr. 72
	Vinten	Plus-X, 2402	580-680 NM	00283	14 Apr. 72
	Vinten	Aerographic infrared 2424	690-760 NM	00284	14 Apr. 72
	Vinten	Aerochrome infrared 2443	510-900 NM	00285	14 Apr. 72
72-077	Vinten	Plus-X, 2402	475-575 NM	00314	3 May 72
	Vinten	Plus-X, 2402	580-680 NM	00315	3 May 72
	Vinten	Aerographic infrared 2424	690-760 NM	00316	3 May 72
	Vinten	Aerochrome infrared 2443	510-900 NM	00317	3 May 72
	Multispectral scanner		500-1100 NM (ERTS MSS bands)	00318	3 May 72
72-100	Vinten	Plus-X, 2402	475-575 NM	00451	15 June 72
	Vinten	Plus-X, 2402	580-680 NM	00452	15 June 72
	Vinten	Aerographic infrared 2424	690-760 NM	00453	15 June 72
	Vinten	Aerochrome infrared 2443	510-900 NM	00454	15 June 72
	RC-10	Aerochrome infrared 2443	510-900 NM	00455	15 June 72

MONO COUNTY, CALIFORNIA
Earth Observation Aircraft Program Data

Earth Resources Research Data Facility
National Aeronautics and Space Administration
Lyndon B. Johnson Space Center
Houston, Texas

AMS Map Sheet 1/250,000	Geographical area	NASA Test Site No.
Mariposa	Mono Lake, California	3

Sensor	Site No.	Mission	Film	Format	Accession No.	Date
ITEK 9 lens	003	13	Plus-X	70 mm	NR-20-EJ-003-00006	
RC-8 camera	003	13	Ektachrome	9-1/2"	NR-22-EJ-003-00006	29 Sept. 65
Wild-Heerbrugg	003	13	Plus-X	9-1/2"	NR-22-EJ-003-00007	30 Sept. 65
	003	13	Ektachrome IR	9-1/2"	NR-22-EJ-003-00008	30 Sept. 65
	003	13	Ektachrome IR	9-1/2"	NR-22-EJ-003-00009	30 Sept. 65
	003	13	Plus-X	9-1/2"	NR-22-EJ-003-00010	1 Oct. 65
	003	30	Ektachrome IR	9-1/2"	NR-22-EJ-003-00084	1 Sept. 66
	003	56	Plus-X, 5401	9-1/2"	NR-22-EJ-003-00158	6-9 Sept. 67
	003	78	8443	9-1/2"	NR-22-EJ-003-00267	28 Aug. 68
	003	78	8401	9-1/2"	NR-22-EJ-003-00272	28 Aug. 68
	003	100	50117/color IR	6"	NR-22-EJ-003-00409	17 Jul. 69
	003	100	2-2AU/color 2448	6"	NR-22-EJ-003-00410	17 Jul. 69
Reconofax IV	003	8		70 mm	NR-23-EJ-003-00012	3-4 Jun. 65
IR scanner	003	21		70 mm	NR-23-EJ-003-00040	6 Apr. 66
HRB Singer	003	30		70 mm	NR-23-EJ-003-00061	3 Sept. 66

MONO COUNTY, CALIFORNIA
Earth Observation Aircraft Program Data (cont'd.)

Sensor	Site No.	Mission	Film	Format	Accession No.	Date
AAS-5 UV camera (HRB Singer)	003	30		35 mm	NR-24-EJ-003-00006	2 Aug. 66
Nikon K-17 camera	003	13	Plus-X	35 mm	NR-25-EJ-003-00015	30 Sept. 65
RS-7 IR scanner	003	56	TRI-X 5498	70 mm	NR-29-EJ-003-00015	6-9 Sept. 67
(Texas Instruments)	003	78	5498 RAR	70 mm	NR-29-EJ-003-00024	27-28 Aug. 68
APQ-97 SLAR	003	99W	Radar	9-1/2"	NR-33-EJ-003-00056	29 Oct. 65
(Westinghouse)	003	100W	Radar	9-1/2"	NR-33-EJ-003-00061	1 Nov. 65
ZEISS Rmk 30/23 camera	003	100	Color IR 50117	12"	NR-35-EJ-003-00003	17 Jul. 69

NYE COUNTY, NEVADA
Pre-ERTS Investigator Support (PEIS) Data

Airborne Science Office
Ames Research Center
Moffett Field, California

High altitude U-2 flight tracks shown in Plate 7

PEIS Flight No.	Sensor	Film	Spectral Band	PEIS Accession No.	Date
72-059	Vinten	Plus-X, 2402	475-575 NM	00282	14 Apr. 72
	Vinten	Plus-X, 2402	580-680 NM	00283	14 Apr. 72
	Vinten	Aerographic infrared 2424	690-760 NM	00284	14 Apr. 72
	Vinten	Aerochrome infrared, 2443	510-900 NM	00285	14 Apr. 72
72-077	Vinten	Plus-X, 2402	475-575 NM	00342	12 May 72
	Vinten	Plus-X, 2402	580-680 NM	00343	12 May 72
	Vinten	Aerographic infrared 2424	690-760 NM	00344	12 May 72
	Vinten	Aerochrome infrared 2443	510-900 NM	00345	12 May 72
	Wild RC-10	Plus-X, 2402	510-700 NM	00346	12 May 72
72-098	RC-10	Panatomic X, 3400	510-700 NM	00445	14 June 72
72-100	Vinten	Plus-X, 2402	475-575 NM	00451	15 June 72
	Vinten	Plus-X, 2402	580-680 NM	00452	15 June 72
	Vinten	Aerographic infrared 2424	690-760 NM	00453	15 June 72
	Vinten	Aerochrome infrared 2443	510-900 NM	00454	15 June 72

NYE COUNTY, NEVADA
Earth Observation Aircraft Program Data

Earth Resources Research Data Facility
National Aeronautics and Space Administration
Lyndon B. Johnson Space Center
Houston, Texas

AMS Map Sheet 1/250,000	Geographical area	NASA Test Site No.
Caliente and Goldfield	Nevada AEC	52
Goldfield	Goldfield, Nevada	75

Sensor	Site No.	Mission	Film	Format	Accession No.	Date
RC-8 camera	052	30	Ektachrome IR	9-1/2"	NR-22-EJ-052-00087	3 Sept. 66
Wild-Heerbrugg	052	44	Plus-X	9-1/2"	NR-22-EJ-052-00121	23 Mar. 67
	052	44	Ektachrome IR	9-1/2"	NR-22-EJ-052-00122	23 Mar. 67
Reconofax IV	052	30		70 mm	NR-23-EJ-052-00964	3 Sept. 66
IR scanner	052	17/S	TRI-X	70 mm	NR-34-EJ-052-00036	10 Aug. 66
(HRB Singer)	075	17/S	TRI-X	70 mm	NR-34-EJ-075-00037	10 Aug. 66
AAS-5 UV	052	30		35 mm	NR-24-EJ-052-00009	2 Aug. 66
Camera (HRB	052	44	TX-417	35 mm	NR-24-EJ-052-00030	24 Mar. 67
Singer)	075	76	TRI-X	35 mm	NR-24-EJ-075-00070	16 Jul. 68
Nikon K-17 camera	052	44	Plus-X	35 mm	NR-25-EJ-052-00080	21-24 Mar. 67
T-11 camera	052	30	Plus-X	9-1/2"	NR-26-EJ-052-00017	3 Sept. 66
(Fairchild)	052	44	Aeroektachrome	9-1/2"	NR-26-EJ-052-00022	23 Mar. 67

NYE COUNTY, NEVADA
Earth Observation Aircraft Program Data (cont'd.)

Sensor	Site No.	Mission	Film	Format	Accession No.	Date
RS-14 Dual Channel IR scanner	075	180	B & W 2498 .3-.5 micrometers		NR-21-EJ-075-00030	10 Oct. 69
RC-8 camera Wild-Heerbrugg	075	76	8442	9-1/2"	NR-22-EJ-075-00254	16 Jul. 68
	075	76	8443	9-1/2"	NR-22-EJ-075-00256	16 Jul. 68
	075	108	SO117 color IR	6"	NR-22-EJ-075-00592	10 Oct. 69

SAN BERNARDINO COUNTY, CALIFORNIA
Pre-ERTS Investigator Support (PEIS) Data

Airborne Science Office
Ames Research Center
Moffett Field, California

High altitude U-2 flight tracks shown in Plate 7

PEIS Flight No.	Sensor	Film	Spectral Band	PEIS Accession No.	Date
72-059	Vinten	Plus-X, 2402	475-575 NM	00282	14 Apr. 72
	Vinten	Plus-X, 2402	580-680 NM	00283	14 Apr. 72
	Vinten	Aerographic infrared 2424	690-760 NM	00284	14 Apr. 72
	Vinten	Aerochrome infrared 2443	510-900 NM	00285	14 Apr. 72
72-077	Vinten	Plus-X, 2402	475-575 NM	00342	12 May 72
	Vinten	Plus-X, 2402	580-680 NM	00343	12 May 72
	Vinten	Aerographic infrared 2424	690-760 NM	00344	12 May 72
	Vinten	Aerochrome infrared 2443	510-900 NM	00345	12 May 72
	Wild RC-10	Plus-X, 2402	510-700 NM	00346	12 May 72
72-100	Vinten	Plus-X, 2402	475-575 NM	00451	15 June 72
	Vinten	Plus-X, 2402	580-680 NM	00452	15 June 72
	Vinten	Aerographic infrared 2424	690-760 NM	00453	15 June 72
	Vinten	Aerochrome infrared 2443	510-900 NM	00454	15 June 72

SAN BERNARDINO COUNTY, CALIFORNIA
Earth Observation Aircraft Program Data

Earth Resources Research Data Facility
National Aeronautics and Space Administration
Lyndon B. Johnson Space Center
Houston, Texas

AMS Map Sheet 1/250,000	Geographical area	NASA Test Site No.
Kingman	Devils Playground, Calif.	25

Sensor	Site No.	Mission	Film	Format	Accession No.	Date
APQ-97 SLAR (Westinghouse)	025	101W	Radar	9-1/2"	NR-33-EJ-025-00066	2 Nov. 65